

**Inflammatory Response as a Mechanism of Perinatal Programming:
Long-term Impact on Pulmonary and Renal Function?**

Inaugural-Dissertation

zur

Erlangung des Doktorgrades

Dr. nat. med.

der Medizinischen Fakultät

und

der Mathematisch-Naturwissenschaftlichen Fakultät

der Universität zu Köln



vorgelegt von

Dr. med. Miguel Angel Alejandre Alcázar

aus Brombachtal

Hundt-Druck GmbH, Köln

Köln, 2012

Berichterstatter: Prof. Dr. T. Benzing

Prof. Dr. Hammerschmidt

Tag der letzten mündlichen Prüfung: 05.07.2012

PARA
VANESSA Y FRANZISKA

TABLE OF CONTENTS

I. TABLE OF CONTENTS

I. Table of contents.....	1
II . Summary	4
III. Zusammenfassung	7
1. Introduction	10
1.1. Lung development.....	10
1.1.1. Stages of Lung Development.....	10
1.1.2. Molecular Mediators of Lung Development.....	13
1.2. The Kidney: Anatomy and Kidney Development.....	16
1.2.1. Stages of Renal Development.....	17
1.2.2. Molecular Mechanisms of Renal Development.....	18
1.3. Perinatal Programming.....	20
1.3.1. Intrauterine Growth Restriction: Definition and Incidence.....	20
1.3.2. Fetal Programming: The Barker Hypothesis.....	21
1.3.3. Metabolic Programming.....	22
1.4. Intrauterine Growth Restriction and Organ-Specific Diseases.....	23
1.4.1. Intrauterine Growth Restriction and Lung Disease	23
1.4.2. Intrauterine Growth Restriction and Renal Disease.....	24
1.4.3. Early Postnatal Hyperalimentation and Metabolic Programming.....	25
1.5. Transforming Growth Factor β Signaling Pathway.....	26
1.5.1 Transforming Growth Factor β Superfamily and its Ligands.....	26
1.5.2 Transforming Growth Factor β Receptors: Classification and Structure.....	27
1.5.3. Transforming Growth Factor β Pathway: Intracellular Signaling.....	28
1.6. Leptin and Interleukin-6 Signaling pathway.....	29
1.6.1. Leptin	29
1.6.2. Interleukin-6.....	30
1.6.3. Intracellular Signaling of Leptin and Interleukin-6: Stat3 and Erk1/2 Signaling Pathway.....	30

TABLE OF CONTENTS

1.7. Aims	33
2. Results.....	34
2.1. Inhibition of TGF- β signaling and decreased apoptosis in IUGR-associated lung disease in rats.....	34
2.2. Developmental regulation of inflammatory cytokine-mediated Stat3 signaling: the missing link between intrauterine growth restriction and pulmonary dysfunction?.....	36
2.3. Persistent changes within the intrinsic kidney-associated NPY system and tubular function by litter size reduction.....	38
2.4. Early postnatal hyperalimentation impairs renal function via SOCS-3 mediated renal postreceptor leptin resistance.....	40
2.5. Hypothalamic JNK1 and IKK β activation and impaired early postnatal glucose metabolism after maternal perinatal high-fat feeding.....	42
2.6. Prevention of early postnatal hyperalimentation restores TGF- β /BMP signaling in the lung subsequent to IUGR.....	43
3. Discussion.....	45
3.1. TGF- β and IUGR-associated Lung Disease.....	45
3.2. Inflammatory Response in the Lung Subsequent to IUGR and Early Postnatal Hyperalimentation.....	47
3.3. Impact of Leptin and Interleukin-6 Signaling in the Kidney Subsequent to Early Postnatal Hyperalimentation.....	51
4. References.....	55
5. Acknowledgments.....	72
6. <i>Curriculum vitae</i>	73
7. Erklärung.....	77
8. Articles	
8.1. Inhibition of TGF- β signaling and decreased apoptosis in IUGR-associated lung disease in rats	
8.2. Developmental Regulation of Inflammatory Cytokine-mediated Stat3 Signaling: The Missing Link between Intrauterine Growth Restriction and Pulmonary Dysfunction?	
8.3. Persistent Changes Within The Intrinsic Kidney-Associated NPY system and Tubular Function by Litter Size Reduction	

TABLE OF CONTENTS

- 8.4. Early Postnatal Hyperalimentation Impairs Renal Function via SOCS-3 mediated Renal Postreceptor Leptin Resistance
- 8.5. Hypothalamic JNK1 and IKK β Activation and Impaired Early Postnatal Glucose Metabolism after Maternal Perinatal High-Fat Feeding

SUMMARY

II. SUMMARY

RATIONALE: Temporal changes in the fetal environment, such as malnutrition and placental insufficiency induce intrauterine growth restriction (IUGR) and lead to a permanent changes of physiological processes later in life. Interestingly, epidemiological studies demonstrated an impairment of lung and renal function in young infants subsequent to IUGR. Complementary, experimental studies showed that IUGR induces a perinatal programming of the developing lung with persisting impairment of pulmonary structure and function. Besides IUGR, early postnatal hyperalimentation (pHA) is discussed as a crucial factor of IUGR-associated diseases. Both extracellular matrix (ECM) and inflammatory processes have been shown to be dysregulated following IUGR and early pHA. However, the underlying molecular mechanisms of IUGR-associated diseases and the potential linkage of ECM and inflammation have not been addressed so far. Therefore, the ultimate goal of this project was to elucidate the role of regulation of ECM and inflammatory cytokines subsequent to IUGR and early pHA.

AIMS: There are three specific aims: (1) to analyze the role of the TGF- β signaling in lung development subsequent to IUGR, (2) to determine the regulation of inflammatory cytokines and ECM-molecules in lungs subsequent to IUGR, and (3) to characterize the pathomechanistic role of early pHA using the example of the kidney.

METHODS: Two simultaneous sets of animal experiments were used. One animal model addressed pre- and postnatal nutritional intervention, the other was restricted to postnatal interventions only: (A) IUGR was induced in Wister rats by isocaloric low protein diet (8% casein; IUGR) during gestation. The control group received normal protein diet (17% casein; Co). At birth the litter size was reduced to 6 male pups to induce early pHA. During lactation the mothers of both groups were fed standard chow. (B) Early pHA was induced by litter size reduction to 6 (LSR6) or 10 (LSR10) male neonates. Home-cage control (HCC; mean litter size of 16) animals without any postnatal manipulation during lactation were included. At postnatal day (P) 28 as well as P70 animals underwent whole body plethysmography and in addition metabolic cages at P70. Serum and samples of lungs and kidney were obtained at P1, P12, P21, P42, and P70 for mRNA extraction, protein extraction as well as histological analyses.

RESULTS: Both respiratory system resistance and compliance were impaired subsequent to IUGR at P28; this impairment was even more significant at P70. (1) These changes were accompanied by persistent attenuated activity of the TGF- β signaling, assessed by

SUMMARY

phosphorylation of Smad2 and Smad3. Expression analysis of TGF- β -regulated ECM components in the lungs of IUGR animals at P1, such as collagen I, elastin, and tenascin N, revealed a significant deregulation. Consistently, in vitro inhibition of TGF- β signaling in NIH/3T3, MLE 12 and endothelial cells by adenovirus-delivered Smad7 demonstrated a direct effect on the expression of ECM components. Interestingly, however, not just a deregulation of ECM components was detected at P1, but also attenuated apoptotic processes, e.g. decreased cleavage of PARP. (2) Since the TGF- β signaling has potent anti-inflammatory effects, we next determined the dynamic expression of pro-inflammatory and pro-fibrotic markers as well of ECM components in the lung subsequent to IUGR at P1, P42 and P70. The expression of ECM components and metabolizing enzymes was markedly deregulated and the deposition of collagen I was strikingly increased at P70. Concomitantly to the pro-fibrotic processes in the lung subsequent to IUGR, the expression of inflammatory cytokines and both the activity and the expression of target genes of Stat3 signaling were dynamically regulated, with unaltered or decreased expression at P1 and significantly increased expression at P70. (3) Assessment of renal function at postnatal day 70 revealed decreased glomerular filtration rate, proteinuria, and increased fractional sodium and potassium secretion following early pHA (LSR6). Moreover, the deposition of ECM molecules, such as collagen I, was increased. Interestingly, despite the elevated expression of pro-inflammatory leptin and IL-6 expression the phosphorylation of Stat3 and ERK1/2 in the kidney, however, was decreased after LSR6. In accordance, neuropeptide Y (NPY) gene expression – sympathetic co-neurotransmitter regulated by Stat3 signaling – was down-regulated. In accordance, suppressor of cytokine signaling (SOCS)3 protein expression, an inhibitor of Stat3 and Erk1/2 signaling, was strongly elevated and colocalized with NPY. Interestingly, NPY is co-localized with SOCS3 in the distal tubules in the cortex and outer medulla, and in the proximal tubules, but no expression of SOCS3 was detectable in glomeruli.

CONCLUSION: Taken together, IUGR has a direct and strong negative impact on respiratory resistance and compliance of the lung. There are two major underlying mechanisms linking IUGR and deregulation of ECM: first, the attenuated TGF- β signaling during late lung development; and second, the increased expression of inflammatory cytokines subsequent to IUGR. In addition, the missing anti-inflammatory effect of TGF- β signaling could contribute to the increased inflammatory response following IUGR. Furthermore we demonstrated that early pHA leads to organ-intrinsic increased expression of NPY via a postreceptor-leptin-receptor leptin resistance. This leptin resistance could

SUMMARY

contribute to the observed profibrotic processes, and ultimately to a long-term impairment of renal function. Thus, both IUGR and early postnatal hyperalimentation have a strong impact on perinatal programming of multi-organ inflammatory response.

III. ZUSAMMENFASSUNG

HINTERGRUND: Kurzzeitige intrauterine Einlüsse, wie maternale Unterernährung oder Plazentainsuffizienz führen zu einer intrauterinen Wachstumsrestriktion (IUGR) und letztlich zu dauerhaften Veränderungen physiologischer Prozesse. Epidemiologische Studien zeigen sowohl renale als auch pulmonale Funktionsstörungen in Kindern nach IUGR. Ergänzende experimentelle Arbeiten konnten zudem perinatale Programmierung persistierender struktureller Veränderungen in Lunge und Niere nach IUGR aufweisen. Neben der IUGR selbst wird die frühe postnatale Hyperalimentation (pHA) als zentraler Faktor der IUGR-assoziierten Erkrankungen diskutiert. Es ist zudem gezeigt worden, dass sowohl die extrazellulären Matrix (ECM) als auch inflammatorische Prozesse nach IUGR und früher pHA dysreguliert sind. Dennoch sind die zugrunde liegenden Mechanismen der IUGR-assoziierten Erkrankungen sowie der potentielle Zusammenhang zwischen Veränderungen der ECM und inflammatorischen Prozessen noch weitgehend ungeklärt. Aus diesem Grunde war das zentrale Ziel dieser Studie, die Rolle der Regulation der ECM und inflammatorischer Zytokine nach IUGR und früher pHA zu untersuchen.

ZIELE: Drei spezifische Ziele sollten an Rattenmodellen verfolgt werden: (1) Analyse der Rolle der TGF- β Signalkaskade in der Lungenentwicklung nach IUGR, (2) Untersuchung der Regulation inflammatorischer Zytokine sowie der ECM-Moleküle nach IUGR, und (3) Charakterisierung der pathomechanistischen Bedeutung früher pHA am Beispiel der Niere.

METHODS: Zwei parallele unabhängige Tierexperimente wurden genutzt. Das erste Tiermodell umfasst prä- und postnatale, das zweite hingegen nur postnatale nutritive Intervention: (A) IUGR wurde in Wistar Ratten induziert durch isokalorische Proteinmangeldiät (8% Casein; IUGR) während der Gestation. Die Kontrollgruppe erhielt Normalproteindiät (17% Casein, Co). An der Geburt wurden die Würfe auf sechs männliche Nachkommen reduziert, um eine frühe pHA zu induzieren. In der Laktationsphase wurde den Muttertieren Standardfutter gefüttert. (B) Frühe pHA wurde durch Wurfreduktion auf 6 (LSR6) beziehungsweise 10 (LSR10) männliche Neonaten induziert. Eine zusätzliche Gruppe ohne Wurfreduktion (HCC; mittlere Wurfgröße 16) wurde ergänzt. Am postnatalen Tag (P) 28 und am P70 wurden Ganzkörperplethysmographie sowie metabolischen Untersuchungen in metabolischen Käfigen am P70 durchgeführt. Serum sowie Lungen- und Nierenproben wurden am P1, P12, P21, P42 und P70 für mRNA Extraktion, Proteinextraktion sowie histologische Untersuchungen gewonnen.

ZUSAMMENFASSUNG

ERGEBNISSE: Sowohl der Atemwegswiderstand als auch die dynamische Compliance waren eingeschränkt nach IUGR am P28. Diese pulmonale Funktionsstörung war am P70 sogar noch ausgeprägter. (1) Die funktionellen Veränderungen der Lunge waren begleitet von einer persistierend erniedrigten Aktivität der TGF- β Signalkaskade mit verminderter Phosphorylierung von Smad2 und Smad3. Dementsprechend wies die Genexpressionsanalyse TGF- β -regulierter ECM Komponenten, wie Collagen I, Elastin und Tenascin N, eine signifikante Dysregulation auf. Im Einklang mit diesen *in vivo* Daten, führte die *in vitro* Inhibition der TGF- β Signalkaskade in NIH/3T3, MLE-12 und Endothelzellen durch adenovirale Überexpression von Smad7 zu den entsprechenden Expressionsveränderungen der ECM Komponenten. Interessanterweise waren am P1 auch apoptotische Prozesse nach IUGR gehemmt. (2) Da TGF- β auch starke anti-inflammatorische Wirkung besitzt, haben wir als nächstes die Expression pro-inflammatorischer und -fibrotischer Marker sowie von ECM Komponenten in der Lunge nach IUGR am P1, P42 und P70 untersucht. Die Expression der ECM-Komponenten und der metabolisierenden Enzyme war deutlich alteriert und zudem die Ablagerung von Collagen I am P70 beachtlich erhöht. Begleitend zu diesen pro-fibrotischen Veränderungen war die Expression inflammatorischer Zytokine und die Aktivität der Stat3 Signalkaskade mit einer signifikanten Steigerung an P70 reguliert. (3) Die Analyse der Nierenfunktion am P70 zeigte eine erniedrigte glomeruläre Filtrationsrate, Proteinurie, erhöhte fraktionelle Natrium- sowie Kaliumsekretion nach früher pHA (LSR6). Strukturell zeigte sich eine gesteigerte Ablagerung von Collagen I in der Niere. Interessanterweise, war trotz der starken Expression des pro-inflammatorischen Leptins und des Interleukin 6 (IL-6) die Phosphorylierung von Stat3 und Erk1/2 in der Niere erniedrigt nach früher pHA. Entsprechend der erniedrigten Aktivität der Stat3 Signalkaskade war die Genexpression von Neuropeptid Y (NPY) – ein von Stat3-regulierter sympathischer Co-Neurotransmitter – erniedrigt. Die Proteinexpression von suppressor of cytokine signaling (SOCS)3 – ein Inhibitor des Stat3 und Erk1/2 Signalweges – war deutlich erhöht. Bemerkenswert ist zudem, dass NPY mit SOCS3 im distalen Tubulus der Nierenrinde und des -marks co-lokalisiert ist, aber SOCS3 nicht im Glomerulus detektierbar war.

SCHLUSSFOLGERUNG: Diese Studie zeigt, dass IUGR einen direkten negativen Einfluss auf den Atemwegswiderstand und die dynamische Compliance der Lunge hat. Zwei zentrale zugrunde liegende Mechanismen wurden aufgewiesen: erstens, die erniedrigte Aktivität der TGF- β Signalkaskade während der späten Lungenentwicklung und zweitens, eine gesteigerte Expression inflammatorischer Zytokine. Zusätzlich kann die fehlende anti-inflammatorische Wirkung von TGF- β nach IUGR zu der erhöhten inflammatorischen Reaktion nach IUGR

ZUSAMMENFASSUNG

beitragen. Des Weiteren konnten wir zeigen, dass die frühe pHA zu einer organspezifischen gesteigerten Expression von NPY über eine postrezeptor-Leptinrezeptor Leptinresistenz führt. Diese Leptinresistenz könnte zu den beobachteten pro-fibrotischen Prozessen und letztlich zu den renalen Langzeitfolgen nach früher pHA beitragen. Zusammenfassend kann man sagen, dass sowohl IUGR als auch frühe pHA eine tragende Rolle in der perinatalen Programmierung inflammatorischer Prozesse haben.

1. INTRODUCTION

1.1. Lung Development

The development of the human lung encompasses a time period starting with the appearance of the trachea as the ventral outpouching of the foregut in the fourth post-conceptional week and ending in early infancy. Lung development occurs in six distinct stages: (1) embryonic, (2) pseudoglandular, (3) canalicular, (4) saccular, (5) alveolar, and finally (6) vascular maturation stage (1-4). The overall goal of these six developmental stages is to maximize the gas exchange surface area, while minimizing the blood-air barrier. To achieve a normal and concerted course of these developmental processes a finely tuned and balanced cellular interaction by growth factors, transcription factors as well as postnatal mechanical forces is mandatory (5-7). Since lung development is highly regulated, it is thus susceptible to influences by environmental conditions. Therefore, both intrauterine and early postnatal environmental changes lead to alterations of pulmonary structure and thereby of lung function (8-13).

1.1.1. Stages of Lung Development

Two major processes are required for maximization of gas exchange surface area: first, branching of the conducting airways up to the terminal bronchi, and second, subdivision of the developing airspaces into alveoli, a process also named septation (2).

The early stage of lung development comprises the embryonic and pseudoglandular phases. In the subsequent canalicular phase the airway branching is completed and the development of the gas exchange region is initiated and represents the start of the stages of late lung development: growth of pulmonary parenchyma, thinning of connective tissue between the airspaces, maturation of the surfactant system, septation of secondary crests as well as vascular maturation are key processes of the saccular, alveolar and vascular stage (1, 14) (figure 1).

INTRODUCTION

	early lung development			late lung development	
	embryonic	pseudoglandular	canalicular	saccular	alveolar
mouse	E 9.5-	E 12-16.5	E 16.5- 17.5	E 17.5-P4	P4-P21
human	4.-7. w.p.c.	4.-17. w.p.c.	16.- 26. w.p.c.	24.-38. w.p.c.	36.w.p.c.-4.year

Figure1: Schema depicting the different stages of early and late lung development in human and mouse

(1) embryonic stage

[4–7 weeks post conception (p.c.) in humans, embryonic day (E) E9.5–E12 in mice]

In the embryonic stage, the lung bud appears as a ventral outpouching of the primordial foregut, which forms the prospective ventral trachea, and the dorsal oesophagus. The ventral trachea elongates caudally and subsequently branches into left and right bronchial buds. These are the primary bronchi, which continue migrating into the mesenchymal tissue by dichotomous branching, creating the conducting airway tree (1, 15, 16).

(2) pseudoglandular stage

(5–17 weeks p.c. in humans, E12–E16.5 in mice).

The dichotomous branching of the initial conducting airways forming the bronchi and finally the terminal bronchioles is the predominant process of the pseudoglandular stage. Arterial branches accompany the newly-formed airways; veins spread in the mesenchymal tissue, and extend between each generation of airway branching. The prospective conductive airways have been formed, and the acinar limits are apparent. Moreover, during pseudoglandular stage the cell differentiation continues: ciliated cells, goblet cells and basal cells appear, while the transition of mesenchymal cells to smooth muscle and cartilage cells begins (1, 15, 16).

(3) canalicular stage

(16–26 weeks p.c. in humans, E16.5–E17.5 in mice)

Once the phase of early lung development with the major aim of airway branching is successfully completed, late lung development proceeds with forming gas exchange airspaces. Therefore, the distal cuboidal epithelium differentiates into type I and type II cells and signals the start of surfactant production. Moreover, vascularization takes place with the formation

INTRODUCTION

and spreading of capillaries in the interstitium. The endothelial cells of the newly-formed capillaries interact with the adjacent respiratory epithelium, and induce thereby the development of the air-blood barrier. Finally, the bronchioli appear, and the interstitial tissue mass diminish. Furthermore, the pulmonary epithelial cells differentiate into different cell types with highly specific functions, such as pulmonary neuroendocrine cells (PNECs) (1, 15, 16).

(4) saccular stage

[24–38 weeks p.c. in humans, E17.5–postnatal day (P) 4]

The distal airways next form saccular units in the saccular stage. There are three key processes preparing the lungs in this period towards extrauterine life: first, the growth of the pulmonary parenchyma; second, the thinning of the connective tissue between the airspaces; and finally, the maturation of the surfactant system to decrease the superficial tension. At the end, the distal airways spread and expand at the expense of the mesenchyme forming the transitory airspaces, also called sacculi (1, 15, 16).

(5) alveolar stage

(36 weeks p.c. to 36 months postnatal in humans; P4–P28 in mice)

Finally, at the end of intrauterine development and at birth the lung is functionally ready. However, the alveoli as the units of gas exchange are missing and therefore the lung structure is still immature. Secondary septa subdivide the sacculi in smaller units, forming the mature alveoli. This process during the alveolar stage is called septation, and finds its origins in low ridges that arise from the saccular wall. The major goal of alveolar stage is to maximize the gas exchange surface of the lung (1, 15, 16).

(6) vascular maturation stage

(36 weeks p.c. to 36 months postnatal in humans; P4–P28 in mice)

The newly-formed secondary septa during alveolar stage contain a double capillary layer separated by a sheet of connective tissue. These immature septa need to undergo further maturation to minimize the blood-air barrier. Therefore the last stage of lung development is characterized by microvascular maturation, consisting of the fusion of the double-layered capillary network within the immature alveolar septum forming a final single layered capillary septum (1, 4, 15, 16).

INTRODUCTION

1.1.2. Molecular Mediators of Lung Development

Both early and late lung development are sequences of finely-tuned processes, which are tightly regulated by the concerted action of growth factors, transcription factors, and mechanical stretching. Each stage of lung development demands the action of certain transcription factors as well as of growth factors (5-7, 14).

Regarding late lung development, there are several growth factors playing a pivotal role, notable amongst them is transforming growth factor β (TGF- β) (16), bone morphogenetic protein (BMP)(15), fibroblast growth factor (FGF) (17, 18), and vascular endothelial growth factor (VEGF) (19, 20).

(a) Transforming growth factor (TGF)- β system and lung development

Transforming growth factor β (TGF- β) exerts pleiotropic roles in regulating cell proliferation, transformation and apoptosis as well as production, deposition and remodeling of extracellular matrix (ECM) (11, 21, 22). In line with these distinct functions, TGF- β has been demonstrated to be a key regulator of branching and alveolarization (2, 23, 24). This signaling pathway is finely-tuned and highly sensitive to perinatal influences, such as mechanical ventilation (25) and oxygen supply (11). Both over-expression and under-expression of TGF- β have been shown to impact alveolarization: rodents over-expressing TGF- β either by adenoviral transfer of TGF- β 1 (26) or by conditional over-expression of bioactive TGF- β 1 (21) exhibited defective alveolarization, yielding lung structural abnormalities, such as reduced numbers of alveoli and lung blood vessels. In line with these findings, in studies with preterm infants with bronchopulmonary dysplasia (BPD) – characterized by thickened alveolar septa as well as fewer alveoli – levels of TGF- β 1 in tracheal aspirates were increased (27, 28). Similar structural abnormalities of the lung and its vasculature – decreased formation of alveoli and microvessels - are evident in animal models of BPD (11, 29, 30). In contrast, blockade of TGF- β signaling by either ablation of Smad3 (31, 32) or Smad3 deficiency in mice (33) resulted in progressive airspace enlargement and disruption of alveolarization. These studies indicate that TGF- β does not only act as a negative regulator but also a potent positive mediator of normal lung development. Thus, TGF- β signaling is finely-regulated during lung development; both too much and also too little TGF- β activity has serious impact on lung structure and lung function.

INTRODUCTION

(b) Bone morphogenetic protein (BMP) system and lung development

Several studies demonstrate that BMP signaling has strong implication in both early and late lung development (15, 34-36). The BMPs have been ascribed numerous functions in lung development, including cell differentiation, migration, proliferation, and apoptosis (37). BMP-4 stimulates lung branching in vitro (38, 39), whereas the dysregulated expression of BMP-4 in the distal lung epithelium causes an enlargement of airspace and consequently leads to an impaired lung growth (35). Bone morphogenetic protein receptor 1a (Bmpr1a) and Bmpr1b play an important role in the regulation of proliferative and apoptotic processes (40). Bmpr1a and Bmpr1b generally promote opposing functions: signaling via Bmpr1a promotes proliferation, while signaling via Bmpr1b is antiproliferative, promoting mitotic arrest and apoptosis (40). In accordance to these findings, prenatal lung epithelial cell-specific abrogation of *bmpr1a* results in strong apoptosis, leading to a disruption of distal airway formation and ultimately to lung malformation and respiratory failure (41). Furthermore, it has been demonstrated that antisense knockdown of *smad1*, a key intracellular transducer of BMP signals, negatively regulates lung branching (2, 42). Moreover, it has been shown that BMP signaling is strongly activated during late lung development and exhibits dramatic changes in spatial localization during late lung development, and thereby these data indicate a strong impact of BMP-signaling in normal late lung development (15). Furthermore, this study gave initial evidence that Bmpr1a-directed signaling is favoured as normal, late lung development proceeds (15). In addition, BMP ligands regulate myocyte differentiation (43), ECM production by pulmonary myofibroblasts (44), and cell cycle in alveolar epithelial cells (45, 46). Taken together, BMP signaling appears to be a key regulator of proliferation and apoptosis during early and postnatal lung development. Dysregulation of this signaling pathway ultimately disrupts normal airway formation and lung maturation.

(c) Fibroblast growth factor (FGF) and lung development

Fibroblast growth factor (FGF) signaling pathway is another growth factor playing a fundamental role in the morphogenesis of branching organs such as the lung (47). The intracellular signaling of the secreted FGFs occurs via the activation of their cognate specific cell surface receptors (FGFRs) encoded by four distinct genes, namely FGFR1-4 (48). In the developing lung, FGF signaling is a pivotal regulator of the crosstalk between mesenchyme and epithelium, directing branching of the airways (49). Only a limited number of FGF

INTRODUCTION

ligands are expressed and present in the lung during embryonic development, notable among this and well investigated are FGF7 and FGF10 (49-51). A disruption of genes encoding these FGFs is known to be involved in the pathogenesis of pulmonary hypertension as well as congenital diaphragmatic hernia (52-56). FGF10 is dynamically expressed and has chemoattractant function in the lung mesenchyme surrounding the distal buds and regulates thereby the induction and outgrowth of lung epithelium through FGFR2 (50, 57). Moreover, *fgf10*^(-/-) mice have been shown to fail to develop lungs, ultimately leading to neonatal death (48, 58). In accordance to the important role of the FGF ligands, also FGFR2 and FGFR3 have been shown in animal studies to be expressed during late lung development, indicating an important role on alveolarization (48). Lung morphometric analyses of *fgfr3*^(-/-) and *fgfr4*^(-/-) mice revealed thinner mesenchyme as well as an enlargement of airspace (59-62). In conclusion, FGF signaling is a key mediator of early and postnatal lung development, directing the crosstalk between mesenchyme and epithelium and thereby regulating branching and alveolarization.

(d) Vascular endothelial growth factor (VEGF) and lung development

Finally, alveolarization is a complex process depending on the interaction of several cell types. It is not only characterized by the subdivision of sacculi by secondary septa and the differentiation of alveolar type I and type II cells but also by the formation of microvessels. Vascular endothelial growth factor (VEGF) is one of the key mediators of vascular development. VEGF is not only essential for the formation of the pulmonary vasculature, but it is also essential for branching morphogenesis of the developing airway epithelium (63) (64). Blocking VEGF signaling decreases the formation of alveoli and lung capillaries in newborn rats, mimicking changes seen in BPD (65). Moreover, VEGFR2 blockade also has been shown to disrupt lung development in neonatal mice, inducing a disruption of normal formation of alveoli (66, 67). However, VEGF treatment restores normal lung architecture and promotes lung capillary formation in neonatal rats exposed to several days of extreme hyperoxia (19). On the one hand these findings clearly demonstrate the key role of VEGF in alveolarization; on the other hand it shows that deregulation of VEGF signaling plays an important role in the pathogenesis of lung diseases, such as ventilation-induced or hyperoxia-induced lung injury (25, 29, 30, 68-72). Taken together, VEGF is a predominant growth factor directing vascularization and thereby alveolarization during late lung development.

INTRODUCTION

1.2. The Kidney: Anatomy and Kidney Development

The kidney serves several vital regulatory functions and essential in whole-body homeostasis: (1) natural filter of the blood, (2) urine production, (3) detoxification of substances such as urea and ammonium, (4) regulation of electrolytes, (5) maintenance of acid-base balance, regulation of blood pressure through maintaining salt and water balance [renin-angiotensin-aldosterone system (RAAS)], (6) reabsorption of water, glucose and amino acids, and finally (7) synthesis of hormones such as calcitriol, erythropoietin, and the enzyme renin. The kidney coordinates these homeostatic functions both independently and in concert with other organs, especially the endocrine system.

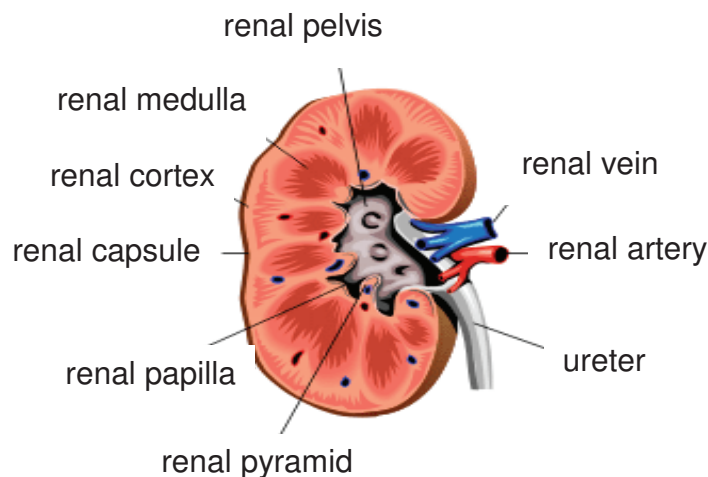


Figure1: **macroscopic anatomy of the kidney:** the kidney is enclosed in a membrane called the renal capsule and divided into two main areas: (1) the outer area called the renal cortex, and (2) the inner area, the renal medulla. Within the medulla there are 8 or more cone-shaped sections known as renal pyramids with the renal papilla at the cone end. The renal pyramids are oriented to the renal pelvis, which extends to the ureter. (modified from: <http://content.p-i-n.com/pics/diabetesaktuell/koerper/nierenanatomie.gif>)

The kidney is composed of renal cortex and renal medulla (figure1). The basic structural and functional unit of the kidney is named nephron –1.2 Million nephrons per adult kidney. Each nephron is subdivided in an initial filtering component (renal corpuscle), and a tubular system (renal tubule). The renal corpuscle is composed of two anatomic structures: (1) the glomerulus, a capillary tuft, receiving its blood supply from an afferent arteriole of the renal circulation; both the oncotic and hydrostatic pressure in the glomerulus induces the filtration of water and soluble substances in the (2) Bowman’s capsule (73). The glomerular filtrate, also called primary urine, is then transferred in the renal tubular system, specialized for reabsorption and secretion, which is subdivided in:

INTRODUCTION

- Proximal convoluted tubule
- Loop of Henle
 - Descending limb of loop of Henle
 - Ascending limb of loop of Henle
 - Thin ascending limb of loop of Henle
 - Thick ascending limb of loop of Henle
- Distal convoluted tubule

Once the glomerular filtrate has passed through the renal tubule and has been concentrated, the filtrate continues to the collecting duct system, which is not part of the nephron. The kidney generates 180 liters of filtrate a day, while reabsorbing a large percentage in the renal tubular system, allowing the generation of only approximately 2 liters of urine (74, 75).

1.2.1. Stages of Renal Development

Kidney development, also called nephrogenesis, has its origin in the intermediate mesoderm and is characterized by three successive phases, starting at day 22 of human gestation and terminating at gestational week 36: (1) the pronephros, (2) mesonephros, and (3) metanephros. The nephrogenesis in vertebrates reflects the phylogenesis of the kidney (76, 77).

(1) Pronephros

The pronephros serves as an excretory organ in less developed fishes and has no specific function in humans. The paired pronephroi develop in the cervical region of the embryo and are apparent towards the cranial end of the intermediate mesoderm during day 22 of human gestation. Next, the epithelial cells form tubules, namely the nephrotomes, which then join laterally with the pronephric duct.

(2) Mesonephros

The pronephric duct proceeds its elongation caudally and induces the intermediate mesoderm to differentiate in epithelial tubules, called mesonephric tubules. Branches of the aorta sprout in these mesonephric tubules and form a capillary tuft inside, allowing the filtration of the blood. The filtrate is drained via the mesonephric tubule to the mesonephric duct, also called Wolffian duct. The mesonephros develops in reptiles, birds and mammals, representing a

INTRODUCTION

transient stage of renal development and degenerating while the mesonephric duct extends towards the cloaca.

(3) Metanephros

The ureteric bud originates from the mesonephric duct as an outpouching during the fifth week of gestation and is called metanephrogenic diverticulum. The elongated stalk of the metanephrogenic diverticulum forms the metanephric duct, the ureter. The ureter undergoes several series of branching and thereby developing the renal pelvis, the renal calices, and the collecting duct system. The tips of the branching ureteric bud interact with the undifferentiated intermediate mesoderm, and induce thereby the formation of renal tubules in the so called metanephrogenic blastema. These newly formed renal tubules coalesce with the connecting ducts of the collecting duct system, allowing a continuous passage from the renal tubule to the collecting duct. At the same time, vascular endothelial cells begin to accumulate at the tips of the renal tubules and to differentiate to the definitive glomerulus. In humans, the formation of the functional unit “nephron” is completed by 32 to 36 weeks of gestation. However, these structures will continue to mature after birth.

Table1: Time course of renal development after Sáxen (76); days of gestation:

	Pronephros	Mesonephros	Metanephros
human	22	24	35-37
rat	10	11.5	12.5
mouse	8	9.5	11

1.2.2. Molecular Mechanisms of Renal Development

The development of mammalian kidneys depends on a tightly regulated program of reciprocal inductive interactions between two primordial tissues: (1) metanephric mesenchyme, and (2) ureteric bud. This interaction induces the branching of the ureteric bud and is directed by the concerted action of numerous transcription factors, growth factors, proteases and components of the extracellular matrix (ECM) (78-81).

INTRODUCTION

(a) Transcription factors and growth factors in renal development

The zinc finger transcription factor Wilms tumor-1 (Wt1) is ubiquitously expressed in the metanephric mesenchyme and is essential for initial differentiation. In line with these findings, mice with *wt-1* null mutation exhibit a kidney agenesis, indicating, that Wt-1 is vital for the initiation and even more for the formation of the ureteric bud (82, 83). Another transcription factor playing a pivotal role in the induction of branching of the ureteric bud and its interaction with the metanephric mesenchyme is paired box gene 2 (Pax-2). In accordance with the findings, mice with *pax-2* null mutation causes kidney agenesis with defective branching morphogenesis (84). Moreover, in *pax-2* knockout mice, expression of glial cell line-derived neurotrophic factor (GDNF) is absent (85). GDNF is expressed in the metanephric mesenchyme area and its receptor “rearranged during transfection” (Ret and its co-receptor Glial cell line-derived neurotrophic factor receptor alpha (Gfra) are expressed in the Wolffian duct (86). It has been shown, that GDNF is one of the key metanephric mesenchyme-derived growth factors of initiation of forming the ureteric bud and its branching afterwards. In accordance, in mice with null mutations of *gdnf*, *ret*, or *gfra* the ureteric outpouching and subsequent elongation and branching is severely affected (87-93). In conclusion, not only growth factors such as GDNF and its receptors are vital for normal renal development, but also the transcription factor, e.g. Pax-2.

Another group of growth factors essential for budding and tubulogenesis is the BMPs, members of the transforming growth factor β (TGF- β) superfamily (94-96). Experimental studies determining the role of BMP family members demonstrated a crucial function of BMPs throughout renal development: For example BMP7 mutant mice die within the first 24h due to renal failure, indicating that BMP7 plays an essential role in branching morphogenesis. It has been suggested that BMP7 may function as an inducer of metanephric mesenchyme, promoting survival (97-100). To conclude, BMP signaling plays a crucial role in early and late renal development, especially in induction of metanephric mesenchyme and regulation of the interaction between the tips of the ureteric bud and the metanephric mesenchyme.

(b) Extracellular matrix components and enzymes in renal development

In addition to transcription factors and growth factors, the ECM appears to play an underestimated role in branching morphogenesis (101, 102). Ureteric bud, for example,

INTRODUCTION

requires type I collagen and matrigel to form tubules in vitro (103). Furthermore, hyaluronic acid prevents cell death and promotes uretric bud branching morphogenesis in three-dimensional cell culture systems (104). Moreover, it has been shown that several integrins, such as $\alpha 3$, $\alpha 6$, $\beta 1$, and $\beta 4$ as well as laminin-5 are involved in branching processes of renal development (105). In line with these findings, *integrin $\alpha 3$* knockout mice exhibit decreased collecting ducts (106). Furthermore, ECM-metabolizing enzymes, such as metalloproteinases (MMP) 9 and MMP2 as well as their cognate inhibitor tissue inhibitor of metalloproteinases (TIMP) have been suggested to regulate branching processes (107-109).

1.3. Perinatal Programming

The term *Perinatal Programming* describes a process during a critical fetal and postnatal period of development, in which various influences, such as nutrition, hormones and inflammation, form permanent physiological processes and organ functions (110, 111). Therefore, disturbances and interruptions in these critical phases of development ultimately lead to permanent alterations of organ structure, and physiological processes with a severe impact on organ function throughout life (112).

The basic concept of *Perinatal Programming* is rooted in the hypothesis of the french biologist Lamarck in 1809: the phenotype could be induced by environmental “programming” (Lamarck JB: Philosophie zoologique. Paris, Dentu, 1809). In the 1960s Dubos et al. introduced the term of “biological Freudianism” (113), particularly referring to the intrauterine influence on the development of postnatal body weight. Günter Dörner at the Charité in Berlin merged these concepts of the last centuries and expanded them to a more fundamental developmental biological and medical ultimate principle. He did not only hypothesize, that alterations of the intrauterine environment has long-term effects in the offspring, but he also introduced the concept of “intrauterine Programming” (114, 115).

1.3.1. Intrauterine Growth Restriction: Definition and Incidence

Small for gestational age (SGA) infants are those, who are small in size for their gestational age, most commonly defined as a weight below the 10th percentile for the gestational age. Intrauterine growth restriction (IUGR) and SGA are often used interchangeably but the distinction is important. IUGR is the pathological form of SGA. Not all infants born SGA are pathologically growth restricted and, actually might be constitutionally small. IUGR refers to an intrauterine condition or insult, which impairs the growth of the fetus and ultimately leads

INTRODUCTION

to restriction of growth, impeding the fetus to reach its growth potential. IUGR incidence in newborns is between 3% and 7% of the pregnancies (116-119). The causes of IUGR are miscellaneous, but they can be subdivided in three major groups:

- (1) **maternal factors:** including poor nutritional status, alcohol and/or drug use, smoking, pulmonary, cardiovascular as well as renal disease, diabetes, and hypertension.
- (2) **Uteroplacental factors:** preeclampsia, uterine malformations, placental insufficiency.
- (3) **and fetal factors:** chromosomal abnormalities, and intrauterine infection.

Over decades the management of early postnatal nutrition of infants with IUGR has been discussed. Since the importance of postnatal environmental nutrition has been recognized for optimal neurological and cognitive development in low birth weight infants (120-122), the issue of whether early postnatal hyperalimentation and thereby catch-up growth might bear in turn impaired renal function, as well as metabolic syndrome is considerable important. Several epidemiological studies investigated the long-term consequences of small size at birth and give compelling evidence, that infants who were born with low birth weight and subsequently showed increased postnatal weight gain, namely catch-up growth, displayed a higher susceptibility for obesity, type 2 diabetes, insulin resistance, and cardiovascular disease (123-133). These controversial observations – low intrauterine growth velocity *versus* accelerated postnatal weight gain – led to the so called “mismatch theory”: though the physiological processes of an infant subsequent to IUGR are adapted to poor nutritional supply – *thrifty phenotype* – they are exposed to nutritional abundance (134). However, the impact of IUGR on catch-up growth, the role of early postnatal hyperalimentation itself, and the exact vulnerable window where increased postnatal weight gain has adverse effects on organ development and function still remains largely unknown.

1.3.2. Fetal Programming: The Barker Hypothesis

The term *fetal programming* reflects the hypothesis that temporary environmental influences during intrauterine development lead to permanent alterations of physiological processes later in life. This ground-breaking idea was coined by Barker et al. in the 1990s, describing the positive correlation between low birth weight at birth (<2.5kg) and the increased relative risk to develop features of metabolic syndrome, such as type II diabetes in adulthood (110, 127). These data imply that maternal nutritional fetal supply has long-term implications for the

INTRODUCTION

health of the fetus in adulthood. Further studies showed that low birth weight is also associated with an increased risk of hypertension (130, 133, 135, 136). This led ultimately to the so called “Fetal Origins Hypothesis”, which proposes that coronary heart disease, and the diseases related to it, originates from responses to undernutrition during fetal life and infancy. In line with these findings, he showed that the lower the birth weight, the higher the risk for coronary heart disease in later life (133). Barker and Hales combined these features of infants born with low birth weight to the so called *thrifty phenotype*. The *thrifty phenotype* hypothesis says that reduced fetal growth results from an adaptation of the fetus in an environment limited in its supply of nutrients. Such an infant is prepared for survival in an environment in which resources are likely to be short. In other words, the *thrifty phenotype* is considered as the capacity of the offspring to respond to environmental cues during early development.

1.3.3. Metabolic Programming

The prevalence of obesity in children is dramatically increasing in the last decades and the incidence of metabolic syndrome is emerging as a worldwide epidemic (137). The incidence of obesity has doubled for children 2 to 5 years of age, almost tripled for youth 6 to 19 years of age. In 2004, the World Health Organization (WHO) estimated that 22 million children under 5 years of age, and 10% of all children 5-17 years of age were overweight or obese, and predicted that childhood obesity will continue to increase in both developed and developing countries (138). Furthermore, there is an increase in the prevalence of pediatric type 2 diabetes in obese children (139-142).

Indeed, there is already no doubt, that food intake and food quality plays a vital role in the development of obesity. Pre- and postnatal nutritional stressors were delineated as central risk factors predisposing the individual to later increased features of metabolic syndrome (143-145). Over half century ago, first studies gave initial evidence, that nutrition during early postnatal life has long-lasting effects showing life-time changes in growth and body size subsequent to early abundant or restricted maternal milk in rodents (146). In the 90s, Barker and Hales coined the concept of *fetal programming* of diseases in adulthood (127). Plagemann et al. next extended this concept on postnatal events, such as nutritional factors and described this process as *metabolic programming* (111).

Metabolic programming describes a process whereby a nutritional stimulus during a vulnerable period of development has permanent effect on organ physiology and function. The idea of perinatal programming of diseases implies that an insult, acting during a narrow

INTRODUCTION

phase of sensitivity in the perinatal period of life induces permanent physiological alterations leading to diseases in adulthood. Since the vital relevance of postnatal environmental nutrition has been recognized over the last decades, numerous studies suggested that accelerated growth and weight gain in the early postnatal period bear the risk of long term impaired renal function, as well as in metabolic syndrome (143, 147-150). However, it still remains unclear, whether enhanced early postnatal nutrition of premature infants may either influence favourably the postnatal continuation of nephrogenesis or accelerate the progression toward renal insufficiency.

1.4. Intrauterine Growth Restriction and Organ-Specific Diseases

1.4.1. Intrauterine Growth Restriction and Lung Disease

The incidence of respiratory illness increased during the past decades (151). Asthma is the most common cause of chronic childhood disease in developed countries. Its prevalence has nearly doubled over the last 2 decades, putting a serious socioeconomic burden on the families (152). The pathomechanisms are based on the interaction between multiple genes and environmental factors (153). Prenatal influences, such as maternal smoking during gestation and intrauterine malnutrition of the fetus adversely affect later respiratory health (154-164). In accordance with these findings, epidemiological studies demonstrated an impairment of lung function with reduced forced expiratory volume (FEV₁) in young infants subsequent to IUGR (8). Interestingly, there is an increasing body of evidence that IUGR induces changes in the developing lung with a persisting impairment of pulmonary structure and function (10, 155, 165, 166). Few experimental studies have demonstrated morphometric pulmonary alterations and imbalance of ECM composition in lungs of animals subsequent to IUGR (167, 168). Furthermore, analysis of lung structure in growth restricted animals revealed an impaired development of the lung, accompanied by a delayed maturation of the surfactant system (10, 163). Moreover, several studies show that a severely perturbed metabolism of the key ECM components contributes to this structural disorder of the lung (167, 168) and thereby suggest a regulatory effect of IUGR on the production and metabolism of the ECM. Consistently, Joss-Moore et al. suggested a pivotal role of ECM molecules, such as elastic fibers in the pathomechanism of IUGR-associated lung disease (167).

Lung structure and function are already determined during early and late lung development (1-3, 5, 14). Interference with the developmental program of the lung during any of these phases

INTRODUCTION

may render the lung less effective in gas exchange or more susceptible to disease. However, the pathogenesis of IUGR-associated lung disease is largely unknown. There are two central processes potentially involved: (1) ECM and its maintenance during alveolarization is thought to play a pivotal role (167, 168). Disruption of critical signaling pathways that direct lung development may contribute to the altered lung structure subsequent to IUGR. (2) Inflammatory cytokines and their effect on the regulation of the composition and function of the ECM.

1.4.2. Intrauterine Growth Restriction and Renal disease

Low birth weight as a result of IUGR has been demonstrated to be directly associated with a rising risk to develop renal diseases in later life or to aggravate their course (169-173). Indeed, there are studies reporting a higher incidence of end-stage renal disease at adulthood in patients with former IUGR (174, 175). Moreover, numerous studies demonstrated a greater incidence of glomerular disease as well as complications and aggravation of nephrotic syndrome in children subsequent to IUGR (176-178). For example, children with IUGR and low birth weight were shown to be at higher risk to develop progressive glomerulosclerosis compared to children without IUGR (179). In line with these findings, another study demonstrated that IUGR is significantly associated with low-normal kidney function (creatinine clearance) (169).

These observations in humans were verified in several experimental animal studies of IUGR either induced by maternal low protein diet or by ligation of the uterine artery (173, 180-182). Furthermore, morphometric investigations give strong evidence, that IUGR impairs nephrogenesis and thereby leads to a reduction of nephron number after birth (182, 183). In line with these results, there is a strong epidemiological relationship between IUGR/low birth weight and adult hypertension (182, 184). In the late 80s, Brenner and Anderson coined the concept “reduction in nephron number” suggesting an inverse correlation between the total renal filtration surface area and the risk of arterial hypertension (185). What impairs nephrogenesis subsequent to IUGR? (1) increased inflammatory response (173, 180); (2) dysbalance of apoptotic processes (186); (3) deregulation of the renin-angiotensin-aldosterone system (RAAS) (187-189); and (4) secondary effects of features of metabolic syndrome, such as hyperglycemia (190). However, the underlying molecular mechanism of IUGR-associated renal diseases still remains unclear and the role of postnatal nutrition requires further elucidation to gain a broader understanding of the effects of IUGR on renal development and maturation.

1.4.3. Early Postnatal Hyperalimentation and Metabolic Programming

It is well known that obesity entails a high risk for pulmonary illness and chronic kidney disease (161, 191-193), independently of diabetes and hypertension (190, 194). These facts underline how obesity is a real threat not only for adults, but also for the health of children and adolescent (195, 196). Both kidney and lung are susceptible to weight gain and obesity-induced disease:

(1) Obesity-related glomerulopathy, a secondary form of focal-segmental glomerulosclerosis (FSGS), presents proteinuria and progressive renal dysfunction (197). Moreover, prenatal risk factors for obesity, such as being small for gestational age or born prematurity, in addition to imposing an additional risk of hypertension, and T2DM later in life, are also risk factors for reduced nephron mass and progression of kidney disease in childhood (174, 175, 182, 198-200). Few studies have addressed the question whether postnatal nutrition can influence nephrogenesis when it is prolonged postnatally (148, 149). Nephrogenesis is achieved prenatally in the human, most nephrons being formed between 28 and 34 weeks of gestation (76). After birth, postnatal maturation consists among other changes of increased glomerular size and tubular length. Postnatal alteration has been experimentally induced by postnatal dietary intervention, showing that, postnatally, ongoing nephrogenesis is influenced by nutrition (148, 149). Furthermore, hyperleptinemia in the obese patients can contribute to renal damage not only because of its profibrotic effects but also because it is a strong stimulus for sympathetic system (201-205). Leptin-mediated sympathetic stimulation could be a relevant player in obesity-related glomerulopathy.

(2) The process of alveolarization begins before birth and proceeds until early infancy (1). Environmental influences during this critical period of pulmonary development have long-term effects on pulmonary structure and function (9, 11, 166). It is intriguing though, that only a few studies have addressed the important question, whether early postnatal hyperalimentation programs lung structure and function (13, 206-208). The results are controversial: one study gives initial evidence, that adult forced expiratory volume in 1 second (FEV1) and forced vital capacity (FVC) are positively associated with weight gain in the first year of life (13, 208). Another study demonstrated that low birth weight and lower weight gain in early childhood correlate with modest reduction in adult lung function with lower diffusing capacity (13). In line with this study, Canoy D. et al. did not only show that

INTRODUCTION

birth weight is continuously associated with adult respiratory function but also that poor growth in early life may restrict normal lung development (209). In contrast to these findings, other studies gave strong evidence that weight gain in infancy is associated with impaired lung function and transient asthma symptoms (208, 210).

However, enhanced early postnatal hyperalimentation may either influence favourably the postnatal continuation of nephrogenesis and alveolarization. To date, the studies are controversial and the effect of early postnatal hyperalimentation remains still unclear.

1.5. Transforming Growth Factor β Signaling Pathway

1.5.1. Transforming Growth Factor β Superfamily and its Ligands

Transforming growth factor- β (TGF- β) superfamily comprises a large number of growth factors – more than 35 structurally-related cytokines – that exert pleiotropic effects on different cell-types. The different members of the TGF- β superfamily play a vital role in developmental processes, cellular differentiation, expression and remodeling of ECM, regulation of proliferation and apoptosis as well as modulation of the immune response. Almost all cell types synthesize TGF- β ; the active form of TGF- β is a 25 kDa dimer in which the two polypeptides interact via a disulfide bond and hydrophobic interactions. TGF- β is initially synthesized as an inactive propeptide precursors, and is then processed and secreted as inactive homodimers, noncovalently bound to a latency-associated peptide (LAP) (211, 212) (213). The inactive precursor molecule consists of: (1) N-terminal signal peptide that is required for secretion, (2) pro-region [called latency associated peptide or (LAP)], and (3) C-terminal region, which represents the mature TGF- β molecule subsequent to release from the pro-region by proteolytic cleavage. The latent form is activated extracellularly through proteolysis by numerous factors: thrombin, thrombospondin, plasmin, metalloproteases, retinoids, low pH, or reactive oxygen species (ROS) (212) . Moreover, the $\alpha\beta_6$ integrin-expressing cells also induce activation of TGF- β_1 (214).

There are three distinct TGF- β isoforms expressed in mammals: TGF- β_1 , TGF- β_2 , and TGF- β_3 , and they are not functionally redundant. In line with these argue, they are encoded by different genes, and exhibit diverse expression patterns *in vivo*. Interestingly, TGF- β_1 is

INTRODUCTION

selectively induced by oncogenes and early genes; in contrast the expression of the other isoforms is more developmentally and hormonally regulated (215, 216).

In particular, TGF- β 1 isoform is secreted by numerous cell types, such as, platelets and immune cells (21, 22, 217). In the lung, especially the fibroblasts and epithelial cells produce this cytokine. Moreover, TGF- β 1 has been shown to have a strong impact on lung development. Several studies have indicated that TGF- β signaling plays a critical and finely-tuned role in branching and alveolarization (2, 5, 16): TGF- β ligands inhibited airway branching *in vitro* (218, 219). Additional studies demonstrate that an abrogation of TGF- β signaling, by genetic down-regulation either of T β RII, or of Smad2, Smad3, or Smad4 enhances lung branching *in vitro* (31, 220). Consistent with these observations, overexpression of Smad7, which antagonizes TGF- β signaling, promoted lung branching *in vitro* (221, 222). However, a conditional overexpression of TGF- β 1 gene in the mouse lung in the postnatal period disrupted lung development (21, 26). Of interest, Smad3 deficiency in mice resulted in progressive airspace enlargement with age (Bonniaud et al., 2004)(32). These studies implicate, that TGF- β signaling is both a positive and a negative regulator of lung branching and alveolarization. Taken together, these data indicate that TGF- β plays a key role in lung development, as well as in the maintenance of pulmonary structure. Furthermore, TGF- β has an important role in diverse human pathologies, such as autoimmune and fibroproliferative diseases, affecting several organs like the kidney, lung and liver.

1.5.2. Transforming Growth Factor β Receptors: Classification and Structure

There are three types of TGF- β receptors:

- (1) TGF- β -receptor I (Tgfbr1; also called T β R-I)
- (2) TGF- β -receptor II (Tgfbr2; also called T β R-II)
- (3) and TGF- β -receptor III (Tgfbr3; also called T β R-III or betaglycan)

Structural and biochemical analyses have shown that they represent transmembrane serine/threonine kinases, which have the ability to associate in a homo- and heteromeric complex. Several studies have demonstrated the impact of both the type II and type I receptors as the signaling mediators. Moreover the type III receptor, is widely expressed in fetal and adult tissues, including mesenchymal, epithelial, neuronal and other cell types. The type III receptor binds all three TGF- β isoforms. Interestingly, recombinant expression of type III receptor does not only lead to the synthesis of a transmembrane protein, but also to a

INTRODUCTION

secreted protein – soluble betaglycan. As a consequence of its ability to bind TGF- β , the soluble type III receptor could competitively inhibit TGF- β -binding to the transmembrane receptors (211, 213, 223-225).

Endoglin is an accessory TGF- β -receptor, which is expressed in a limited set of cell types, primarily vascular endothelial cells and several hematopoietic cell types. Endoglin binds all three TGF- β isoforms: TGF- β 1 and - β 3 (211, 225, 226).

1.5.3. Transforming Growth Factor β Pathway: Intracellular Signaling

Intracellular TGF- β signaling is primarily mediated by Smad signaling molecules. The name Smad is derived from the founding members of this family, the *Drosophila melanogaster* protein MAD (mothers against decapentaplegic). The Smad family of transcription factors is composed of eight proteins: Smad1 through to Smad8 (224, 227). They are functionally subdivided in three groups:

1) Receptor-regulated Smads (R-Smads): Smad2 and Smad3

The R-Smads represent cytoplasmic effector molecules, which are receptor-associated. They are directly phosphorylated by the type I receptor kinases (211, 227, 228).

2) Common-partner Smad (Co-Smad): Smad4

The interaction between the R-Smads and various DNA-binding proteins is mediated by Smad4. Moreover, it plays a central role for the nuclear import of the R-Smads, and in the activation of gene transcription (211).

3) Inhibitory Smads (I-Smads): Smad6 and Smad7

The I-Smads are antagonistic Smads; they inhibit the TGF- β signaling cascade by associating with the activated type I receptor and thereby preventing the binding and activation of the R-Smads (224, 228).

TGF- β signaling is initiated by binding of TGF- β to the type II TGF- β receptor (T β RII), which subsequently forms a complex with the type I receptor [also called activin-like kinase (ALK)-5] or Acvrl1 (also called ALK-1). The type I receptor transmits signals within the cell via second-messenger R-Smad proteins, namely Smads 2 and 3. Moreover, transforming

INTRODUCTION

growth factor- β signaling is also regulated by the inhibitory Smads, Smad6 and Smad7, which antagonize TGF- β signaling. The phosphorylated and thereby activated R-Smads bind Smad 4 and are then translocated into the nucleus, where these R-Smads regulate gene transcription, and hence, cell function (211, 228) (figure2).

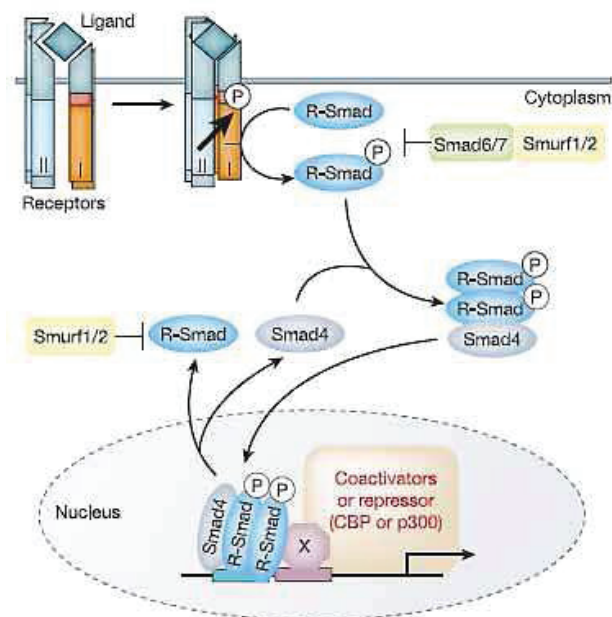


Figure 2: **Schematic diagram of the transforming growth factor- β signaling pathway from the cell membrane to the nucleus.** The arrows indicate signal flow. At the cell surface, the ligand binds to the type I and type II receptor complex, and induces phosphorylation of the GS segment (red) of the type I receptor. Consequently, receptor-regulated Smads (R-Smads) are phosphorylated at the C-terminal serine residues, which then form a complex with Smad4. This complex translocates into the nucleus to regulate the transcription of target genes, assisted by either co-activators or co-repressors. Both R-Smads and Smad4 shuttle between the nucleus and the cytoplasm. Smurf1, Smurf2, Smad6, and Smad7 function as inhibitors of the phosphorylation of the R-Smads [copyright permission is existent].

1.6. Leptin and Interleukin-6 signaling pathway

1.6.1. Leptin

Leptin is a 16-kDa protein, encoded by the *ob* gene, and mainly produced in adipocytes of white adipose tissue. Recent evidence has shown that placenta, skeletal muscle and possibly kidney are additional sites of leptin synthesis (229, 230). There is an accumulating body of

INTRODUCTION

evidence that leptin exerts as a multifunctional hormone diverse actions, extending beyond those involved in regulation of appetite and body weight. Some of these include proliferation, sympathetic nervous activation, wound healing, fibrosis, and inflammation (201-205). However, a more direct role for leptin in promoting renal pathophysiology via leptin receptors has arisen in the last years. Leptin stimulates the proliferation of cultured glomerular endothelial cells (201). Moreover, leptin increases type I collagen mRNA and protein production (204). Glomerular expression of type IV collagen was significantly enhanced in, and urinary protein excretion significantly increased leptin-treated rats (201).

1.6.2. Interleukin-6

Interleukin 6 (IL-6) was first described as a B-cell differentiation factor, which activates B-cells into immunoglobulin-producing cells. Consequently, it was initially named B-cell stimulatory factor 2 (B-cell stimulatory factor-2) (231). IL-6 is synthesized by numerous cell types, including immune cells (T-cells, B-cells, and monocytes), fibroblasts, endothelial cells, mesangial cells, and adipocytes and exerts a variety of biological functions (232). Interestingly, the IL-6 signaling cascade is involved in multiple physiological and pathological processes: (1) organ development (233), (2) inflammatory processes (234, 235), (3) growth and cell differentiation, (4) apoptosis, (5) pathogenesis of tumors, (6) bone and cartilage metabolism as well as rheumatoid arthritis, (7) lipid and glucose metabolism (232).

1.6.3. Intracellular Signaling of Leptin and Interleukin-6: Stat3 and Erk1/2 Signaling Pathway

Leptin acts through leptin receptor (ObR), which belongs to the interleukin 6 (IL-6) family of class 1 cytokine receptors. Five alternatively spliced isoforms of ObR with different lengths of C-termini have been identified in mice (236-238). Long form (ObRb) and short form (ObRa) are the most studied isoforms; only ObRb is fully capable of activating intracellular signaling (239-242) (figure3).

INTRODUCTION

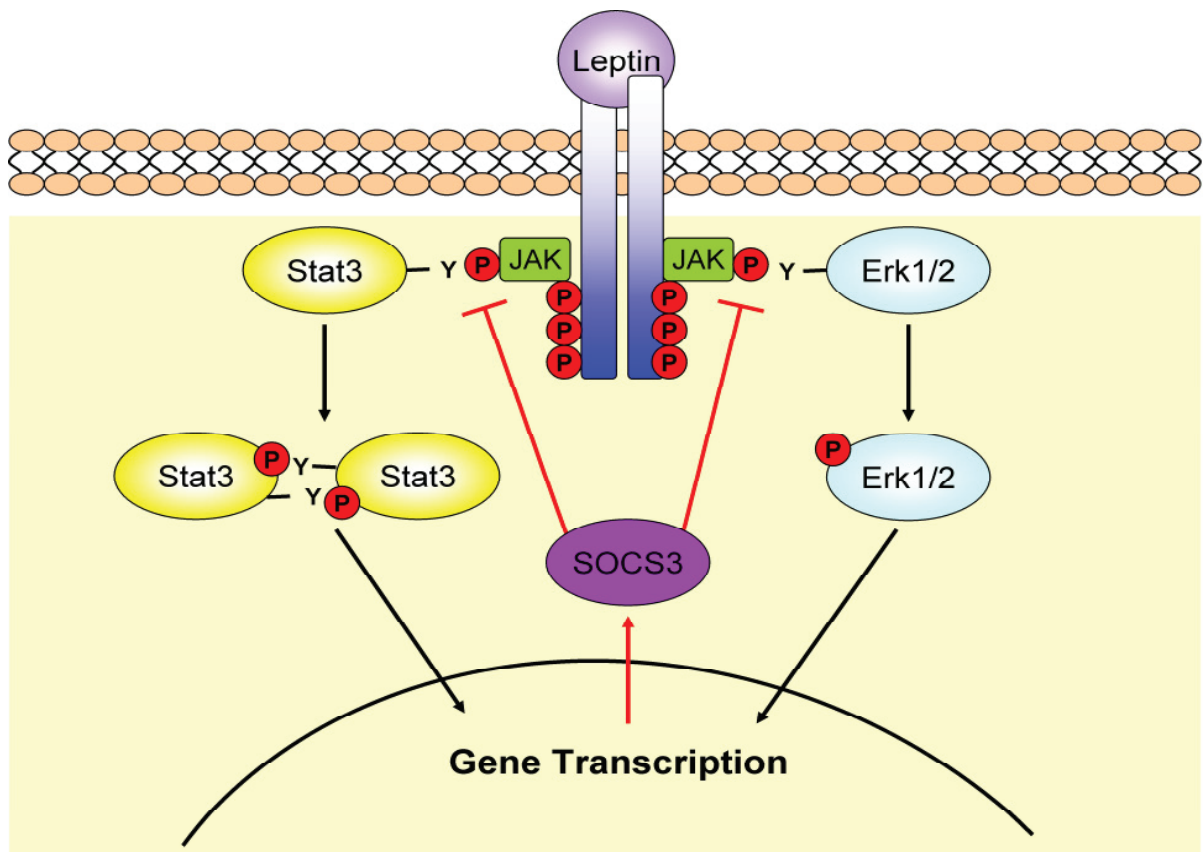


Figure 3: **Schematic diagram of the leptin signaling pathway:** leptin binds to the full length form of the leptin receptor (ObRb) and initiates thereby the janus-kinase (JAK)-mediated phosphorylation of three intracellular tyrosine residues of the receptor. This leads to the phosphorylation of signal transducer and activator of transcription (Stat) 3 molecules as well as extracellular-signal regulated kinase (Erk) 1/2. The activated Stat3 and Erk1/2 translocate to the nucleus and induce transcription of numerous target genes, notable among these suppressor of cytokine signaling (SOCS)3, which in turn negatively regulates the activation of Stat3 and Erk1/2, representing a negative feedback loop.

Interleukin-6 (IL-6) exerts its biological function via IL-6 receptor (IL-6R, also called IL-6R α , gp80, and CD126) and gp130 (also named IL-6R β , and CD130). IL-6R is essential for ligand binding, whereas the cytoplasmic domain of gp130 is the central mediator of intracellular signaling (243-246). Interestingly, gp130 initiates downstream signaling *via* an intrinsic kinase domain, but through various regions, which then associate with a non-receptor tyrosine kinase: Janus-kinase, also called JAK (232). Binding of IL-6 to the membrane-bound IL-6R induces a homodimerization with gp130 and thereby forming a functional receptor complex of IL-6, IL-6R, and gp130. In addition, the soluble IL-6R (sIL-6R), which lacks the intracytoplasmic domain, can also bind IL-6, and consequently form a complex with gp130 (IL-6 trans-signaling) (232, 247). Based on the fact, that membrane-bound gp130 is expressed ubiquitously, the IL-6-sIL-6R complex can bind to each cell type and thereby mediate IL-6

INTRODUCTION

function. However, gp130 is also circulating as soluble form (sgp130) and has the ability to bind IL-6-sIL-6R complex and thereby acting as a natural inhibitor of IL-6 signaling (248, 249) (figure4).

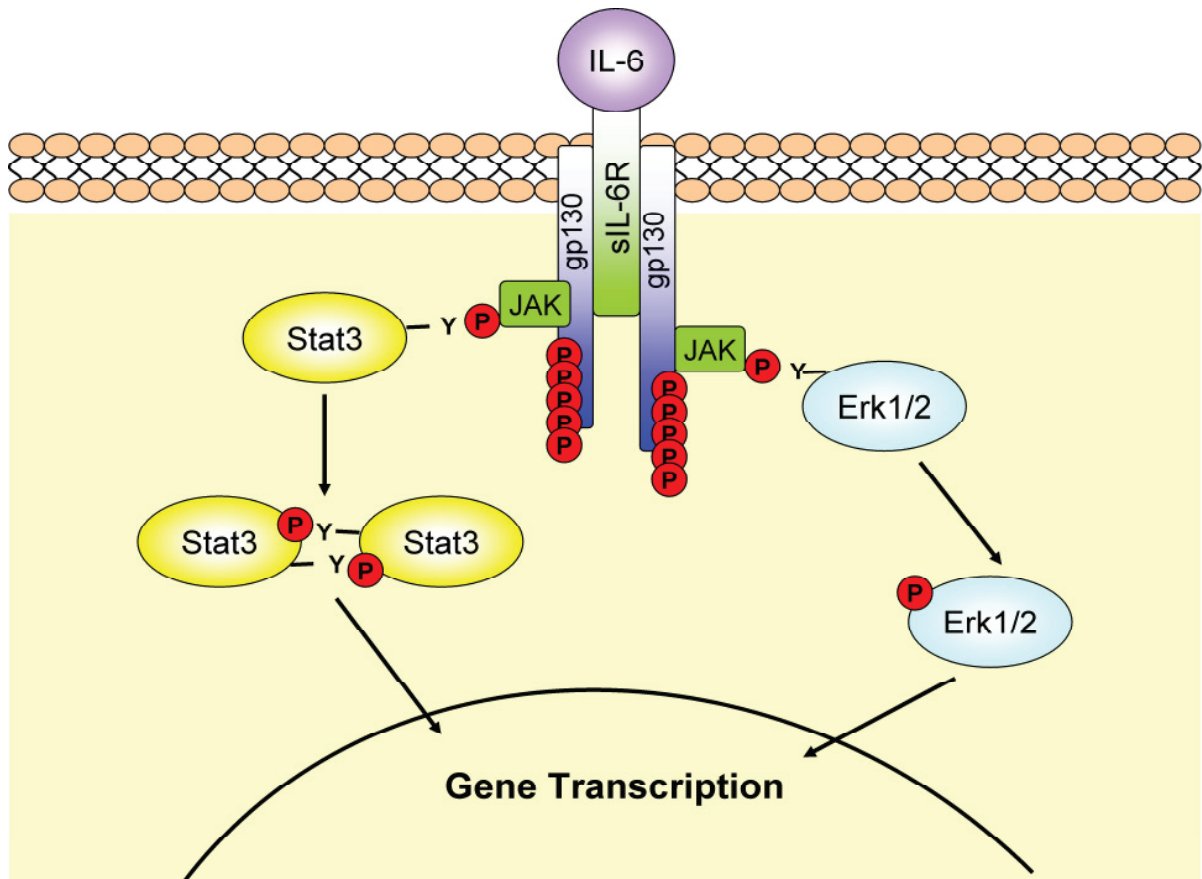


Figure 4: **Schematic diagram of the Interleukin (IL)-6 signaling pathway:** IL-6 binds to interleukin-6 receptor (IL-6R), which then forms a complex with the membran-bound glycoprotein (gp)130 and thereby initiates the janus-kinase (JAK)-mediated phosphorylation of the intracellular tyrosin residues of the receptor. This leads to the phosphorylation of signal transducer and activator of transcription (Stat) 3 molecules as well as extracellular-signal regulated kinase (Erk) 1/2. The activated Stat3 and Erk1/2 translocate to the nucleus and induces transcription of numerous target genes.

Moreover, gp130 is also transmits the intracellular signaling of other members of the IL-6 family, including LIF (leukaemia inhibitory factor), CNTF (ciliary neurotrophic factor), and IL-11 (232, 250).

INTRODUCTION

1.7. Aims

A growing body of evidence has suggested that nutritional stimuli play a pivotal role in organ development, and that both IUGR and early postnatal hyperalimentation are known to have an impact on perinatal programming of lung and renal function. However, the underlying mechanism of pulmonary and renal perinatal programming remains still unclear. It is the *overall goal* of this study to investigate the mechanisms perinatal programming of pulmonary and renal organ function. Therefore, we will test the hypothesis that inflammatory processes as well as the TGF- β signaling are regulated subsequent to nutritional stimuli in the perinatal period.

This idea will be explored in the following four sub-hypotheses:

1. TGF- β signaling is regulated in the lung and contributes to the impairment of lung function subsequent to IUGR.
2. Key inflammatory cytokines are increased in the lung subsequent to IUGR and early postnatal hyperalimentation.
3. Early postnatal hyperalimentation has an impact on renal function.
4. Leptin and interleukin-6 signaling in the play a role in the pathogenesis of renal disease subsequent to early postnatal hyperalimentation.

RESULTS

2. RESULTS

2.1. Inhibition of TGF- β signaling and decreased apoptosis in IUGR-associated lung disease in rats

Alejandro Alcázar MA, Morty RE, Lenzian L, Vohlen C, Oestreicher I, Plank C, Schneider H, Dötsch J. PLoS One, 2011

Intrauterine growth restriction is associated with impaired lung function in adulthood. It is unknown whether such impairment of lung function is linked to the transforming growth factor (TGF)- β system in the lung. Therefore, we investigated the effects of IUGR on lung function, expression of extracellular matrix (ECM) components and TGF- β signaling in rats. IUGR was induced in rats by isocaloric protein restriction during gestation. Lung function was assessed with direct plethysmography at postnatal day (P) 70. Pulmonary activity of the TGF- β system was determined at P1 and P70. TGF- β signaling was blocked *in vitro* using adenovirus-delivered Smad7.

At P70, respiratory airway compliance was significantly impaired after IUGR. These changes were accompanied by decreased expression of TGF- β 1 at P1 and P70 and a consistently dampened phosphorylation of Smad2 and Smad3. Furthermore, the mRNA expression levels of inhibitors of TGF- β signaling (Smad7 and Smurf2) were reduced, and the expression of TGF- β -regulated ECM components (e.g. collagen I) was decreased in the lungs of IUGR animals at P1; whereas elastin and tenascin N expression was significantly upregulated. *In vitro* inhibition of TGF- β signaling in NIH/3T3, MLE 12 and endothelial cells by adenovirus-delivered Smad7 demonstrated a direct effect on the expression of ECM components. Taken together, these data demonstrate a significant impact of IUGR on lung development and function and suggest that attenuated TGF- β signaling may contribute to the pathological processes of IUGR-associated lung disease.

Contribution to Publication I

Once I had formed the hypothesis and designed the experiments for this project, I established and validated successfully a new system for whole body plethysmography in rats. I next instructed Lisa Lenzian, who then conducted the experiments for P70 by herself as part of her MD-thesis. Furthermore, as it was in part a joined project of her and mine, she performed

RESULTS

the western blots and real-time RT-PCR for P1 as part of her MD-thesis, whereas I assessed these experiments for P70 and in addition the immunohistochemical stainings. Moreover, Dr. Rory Morty supported me greatly with the morphometric analyses. I designed and performed the western blots for apoptotic processes as well as the cell culture experiments using adenoviral Smad7 vector. I finally calculated the statistics, designed and wrote the manuscript. The manuscript was proofread by Prof. Dr. Holm Schneider, and Prof. Dr. Dötsch.

Table1

Primers and TaqMan probes were designed by **Miguel Angel Alejandro Alcazar**.

Figure1:

Physiological data of the animals and respiratory system compliance at P70 were assessed, and illustrated by Lisa Lenzian, whereas the morphometric analyses of the lung and the assessment of the mRNA expression of genes encoding surfactant proteins were performed by **Miguel Angel Alejandro Alcazar**.

Figure2, Figure3, Figure4, and Figure 5, and Figure6

The assessment of mRNA expression of extracellular matrix (ECM) proteins and modulators of the ECM as well as of the TGF- β signaling machinery and the activity of the TGF- β signaling in neonatal rat lungs (P1) was performed by Lisa Lenzian, whereas **Miguel Angel Alejandro Alcazar** assessed the same set of experiments for P70. In addition, **Miguel Angel Alejandro Alcazar** performed immunostaining for phosphorylated Smad2 and phosphorylated Smad3 at P70 as well as western blots for apoptotic processes at P1.

Figure7:

Miguel Angel Alejandro Alcazar explored the effects of the inhibition of intracellular TGF- β signaling by adenoviral Smad7 overexpression on the expression of ECM components *in vitro*.

RESULTS

2.2. Developmental Regulation of Inflammatory Cytokine-Mediated Stat3 Signaling: The Missing Link between Intrauterine Growth Restriction and Pulmonary Dysfunction?

Alejandro Alcazar MA, Ostreicher I, Appel S, Rother E, Vohlen C, Plank C, Dötsch J. J Mol Med, 2012

Intrauterine growth restriction (IUGR) is a risk factor for impairment of lung function in adolescence and adulthood. Inflammatory and proliferative processes linking IUGR and perturbed extracellular matrix (ECM) as an underlying mechanism have not been addressed so far. Therefore, in this study we aimed to investigate the developmental regulation of inflammatory and profibrotic processes in the lung subsequent to IUGR.

IUGR was induced in rats by isocaloric protein restriction during gestation. Lung function was assessed with direct plethysmography at postnatal day (P) 28 and P70. Lungs were obtained at P1, P42 and P70 for assessment of mRNA, protein expression, immunohistochemistry, and gelatinolytic activity.

Both, respiratory system resistance and compliance were impaired subsequent to IUGR at P28 and this impairment was even more pronounced at P70. In line with these results, the expression of ECM components and metabolizing enzymes was deregulated. The deposition of collagen was increased at P70. In addition, the expression of inflammatory cytokines and both the activity and the expression of target genes of Stat3 signaling were dynamically regulated, with unaltered or decreased expression at P1 and significantly increased expression at P70.

Taken together, these data give evidence for an age-dependent impairment of lung function as a result of a developmentally regulated increase of inflammatory and profibrotic processes subsequent to IUGR.

Contribution to Publication II

As I described in the “Contribution to Publication I” I established and validated successfully a new system for whole body plethysmography in rats. I next performed the lung function tests, including provocation of bronchoconstriction *via* inhalation of methacholine at P28, and after I instructed Lisa Lenzian she conducted the experiments for a later time point P70 by herself

RESULTS

as part of her MD-thesis. Furthermore, I formed the hypothesis and designed the experiments. Dr. med. Iris Östreicher assessed part of mRNA expression of inflammatory cytokines. Moreover, Christina Vohlen supported me greatly with the performance of western blot analyses. I finally calculated the statistics, designed and wrote the manuscript by myself. The manuscript was proofread by Dr. rer. nat. Sarah Appel, Dr. med. Eva Rother, PD Dr. med. Christian Plank, and Prof. Dr. Dötsch.

Table1

Primers and TaqMan probes were designed by a joint project of Iris Östreicher and **Miguel Angel Alejandro Alcazar**.

Figure1, Figure2

Physiological data of the mothers as well of the offspring were calculated and analysed by **Miguel Angel Alejandro Alcazar**. Respiratory function was assessed using whole body plethysmography by **Miguel Angel Alejandro Alcazar** at P28 and by Lisa Lenzian at P70.

Figure3, Figure4, Figure7

The expression of genes encoding adrenoceptor $\beta 1$ and $\beta 2$ as well as ECM molecules and modulators of the ECM was assessed by **Miguel Angel Alejandro Alcazar**.

Figure5, Figure6

The composition of the ECM as well as proliferation in the lung was analyzed by **Miguel Angel Alejandro Alcazar** using real-time PCR, western blots, gelatine zymographie as well as immunohistochemistry.

Figure7, Figure8

The expression of genes encoding inflammatory and profibrotic cytokines was assessed by Iris Östreicher and **Miguel Angel Alejandro Alcazar**. The western blots for Stat3 signaling were analyzed by **Miguel Angel Alejandro Alcazar**.

RESULTS

2.3. Persistent Changes within the Intrinsic Kidney-Associated NPY system and Tubular Function by Litter Size Reduction

Alejandro Alcázar MA, Boehler E, Amann K, Klaffenbach D, Hartner A, Allabauer I, Wagner L, von Hörsten S, Plank C, Dötsch J. *Nephrology Dialysis and Transplantation*, 2011. Intrauterine growth restriction (IUGR) is associated with an increased risk of renal diseases in adulthood. However, while low-birth-weight-infants often undergo accelerated postnatal growth, the impact of postnatal environmental factors such as nutrition and early postnatal stressors on renal development and function remains unclear. In this context, Neuropeptide Y (NPY) may act as a critical factor. NPY is a sympathetic coneurotransmitter involved in blood pressure regulation and tubular function. Yet, little is known about the expression and function of endogenous NPY in the kidney and the functional relevance for the transmission of persistent postnatal-induced effects.

IUGR was induced in Wistar rats by isocaloric protein restriction in pregnant dams. We reduced the litter size to 6 (LSR6) or 10 (LSR10) male neonates. To differentiate the effect of postnatal nutrition and stressors we additionally included home-cage-control (HCC) animals without any postnatal manipulation. Animals were sacrificed at day 70. Litter size reduction (LSR6) but not IUGR increased mRNA expression of endogenous NPY and downregulated the NPY-receptors Y1 and Y2. Furthermore dipeptidylpeptidase IV (DPPIV) – an enzyme that cleaves NPY – was decreased after litter size reduction (LSR). The expression and the phosphorylation of MAPKinase 42/44 (intracellular signalling pathway of the receptor Y1) were altered. An impaired renal function with pronounced kaliuresis and natriuresis was observed at day 70 after LSR. In conclusion, postnatal nutrition and stressors such as LSR lead to dysregulated signaling of NPY. These data demonstrate that factors in the early postnatal environment exert important changes in the tubular function, which may predispose to corresponding pathology.

Contribution to Publication III

In this project I designed the concept and established the experimental techniques, such as real-time RT-PCR, protein purification, western blotting as well immunohistochemistry. Once the mRNA extraction and the real-time RT-PCR were ready-to-use, I instructed Eva Böhler on the assessment of the expression of Neuropeptide Y (NPY), NPY-receptor 1 (Y1) and Y2,

RESULTS

which was part of her MD-thesis. Both Prof. Dr. Amann as well as Ida Allabauer supported me regarding immunohistochemical stainings and access to microscopy facilities. Moreover, Leona Wagner performed the DPPIV enzyme-activity assays. Furthermore, I assessed the physiological data, the parameters of renal function as well as the western blot analyses. I finally calculated the statistics, designed and wrote the manuscript. The manuscript was proofread by Dr. med. Daniela Klaffenbach, Prof. Dr. Stephan v. Hoersten, PD Dr. med. Christian Plank, and Prof. Dr. Dötsch.

Table1, Table2, Table3 and Figure1

Primers and TaqMan probes were designed as well as physiological data of animals were assessed using results of metabolic studies, weight and length of the animal by **Miguel Angel Alejandro Alcazar**.

Figure2, Figure3, Figure4, and Figure5

Localization of NPY, Y1 and Y2 receptor in the kidney using immunofluorescence was analyzed by **Miguel Angel Alejandro Alcazar** with the kind support of Prof. Dr. Amann's and Prof. Dr. v. Hörsten's lab. The Expression pattern of NPY, Y1 and Y2 was assessed by Eva Böhler, whereas the expression of mineral corticoid receptor (MCR), renin, angiotensin receptor (ATR) 1a, and ATR1b was assessed by **Miguel Angel Alejandro Alcazar** using real-time RT-PCR.

Figure 6, and Figure7

The DPPIV enzyme activity was assessed by Leona Wagner. The western blots for DPPIV, phosphorylated MAPK 42/44, total MAPK 42/44, and β -Actin were performed by **Miguel Angel Alejandro Alcazar**.

Figure8

The calculation of sodium and potassium excretion in the urine for 24h as well as excreted fraction of the filtered sodium (FeNa), and excreted fraction of the filtered potassium (FeK) were calculated and analyzed by **Miguel Angel Alejandro Alcazar**.

RESULTS

2.4. Early Postnatal Hyperalimentation Impairs Renal Function via SOCS-3 Mediated Renal Postreceptor Leptin Resistance

Alejandro Alcázar MA, Boehler E, Rother E, Amann K, Vohlen C, von Hörsten S, Plank C, Dötsch J. *Endocrinology*, 2012

Early postnatal hyperalimentation (pHA) has long-term implications for obesity and developing renal disease. Suppressor of cytokine signalling (SOCS) 3 inhibits phosphorylation of Stat3 and ERK1/2, and plays thereby a pivotal role in mediating leptin resistance. In addition, SOCS-3 is induced by both leptin and inflammatory cytokines. However, little is known about the intrinsic-renal leptin synthesis and function. Therefore, this study aims to elucidate the implications of early pHA on renal function and on the intrinsic-renal leptin signaling.

Early pHA in Wistar rats during lactation was induced by litter size reduction at birth either to 10 (LSR10) or 6 (LSR6), compared to home-cage-control (HCC) male rats. Assessment of renal function at postnatal day 70 (P70) revealed decreased glomerular filtration rate, and proteinuria after LSR6. In line with this impairment of renal function, renal inflammation and expression and deposition of ECM molecules, such as collagen I, were increased. Furthermore, renal expression of leptin and interleukin-6 was upregulated subsequent to LSR6. Interestingly, the phosphorylation of Stat3 and of Erk1/2 in the kidney, however, was decreased after LSR6, indicating postreceptor leptin resistance. In accordance, NPY gene-expression was downregulated. Moreover, SOCS-3 protein expression – a mediator of postreceptor leptin resistance – was strongly elevated and colocalized with NPY.

Thus, our findings do not only demonstrate impaired renal function and profibrotic processes, but also provide compelling evidence of a SOCS-3-mediated intrinsic-renal leptin resistance and concomitant upregulated NPY-expression as an underlying mechanism.

Contribution to Publication IV

Within this study I generated the hypothesis and the major aims as well as the designing of the experiments. I established the experimental techniques, such as real-time RT-PCR, protein purification, western blotting as well immunohistochemistry. Once I instructed Eva Böhler on western blot and immunohistochemistry, she performed the assessment of Stat3 expression, phosphorylation of Stat3, SOCS-3, and β -Actin as well as the localization and quantification

RESULTS

of collagen I by herself as part of her MD-thesis. In addition, she calculated the glomerular filtration rate as well as the proteinuria using the metabolic study, also as part of her MD-thesis. Prof. Dr. Amann supported me regarding immunohistochemical staining, assessment of indices of renal damage, and access to microscopy facilities. PD Dr. med. Christian Plank performed the measurement of blood pressure. I finally calculated the statistics, designed and wrote the manuscript. The manuscript was proofread by Prof. Dr. Stephan v. Hoersten, and Prof. Dr. Dötsch.

Table1, Figure1, and Figure2

Primers and TaqMan probes were designed as well as leptin ELISA, and analysis of data regarding indices of renal damage were conducted by **Miguel Angel Alejandro Alcazar**. Eva Böhler calculated the physiological data of animals, such as body weight, body length, and glomerular filtration rate as well as proteinuria and supported me with the ELISA. PD Dr. med. Christian Plank performed the measurements of blood pressure.

Figure3, and Figure4

The mRNA expression of ECM-metabolizing enzymes was assessed by **Miguel Angel Alejandro Alcazar**. The deposition of collagen I and collagen IV was quantified as a joined project of Eva Böhler (collagen I), and **Miguel Angel Alejandro Alcazar** (collagen IV). Accordingly, we also assessed the proliferation within the different compartment of the kidney using immunohistochemical staining of PCNA.

Figure5, and Figure6:

The measurements of the intrinsic renal, and adipose tissue mRNA expression of *leptin*, obese receptor b (*Obrb*), and *ObRa* was assessed by **Miguel Angel Alejandro Alcazar**. The localization of leptin within the kidney was analyzed by **Miguel Angel Alejandro Alcazar** with the kind support of Prof. Dr. Amann's lab. The western blots for phosphorylation of Stat3 was performed by Eva Böhler, whereas western blots of Erk1/2 signaling was conducted by **Miguel Angel Alejandro Alcazar**.

Figure7

The expression of proinflammatory cytokines as well as of genes encoding adrenoceptors- α 1a, α 1d, β 1, and β 2 was assessed by **Miguel Angel Alejandro Alcazar**.

RESULTS

Figure 8

The assessment of the expression of SOCS-3 was performed by Eva Böhler using western Blot analysis. The analysis of the renal localization and expression of SOCS-3 was conducted by **Miguel Angel Alejandre Alcazar**.

2.5. Hypothalamic JNK1 and IKK β Activation and Impaired Early Postnatal Glucose Metabolism after Maternal Perinatal High-Fat Feeding

Rother E, Kuschewski R, **Alejandre Alcazar MA**, Oberthuer A, Bae-Gartz I, Vohlen C, Roth B, Dötsch J. *Endocrinology*, 2012.

Hypothalamic inflammation has been demonstrated to be an important mechanism in the pathogenesis of obesity-induced type 2 diabetes mellitus. Feeding pregnant and lactating rodents a diet rich in saturated fatty acids has consistently been shown to predispose the offspring for the development of obesity and impaired glucose metabolism. However, hypothalamic inflammation in the offspring has not been addressed as a potential underlying mechanism. In this study, virgin female C57BL/6 mice received high-fat feeding starting at conception until weaning of the offspring at postnatal d 21. The offspring developed increased body weight, body fat content, and serum leptin concentrations during the nursing period. Analysis of hypothalamic tissue of the offspring at postnatal d 21 showed up-regulation of several members of the toll-like receptor 4 signaling cascade and subsequent activation of c-Jun N-terminal kinase 1 and I κ B kinase- β inflammatory pathways. Interestingly, glucose tolerance testing in the offspring revealed signs of impaired glucose tolerance along with increased hepatic expression of the key gluconeogenic enzyme phosphoenolpyruvate carboxykinase. In addition, significantly increased hepatic and pancreatic PGC1 α expression suggests a role for sympathetic innervation in mediating the effects of hypothalamic inflammation to the periphery. Taken together, our data indicate an important role for hypothalamic inflammation in the early pathogenesis of glucose intolerance after maternal perinatal high-fat feeding.

Contribution to Publication V

In this project I supported Dr. med. Eva Rother with the analyses of the western blots for JNK1/2 signaling, I κ B kinase- β inflammatory pathways as well as insulin-stimulated Akt

RESULTS

phosphorylation in liver. Furthermore I contributed to discussion of the results and to proofreading of the manuscript.

Figure1, and Figure2

The physiological data of the mothers and the offspring were assessed by Eva Rother and Ruth Kuschewski.

Figure3

Three-dimensional view of a principal component analysis performed with global gene expression information was assessed by André Oberthür.

Figure4, Figure5, and Figure6

The mRNA expression was assessed by Eva Rother using real-time RT-PCR. The western blot analysis was performed as a joined project by Eva Rother and **Miguel Angel Alejandro Alcazar**. Moreover the densitometric analyses were assessed by **Miguel Angel Alejandro Alcazar**.

2.6. Prevention of Early Postnatal Hyperalimentation Restores TGF- β /BMP Signaling in the Lung subsequent to IUGR

Alejandro Alcazar MA, Vohlen C, Rother E, Plank C, Dötsch J. (Manuscript in Preparation)

Intrauterine growth restriction (IUGR) is intimately linked with accelerated postnatal catch-up growth leading to an impairment of lung structure and function in infancy and adulthood. Deregulation of Transforming Growth Factor β (TGF- β) superfamily as well as inflammatory processes has been shown to play a vital role in the underlying mechanism of IUGR-associated lung disease. Interestingly, to date, the programming impact of early postnatal hyperalimentation (pHA) has not been addressed so far. Therefore, in this study we aimed to investigate whether prevention of pHA shield the lung from programming of vital mechanisms involved in IUGR-associated lung disease: (1) TGF- β /BMP pathway, (2) IL-6 signaling, and (3) extracellular matrix composition (ECM).

IUGR was induced in rats by isocaloric protein restriction during gestation. At birth litter size was either reduced to 6 to induce pHA (IUGR-pHA) or adjusted to 10 (IUGR). In addition, we examined a control group without IUGR and litter size adjustment to 10 (Co). Lungs were

RESULTS

obtained at P70 for assessment of mRNA and protein expression as well as gelatinolytic activity.

Analysis of lung homogenates demonstrated: (1) Prevention of pHA restores mRNA expression pattern of the TGF- β /BMP signaling machinery, namely *tgfr1*, *tgfr3*, *tgfr3*, *bmpr1a*, *bmpr1b*, *bmpr2*, *smad1*, *smad2*, *smad3*, *smad4*, and *smad5*). In line with these results we demonstrated a reconstitution of the TGF- β /BMP activity in the lungs of former IUGR rats using immunoblot of phosphorylated Smad2 and Smad3 (TGF- β system) as well as phosphorylated Smad1/5/8 (BMP system). Consistently, we showed a normalization of the expression of a target gene of the BMP system encoding inhibitor of differentiation 1 (*id1*). (2) Additionally, we observed massively increased expression of Interleukin-6 and its target gene AP-1 following pHA, while prevention of pHA completely normalized the expression of both. Moreover, we detected the same effect of prevention of pHA on IL-13, another proinflammatory cytokine, whereas the anti-inflammatory cytokine IL-10 was even upregulated preventing pHA subsequent to IUGR. (3) Finally, perturbed expression of collagen1 α 1, osteopontin, and metalloproteinases (MMP), important components of the pulmonary extracellular matrix, could be restored by prevention of pHA. Assessment of MMP-2 by gelatinase zymography showed a normalization of expression when pHA subsequent to IUGR is prevented.

In conclusion, these data give strong evidence that prevention of pHA subsequent to IUGR has massive effect on key regulatory mechanisms of IUGR-associated lung disease offering new avenues to expand this knowledge to develop innovative preventive strategies for perinatal programming of lung diseases later in life.

Contribution to Publication VI

Within this study I formed the hypothesis and designed the experiments. I designed the primers and established the RT-PCR. Once I instructed Christina Vohlen she supported me with the mRNA extraction as well as with the RT-PCR. The protein purification as well as the western blots were performed by myself. Moreover, Christina Vohlen supported me greatly with the assessment of gelatinase activity. I finally calculated the statistics, designed and wrote the manuscript by myself. The manuscript is now in preparation and is proofread by Dr. med. Eva Rother, PD Dr. med. Christian Plank, and Prof. Dr. Dötsch.

3. DISCUSSION

3.1. TGF- β and IUGR-associated Lung Disease¹

Intrauterine growth restriction (IUGR) does not only have an impact on lung morphometry, but also on lung structure in childhood. Only a few studies have addressed the underlying mechanism of IUGR-associated lung disease, most of them referring to the role of ECM, its composition as well as its metabolism. However, none so far has addressed lung function and the impact of TGF- β on the IUGR-associated lung disease. Therefore, I aimed to elucidate mechanistic clues linking TGF- β signaling and changes in pulmonary structure and function subsequent to IUGR

Our data demonstrate that IUGR in rats leads to a reduced dynamic compliance and increased respiratory system resistance later in life. This is in line with human studies demonstrating an impairment of lung function with decreased forced expiratory volume (FEV) in former IUGR infants (8). In accordance with this functional impairment, morphometric analysis at P70 revealed a increased alveolar tissue/alveolarization, assessed by measurement of a decreased mean linear intercept (MLI) after IUGR. These results are in contrast to previously reported morphometric lung analyses subsequent to IUGR demonstrating an impaired alveolarization (10, 165). However, those previous studies differ from our in various points: (1) species, (2) induction of IUGR and (3) catch up growth.

Extracellular matrix components are essential for forming alveoli and determine thereby lung function. Interestingly, the expression analysis revealed a clear deregulation of both ECM components, such as elastin, and tenascin as well as ECM regulators, such as matrix metalloproteinases-2 (MMP-2) and tissue inhibitor of metalloproteinases-2 (TIMP-2). How is ECM production and metabolism regulated during lung development subsequent to IUGR? TGF- β signaling is known to regulate key cell proliferative and migratory pathways and is active during late lung development (11, 251-253). Both over-expression and inhibition of TGF- β have been shown to impact alveolarization: rodents over-expressing TGF- β exhibited defective alveolarization (21, 26), including reduced numbers of alveoli; inhibition of TGF- β signaling in mice by genetic ablation of Smad3, or Smad3 deficiency, resulted in progressive airspace enlargement with age (Bonniaud et al., 2004)(32).

¹ This section of the discussion is predominantly extracted of the publication of Alejandro-Alcazar et al., PLoS One, 2011

DISCUSSION

In line with the altered alveolar structure in former IUGR rats, we demonstrate in these lungs that IUGR decreases pulmonary TGF- β signaling persistently. TGF- β 1 mRNA and protein levels were reduced immediately after birth and at P70. In accordance, the activation of the intracellular signaling, assessed by phosphorylation of both Smad2 and Smad3 is significantly derogated at both P1 and P70 in the rat lung. Based on the fact that TGF- β positively regulates ECM components, we demonstrated that the damped Smad2 and Smad3 activation is accompanied by reduced expression of genes encoding collagen I, collagen III, and fibrillin mRNA. Moreover, in animals of arrest of alveolarization MMP-2 is decreased and TIMP-1 is increased (Hosford et al., 2004, Dik et al., 2001). In contrast to these findings, we show in our study an increment of alveolar tissue and opposing regulation of MMP-2 and TIMP-1. Taken together, this study gives strong evidence that IUGR leads to an inhibition of the TGF- β signaling and consistently to a decreased expression of TGF- β -regulated ECM components.

In addition to the *in vivo* study, we investigated *in vitro* the impact of an inhibition of the TGF- β activity by adenoviral Smad7 on mRNA expression of previously named TGF- β -regulated ECM molecules. Interestingly, we detected distinct effects depending on the cell type used, confirming that it is essential to differentiate between the cell types of the compartments of the lung. While an inhibition of TGF- β signaling led to a tremendous upregulation of elastin and tenascin N in alveolar epithelial cells (MLE-12), the gene expression of these molecules was either unaffected in fibroblasts (NIH/3T3) or even down-regulated in murine endothelial cells. Moreover, we observed a marked effect of the inhibition of the TGF- β signaling on ECM-metabolizing enzymes: MMP-2 as well as TIMP-2 were dramatically decreased in NIH/3T3, whereas the expression of MMP-9 was unchanged and even increased in MLE-12. In summary, these data demonstrate that the expression of genes encoding ECM components is regulated by an inhibition of the TGF- β signaling. In addition, these results suggest that there is a causal link between the inhibited TGF- β activity in lungs and the perturbed ECM as well as the altered pulmonary structure subsequent to IUGR.

Despite regulation of ECM composition and metabolism, TGF- β signaling has further vital functions in the process of alveolarization, such as proliferation and cell differentiation of type II pneumocytes (254, 255). Our study shows that in lungs of IUGR rats the decreased activation of the TGF- β system is accompanied by reduced expression and cleavage of caspase-3 and consistently by reduced cleavage of Poly(ADP-ribose)-Polymerase 1 (PARP). These findings indicate disturbed apoptotic processes. Furthermore, these results are endorsed

DISCUSSION

by the fact that caspase-3 is a downstream molecule of the TGF- β system (256), whereby TGF- β signaling has potent antiproliferative and pro-apoptotic effects on epithelial cells (251, 252, 257, 258).

Interestingly, in our study the mRNA expression of *tgfr3* is significantly upregulated in IUGR lungs at P1. Based on the fact that the soluble type III receptor could competitively inhibit TGF- β binding to the transmembrane receptors (211, 224-226), an increased expression of *tgfr3* could have additional inhibitory effect on the TGF- β signaling subsequent to IUGR and thereby contribute to the observed altered pulmonary structure. In addition, another group postulates that TGF- β receptor III (T β RIII) could act as a protective factor in apoptotic processes in cardiac fibroblasts by negative regulation and inhibition of TGF- β signaling (259).

In conclusion, the data presented here suggest that IUGR affects lung structure and lung function by at least two functional consequences: 1) IUGR attenuates TGF- β signaling after IUGR which leads to a dysregulated expression of ECM and ECM-remodeling components, and 2) IUGR decreases apoptosis in the lung. These mechanisms significantly contribute to the altered lung development and impaired lung function after IUGR. The amenability of these pathways to genetic and pharmacological manipulation could provide alternative avenues for the therapy of IUGR-associated lung disease.

3.2. Inflammatory Response in the Lung Subsequent to IUGR and Early Postnatal Hyperalimentation²

We demonstrated that IUGR decreases the activity of TGF- β signaling in the lung subsequent to IUGR. Furthermore, these findings were accompanied by perturbed expression of key molecules of the ECM as well as decreased apoptosis in the lung and thereby contributing to the pathomechanisms of IUGR-associated lung disease. Interestingly, TGF- β does not only regulate ECM and apoptosis, but has also anti-inflammatory function in the lung. However, the underlying molecular mechanisms of IUGR-associated lung disease still remain unclear. It is intriguing though, that the impact of pulmonary inflammation as a potential link between IUGR

² This section of the discussion is predominantly extracted of the publication of Alejandre-Alcazar et al., Journal of Molecular Medicine, 2012

DISCUSSION

and pulmonary disease has not been addressed to date. Therefore, we aimed to explore the inflammatory processes as well as ECM over time, starting at P1 and terminating at P70.

In line with human studies as well as animal studies (8, 260), we show increased airway hyperresponsiveness in former IUGR rats. Based on the fact, that enhanced deposition and a deregulated expression of ECM is associated with obstructive lung disease (261, 262), as well as ECM composition in the lung is regulated by IUGR, we investigated the expression of ECM components and ECM-metabolizing enzymes subsequent to IUGR over time using real-time PCR, western blot, immunohistochemistry and gelatine zymograph. Analyses of the results revealed an interesting time-dependent pattern: at P1 we detected a decreased production of ECM molecules, such as collagen III and fibrillin, whereas the expression increased steadily over time with a significant increment at P70. Interestingly, not only the gene expression of ECM components was increased, but there was also a striking increment of deposition of collagen I α in the different compartments of the lung at P70, indicating profibrotic processes. These results are in line with experimental studies of Maritz et al. (10, 165), giving strong evidence of a persistently thicker blood-air barrier and thicker septa in lungs subsequent IUGR.

The ECM is continuously metabolized and remodelled by a variety of proteases, notable among them the matrix-metalloproteinases (MMP) and their cognate inhibitors, tissue inhibitor of metalloproteinases (TIMP). Both of them are strongly expressed in rodents during lung development (263) and also in fibrotic processes (264) indicating thereby a pivotal role of matrix remodelling in the lung. In our study, we demonstrate that IUGR decreased expression of pro-MMP-2 at P70, assessed by gelatine zymography. In line with this deregulation, we detected a significantly increased expression of TIMP-1 and TIMP-2 at P70. Both findings – decreased synthesis of MMP-2 and increased expression of its inhibitors – indicate a perturbed ECM metabolism. Interestingly, an augmented deposition of collagen I α in the lung was detected by immunohistochemical analyses at the same time. To sum up, our data collectively suggest that IUGR swing the balance in favour of interstitial ECM deposition preventing thereby turnover of ECM components in the lung.

Based on the fact, that fibrotic processes are not only characterized by increased deposition of ECM components, but also by increased proliferative processes, we next determined whether proliferation is regulated in lungs at P70 subsequent to IUGR. The gene expression p21 as well as the synthesis of proliferating cell nuclear antigen (PCNA) were increased at P70. Several studies report the impact of p21 on the regulation of cell cycle and cell ageing/senescence by inhibiting the activity of cyclin-dependent kinases (265). In line with the pronounced

DISCUSSION

proliferative state in IUGR-lungs at P70, our group demonstrated that rats following IUGR exhibit an increased amount of alveolar tissue and a dampened apoptosis. Thus, the findings we describe in both studies give a strong body of evidence that the balance between apoptosis and proliferation is perturbed and proliferation is favoured the more development and age proceed.

It is intriguing that inflammatory response over time as a potential underlying molecular mechanism of perturbed tissue remodeling and subsequent fibrosis in IUGR-animals has not been addressed to date. Strikingly, this study clearly shows a continuously increasing expression of inflammatory cytokines, such as IL-6, IL-13 and plasminogen activator inhibitor (PAI-1), starting being markedly decreased at P1 and significantly upregulated at later time points (P42 and P70). There are only a few studies giving initial evidence of fibrosis and inflammation in other organs subsequent to IUGR (173) and the potential role of IL-6 in the pathomechanism (266). For example, it has been shown, that IUGR aggravates the course of thy1-glomerulonephritis. The kidneys presented clear features of renal inflammation and fibrosis (173): (1) upregulated renal expression of IL-6, PAI-1 and monocyte chemoattractant protein-1 (MCP-1), and (2) augmented deposition of ECM components. Inflammatory cytokines, such as IL-6, does not only mediate inflammation and subepithelial fibrosis with collagen deposition (267), but does also play a pivotal role in lung development. There is strong evidence, that IL-6 induces catch-up growth of hypoplastic lungs (233). Interestingly, in our study, the expression of IL-6 is significantly downregulated at the transition from saccular to alveolar phase at P1 – a critical and vulnerable period in lung development – and could thereby contribute to the deregulation of lung morphogenesis subsequent to IUGR. At P42 and P70, however, the expression of IL-6 is reversed: not only the expression of IL-6, but also the expression of other cytokines, such as IL-13, PAI-1 and tumor necrosis factor (TNF)- α is significantly increased. In conclusion, our data suggest three roles of IL-6 in the lungs of former IUGR rats with postnatal catch-up growth: (1) a pivotal role during lung morphogenesis at the early stage of life (P1); (2) and inducer of catch-up growth of the lung; and finally (3) a pro-inflammatory and profibrotic function at P70. Therefore IL-6 may be a link between IUGR and the observed lung disease in former IUGR rats.

Other central cytokines, markedly regulated in lungs subsequent to IUGR are IL-13 and PAI-1, both of them shown to promote fibrosis and inflammation. Zhu and colleagues (268) demonstrated a strong impact of IL-13 in the pathogenesis of an asthmatic phenotype. This cytokine was associated with mononuclear inflammation, subepithelial fibrosis, and airway

DISCUSSION

obstruction. In addition, PAI-1 and the plasminogen system inhibit MMPs and thereby prevents degradation of ECM (269). Moreover, it has been demonstrated that PAI-1-deficient mice are protected from bleomycin-induced pulmonary fibrosis (270).

Previous studies of our group showed that IL-6 was the cytokine with the most striking increment in gene expression subsequent to either IUGR (173). Interestingly, IL-6 is also strongly elevated in the present study. However, the intracellular signaling of IL-6 via Stat3 has not been addressed so far in lungs subsequent to IUGR and catch-up growth. Therefore, we analyzed the activity of Stat3 signaling over time, starting at P1 and terminating at P70, using western blot technique. In accordance to the IL-6 expression, the analysis of Stat3 phosphorylation revealed a significant deregulation. Strikingly, we detected an augmentation in phosphorylation over time, starting with no changes at P1 and terminating with a significant increment on phosphorylation compared to the control group at P70. In accordance to the significantly increased activity of Stat3 at P70, we detected an elevated gene expression of the Stat3 target genes encoding TIMP-1 and activator protein (AP-1).

In this study, we demonstrate that the increment of inflammatory response is paralleled by elevated expression and deposition of ECM components. In conclusion, these findings suggest that inflammation may be a potential underlying mechanism of the profibrotic pulmonary processes observed in lungs subsequent to IUGR.

It will be promising to determine the effect of an anti-inflammatory therapy on the development of IUGR-associated lung diseases in further studies in order to address the question whether such treatment strategies may help to prevent the onset of pulmonary damage and improve long term lung function following IUGR.

In conclusion, the present study shows that IUGR with catch-up growth leads to a dynamic upregulation of inflammatory cytokines in the lung and subsequent activation of intracellular Stat3 signaling. These pro-inflammatory processes could contribute to a profibrotic remodeling of ECM in the lung over time. Thus, our study does not only provide evidence to gain a broader understanding of IUGR in infants, but also elucidates the pathomechanistic aspects of IUGR-associated lung disease.

3.3. Impact of Leptin and Interleukin-6 Signaling in the Kidney Subsequent to Early Postnatal Hyperalimentation³

As described under 3.2. IUGR with subsequent catch-up growth leads to impaired pulmonary function, in particular to an airway hyperresponsiveness in later life. Focussing on the underlying molecular mechanism, we deciphered a vital role of an enhanced inflammatory response as well as profibrotic processes. However, the impact of early postnatal hyperalimentation (early pHA) as well as the question whether these effects are lung-specific remain poorly understood. Therefore, we next tested the hypothesis, that early postnatal hyperalimentation induced by litter size reduction leads to a deregulation of inflammatory response and ultimately to an impairment of renal function.

Interestingly, clinical studies support these idea demonstrating elevated serum inflammatory markers in overweight children and adolescents (271), as well as in patients with CKD (272). Furthermore, there is arising evidence for obesity-related nephropathy in infant, adolescent and adult humans (273) (110) (198, 199). In accordance to these findings in humans, we demonstrated in our study an impairment of both glomerular and tubular function in adult rats at P70 subsequent to early pHA. In particular, the animals exhibited the following impairment of renal function: (1) decreased glomerular filtration rate, (2) proteinuria, (3) increased fractional sodium excretion, and (4) increased fractional potassium excretion. Note, that this impaired glomerular and tubular function was not accompanied by a metabolic syndrome. Several studies support our findings by giving evidence that obese individuals often develop renal dysfunction before the occurrence of diabetes and severe hypertension (200, 274).

Adipose tissue-secreted adipocytokines, such as IL-6 and PAI-1 exert numerous inflammatory and atherosclerotic effects: (1) increase of sympathetic activity, (2) contribution to insulin resistance as well as hypertension, and (4) impairment of renal function. Moreover, there are also peptide hormones, such as leptin, closely linked to obesity-related diseases (275). Interestingly, there are several studies demonstrating not only an adipose-tissue specific but also an intrinsic renal synthesis (230) and function of leptin (201, 202, 229). Leptin exerts a variety of biological functions, notable among these profibrotic, proliferative effects (204, 229), and stimulation of sympathetic nervous system (203). In the present study, leptin plasma levels were not significant elevated in the group following early pHA. However, the intrinsic

³ This section of the discussion is predominantly extracted of the publication of Alejandro-Alcazar et al., *Endocrinology*, 2012

DISCUSSION

renal expression of leptin and its receptor (obRb) is strikingly upregulated after early pHA. Thus, intrinsic renal leptin could exhibit an auto- and paracrine effect, independent of circulating leptin secreted by adipose tissue. Furthermore, we detected an increased expression of IL-6 in the kidney of rats subsequent to early pHA.

Both IL-6 and leptin regulate various functions within the kidney, such as renal cell proliferation (201, 205), differentiation, and production of components and metabolizing enzymes of the ECM (229, 276-278). In accordance, our study shows that an elevated expression of IL-6 and leptin goes along with perturbed ECM deposition and metabolism. Specifically, we demonstrate a decreased expression of ECM-metabolizing enzymes (TIMP-1 and TIMP-2) and increased deposition of collagen I and collagen IV in the renal interstitium and glomeruli.

The effects of IL-6 as well as of leptin are both mediated *via* Stat3 and Erk1/2 signaling pathway. Interestingly, the target genes of these signaling pathways, such as TIMP-1, TIMP-2 (279, 280) and anti-inflammatory cytokines as IL-10 (281) are markedly downregulated in kidney homogenates subsequent to early pHA, whereas the sympathetic co-neurotransmitter Neurotransmitter (NPY) is strikingly upregulated (282, 283). These findings suggest an inhibition of the Stat3 and Erk1/2 signaling and are indeed in contrast to the detected elevated levels of IL-6 and leptin in the kidneys following early pHA. To gain a better understanding of these initially controversially data, we performed western blot analysis to determine the phosphorylation of Stat3 as well as of Erk1/2. These analyses revealed a strong inhibition of both signaling pathways subsequent to early pHA. In conclusion, the elevated intrinsic-renal specific leptin expression combined with an inhibition of Stat3 and Erk1/2 signaling as well as the increased expression of NPY indicates a peripheral leptin resistance subsequent to pHA.

Neuropeptide Y does not only have orexigenic function regulating energy homeostasis, but does also have direct proinflammatory and renal tubular function affecting natriuresis and kaliuresis via NPY-receptors Y1 and Y2 (284, 285). Thus, our study suggests that NPY and the resulting neuro-immune interaction could enhance the inflammatory response after early pHA and thereby contribute to the obesity-related nephropathy. Further experiments showed a significant renal downregulation of the NPY-receptor 1 (Y1) and Y2 following early pHA. But how does an increased renal NPY expression exert an inflammatory effect *via* a decreased expression Y1 receptor? The inflammatory effects of NPY are predominantly mediated *via* Y1-receptor, which is present on the surface of macrophages and granulocytes (285-287).

DISCUSSION

Therefore, the renal-specific Y1-receptors might not be essential for the NPY-mediated inflammatory effect on renal tissue, but the Y1 receptors of both granulocytes and/or macrophages.

How is intrinsic renal leptin resistance mediated without systemic hyperleptinemia and an underlying metabolic syndrome? There is initial evidence of an obesity-induced leptin-independent leptin resistance (288). The underlying mechanisms are controversially discussed: (1) endoplasmic reticulum stress-associated leptin resistance (289), and (2) inflammation (IL-6) and therefore postreceptor-mediated leptin resistance (278, 290). Suppressor of cytokine signaling 3 (SOCS-3) is induced by phosphorylated Stat3 *via* IL-6. Interestingly, SOCS-3 – inhibitor of Stat3 and Erk 1/2 phosphorylation – represents endogenous negative feedback mechanism of Stat3 signaling and is thereby thought to be causal for postreceptor leptin resistance (290). Therefore, we explored the SOCS-3 localization and expression in kidney. First, we determined that SOCS-3 is strikingly upregulated subsequent to pHA. Interestingly, we did not detect SOCS-3 in the glomeruli. Consequently, based on the fact, that Stat3 and Erk1/2 signaling are not inhibited by SOCS-3 in the glomeruli, both leptin as well as IL-6 can exert its glomerular proliferative effect subsequent to early pHA. This idea is supported by Rodrigues AL et al. (282) who demonstrated that pHA leads to a higher SOCS3 expression in the hypothalamus. However, Gomez-Guerrero et al. (291) give initial evidence that SOCS-3 reduces renal lesions in an animal model of diabetic nephropathy and improves thereby renal function in diabetic rodents. At first glance these results are in contrast to our study, but, interestingly, SOCS-3 was not just localized in the interstitial compartment of diabetic kidneys, but also in the glomeruli. These facts indicate that the underlying pathomechanism of hyperglycemia-induced renal damage is distinct to the one to pHA.

Obesity and early pHA disrupt critical signaling pathway which have a strong regulatory impact on numerous biological function, such as cell proliferation, ECM composition, and renal function. There are numerous underlying mechanisms discussed: 1) adipocytokines (IL-6, PAI-1) directly induce renal cell proliferation and fibrotic processes. 2) hyperleptinemia due to obesity and pHA stimulate sympathetic activity and thereby contributes to renal damage and 3) hyperleptinemia-independent intrinsic renal leptin resistance leads to increased expression of NPY and enhances proinflammatory processes. Furthermore, we demonstrate in our study an alteration of the NPY-System: we detected an increased expression of NPY and a decreased expression of its receptors Y1 and Y2 subsequent to pHA, potentially indicating

DISCUSSION

an increased sympathetic activity. In line with the deregulation of NPY we observed in our study a downregulation of adrenoceptors $\alpha 1a$ and $\alpha 1d$ following early pHA, whereas adrenoceptor $\beta 1$ and $\beta 2$ were significantly upregulated, supporting the idea of an increased activity of the sympathetic system after pHA.

To sum up, early pHA contributes to impaired renal function in later life. This study presents evidence for (1) a role of SOCS-3 in mediating postreceptor leptin resistance, and (2) subsequent regulation of sympathetic activity (NPY) and inflammatory response in the underlying pathomechanism of pHA-induced nephropathy.

In conclusion, this study gives an accumulating body of evidence, that the early postnatal period and the environmental influence, in particular nutrition has a dramatic impact not just on weight gain, but also on organ-specific inflammatory response and ultimately on organ function. A more profound understanding of the underlying mechanistic aspects of early postnatal hyperalimentation will ultimately allow defining more effective preventional and therapeutic strategies of nephropathy in childhood and beyond.

REFERENCES

4. REFERENCES

1. **Copland I, Post M** 2004 Lung development and fetal lung growth. *Paediatr Respir Rev* 5 Suppl A:S259-264
2. **Roth-Kleiner M, Post M** 2005 Similarities and dissimilarities of branching and septation during lung development. *Pediatr Pulmonol* 40:113-134
3. **Roth-Kleiner M, Post M** 2003 Genetic control of lung development. *Biol Neonate* 84:83-88
4. **Schachtner SK, Wang Y, Scott Baldwin H** 2000 Qualitative and quantitative analysis of embryonic pulmonary vessel formation. *Am J Respir Cell Mol Biol* 22:157-165
5. **Jankov RP, Keith Tanswell A** 2004 Growth factors, postnatal lung growth and bronchopulmonary dysplasia. *Paediatr Respir Rev* 5 Suppl A:S265-275
6. **Warburton D, Bellusci S** 2004 The molecular genetics of lung morphogenesis and injury repair. *Paediatr Respir Rev* 5 Suppl A:S283-287
7. **Cardoso WV** 2001 Molecular regulation of lung development. *Annu Rev Physiol* 63:471-494
8. **Kotecha SJ, Watkins WJ, Heron J, Henderson J, Dunstan FD, Kotecha S** 2010 Spirometric lung function in school-age children: effect of intrauterine growth retardation and catch-up growth. *Am J Respir Crit Care Med* 181:969-974
9. **Joss-Moore LA, Lane RH** 2009 The developmental origins of adult disease. *Curr Opin Pediatr* 21:230-234
10. **Maritz GS, Cock ML, Louey S, Suzuki K, Harding R** 2004 Fetal growth restriction has long-term effects on postnatal lung structure in sheep. *Pediatr Res* 55:287-295
11. **Alejandre-Alcazar MA, Kwapiszewska G, Reiss I, Amarie OV, Marsh LM, Sevilla-Perez J, Wygrecka M, Eul B, Kobrich S, Hesse M, Schermuly RT, Seeger W, Eickelberg O, Morty RE** 2007 Hyperoxia modulates TGF-beta/BMP signaling in a mouse model of bronchopulmonary dysplasia. *Am J Physiol Lung Cell Mol Physiol* 292:L537-549
12. **Bland RD** 2005 Neonatal chronic lung disease in the post-surfactant era. *Biol Neonate* 88:181-191
13. **Hancox RJ, Poulton R, Greene JM, McLachlan CR, Pearce MS, Sears MR** 2009 Associations between birth weight, early childhood weight gain and adult lung function. *Thorax* 64:228-232
14. **Warburton D, Schwarz M, Tefft D, Flores-Delgado G, Anderson KD, Cardoso WV** 2000 The molecular basis of lung morphogenesis. *Mech Dev* 92:55-81
15. **Alejandre-Alcazar MA, Shalamanov PD, Amarie OV, Sevilla-Perez J, Seeger W, Eickelberg O, Morty RE** 2007 Temporal and spatial regulation of bone morphogenetic protein signaling in late lung development. *Dev Dyn* 236:2825-2835
16. **Alejandre-Alcazar MA, Michiels-Corsten M, Vicencio AG, Reiss I, Ryu J, de Krijger RR, Haddad GG, Tibboel D, Seeger W, Eickelberg O, Morty RE** 2008 TGF-beta signaling is dynamically regulated during the alveolarization of rodent and human lungs. *Dev Dyn* 237:259-269
17. **Morrisey EE, Hogan BL** 2010 Preparing for the first breath: genetic and cellular mechanisms in lung development. *Dev Cell* 18:8-23
18. **Lebeche D, Malpel S, Cardoso WV** 1999 Fibroblast growth factor interactions in the developing lung. *Mech Dev* 86:125-136
19. **Thebaud B, Ladha F, Michelakis ED, Sawicka M, Thurston G, Eaton F, Hashimoto K, Harry G, Haromy A, Korbitt G, Archer SL** 2005 Vascular endothelial growth factor gene therapy increases survival, promotes lung angiogenesis,

REFERENCES

- and prevents alveolar damage in hyperoxia-induced lung injury: evidence that angiogenesis participates in alveolarization. *Circulation* 112:2477-2486
20. **Ferrara N** 2000 Vascular endothelial growth factor and the regulation of angiogenesis. *Recent Prog Horm Res* 55:15-35; discussion 35-16
 21. **Vicencio AG, Lee CG, Cho SJ, Eickelberg O, Chuu Y, Haddad GG, Elias JA** 2004 Conditional overexpression of bioactive transforming growth factor-beta1 in neonatal mouse lung: a new model for bronchopulmonary dysplasia? *Am J Respir Cell Mol Biol* 31:650-656
 22. **Morty RE, Konigshoff M, Eickelberg O** 2009 Transforming growth factor-beta signaling across ages: from distorted lung development to chronic obstructive pulmonary disease. *Proc Am Thorac Soc* 6:607-613
 23. **Bartram U, Speer CP** 2004 The role of transforming growth factor beta in lung development and disease. *Chest* 125:754-765
 24. **Grande JP** 1997 Role of transforming growth factor-beta in tissue injury and repair. *Proc Soc Exp Biol Med* 214:27-40
 25. **Bland RD, Ertsey R, Mokres LM, Xu L, Jacobson BE, Jiang S, Alvira CM, Rabinovitch M, Shinwell ES, Dixit A** 2008 Mechanical ventilation uncouples synthesis and assembly of elastin and increases apoptosis in lungs of newborn mice. Prelude to defective alveolar septation during lung development? *Am J Physiol Lung Cell Mol Physiol* 294:L3-14
 26. **Gauldie J, Galt T, Bonniaud P, Robbins C, Kelly M, Warburton D** 2003 Transfer of the active form of transforming growth factor-beta 1 gene to newborn rat lung induces changes consistent with bronchopulmonary dysplasia. *Am J Pathol* 163:2575-2584
 27. **Kotecha S, Wangoo A, Silverman M, Shaw RJ** 1996 Increase in the concentration of transforming growth factor beta-1 in bronchoalveolar lavage fluid before development of chronic lung disease of prematurity. *J Pediatr* 128:464-469
 28. **Lecart C, Cayabyab R, Buckley S, Morrison J, Kwong KY, Warburton D, Ramanathan R, Jones CA, Minoo P** 2000 Bioactive transforming growth factor-beta in the lungs of extremely low birthweight neonates predicts the need for home oxygen supplementation. *Biol Neonate* 77:217-223
 29. **Bland RD, Xu L, Ertsey R, Rabinovitch M, Albertine KH, Wynn KA, Kumar VH, Ryan RM, Swartz DD, Csiszar K, Fong KS** 2007 Dysregulation of pulmonary elastin synthesis and assembly in preterm lambs with chronic lung disease. *Am J Physiol Lung Cell Mol Physiol* 292:L1370-1384
 30. **Bland RD, Mokres LM, Ertsey R, Jacobson BE, Jiang S, Rabinovitch M, Xu L, Shinwell ES, Zhang F, Beasley MA** 2007 Mechanical ventilation with 40% oxygen reduces pulmonary expression of genes that regulate lung development and impairs alveolar septation in newborn mice. *Am J Physiol Lung Cell Mol Physiol* 293:L1099-1110
 31. **Zhao J, Lee M, Smith S, Warburton D** 1998 Abrogation of Smad3 and Smad2 or of Smad4 gene expression positively regulates murine embryonic lung branching morphogenesis in culture. *Dev Biol* 194:182-195
 32. **Chen H, Sun J, Buckley S, Chen C, Warburton D, Wang XF, Shi W** 2005 Abnormal mouse lung alveolarization caused by Smad3 deficiency is a developmental antecedent of centrilobular emphysema. *Am J Physiol Lung Cell Mol Physiol* 288:L683-691
 33. **Bonniaud P, Kolb M, Galt T, Robertson J, Robbins C, Stampfli M, Lavery C, Margetts PJ, Roberts AB, Gauldie J** 2004 Smad3 null mice develop airspace enlargement and are resistant to TGF-beta-mediated pulmonary fibrosis. *J Immunol* 173:2099-2108

REFERENCES

34. **Weaver M, Dunn NR, Hogan BL** 2000 Bmp4 and Fgf10 play opposing roles during lung bud morphogenesis. *Development* 127:2695-2704
35. **Bellusci S, Henderson R, Winnier G, Oikawa T, Hogan BL** 1996 Evidence from normal expression and targeted misexpression that bone morphogenetic protein (Bmp-4) plays a role in mouse embryonic lung morphogenesis. *Development* 122:1693-1702
36. **Dewulf N, Verschueren K, Lonnoy O, Moren A, Grimsby S, Vande Spiegle K, Miyazono K, Huylebroeck D, Ten Dijke P** 1995 Distinct spatial and temporal expression patterns of two type I receptors for bone morphogenetic proteins during mouse embryogenesis. *Endocrinology* 136:2652-2663
37. **Miyazono K, Maeda S, Imamura T** 2005 BMP receptor signaling: transcriptional targets, regulation of signals, and signaling cross-talk. *Cytokine Growth Factor Rev* 16:251-263
38. **Bragg AD, Moses HL, Serra R** 2001 Signaling to the epithelium is not sufficient to mediate all of the effects of transforming growth factor beta and bone morphogenetic protein 4 on murine embryonic lung development. *Mech Dev* 109:13-26
39. **Shi W, Zhao J, Anderson KD, Warburton D** 2001 Gremlin negatively modulates BMP-4 induction of embryonic mouse lung branching morphogenesis. *Am J Physiol Lung Cell Mol Physiol* 280:L1030-1039
40. **Panchision DM, Pickel JM, Studer L, Lee SH, Turner PA, Hazel TG, McKay RD** 2001 Sequential actions of BMP receptors control neural precursor cell production and fate. *Genes Dev* 15:2094-2110
41. **Sun J, Chen H, Chen C, Whitsett JA, Mishina Y, Bringas P, Jr., Ma JC, Warburton D, Shi W** 2008 Prenatal lung epithelial cell-specific abrogation of Alk3-bone morphogenetic protein signaling causes neonatal respiratory distress by disrupting distal airway formation. *Am J Pathol* 172:571-582
42. **Chen C, Chen H, Sun J, Bringas P, Jr., Chen Y, Warburton D, Shi W** 2005 Smad1 expression and function during mouse embryonic lung branching morphogenesis. *Am J Physiol Lung Cell Mol Physiol* 288:L1033-1039
43. **Jeffery TK, Upton PD, Trembath RC, Morrell NW** 2005 BMP4 inhibits proliferation and promotes myocyte differentiation of lung fibroblasts via Smad1 and JNK pathways. *Am J Physiol Lung Cell Mol Physiol* 288:L370-378
44. **Izumi N, Mizuguchi S, Inagaki Y, Saika S, Kawada N, Nakajima Y, Inoue K, Suehiro S, Friedman SL, Ikeda K** 2006 BMP-7 opposes TGF-beta1-mediated collagen induction in mouse pulmonary myofibroblasts through Id2. *Am J Physiol Lung Cell Mol Physiol* 290:L120-126
45. **Buckley S, Shi W, Driscoll B, Ferrario A, Anderson K, Warburton D** 2004 BMP4 signaling induces senescence and modulates the oncogenic phenotype of A549 lung adenocarcinoma cells. *Am J Physiol Lung Cell Mol Physiol* 286:L81-86
46. **Eblaghie MC, Reedy M, Oliver T, Mishina Y, Hogan BL** 2006 Evidence that autocrine signaling through Bmpr1a regulates the proliferation, survival and morphogenetic behavior of distal lung epithelial cells. *Dev Biol* 291:67-82
47. **Han RN, Liu J, Tanswell AK, Post M** 1992 Expression of basic fibroblast growth factor and receptor: immunolocalization studies in developing rat fetal lung. *Pediatr Res* 31:435-440
48. **Moura RS, Coutinho-Borges JP, Pacheco AP, Damota PO, Correia-Pinto J** 2011 FGF signaling pathway in the developing chick lung: expression and inhibition studies. *PLoS One* 6:e17660
49. **Post M, Souza P, Liu J, Tseu I, Wang J, Kuliszewski M, Tanswell AK** 1996 Keratinocyte growth factor and its receptor are involved in regulating early lung branching. *Development* 122:3107-3115

REFERENCES

50. **Bellusci S, Grindley J, Emoto H, Itoh N, Hogan BL** 1997 Fibroblast growth factor 10 (FGF10) and branching morphogenesis in the embryonic mouse lung. *Development* 124:4867-4878
51. **Shiratori M, Oshika E, Ung LP, Singh G, Shinozuka H, Warburton D, Michalopoulos G, Katyal SL** 1996 Keratinocyte growth factor and embryonic rat lung morphogenesis. *Am J Respir Cell Mol Biol* 15:328-338
52. **Wedgwood S, Devol JM, Grobe A, Benavidez E, Azakie A, Fineman JR, Black SM** 2007 Fibroblast growth factor-2 expression is altered in lambs with increased pulmonary blood flow and pulmonary hypertension. *Pediatr Res* 61:32-36
53. **Izikki M, Guignabert C, Fadel E, Humbert M, Tu L, Zadigue P, Darteville P, Simonneau G, Adnot S, Maitre B, Raffestin B, Eddahibi S** 2009 Endothelial-derived FGF2 contributes to the progression of pulmonary hypertension in humans and rodents. *J Clin Invest* 119:512-523
54. **Dingemann J, Doi T, Ruttensstock EM, Puri P** 2011 Downregulation of FGFR1 contributes to the development of the diaphragmatic defect in the nitrofen model of congenital diaphragmatic hernia. *Eur J Pediatr Surg* 21:46-49
55. **Teramoto H, Yoneda A, Puri P** 2003 Gene expression of fibroblast growth factors 10 and 7 is downregulated in the lung of nitrofen-induced diaphragmatic hernia in rats. *J Pediatr Surg* 38:1021-1024
56. **Friedmacher F, Doi T, Gosemann JH, Fujiwara N, Kutasy B, Puri P** 2012 Upregulation of fibroblast growth factor receptor 2 and 3 in the late stages of fetal lung development in the nitrofen rat model. *Pediatr Surg Int* 28:195-199
57. **Park WY, Miranda B, Lebeche D, Hashimoto G, Cardoso WV** 1998 FGF-10 is a chemotactic factor for distal epithelial buds during lung development. *Dev Biol* 201:125-134
58. **Sekine K, Ohuchi H, Fujiwara M, Yamasaki M, Yoshizawa T, Sato T, Yagishita N, Matsui D, Koga Y, Itoh N, Kato S** 1999 Fgf10 is essential for limb and lung formation. *Nat Genet* 21:138-141
59. **Orr-Urtreger A, Bedford MT, Burakova T, Arman E, Zimmer Y, Yayon A, Givol D, Lonai P** 1993 Developmental localization of the splicing alternatives of fibroblast growth factor receptor-2 (FGFR2). *Dev Biol* 158:475-486
60. **De Moerlooze L, Spencer-Dene B, Revest JM, Hajihosseini M, Rosewell I, Dickson C** 2000 An important role for the IIIb isoform of fibroblast growth factor receptor 2 (FGFR2) in mesenchymal-epithelial signalling during mouse organogenesis. *Development* 127:483-492
61. **Celli G, LaRochelle WJ, Mackem S, Sharp R, Merlino G** 1998 Soluble dominant-negative receptor uncovers essential roles for fibroblast growth factors in multi-organ induction and patterning. *EMBO J* 17:1642-1655
62. **Hokuto I, Perl AK, Whitsett JA** 2003 Prenatal, but not postnatal, inhibition of fibroblast growth factor receptor signaling causes emphysema. *J Biol Chem* 278:415-421
63. **Thebaud B, Abman SH** 2007 Bronchopulmonary dysplasia: where have all the vessels gone? Roles of angiogenic growth factors in chronic lung disease. *Am J Respir Crit Care Med* 175:978-985
64. **Ferrara N, Gerber HP, LeCouter J** 2003 The biology of VEGF and its receptors. *Nat Med* 9:669-676
65. **Carmeliet P, Ferreira V, Breier G, Pollefeyt S, Kieckens L, Gertsenstein M, Fahrig M, Vandenhoek A, Harpal K, Eberhardt C, Declercq C, Pawling J, Moons L, Collen D, Risau W, Nagy A** 1996 Abnormal blood vessel development and lethality in embryos lacking a single VEGF allele. *Nature* 380:435-439

REFERENCES

66. **Kasahara Y, Tudor RM, Taraseviciene-Stewart L, Le Cras TD, Abman S, Hirth PK, Waltenberger J, Voelkel NF** 2000 Inhibition of VEGF receptors causes lung cell apoptosis and emphysema. *J Clin Invest* 106:1311-1319
67. **Le Cras TD, Markham NE, Tudor RM, Voelkel NF, Abman SH** 2002 Treatment of newborn rats with a VEGF receptor inhibitor causes pulmonary hypertension and abnormal lung structure. *Am J Physiol Lung Cell Mol Physiol* 283:L555-562
68. **Bland RD, Albertine KH, Carlton DP, Kullama L, Davis P, Cho SC, Kim BI, Dahl M, Tabatabaei N** 2000 Chronic lung injury in preterm lambs: abnormalities of the pulmonary circulation and lung fluid balance. *Pediatr Res* 48:64-74
69. **Mokres LM, Parai K, Hilgendorff A, Ertsey R, Alvira CM, Rabinovitch M, Bland RD** 2010 Prolonged mechanical ventilation with air induces apoptosis and causes failure of alveolar septation and angiogenesis in lungs of newborn mice. *Am J Physiol Lung Cell Mol Physiol* 298:L23-35
70. **Maniscalco WM, Watkins RH, Pryhuber GS, Bhatt A, Shea C, Huyck H** 2002 Angiogenic factors and alveolar vasculature: development and alterations by injury in very premature baboons. *Am J Physiol Lung Cell Mol Physiol* 282:L811-823
71. **Bhatt AJ, Pryhuber GS, Huyck H, Watkins RH, Metlay LA, Maniscalco WM** 2001 Disrupted pulmonary vasculature and decreased vascular endothelial growth factor, Flt-1, and TIE-2 in human infants dying with bronchopulmonary dysplasia. *Am J Respir Crit Care Med* 164:1971-1980
72. **Lassus P, Turanlahti M, Heikkila P, Andersson LC, Nupponen I, Sarnesto A, Andersson S** 2001 Pulmonary vascular endothelial growth factor and Flt-1 in fetuses, in acute and chronic lung disease, and in persistent pulmonary hypertension of the newborn. *Am J Respir Crit Care Med* 164:1981-1987
73. **Wallace MA** 1998 Anatomy and physiology of the kidney. *AORN J* 68:800, 803-816, 819-820; quiz 821-804
74. **Preuss HG** 1993 Basics of renal anatomy and physiology. *Clin Lab Med* 13:1-11
75. **Pellatt GC** 2007 Anatomy and physiology of urinary elimination. Part 1. *Br J Nurs* 16:406-410
76. **Saxen L, Sariola H** 1987 Early organogenesis of the kidney. *Pediatr Nephrol* 1:385-392
77. **Jose PA, Fildes RD** 1988 Postnatal development of renal function. *Mead Johnson Symp Perinat Dev Med*:71-76
78. **Lechner MS, Dressler GR** 1997 The molecular basis of embryonic kidney development. *Mech Dev* 62:105-120
79. **Bates CM** 2000 Kidney development: regulatory molecules crucial to both mice and men. *Mol Genet Metab* 71:391-396
80. **Dressler GR** 2009 Advances in early kidney specification, development and patterning. *Development* 136:3863-3874
81. **Burrow CR** 2000 Regulatory molecules in kidney development. *Pediatr Nephrol* 14:240-253
82. **Donovan MJ, Natoli TA, Sainio K, Amstutz A, Jaenisch R, Sariola H, Kreidberg JA** 1999 Initial differentiation of the metanephric mesenchyme is independent of WT1 and the ureteric bud. *Dev Genet* 24:252-262
83. **Kreidberg JA, Sariola H, Loring JM, Maeda M, Pelletier J, Housman D, Jaenisch R** 1993 WT-1 is required for early kidney development. *Cell* 74:679-691
84. **Torres M, Gomez-Pardo E, Dressler GR, Gruss P** 1995 Pax-2 controls multiple steps of urogenital development. *Development* 121:4057-4065
85. **Brophy PD, Ostrom L, Lang KM, Dressler GR** 2001 Regulation of ureteric bud outgrowth by Pax2-dependent activation of the glial derived neurotrophic factor gene. *Development* 128:4747-4756

REFERENCES

86. **Sakurai H** 2003 Molecular mechanism of ureteric bud development. *Semin Cell Dev Biol* 14:217-224
87. **Durbec P, Marcos-Gutierrez CV, Kilkenny C, Grigoriou M, Wartiovaara K, Suvanto P, Smith D, Ponder B, Costantini F, Saarma M, et al.** 1996 GDNF signalling through the Ret receptor tyrosine kinase. *Nature* 381:789-793
88. **Moore MW, Klein RD, Farinas I, Sauer H, Armanini M, Phillips H, Reichardt LF, Ryan AM, Carver-Moore K, Rosenthal A** 1996 Renal and neuronal abnormalities in mice lacking GDNF. *Nature* 382:76-79
89. **Pichel JG, Shen L, Sheng HZ, Granholm AC, Drago J, Grinberg A, Lee EJ, Huang SP, Saarma M, Hoffer BJ, Sariola H, Westphal H** 1996 Defects in enteric innervation and kidney development in mice lacking GDNF. *Nature* 382:73-76
90. **Sainio K, Suvanto P, Davies J, Wartiovaara J, Wartiovaara K, Saarma M, Arumae U, Meng X, Lindahl M, Pachnis V, Sariola H** 1997 Glial-cell-line-derived neurotrophic factor is required for bud initiation from ureteric epithelium. *Development* 124:4077-4087
91. **Sanchez MP, Silos-Santiago I, Frisen J, He B, Lira SA, Barbacid M** 1996 Renal agenesis and the absence of enteric neurons in mice lacking GDNF. *Nature* 382:70-73
92. **Schuchardt A, D'Agati V, Pachnis V, Costantini F** 1996 Renal agenesis and hypodysplasia in ret-k- mutant mice result from defects in ureteric bud development. *Development* 122:1919-1929
93. **Vega QC, Worby CA, Lechner MS, Dixon JE, Dressler GR** 1996 Glial cell line-derived neurotrophic factor activates the receptor tyrosine kinase RET and promotes kidney morphogenesis. *Proc Natl Acad Sci U S A* 93:10657-10661
94. **Rogers SA, Ryan G, Hammerman MR** 1992 Metanephric transforming growth factor-alpha is required for renal organogenesis in vitro. *Am J Physiol* 262:F533-539
95. **Rogers SA, Ryan G, Purchio AF, Hammerman MR** 1993 Metanephric transforming growth factor-beta 1 regulates nephrogenesis in vitro. *Am J Physiol* 264:F996-1002
96. **Ritvos O, Tuuri T, Eramaa M, Sainio K, Hilden K, Saxen L, Gilbert SF** 1995 Activin disrupts epithelial branching morphogenesis in developing glandular organs of the mouse. *Mech Dev* 50:229-245
97. **Dudley AT, Lyons KM, Robertson EJ** 1995 A requirement for bone morphogenetic protein-7 during development of the mammalian kidney and eye. *Genes Dev* 9:2795-2807
98. **Godin RE, Robertson EJ, Dudley AT** 1999 Role of BMP family members during kidney development. *Int J Dev Biol* 43:405-411
99. **Dudley AT, Godin RE, Robertson EJ** 1999 Interaction between FGF and BMP signaling pathways regulates development of metanephric mesenchyme. *Genes Dev* 13:1601-1613
100. **Luo G, Hofmann C, Bronckers AL, Sohocki M, Bradley A, Karsenty G** 1995 BMP-7 is an inducer of nephrogenesis, and is also required for eye development and skeletal patterning. *Genes Dev* 9:2808-2820
101. **Davies J** 2001 Intracellular and extracellular regulation of ureteric bud morphogenesis. *J Anat* 198:257-264
102. **Santos OF, Nigam SK** 1993 HGF-induced tubulogenesis and branching of epithelial cells is modulated by extracellular matrix and TGF-beta. *Dev Biol* 160:293-302
103. **Sakurai H, Barros EJ, Tsukamoto T, Barasch J, Nigam SK** 1997 An in vitro tubulogenesis system using cell lines derived from the embryonic kidney shows dependence on multiple soluble growth factors. *Proc Natl Acad Sci U S A* 94:6279-6284

REFERENCES

104. **Pohl M, Sakurai H, Stuart RO, Nigam SK** 2000 Role of hyaluronan and CD44 in in vitro branching morphogenesis of ureteric bud cells. *Dev Biol* 224:312-325
105. **Zent R, Bush KT, Pohl ML, Quaranta V, Koshikawa N, Wang Z, Kreidberg JA, Sakurai H, Stuart RO, Nigam SK** 2001 Involvement of laminin binding integrins and laminin-5 in branching morphogenesis of the ureteric bud during kidney development. *Dev Biol* 238:289-302
106. **Kreidberg JA, Donovan MJ, Goldstein SL, Rennke H, Shepherd K, Jones RC, Jaenisch R** 1996 Alpha 3 beta 1 integrin has a crucial role in kidney and lung organogenesis. *Development* 122:3537-3547
107. **Pohl M, Sakurai H, Bush KT, Nigam SK** 2000 Matrix metalloproteinases and their inhibitors regulate in vitro ureteric bud branching morphogenesis. *Am J Physiol Renal Physiol* 279:F891-900
108. **Lelongt B, Trugnan G, Murphy G, Ronco PM** 1997 Matrix metalloproteinases MMP2 and MMP9 are produced in early stages of kidney morphogenesis but only MMP9 is required for renal organogenesis in vitro. *J Cell Biol* 136:1363-1373
109. **Ota K, Stetler-Stevenson WG, Yang Q, Kumar A, Wada J, Kashihara N, Wallner EI, Kanwar YS** 1998 Cloning of murine membrane-type-1-matrix metalloproteinase (MT-1-MMP) and its metanephric developmental regulation with respect to MMP-2 and its inhibitor. *Kidney Int* 54:131-142
110. **Barker DJ** 1995 Intrauterine programming of adult disease. *Mol Med Today* 1:418-423
111. **Plagemann A** 2005 Perinatal programming and functional teratogenesis: impact on body weight regulation and obesity. *Physiol Behav* 86:661-668
112. **Nuyt AM** 2008 Mechanisms underlying developmental programming of elevated blood pressure and vascular dysfunction: evidence from human studies and experimental animal models. *Clin Sci (Lond)* 114:1-17
113. **Dubos R, Savage D, Schaedler R** 1966 Biological Freudianism. Lasting effects of early environmental influences. *Pediatrics* 38:789-800
114. **Dorner G** 1977 Hormones, brain differentiation and fundamental processes of life. *J Steroid Biochem* 8:531-536
115. **Dorner G** 1986 Influences of nutrition on brain differentiation mediated by systemic hormones and neurotransmitters. *Bibl Nutr Dieta*:27-38
116. **Romo A, Carceller R, Tobajas J** 2009 Intrauterine growth retardation (IUGR): epidemiology and etiology. *Pediatr Endocrinol Rev* 6 Suppl 3:332-336
117. **Di Cesare Merlone A, Bozzola E, Cerbo RM, Rondini G** 2004 [Intrauterine growth retardation: diagnostic and therapeutic approach]. *Minerva Pediatr* 56:183-188
118. **Chatelain P** 2000 Children born with intra-uterine growth retardation (IUGR) or small for gestational age (SGA): long term growth and metabolic consequences. *Endocr Regul* 34:33-36
119. **Maulik D** 2006 Fetal growth compromise: definitions, standards, and classification. *Clin Obstet Gynecol* 49:214-218
120. **Agosti M, Vegni C, Calciolari G, Marini A** 2003 Post-discharge nutrition of the very low-birthweight infant: interim results of the multicentric GAMMA study. *Acta Paediatr Suppl* 91:39-43
121. **Were FN, Bwibo NO** 2007 Neonatal nutrition and later outcomes of very low birth weight infants at Kenyatta National Hospital. *Afr Health Sci* 7:108-114
122. **Neubauer AP, Voss W, Kattner E** 2008 Outcome of extremely low birth weight survivors at school age: the influence of perinatal parameters on neurodevelopment. *Eur J Pediatr* 167:87-95
123. **Yajnik CS** 2004 Early life origins of insulin resistance and type 2 diabetes in India and other Asian countries. *J Nutr* 134:205-210

REFERENCES

124. **Yajnik C** 2000 Interactions of perturbations in intrauterine growth and growth during childhood on the risk of adult-onset disease. *Proc Nutr Soc* 59:257-265
125. **Forsen T, Eriksson J, Tuomilehto J, Reunanen A, Osmond C, Barker D** 2000 The fetal and childhood growth of persons who develop type 2 diabetes. *Ann Intern Med* 133:176-182
126. **Crowther NJ, Cameron N, Trusler J, Gray IP** 1998 Association between poor glucose tolerance and rapid post natal weight gain in seven-year-old children. *Diabetologia* 41:1163-1167
127. **Hales CN, Barker DJ, Clark PM, Cox LJ, Fall C, Osmond C, Winter PD** 1991 Fetal and infant growth and impaired glucose tolerance at age 64. *BMJ* 303:1019-1022
128. **Ravelli AC, van der Meulen JH, Michels RP, Osmond C, Barker DJ, Hales CN, Bleker OP** 1998 Glucose tolerance in adults after prenatal exposure to famine. *Lancet* 351:173-177
129. **Knip M, Akerblom HK** 2005 Early nutrition and later diabetes risk. *Adv Exp Med Biol* 569:142-150
130. **Eriksson JG, Forsen T, Tuomilehto J, Winter PD, Osmond C, Barker DJ** 1999 Catch-up growth in childhood and death from coronary heart disease: longitudinal study. *BMJ* 318:427-431
131. **Ong KK, Ahmed ML, Emmett PM, Preece MA, Dunger DB** 2000 Association between postnatal catch-up growth and obesity in childhood: prospective cohort study. *BMJ* 320:967-971
132. **Levy-Marchal C, Jaquet D, Czernichow P** 2004 Long-term metabolic consequences of being born small for gestational age. *Semin Neonatol* 9:67-74
133. **Barker DJ, Osmond C, Forsen TJ, Kajantie E, Eriksson JG** 2005 Trajectories of growth among children who have coronary events as adults. *N Engl J Med* 353:1802-1809
134. **Hales CN** 1997 Fetal and infant growth and impaired glucose tolerance in adulthood: the "thrifty phenotype" hypothesis revisited. *Acta Paediatr Suppl* 422:73-77
135. **Barker DJ, Osmond C, Golding J, Kuh D, Wadsworth ME** 1989 Growth in utero, blood pressure in childhood and adult life, and mortality from cardiovascular disease. *BMJ* 298:564-567
136. **Huxley RR, Shiell AW, Law CM** 2000 The role of size at birth and postnatal catch-up growth in determining systolic blood pressure: a systematic review of the literature. *J Hypertens* 18:815-831
137. **Wang Y, Chen X, Klag MJ, Caballero B** 2006 Epidemic of childhood obesity: implications for kidney disease. *Adv Chronic Kidney Dis* 13:336-351
138. **Zimmet P, Alberti KG, Kaufman F, Tajima N, Silink M, Arslanian S, Wong G, Bennett P, Shaw J, Caprio S** 2007 The metabolic syndrome in children and adolescents - an IDF consensus report. *Pediatr Diabetes* 8:299-306
139. **Hedley AA, Ogden CL, Johnson CL, Carroll MD, Curtin LR, Flegal KM** 2004 Prevalence of overweight and obesity among US children, adolescents, and adults, 1999-2002. *JAMA* 291:2847-2850
140. **Ogden CL, Carroll MD, Curtin LR, McDowell MA, Tabak CJ, Flegal KM** 2006 Prevalence of overweight and obesity in the United States, 1999-2004. *JAMA* 295:1549-1555
141. **Rewers M, LaPorte RE, King H, Tuomilehto J** 1988 Trends in the prevalence and incidence of diabetes: insulin-dependent diabetes mellitus in childhood. *World Health Stat Q* 41:179-189
142. **Liese AD, D'Agostino RB, Jr., Hamman RF, Kilgo PD, Lawrence JM, Liu LL, Loots B, Linder B, Marcovina S, Rodriguez B, Standiford D, Williams DE** 2006

REFERENCES

- The burden of diabetes mellitus among US youth: prevalence estimates from the SEARCH for Diabetes in Youth Study. *Pediatrics* 118:1510-1518
143. **Dyer JS, Rosenfeld CR** 2011 Metabolic imprinting by prenatal, perinatal, and postnatal overnutrition: a review. *Semin Reprod Med* 29:266-276
 144. **Fernandez-Twinn DS, Ozanne SE** 2010 Early life nutrition and metabolic programming. *Ann N Y Acad Sci* 1212:78-96
 145. **Innis SM** 2011 Metabolic programming of long-term outcomes due to fatty acid nutrition in early life. *Matern Child Nutr* 7 Suppl 2:112-123
 146. **Widdowson EM, McCance RA** 1963 The Effect of Finite Periods of Undernutrition at Different Ages on the Composition and Subsequent Development of the Rat. *Proc R Soc Lond B Biol Sci* 158:329-342
 147. **Plagemann A, Heidrich I, Gotz F, Rohde W, Dorner G** 1992 Obesity and enhanced diabetes and cardiovascular risk in adult rats due to early postnatal overfeeding. *Exp Clin Endocrinol* 99:154-158
 148. **Boubred F, Daniel L, Buffat C, Feuerstein JM, Tsimaratos M, Oliver C, Dignat-George F, Lelievre-Pegorier M, Simeoni U** 2009 Early postnatal overfeeding induces early chronic renal dysfunction in adult male rats. *Am J Physiol Renal Physiol* 297:F943-951
 149. **Boubred F, Buffat C, Feuerstein JM, Daniel L, Tsimaratos M, Oliver C, Lelievre-Pegorier M, Simeoni U** 2007 Effects of early postnatal hypernutrition on nephron number and long-term renal function and structure in rats. *Am J Physiol Renal Physiol* 293:F1944-1949
 150. **Gubhaju L, Sutherland MR, Black MJ** 2011 Preterm birth and the kidney: implications for long-term renal health. *Reprod Sci* 18:322-333
 151. **Meetoo D** 2008 Chronic diseases: the silent global epidemic. *Br J Nurs* 17:1320-1325
 152. **Ljustina-Pribic R, Petrovic S, Tomic J** 2010 [Childhood asthma and risk factors]. *Med Pregl* 63:516-521
 153. **Bloomberg GR** 2011 The influence of environment, as represented by diet and air pollution, upon incidence and prevalence of wheezing illnesses in young children. *Curr Opin Allergy Clin Immunol* 11:144-149
 154. **Gilliland FD, Li YF, Peters JM** 2001 Effects of maternal smoking during pregnancy and environmental tobacco smoke on asthma and wheezing in children. *Am J Respir Crit Care Med* 163:429-436
 155. **Maritz GS, Morley CJ, Harding R** 2005 Early developmental origins of impaired lung structure and function. *Early Hum Dev* 81:763-771
 156. **Petre MA, Petrik J, Ellis R, Inman MD, Holloway AC, Labiris NR** 2011 Fetal and neonatal exposure to nicotine disrupts postnatal lung development in rats: role of VEGF and its receptors. *Int J Toxicol* 30:244-252
 157. **Hylkema MN, Blacchiere MJ** 2009 Intrauterine effects of maternal smoking on sensitization, asthma, and chronic obstructive pulmonary disease. *Proc Am Thorac Soc* 6:660-662
 158. **Maritz GS, Harding R** 2011 Life-long programming implications of exposure to tobacco smoking and nicotine before and soon after birth: evidence for altered lung development. *Int J Environ Res Public Health* 8:875-898
 159. **Carroll KN, Gebretsadik T, Griffin MR, Dupont WD, Mitchel EF, Wu P, Enriquez R, Hartert TV** 2007 Maternal asthma and maternal smoking are associated with increased risk of bronchiolitis during infancy. *Pediatrics* 119:1104-1112
 160. **Sekhon HS, Keller JA, Benowitz NL, Spindel ER** 2001 Prenatal nicotine exposure alters pulmonary function in newborn rhesus monkeys. *Am J Respir Crit Care Med* 164:989-994

REFERENCES

161. **Mai XM, Gaddlin PO, Nilsson L, Leijon I** 2005 Early rapid weight gain and current overweight in relation to asthma in adolescents born with very low birth weight. *Pediatr Allergy Immunol* 16:380-385
162. **McGrath-Morrow S, Rangasamy T, Cho C, Sussan T, Neptune E, Wise R, Tudor RM, Biswal S** 2008 Impaired lung homeostasis in neonatal mice exposed to cigarette smoke. *Am J Respir Cell Mol Biol* 38:393-400
163. **Chen CM, Wang LF, Su B** 2004 Effects of maternal undernutrition during late gestation on the lung surfactant system and morphometry in rats. *Pediatr Res* 56:329-335
164. **Morsing E, Gustafsson P, Brodzski J** 2012 Lung function in children born after foetal growth restriction and very preterm birth. *Acta Paediatr* 101:48-54
165. **Maritz GS, Cock ML, Louey S, Joyce BJ, Albuquerque CA, Harding R** 2001 Effects of fetal growth restriction on lung development before and after birth: a morphometric analysis. *Pediatr Pulmonol* 32:201-210
166. **Lipsett J, Tamblyn M, Madigan K, Roberts P, Cool JC, Runciman SI, McMillen IC, Robinson J, Owens JA** 2006 Restricted fetal growth and lung development: a morphometric analysis of pulmonary structure. *Pediatr Pulmonol* 41:1138-1145
167. **Joss-Moore LA, Wang Y, Yu X, Campbell MS, Callaway CW, McKnight RA, Wint A, Dahl MJ, Dull RO, Albertine KH, Lane RH** 2011 IUGR decreases elastin mRNA expression in the developing rat lung and alters elastin content and lung compliance in the mature rat lung. *Physiol Genomics* 43:499-505
168. **Rehan VK, Sakurai R, Li Y, Karadag A, Corral J, Bellusci S, Xue YY, Belperio J, Torday JS** 2012 Effects of maternal food restriction on offspring lung extracellular matrix deposition and long term pulmonary function in an experimental rat model. *Pediatr Pulmonol* 47:162-171
169. **Hallan S, Euser AM, Irgens LM, Finken MJ, Holmen J, Dekker FW** 2008 Effect of intrauterine growth restriction on kidney function at young adult age: the Nord Trondelag Health (HUNT 2) Study. *Am J Kidney Dis* 51:10-20
170. **Bacchetta J, Harambat J, Dubourg L, Guy B, Liutkus A, Canterino I, Kassai B, Putet G, Cochat P** 2009 Both extrauterine and intrauterine growth restriction impair renal function in children born very preterm. *Kidney Int* 76:445-452
171. **Johansson S, Iliadou A, Bergvall N, Tuvemo T, Norman M, Cnattingius S** 2005 Risk of high blood pressure among young men increases with the degree of immaturity at birth. *Circulation* 112:3430-3436
172. **Hughson MD, Douglas-Denton R, Bertram JF, Hoy WE** 2006 Hypertension, glomerular number, and birth weight in African Americans and white subjects in the southeastern United States. *Kidney Int* 69:671-678
173. **Plank C, Ostreicher I, Hartner A, Marek I, Struwe FG, Amann K, Hilgers KF, Rascher W, Dotsch J** 2006 Intrauterine growth retardation aggravates the course of acute mesangioproliferative glomerulonephritis in the rat. *Kidney Int* 70:1974-1982
174. **Lackland DT, Egan BM, Fan ZJ, Syddall HE** 2001 Low birth weight contributes to the excess prevalence of end-stage renal disease in African Americans. *J Clin Hypertens (Greenwich)* 3:29-31
175. **Lackland DT, Bendall HE, Osmond C, Egan BM, Barker DJ** 2000 Low birth weights contribute to high rates of early-onset chronic renal failure in the Southeastern United States. *Arch Intern Med* 160:1472-1476
176. **Na YW, Yang HJ, Choi JH, Yoo KH, Hong YS, Lee JW, Kim SK** 2002 Effect of intrauterine growth retardation on the progression of nephrotic syndrome. *Am J Nephrol* 22:463-467

REFERENCES

177. **Sheu JN, Chen JH** 2001 Minimal change nephrotic syndrome in children with intrauterine growth retardation. *Am J Kidney Dis* 37:909-914
178. **Zidar N, Avgustin Cavic M, Kenda RB, Ferluga D** 1998 Unfavorable course of minimal change nephrotic syndrome in children with intrauterine growth retardation. *Kidney Int* 54:1320-1323
179. **Zidar N, Cavic MA, Kenda RB, Koselj M, Ferluga D** 1998 Effect of intrauterine growth retardation on the clinical course and prognosis of IgA glomerulonephritis in children. *Nephron* 79:28-32
180. **Plank C, Nusken KD, Menendez-Castro C, Hartner A, Ostreicher I, Amann K, Baumann P, Peters H, Rascher W, Dotsch J** 2010 Intrauterine growth restriction following ligation of the uterine arteries leads to more severe glomerulosclerosis after mesangioproliferative glomerulonephritis in the offspring. *Am J Nephrol* 32:287-295
181. **Zanardo V, Fanelli T, Weiner G, Fanos V, Zaninotto M, Visentin S, Cavallin F, Trevisanuto D, Cosmi E** 2011 Intrauterine growth restriction is associated with persistent aortic wall thickening and glomerular proteinuria during infancy. *Kidney Int* 80:119-123
182. **Wlodek ME, Westcott K, Siebel AL, Owens JA, Moritz KM** 2008 Growth restriction before or after birth reduces nephron number and increases blood pressure in male rats. *Kidney Int* 74:187-195
183. **Moritz KM, Mazzuca MQ, Siebel AL, Mibus A, Arena D, Tare M, Owens JA, Wlodek ME** 2009 Uteroplacental insufficiency causes a nephron deficit, modest renal insufficiency but no hypertension with ageing in female rats. *J Physiol* 587:2635-2646
184. **Ojeda NB, Grigore D, Alexander BT** 2008 Intrauterine growth restriction: fetal programming of hypertension and kidney disease. *Adv Chronic Kidney Dis* 15:101-106
185. **Brenner BM, Anderson S** 1992 The interrelationships among filtration surface area, blood pressure, and chronic renal disease. *J Cardiovasc Pharmacol* 19 Suppl 6:S1-7
186. **Vehaskari VM, Aviles DH, Manning J** 2001 Prenatal programming of adult hypertension in the rat. *Kidney Int* 59:238-245
187. **Woods LL, Ingelfinger JR, Nyengaard JR, Rasch R** 2001 Maternal protein restriction suppresses the newborn renin-angiotensin system and programs adult hypertension in rats. *Pediatr Res* 49:460-467
188. **Grigore D, Ojeda NB, Robertson EB, Dawson AS, Huffman CA, Bourassa EA, Speth RC, Brosnihan KB, Alexander BT** 2007 Placental insufficiency results in temporal alterations in the renin angiotensin system in male hypertensive growth restricted offspring. *Am J Physiol Regul Integr Comp Physiol* 293:R804-811
189. **Riviere G, Michaud A, Breton C, VanCamp G, Laborie C, Enache M, Lesage J, Deloof S, Corvol P, Vieau D** 2005 Angiotensin-converting enzyme 2 (ACE2) and ACE activities display tissue-specific sensitivity to undernutrition-programmed hypertension in the adult rat. *Hypertension* 46:1169-1174
190. **Guarnieri G, Zanetti M, Vinci P, Cattin MR, Pirulli A, Barazzoni R** 2010 Metabolic syndrome and chronic kidney disease. *J Ren Nutr* 20:S19-23
191. **Adelman RD** 2002 Obesity and renal disease. *Curr Opin Nephrol Hypertens* 11:331-335
192. **Cleal JK, Poore KR, Boullin JP, Khan O, Chau R, Hambidge O, Torrens C, Newman JP, Poston L, Noakes DE, Hanson MA, Green LR** 2007 Mismatched pre- and postnatal nutrition leads to cardiovascular dysfunction and altered renal function in adulthood. *Proc Natl Acad Sci U S A* 104:9529-9533
193. **Litonjua AA, Gold DR** 2008 Asthma and obesity: common early-life influences in the inception of disease. *J Allergy Clin Immunol* 121:1075-1084; quiz 1085-1076

REFERENCES

194. **Coresh J, Selvin E, Stevens LA, Manzi J, Kusek JW, Eggers P, Van Lente F, Levey AS** 2007 Prevalence of chronic kidney disease in the United States. *JAMA* 298:2038-2047
195. **Hall JE, Crook ED, Jones DW, Wofford MR, Dubbert PM** 2002 Mechanisms of obesity-associated cardiovascular and renal disease. *Am J Med Sci* 324:127-137
196. **Savino A, Pelliccia P, Chiarelli F, Mohn A** 2010 Obesity-related renal injury in childhood. *Horm Res Paediatr* 73:303-311
197. **Camici M, Galetta F, Abraham N, Carpi A** 2012 Obesity-related glomerulopathy and podocyte injury: a mini review. *Front Biosci (Elite Ed)* 4:1058-1070
198. **Kasiske BL, Crosson JT** 1986 Renal disease in patients with massive obesity. *Arch Intern Med* 146:1105-1109
199. **Adelman RD, Restaino IG, Alon US, Blowey DL** 2001 Proteinuria and focal segmental glomerulosclerosis in severely obese adolescents. *J Pediatr* 138:481-485
200. **Henegar JR, Bigler SA, Henegar LK, Tyagi SC, Hall JE** 2001 Functional and structural changes in the kidney in the early stages of obesity. *J Am Soc Nephrol* 12:1211-1217
201. **Wolf G, Hamann A, Han DC, Helmchen U, Thaïss F, Ziyadeh FN, Stahl RA** 1999 Leptin stimulates proliferation and TGF-beta expression in renal glomerular endothelial cells: potential role in glomerulosclerosis [see comments]. *Kidney Int* 56:860-872
202. **Aizawa-Abe M, Ogawa Y, Masuzaki H, Ebihara K, Satoh N, Iwai H, Matsuoka N, Hayashi T, Hosoda K, Inoue G, Yoshimasa Y, Nakao K** 2000 Pathophysiological role of leptin in obesity-related hypertension. *J Clin Invest* 105:1243-1252
203. **Haynes WG, Sivitz WI, Morgan DA, Walsh SA, Mark AL** 1997 Sympathetic and cardiorenal actions of leptin. *Hypertension* 30:619-623
204. **Han DC, Isono M, Chen S, Casaretto A, Hong SW, Wolf G, Ziyadeh FN** 2001 Leptin stimulates type I collagen production in db/db mesangial cells: glucose uptake and TGF-beta type II receptor expression. *Kidney Int* 59:1315-1323
205. **Wolf G, Ziyadeh FN** 2006 Leptin and renal fibrosis. *Contrib Nephrol* 151:175-183
206. **Lucas JS, Inskip HM, Godfrey KM, Foreman CT, Warner JO, Gregson RK, Clough JB** 2004 Small size at birth and greater postnatal weight gain: relationships to diminished infant lung function. *Am J Respir Crit Care Med* 170:534-540
207. **Ubilla C, Bustos P, Amigo H, Oyarzun M, Rona RJ** 2008 Nutritional status, especially body mass index, from birth to adulthood and lung function in young adulthood. *Ann Hum Biol* 35:322-333
208. **Turner S, Zhang G, Young S, Cox M, Goldblatt J, Landau L, Le Souef P** 2008 Associations between postnatal weight gain, change in postnatal pulmonary function, formula feeding and early asthma. *Thorax* 63:234-239
209. **Canoy D, Pekkanen J, Elliott P, Pouta A, Laitinen J, Hartikainen AL, Zitting P, Patel S, Little MP, Jarvelin MR** 2007 Early growth and adult respiratory function in men and women followed from the fetal period to adulthood. *Thorax* 62:396-402
210. **Turner SW, Young S, Goldblatt J, Landau LI, Le Souef PN** 2009 Childhood asthma and increased airway responsiveness: a relationship that begins in infancy. *Am J Respir Crit Care Med* 179:98-104
211. **Massague J** 1998 TGF-beta signal transduction. *Annu Rev Biochem* 67:753-791
212. **Derynck R, Zhang YE** 2003 Smad-dependent and Smad-independent pathways in TGF-beta family signalling. *Nature* 425:577-584
213. **Mehra A, Wrana JL** 2002 TGF-beta and the Smad signal transduction pathway. *Biochem Cell Biol* 80:605-622
214. **Munger JS, Huang X, Kawakatsu H, Griffiths MJ, Dalton SL, Wu J, Pittet JF, Kaminski N, Garat C, Matthey MA, Rifkin DB, Sheppard D** 1999 The integrin

REFERENCES

- alpha v beta 6 binds and activates latent TGF beta 1: a mechanism for regulating pulmonary inflammation and fibrosis. *Cell* 96:319-328
215. **Sun PD, Davies DR** 1995 The cystine-knot growth-factor superfamily. *Annu Rev Biophys Biomol Struct* 24:269-291
216. **Taipale J, Saharinen J, Keski-Oja J** 1998 Extracellular matrix-associated transforming growth factor-beta: role in cancer cell growth and invasion. *Adv Cancer Res* 75:87-134
217. **Chen YG, Hata A, Lo RS, Wotton D, Shi Y, Pavletich N, Massague J** 1998 Determinants of specificity in TGF-beta signal transduction. *Genes Dev* 12:2144-2152
218. **Sakurai H, Nigam SK** 1997 Transforming growth factor-beta selectively inhibits branching morphogenesis but not tubulogenesis. *Am J Physiol* 272:F139-146
219. **Liu J, Tseu I, Wang J, Tanswell K, Post M** 2000 Transforming growth factor beta2, but not beta1 and beta3, is critical for early rat lung branching. *Dev Dyn* 217:343-360
220. **Zhao J, Bu D, Lee M, Slavkin HC, Hall FL, Warburton D** 1996 Abrogation of transforming growth factor-beta type II receptor stimulates embryonic mouse lung branching morphogenesis in culture. *Dev Biol* 180:242-257
221. **Zhao J, Shi W, Chen H, Warburton D** 2000 Smad7 and Smad6 differentially modulate transforming growth factor beta -induced inhibition of embryonic lung morphogenesis. *J Biol Chem* 275:23992-23997
222. **Zhao J, Crowe DL, Castillo C, Wuenschell C, Chai Y, Warburton D** 2000 Smad7 is a TGF-beta-inducible attenuator of Smad2/3-mediated inhibition of embryonic lung morphogenesis. *Mech Dev* 93:71-81
223. **Krishnaveni MS, Hansen JL, Seeger W, Morty RE, Sheikh SP, Eickelberg O** 2006 Constitutive homo- and hetero-oligomerization of TbetaRII-B, an alternatively spliced variant of the mouse TGF-beta type II receptor. *Biochem Biophys Res Commun* 351:651-657
224. **Miyazawa K, Shinozaki M, Hara T, Furuya T, Miyazono K** 2002 Two major Smad pathways in TGF-beta superfamily signalling. *Genes Cells* 7:1191-1204
225. **Wrana JL, Attisano L, Carcamo J, Zentella A, Doody J, Laiho M, Wang XF, Massague J** 1992 TGF beta signals through a heteromeric protein kinase receptor complex. *Cell* 71:1003-1014
226. **Wrana JL, Carcamo J, Attisano L, Cheifetz S, Zentella A, Lopez-Casillas F, Massague J** 1992 The type II TGF-beta receptor signals diverse responses in cooperation with the type I receptor. *Cold Spring Harb Symp Quant Biol* 57:81-86
227. **Moustakas A, Souchelnytskyi S, Heldin CH** 2001 Smad regulation in TGF-beta signal transduction. *J Cell Sci* 114:4359-4369
228. **ten Dijke P, Hill CS** 2004 New insights into TGF-beta-Smad signalling. *Trends Biochem Sci* 29:265-273
229. **Wolf G, Chen S, Han DC, Ziyadeh FN** 2002 Leptin and renal disease. *Am J Kidney Dis* 39:1-11
230. **Meissner U, Hanisch C, Ostreicher I, Knerr I, Hofbauer KH, Blum WF, Allabauer I, Rascher W, Dotsch J** 2005 Differential regulation of leptin synthesis in rats during short-term hypoxia and short-term carbon monoxide inhalation. *Endocrinology* 146:215-220
231. **Hirano T, Yasukawa K, Harada H, Taga T, Watanabe Y, Matsuda T, Kashiwamura S, Nakajima K, Koyama K, Iwamatsu A, et al.** 1986 Complementary DNA for a novel human interleukin (BSF-2) that induces B lymphocytes to produce immunoglobulin. *Nature* 324:73-76

REFERENCES

232. **Mihara M, Hashizume M, Yoshida H, Suzuki M, Shiina M** 2012 IL-6/IL-6 receptor system and its role in physiological and pathological conditions. *Clin Sci (Lond)* 122:143-159
233. **Nogueira-Silva C, Moura RS, Esteves N, Gonzaga S, Correia-Pinto J** 2008 Intrinsic catch-up growth of hypoplastic fetal lungs is mediated by interleukin-6. *Pediatr Pulmonol* 43:680-689
234. **Pedroza M, Schneider DJ, Karmouty-Quintana H, Coote J, Shaw S, Corrigan R, Molina JG, Alcorn JL, Galas D, Gelinis R, Blackburn MR** 2011 Interleukin-6 contributes to inflammation and remodeling in a model of adenosine mediated lung injury. *PLoS One* 6:e22667
235. **Mihara M, Nishimoto N, Ohsugi Y** 2005 The therapy of autoimmune diseases by anti-interleukin-6 receptor antibody. *Expert Opin Biol Ther* 5:683-690
236. **Fei H, Okano HJ, Li C, Lee GH, Zhao C, Darnell R, Friedman JM** 1997 Anatomic localization of alternatively spliced leptin receptors (Ob-R) in mouse brain and other tissues. *Proc Natl Acad Sci U S A* 94:7001-7005
237. **Elmqvist JK, Bjorbaek C, Ahima RS, Flier JS, Saper CB** 1998 Distributions of leptin receptor mRNA isoforms in the rat brain. *J Comp Neurol* 395:535-547
238. **Bjorbaek C, Elmqvist JK, Michl P, Ahima RS, van Bueren A, McCall AL, Flier JS** 1998 Expression of leptin receptor isoforms in rat brain microvessels. *Endocrinology* 139:3485-3491
239. **Baumann H, Morella KK, White DW, Dembski M, Bailon PS, Kim H, Lai CF, Tartaglia LA** 1996 The full-length leptin receptor has signaling capabilities of interleukin 6-type cytokine receptors. *Proc Natl Acad Sci U S A* 93:8374-8378
240. **Morris DL, Rui L** 2009 Recent advances in understanding leptin signaling and leptin resistance. *Am J Physiol Endocrinol Metab* 297:E1247-1259
241. **Myers MG, Cowley MA, Munzberg H** 2008 Mechanisms of leptin action and leptin resistance. *Annu Rev Physiol* 70:537-556
242. **Munzberg H, Bjornholm M, Bates SH, Myers MG, Jr.** 2005 Leptin receptor action and mechanisms of leptin resistance. *Cell Mol Life Sci* 62:642-652
243. **Hibi M, Murakami M, Saito M, Hirano T, Taga T, Kishimoto T** 1990 Molecular cloning and expression of an IL-6 signal transducer, gp130. *Cell* 63:1149-1157
244. **Saito M, Yoshida K, Hibi M, Taga T, Kishimoto T** 1992 Molecular cloning of a murine IL-6 receptor-associated signal transducer, gp130, and its regulated expression in vivo. *J Immunol* 148:4066-4071
245. **Martens AS, Bode JG, Heinrich PC, Graeve L** 2000 The cytoplasmic domain of the interleukin-6 receptor gp80 mediates its basolateral sorting in polarized madin-darby canine kidney cells. *J Cell Sci* 113 (Pt 20):3593-3602
246. **Heinrich PC, Bode JG, Graeve L, Haan C, Martens A, Muller-Newen G, Nimmegern A, Schaper F, Schmitz J, Siewert E** 2000 Modulation and termination of interleukin-6 signalling. *Eur Cytokine Netw* 11:512-513
247. **Rose-John S, Neurath MF** 2004 IL-6 trans-signaling: the heat is on. *Immunity* 20:2-4
248. **Narazaki M, Yasukawa K, Saito T, Ohsugi Y, Fukui H, Koishihara Y, Yancopoulos GD, Taga T, Kishimoto T** 1993 Soluble forms of the interleukin-6 signal-transducing receptor component gp130 in human serum possessing a potential to inhibit signals through membrane-anchored gp130. *Blood* 82:1120-1126
249. **Jostock T, Mullberg J, Ozbek S, Atreya R, Blinn G, Voltz N, Fischer M, Neurath MF, Rose-John S** 2001 Soluble gp130 is the natural inhibitor of soluble interleukin-6 receptor transsignaling responses. *Eur J Biochem* 268:160-167
250. **Taga T, Kishimoto T** 1997 Gp130 and the interleukin-6 family of cytokines. *Annu Rev Immunol* 15:797-819

REFERENCES

251. **Ryan RM, Mineo-Kuhn MM, Kramer CM, Finkelstein JN** 1994 Growth factors alter neonatal type II alveolar epithelial cell proliferation. *Am J Physiol* 266:L17-22
252. **Zhang F, Nielsen LD, Lucas JJ, Mason RJ** 2004 Transforming growth factor-beta antagonizes alveolar type II cell proliferation induced by keratinocyte growth factor. *Am J Respir Cell Mol Biol* 31:679-686
253. **Seay U, Sedding D, Krick S, Hecker M, Seeger W, Eickelberg O** 2005 Transforming growth factor-beta-dependent growth inhibition in primary vascular smooth muscle cells is p38-dependent. *J Pharmacol Exp Ther* 315:1005-1012
254. **Kasai H, Allen JT, Mason RM, Kamimura T, Zhang Z** 2005 TGF-beta1 induces human alveolar epithelial to mesenchymal cell transition (EMT). *Respir Res* 6:56
255. **McDevitt TM, Gonzales LW, Savani RC, Ballard PL** 2007 Role of endogenous TGF-beta in glucocorticoid-induced lung type II cell differentiation. *Am J Physiol Lung Cell Mol Physiol* 292:L249-257
256. **Freathy C, Brown DG, Roberts RA, Cain K** 2000 Transforming growth factor-beta(1) induces apoptosis in rat FaO hepatoma cells via cytochrome c release and oligomerization of Apaf-1 to form a approximately 700-kd apoptosome caspase-processing complex. *Hepatology* 32:750-760
257. **Gal A, Sjoblom T, Fedorova L, Imreh S, Beug H, Moustakas A** 2008 Sustained TGF beta exposure suppresses Smad and non-Smad signalling in mammary epithelial cells, leading to EMT and inhibition of growth arrest and apoptosis. *Oncogene* 27:1218-1230
258. **Undevia NS, Dorscheid DR, Marroquin BA, Gugliotta WL, Tse R, White SR** 2004 Smad and p38-MAPK signaling mediates apoptotic effects of transforming growth factor-beta1 in human airway epithelial cells. *Am J Physiol Lung Cell Mol Physiol* 287:L515-524
259. **Chu W, Li X, Li C, Wan L, Shi H, Song X, Liu X, Chen X, Zhang C, Shan H, Lu Y, Yang B** 2011 TGFBR3, a potential negative regulator of TGF-beta signaling, protects cardiac fibroblasts from hypoxia-induced apoptosis. *J Cell Physiol* 226:2586-2594
260. **Joyce BJ, Louey S, Davey MG, Cock ML, Hooper SB, Harding R** 2001 Compromised respiratory function in postnatal lambs after placental insufficiency and intrauterine growth restriction. *Pediatr Res* 50:641-649
261. **Wynn TA** 2003 IL-13 effector functions. *Annu Rev Immunol* 21:425-456
262. **Gueders MM, Foidart JM, Noel A, Cataldo DD** 2006 Matrix metalloproteinases (MMPs) and tissue inhibitors of MMPs in the respiratory tract: potential implications in asthma and other lung diseases. *Eur J Pharmacol* 533:133-144
263. **Ryu J, Vicencio AG, Yeager ME, Kashgarian M, Haddad GG, Eickelberg O** 2005 Differential expression of matrix metalloproteinases and their inhibitors in human and mouse lung development. *Thromb Haemost* 94:175-183
264. **Oggionni T, Morbini P, Inghilleri S, Palladini G, Tozzi R, Vitulo P, Fenoglio C, Perlini S, Pozzi E** 2006 Time course of matrix metalloproteinases and tissue inhibitors in bleomycin-induced pulmonary fibrosis. *Eur J Histochem* 50:317-325
265. **Sherr CJ, Roberts JM** 1995 Inhibitors of mammalian G1 cyclin-dependent kinases. *Genes Dev* 9:1149-1163
266. **Saito-Fujita T, Iwakawa M, Nakamura E, Nakawatari M, Fujita H, Moritake T, Imai T** 2011 Attenuated lung fibrosis in interleukin 6 knock-out mice after C-ion irradiation to lung. *J Radiat Res (Tokyo)* 52:270-277
267. **Gharaee-Kermani M, Phan SH** 2005 Molecular mechanisms of and possible treatment strategies for idiopathic pulmonary fibrosis. *Curr Pharm Des* 11:3943-3971
268. **Zhu Z, Homer RJ, Wang Z, Chen Q, Geba GP, Wang J, Zhang Y, Elias JA** 1999 Pulmonary expression of interleukin-13 causes inflammation, mucus hypersecretion,

REFERENCES

- subepithelial fibrosis, physiologic abnormalities, and eotaxin production. *J Clin Invest* 103:779-788
269. **Kucharewicz I, Kowal K, Buczek W, Bodzenta-Lukaszyk A** 2003 The plasmin system in airway remodeling. *Thromb Res* 112:1-7
270. **Hattori N, Mizuno S, Yoshida Y, Chin K, Mishima M, Sisson TH, Simon RH, Nakamura T, Miyake M** 2004 The plasminogen activation system reduces fibrosis in the lung by a hepatocyte growth factor-dependent mechanism. *Am J Pathol* 164:1091-1098
271. **Neuman G, Sagi R, Shalitin S, Reif S** 2010 Serum inflammatory markers in overweight children and adolescents with non-alcoholic fatty liver disease. *Isr Med Assoc J* 12:410-415
272. **Teplan V, Jr., Vyhnanek F, Gurlich R, Haluzik M, Racek J, Vyhnanekova I, Stollova M, Teplan V** 2010 Increased proinflammatory cytokine production in adipose tissue of obese patients with chronic kidney disease. *Wien Klin Wochenschr* 122:466-473
273. **Zoccali C, Mallamaci F** 2011 Does adipose tissue have a key role in inflammation in CKD? *J Intern Med* 269:407-409
274. **Morales E, Valero MA, Leon M, Hernandez E, Praga M** 2003 Beneficial effects of weight loss in overweight patients with chronic proteinuric nephropathies. *Am J Kidney Dis* 41:319-327
275. **Velkoska E, Cole TJ, Morris MJ** 2005 Early dietary intervention: long-term effects on blood pressure, brain neuropeptide Y, and adiposity markers. *Am J Physiol Endocrinol Metab* 288:E1236-1243
276. **Fernandez-Riejos P, Najib S, Santos-Alvarez J, Martin-Romero C, Perez-Perez A, Gonzalez-Yanes C, Sanchez-Margalet V** 2010 Role of leptin in the activation of immune cells. *Mediators Inflamm* 2010:568343
277. **Eder K, Baffy N, Falus A, Fulop AK** 2009 The major inflammatory mediator interleukin-6 and obesity. *Inflamm Res* 58:727-736
278. **Galic S, Oakhill JS, Steinberg GR** 2010 Adipose tissue as an endocrine organ. *Mol Cell Endocrinol* 316:129-139
279. **Lin S, Saxena NK, Ding X, Stein LL, Anania FA** 2006 Leptin increases tissue inhibitor of metalloproteinase 1 (TIMP-1) gene expression by a specificity protein 1/signal transducer and activator of transcription 3 mechanism. *Mol Endocrinol* 20:3376-3388
280. **Nakamura K, Nonaka H, Saito H, Tanaka M, Miyajima A** 2004 Hepatocyte proliferation and tissue remodeling is impaired after liver injury in oncostatin M receptor knockout mice. *Hepatology* 39:635-644
281. **Braunschweig A, Poehlmann TG, Busch S, Schleussner E, Markert UR** 2011 Signal Transducer and Activator of Transcription 3 (STAT3) and Suppressor of Cytokine Signaling (SOCS3) Balance Controls Cytotoxicity and IL-10 Expression in Decidual-Like Natural Killer Cell Line NK-92. *Am J Reprod Immunol*
282. **Rodrigues AL, de Moura EG, Passos MC, Trevenzoli IH, da Conceicao EP, Bonono IT, Neto JF, Lisboa PC** 2011 Postnatal early overfeeding induces hypothalamic higher SOCS3 expression and lower STAT3 activity in adult rats. *J Nutr Biochem* 22:109-117
283. **Bates SH, Stearns WH, Dundon TA, Schubert M, Tso AW, Wang Y, Banks AS, Lavery HJ, Haq AK, Maratos-Flier E, Neel BG, Schwartz MW, Myers MG, Jr.** 2003 STAT3 signalling is required for leptin regulation of energy balance but not reproduction. *Nature* 421:856-859

REFERENCES

284. **Alejandre Alcazar MA, Boehler E, Amann K, Klaffenbach D, Hartner A, Allabauer I, Wagner L, von Horsten S, Plank C, Dotsch J** 2011 Persistent changes within the intrinsic kidney-associated NPY system and tubular function by litter size reduction. *Nephrol Dial Transplant* 26:2453-2465
285. **Straub RH, Schaller T, Miller LE, von Horsten S, Jessop DS, Falk W, Scholmerich J** 2000 Neuropeptide Y cotransmission with norepinephrine in the sympathetic nerve-macrophage interplay. *J Neurochem* 75:2464-2471
286. **Dimitrijevic M, Stanojevic S, Micic S, Vujic V, Kovacevic-Jovanovic V, Mitic K, von Horsten S, Kosec D** 2006 Neuropeptide Y (NPY) modulates oxidative burst and nitric oxide production in carrageenan-elicited granulocytes from rat air pouch. *Peptides* 27:3208-3215
287. **Bedoui S, Lechner S, Gebhardt T, Nave H, Beck-Sickinger AG, Straub RH, Pabst R, von Horsten S** 2002 NPY modulates epinephrine-induced leukocytosis via Y-1 and Y-5 receptor activation in vivo: sympathetic co-transmission during leukocyte mobilization. *J Neuroimmunol* 132:25-33
288. **White CL, Whittington A, Barnes MJ, Wang Z, Bray GA, Morrison CD** 2009 HF diets increase hypothalamic PTP1B and induce leptin resistance through both leptin-dependent and -independent mechanisms. *Am J Physiol Endocrinol Metab* 296:E291-299
289. **Ozcan L, Ergin AS, Lu A, Chung J, Sarkar S, Nie D, Myers MG, Jr., Ozcan U** 2009 Endoplasmic reticulum stress plays a central role in development of leptin resistance. *Cell Metab* 9:35-51
290. **Lubis AR, Widia F, Soegondo S, Setiawati A** 2008 The role of SOCS-3 protein in leptin resistance and obesity. *Acta Med Indones* 40:89-95
291. **Ortiz-Munoz G, Lopez-Parra V, Lopez-Franco O, Fernandez-Vizarra P, Mallavia B, Flores C, Sanz A, Blanco J, Mezzano S, Ortiz A, Egido J, Gomez-Guerrero C** 2010 Suppressors of cytokine signaling abrogate diabetic nephropathy. *J Am Soc Nephrol* 21:763-772

ACKNOWLEDGEMENTS

5. ACKNOWLEDGEMENTS

The present study was carried out at the laboratory of Prof. Dötsch at the University of Cologne and at the University Hospital of Erlangen, in cooperation with the Department of Pathology (Prof. Dr. Amann's lab) and the section of experimental therapy (Prof. Dr. v. Hörsten) of the University Hospital of Erlangen as well as with the University of Giessen Lung Centre (Dr. Morty's lab). This work was financially supported by the Erlanger Leistungsbezogene Anschubfinanzierung und Nachwuchsförderung (ELAN), the Collaborative Research Center (SFB) 423: kidney injury: pathogenesis and regenerative mechanisms, and the research grant Köln Fortune of the University of Cologne.

I'm sincerely grateful to my supervisor, Prof. Dr. Jörg Dötsch for providing a unique opportunity to pursue my PhD thesis, for all his teaching, support and patience and the ability to create a stimulating research atmosphere.

I also thank PD Dr. Christian Plank and Prof. Holm Schneider for their teaching and patience with the animal models and the cell culture experiments.

I'm deeply in debt with my colleagues and friends Daniela Klaffenbach, Eva Rother, Christina Vohlen, Julia Dobner, Yvonne Birkner, and Ida Allabauer for all their support, patience, and understanding, also for the stimulating scientific discussions.

Por último, quisiera agradecerles a mis queridos padres Carlota Alcázar Esquinas y Enrique Alejandro Expósito, mi hermano Enrique Alejandro Alcázar, Daniela Alejandro Alcázar y mis dos alegrías Vanessa y Francisca por todo su amor, sus sabios consejos y el apoyo durante mi carrera científica y en medicina. Os llevo y os llevaré en mi corazón por donde me lleve la vida.

6. CURRICULUM VITAE

Personal Data

Name: Miguel Angel Alejandro Alcázar

Address (official): Department of Pediatric and Adolescent Medicine
University of Cologne
Kerpener Strasse 62
D-50937 Cologne

Address (private): Brucknerstrasse 1
D-50931 Cologne

Phone: +49 (0)221 / 27783071 (private)
+49 (0)179 / 7918194 (mobile)
+49 (0)221 / 478 96876 (office)

Email: miguel.alejandre-alcazar@uk-koeln.de

Date of birth: 03/14/1980

Place of birth: Erbach/Odw.

Nationality: Spanish

School education

09/90 – 06/99 Gymnasium Michelstadt, High School diploma (Abitur)
Final grade: 1.6

09/86 – 06/90 elementary school, Bad König

Professional experience

since 07/10 Postdoctoral Fellow, lab of „Perinatal Programming“, Department of Pediatric and Adolescent Medicine, University of Cologne, Germany

10/09 – 06/10 Resident, Department of Pediatric and Adolescent Medicine, University Hospital Erlangen, Germany

03/09 – 09/09 Postdoctoral Fellow [*interdisziplinäres Zentrum für klinische Forschung (IZKF)*], Research lab of the department of Pediatric and Adolescent Medicine, University Hospital Erlangen, Germany

CURRICULUM VITAE

08/06 – 03/09 Resident, Department of Pediatric and Adolescent Medicine, University Hospital Erlangen, Germany

Academic education

12/05 – 05/06 Justus Liebig University Giessen, School of Medicine
Third State examination and Medical license
Final grade: 1.9

06/05 – 08/05 University of Toronto (Canada), Hospital for Sick Children, Department of pediatric surgery, Faculty of Medicine, *Internship*

08/05 – 12/05 Mount Sinai School of Medicine, New York (USA), Department of Pediatrics, *Internship*

05/03 – 05/05 Justus Liebig University Giessen, School of Medicine
Second State examination

09/02 – 04/03 Erasmus Scholarship, Facultad de Medicina de Granada, Spain

09/01 – 08/02 Justus Liebig University Giessen, School of Medicine
First State examination

10/99 – 08/01 Justus Liebig University Giessen, School of Medicine
Physikum

Research Career

06/2009 – to date PhD thesis at the Department of Pediatric and Adolescent Medicine, University Hospital Erlangen (- 06/2010), and University of Cologne (7/2010 – to date) (Prof. Dr. Dötsch's lab): "*Inflammatory response as a mechanism of perinatal programming: long-term impact on pulmonary and renal function?*"
Predicted PhD-completion: summer 2012.

07/2010 – to date Interdisciplinary Program of Molecular Medicine (IPMM), Cologne Dötsch's lab "*Perinatal programming*"

01/2008 – 12/2009 Postdoctoral fellowship in the department of Pediatric and Adolescent Medicine at the University of Erlangen-Nuremberg (Prof. Rascher's and Prof. Dötsch's lab). Project entitled: "Fetal programming of the lung after IUGR"

02/2004 – 08/2006 M.D. thesis in the Morty Laboratory, University of Giessen Lung Center (UGLC), Department of Internal Medicine II.
"*TGF- β /BMP system is dynamically regulated during late lung dedevelopment and altered by hyperoxia-induced lung injury: implication for the pathogenesis of bronchopulmonary dysplasia*"

CURRICULUM VITAE

Awards:

- 04/11 Award for Poster Presentation, Gesellschaft für Pädiatrische Pneumologie (GPP): *“Die frühe postnatalen Hyperalimentation in der IUGR-assoziierten Lungenerkrankung: Induktor inflammatorischer Prozesse?”*
- 04/11 Award for Poster Presentation, Gesellschaft für Pädiatrische Nephrologie (GPN): *“Frühe postnatale Hyperalimentation prädisponiert für Nierenfunktionsstörungen: SOCS3 als zentraler Regulator der renal intrinsischen Leptin-NPY Achse in der Ratte“*
- 04/10 Award for best oral presentation der Süddeutschen Gesellschaft für Kinder- und Jugendmedizin (SGKJ): *„Prädisposition für Atemwegserkrankung nach intrauteriner Wachstumsrestriktion“*

3rd and industrial Funding

- 01/2011 – 12/2011 Seed funding, SFB-829 *“Molecular mechanisms regulating skin homeostasis”*
- 01/2011 – to date Köln Fortune research grant, University of Cologne project entitled: *„Mechanismen der Hautveränderungen nach intrauteriner Wachstumsrestriktion“*
- 11/2008 – 10/2009 ELAN (Erlanger leistungsorientierte Anschubfinanzierung und Nachwuchsförderung), University Hospital of Erlangen, project entitled: *„Einfluss der intrauterinen Wachstumsrestriktion auf Th1/Th2-Verlagerung und pulmonale Inflammation bei allergisch induziertem Asthma bronchiale“*
- 03/2009 – 09/2009 IZKF-research scholarship, University of Erlangen

CURRICULUM VITAE

Publications:

Alejandro Alcázar MA, Vohlen C, Rother E, Plank C, Dötsch J.

Prevention of early postnatal hyperalimentation restores TGF- β /BMP signaling in the lung subsequent to IUGR (in preparation).

Alejandro Alcázar MA, Östreicher I, Appel S, Rother E, Vohlen C, Plank C, Dötsch J. Developmental regulation of Stat3-mediated inflammation: the missing link between intrauterine growth restriction and pulmonary dysfunction? *J Molec Med*, 2012.

Alejandro-Alcázar MA, Boehler E, Rother E, Amann K, von Hörsten S, Plank C, Dötsch J. Early postnatal hyperalimentation leads to impaired renal function partially via renal postreceptor leptin resistance, *Endocrinology*, 2012.

Rother E, Kuschewski R, **Alejandro Alcázar MA**, Oberthuer A, Bae-Gartz I, Vohlen C, Roth B, Dötsch J, Hypothalamic JNK1 and IKK β Activation and Impaired Early Postnatal Glucose Metabolism after Maternal Perinatal High-Fat Feeding, *Endocrinology*. 2012

Alejandro Alcázar MA, Morty RE, Lenzian L, Vohlen C, Oestreicher I, Plank C, Schneider H, Dötsch J. Inhibition of TGF- β Signaling and Decreased Apoptosis in IUGR-Associated Lung Disease in Rats, *PLoS One*, 2011.

Alejandro Alcázar MA, Boehler E, Amann K, Klaffenbach D, Hartner A, Allabauer I, Wagner L., v. Hörsten S., Plank C., Dötsch J. Persistent changes within the intrinsic kidney-associated NPY system and tubular function by litter size reduction, *Nephrol Dial Transplant*, 2011.

Klaffenbach D, Meissner U, Raake M, Fahlbusch F, **Alejandro Alcázar MA**, Allabauer I, Kratzsch J, Rascher W, Dötsch J. Upregulation of leptin-receptor in placental cells by hypoxia, *Regul Pept*. 2011

Schenke C, **Alejandro Alcázar MA**, Holter W, Korn K, Papadopoulos T, Köhler H. Aplastic anemia following hepatitis associated with human herpesvirus 6, *J Pediatr Gastroenterol Nutr*. 2010

Alejandro Alcázar MA, Michiels-Corsten M, Vicencio AG, Reiss I, Ryu J, de Krijger RR, Haddad GG, Tibboel D, Seeger W, Eickelberg O, Morty RE. TGF-beta signaling is dynamically regulated during the alveolarization of rodent and human lungs, *Dev Dyn*, 2008

Alejandro Alcázar MA, Shalamanov PD, Amarie OV, Sevilla-Pérez J, Seeger W, Eickelberg O, Morty RE. Temporal and spatial regulation of bone morphogenetic protein signaling in late lung development, *Dev Dyn*, 2007.

Alejandro Alcázar MA, Kwapiszewska G, Reiss I, Amarie OV, Marsh LM, Sevilla-Pérez J, Wygrecka M, Eul B, Köbrich S, Hesse M, Shermuly RT, Seeger W, Eickelberg O, Morty RE. Hyperoxia modulates TGF- β /BMP signaling in the neonatal lung: implications for the pathogenesis of bronchopulmonary dysplasia, *Am J Physiol Lung Cell Mol Physiol*, 2007.

7. ERKLÄRUNG

Ich versichere, dass ich die mir vorgelegte Dissertation selbständig angefertigt, die benutzten Quellen und Hilfsmittel vollständig angegeben und die Stellen der Arbeit - einschließlich Tabellen, Karten, und Abbildungen - , die anderen Werken im Wortlaut oder dem Sinn nach entnommen sind, in jedem Einzelfall als Entlehnung kenntlich gemacht habe; dass diese Dissertation noch keiner anderen Fakultät oder Universität zur Prüfung vorgelegen hat; dass sie – abgesehen von unten angegebenen Teilpublikationen – noch nicht veröffentlicht worden ist sowie, dass ich eine solche Veröffentlichung vor Abschluss des Promotionsverfahrens nicht vornehmen werde.

Die Bestimmungen dieser Promotionsordnung sind mir bekannt. Die von mir vorgelegte Dissertation ist von **Prof. Dr. med. Jörg Dötsch** betreut worden.

Übersicht der Publikationen (bei Bedarf Seite anfügen):
(veröffentlichte, in Revision sowie submitted (unter Angabe des Journals) einfügen

Ich versichere, dass ich alle Angaben wahrheitsgemäß nach bestem Wissen und Gewissen gemacht habe und verpflichte mich, jedmögliche, die obigen Angaben betreffenden Veränderungen, dem Promotionsausschuss unverzüglich mitzuteilen.

Köln, 08.05.2012
Datum

.....
Miguel Angel Alejandro Alcázar

ERKLÄRUNG

Publikationen:

Alejandro Alcázar MA, Vohlen C, Rother E, Plank C, Dötsch J.

Prevention of early postnatal hyperalimentation restores TGF- β /BMP signaling in the lung subsequent to IUGR (in preparation).

Alejandro Alcázar MA, Östreicher I, Appel S, Rother E, Vohlen C, Plank C, Dötsch J.

Developmental regulation of Stat3-mediated inflammation: the missing link between intrauterine growth restriction and pulmonary dysfunction? J Molec Med, 2012.

Alejandro-Alcázar MA, Boehler E, Rother E, Amann K, von Hörsten S, Plank C, Dötsch J.

Early postnatal hyperalimentation leads to impaired renal function partially via renal postreceptor leptin resistance, Endocrinology, 2012.

Rother E, Kuschewski R, **Alejandro Alcázar MA**, Oberthuer A, Bae-Gartz I, Vohlen C, Roth

B, Dötsch J, Hypothalamic JNK1 and IKK β Activation and Impaired Early Postnatal Glucose Metabolism after Maternal Perinatal High-Fat Feeding, Endocrinology. 2012

Alejandro Alcázar MA, Morty RE, Lenzian L, Vohlen C, Oestreicher I, Plank C, Schneider

H, Dötsch J. Inhibition of TGF- β Signaling and Decreased Apoptosis in IUGR-Associated Lung Disease in Rats, PLoS One, 2011.

Alejandro Alcázar MA, Boehler E, Amann K, Klaffenbach D, Hartner A, Allabauer I,

Wagner L., v. Hörsten S., Plank C., Dötsch J. Persistent changes within the intrinsic kidney-associated NPY system and tubular function by litter size reduction, Nephrol Dial Transplant, 2011.

Inhibition of TGF- β Signaling and Decreased Apoptosis in IUGR-Associated Lung Disease in Rats

Miguel Angel Alejandro Alcázar^{1*}, Rory E. Morty², Lisa Lenzian³, Christina Vohlen¹, Iris Oestreicher⁴, Christian Plank³, Holm Schneider³, Jörg Dötsch¹

1 Department of Pediatrics and Adolescent Medicine, University of Cologne, Cologne, Germany, **2** Department of Internal Medicine, University of Giessen Lung Centre, Justus-Liebig University, Giessen, Germany, **3** Department of Pediatrics and Adolescent Medicine, University Hospital Erlangen, Erlangen, Germany, **4** Department of Neonatology, Charité University Medical Center, Berlin, Germany

Abstract

Intrauterine growth restriction is associated with impaired lung function in adulthood. It is unknown whether such impairment of lung function is linked to the transforming growth factor (TGF)- β system in the lung. Therefore, we investigated the effects of IUGR on lung function, expression of extracellular matrix (ECM) components and TGF- β signaling in rats. IUGR was induced in rats by isocaloric protein restriction during gestation. Lung function was assessed with direct plethysmography at postnatal day (P) 70. Pulmonary activity of the TGF- β system was determined at P1 and P70. TGF- β signaling was blocked *in vitro* using adenovirus-delivered Smad7. At P70, respiratory airway compliance was significantly impaired after IUGR. These changes were accompanied by decreased expression of TGF- β 1 at P1 and P70 and a consistently dampened phosphorylation of Smad2 and Smad3. Furthermore, the mRNA expression levels of inhibitors of TGF- β signaling (Smad7 and Smurf2) were reduced, and the expression of TGF- β -regulated ECM components (e.g. collagen I) was decreased in the lungs of IUGR animals at P1; whereas elastin and tenascin N expression was significantly upregulated. *In vitro* inhibition of TGF- β signaling in NIH/3T3, MLE 12 and endothelial cells by adenovirus-delivered Smad7 demonstrated a direct effect on the expression of ECM components. Taken together, these data demonstrate a significant impact of IUGR on lung development and function and suggest that attenuated TGF- β signaling may contribute to the pathological processes of IUGR-associated lung disease.

Citation: Alejandro Alcázar MA, Morty RE, Lenzian L, Vohlen C, Oestreicher I, et al. (2011) Inhibition of TGF- β Signaling and Decreased Apoptosis in IUGR-Associated Lung Disease in Rats. PLoS ONE 6(10): e26371. doi:10.1371/journal.pone.0026371

Editor: Dominik Hartl, University of Tübingen, Germany

Received: July 18, 2011; **Accepted:** September 25, 2011; **Published:** October 20, 2011

Copyright: © 2011 Alejandro Alcázar et al. This is an open-access article distributed under the terms of the Creative Commons Attribution License, which permits unrestricted use, distribution, and reproduction in any medium, provided the original author and source are credited.

Funding: The animal experiments were in part supported by a grant to Jörg Dötsch, Christian Plank and Wolfgang Rascher by the Deutsche Forschungsgemeinschaft, Bonn, Germany; SFB 423, Collaborative Research Centre of the German Research Foundation: Kidney Injury: Pathogenesis and Regenerative Mechanisms, Project B13; by a grant to Christian Plank and Miguel Angel Alejandro Alcázar by the Erlanger Leistungsbezogene Anschubfinanzierung und Nachwuchsförderung (ELAN) Erlangen; and by a grant to Miguel Angel Alejandro Alcázar by Köln Fortune, University of Cologne. The funders had no role in study design, data collection and analysis, decision to publish, or preparation of the manuscript.

Competing Interests: The authors have declared that no competing interests exist.

* E-mail: miguel.alejandre-alcazar@uk-koeln.de

Introduction

The term fetal programming reflects the assumption that a temporary environmental influence during intrauterine development may lead to permanent alterations of physiological processes later in life [1], [2], [3]. Intrauterine undernourishment can represent such an environmental factor, leading to intrauterine growth restriction (IUGR) and, in most cases, to low birth weight (LBW). Furthermore, there is evidence that being born with LBW also has an impact on lung development and function [4], [5], [6].

Organogenesis of the lung occurs in five stages: 1.) the embryonic stage, 2.) the pseudoglandular stage, 3.) the canalicular stage, 4.) the sacular stage, and 5.) the alveolar stage. A sixth stage - microvascular maturation - has also been proposed [7]. The process of lung development is highly regulated and thus susceptible to modification by perinatal environmental conditions [7], [8]. Consequently, disturbed intrauterine growth may induce changes in lung structure, which predispose lungs to later disease. Several observational studies have described decreased lung function with reduced forced expiratory volume in one second (FEV₁) in young infants [9], in school children [10], and in young

adults born with LBW [11], [12]. The terms IUGR and “small for gestational” age (SGA) are often used synonymously, but the distinction between them is important. IUGR is the pathological form of SGA. It affects growth and predisposes to diseases later in life. Intrauterine protein restriction has been shown to be a reliable animal model of IUGR [13], [14], and several animal studies addressing structural changes of the pulmonary system have also demonstrated reduced lung function following IUGR [15], [16], [17].

Lung structure and function are determined during early and late lung development [18], [19], [20]. While the pathogenic processes leading to IUGR-associated lung disease have not yet been elucidated, extracellular matrix (ECM) and its maintenance during alveolarization is thought to play a pivotal role in disease pathogenesis [21], [22]. Disruption of critical signaling pathways may be involved [19], [23], including signaling by the transforming growth factor (TGF)- β superfamily [23], [24]. TGF- β signaling is initiated by binding of TGF- β to the type II TGF- β receptor (T β RII), which then forms a complex with either the type I receptor (T β RI) or activin A receptor type II-like 1 (Acvr11, also called ALK-1). The type I receptor transmits signals within the cell

via second-messenger Smad proteins, namely Smad1-Smad4, or by Smad-independent pathways [25]. TGF- β signaling is also regulated by Smad6 and Smad7, inhibitory Smads which antagonize TGF- β signaling. Several studies have indicated that TGF- β signaling plays a critical and finely tuned role in pulmonary branching and alveolarization [18], [23], since TGF- β ligands inhibited airway branching *in vitro* [26], [27]. Furthermore; abrogation of TGF- β signaling by genetic ablation of T β RII [28], Smad2, Smad3 or Smad4 enhanced lung branching *in vitro* [29]. Consistent with these observations, overexpression of Smad7 promoted lung branching [30]. However, conditional overexpression of the TGF- β 1 gene in the mouse lung during the postnatal period disrupts lung development [31]. Interestingly, Smad3 deficiency in mice results in progressive airspace enlargement with age [32]. These studies implicate TGF- β signaling as a regulator of lung branching and alveolarization. Together with reports that TGF- β might be associated with fetal growth in pregnancy [33], they have led us to hypothesize that IUGR due to protein restriction during gestation may influence TGF- β signaling and contribute to impaired lung function and structural changes in later life.

Methods

Induction of intrauterine growth restriction

All procedures performed on animals were done in accordance with the German regulations and legal requirements and were approved by the local government authorities (Regierung von Mittelfranken, AZ # 621-2531.31-11/02 and AZ # 621-2531.31-14/05).

Adult and neonatal Wistar rats were housed in humidity- and temperature controlled rooms on a 12:12-h light-dark cycle. IUGR in rats was induced as previously described [14]. In brief, virgin female Wistar rats were obtained from our own colony. Dams were time-mated by the appearance of sperm plugs, then fed either a normal diet containing 17.0% protein (control group) or a low protein isocaloric diet containing 8.0% protein (casein) throughout pregnancy (IUGR group). Diets were obtained from Altromin, Germany (# C1000, C1003). Rats delivered spontaneously at day 23 of pregnancy. On the first postnatal day (P1) the litters were reduced to six pups per dam. During lactation, dams were fed standard chow. Weaning was at P23. IUGR and control animals were sacrificed at P1 and P70 and assigned to four groups: IUGR P1, Control P1, IUGR P70, and Control P70. Body weight and weight of the lung were obtained immediately after sacrificing the animals. Means \pm standard error of the mean were calculated.

Measurement of airway responsiveness

At P70, lung function was assessed by measuring respiratory system dynamic compliance (C_{dyn}) with direct plethysmography (FinePointeTM RC; Wellington, NC, USA). C_{dyn} is defined as a measure of the ability of the lung to distend in response to pressure. Decreased compliance means that a greater change in pressure is needed for a given change in volume, as in atelectasis, edema, fibrosis, pneumonia, or absence of surfactant. Rats were deeply anesthetized by intramuscular injection of ketamine (100 mg/kg body weight) and midazolam (5 mg/kg body weight), tracheotomized and ventilated. C_{dyn} was measured at baseline.

Processing of lung tissue and morphometric analysis

Following anesthesia with ketamine (100 mg/kg body weight) and midazolam (5 mg/kg body weight) the animals were exsanguinated by aortic transection. Neonatal animals at P1 were

euthanized by decapitation. The right lobe of the lung was removed after ligation of the bronchus, and one portion was immediately snap-frozen in liquid nitrogen for mRNA and protein analysis. The left lobe was inflated via tracheotomy and pressure-fixed at 20 cm H₂O with 4% (mass/vol) paraformaldehyde, and the trachea was ligated. Lungs and hearts were excised *en bloc*, submersed in 4% (mass/vol) paraformaldehyde overnight for paraffin embedding and sectioning as described previously [34]. Paraffin sections (1 μ m) were mounted on poly-L-lysine-coated glass slides, dewaxed with xylene (3–5 min) and rehydrated in a graduated series of ethanol solutions (100%, 95%, and 70% (vol/vol), finally PBS). The mean linear intercept (MLI) and septal thickness were determined on sections stained for smooth muscle actin and counter-stained with hematoxylin and eosin as described previously [35], [36].

RNA extraction and real-time PCR

Total RNA was isolated from unfixed lung tissue or cultured cells as previously described [37], followed by DNase treatment to remove any contaminating genomic DNA. Total RNA was screened for mRNA encoding ALK-1, ALK-5, T β RII, T β RIII, Smad2, Smad3, Smad4, Smad6, Smad7, Smurf2, elastin (Eln), tenascin N (TenN), collagen I (Coll I), collagen III (Coll III), fibrillin (Fbl), matrix metalloproteinases (MMP) 2, MMP 9, tissue inhibitor of matrix metalloproteinases (TIMP) 1, TIMP 2, plasminogen activator inhibitor-1 (PAI-1), surfactant protein A (SP-A), SP-C, and SP-D. Quantitative changes in mRNA expression were assessed by quantitative real-time PCR as described previously [14] using the IQTM SYBR-Green[®] Supermix and a BioRad iQ5-Cycler (Bio-Rad Laboratories, Hercules, CA, USA) or the 7500 Real-time PCR system (Applied Biosystem, Foster City, CA, USA) [14]. In all samples, the relative amount of specific mRNA was normalized to the ubiquitously expressed glyceraldehyd-3-phosphat-dehydrogenase (GAPDH) and β -actin gene. Primer pairs and TaqMan probes are listed in Table 1. Oligonucleotides were designed with Primer Express software (Perkin-Elmer, Foster City, CA, USA).

Protein detection by immunoblot

Frozen unfixed lung tissue was homogenized in lysis buffer as previously described [14]. Cultures cells were harvested using a cell scraper and lysed in the same buffer. Protein concentration was determined with a Bio-Rad DC protein assay (Bio-Rad, Hercules, CA). Lysates resolved on a 10% reducing SDS-PAGE gel were transferred to a nitrocellulose membrane. Blots were probed with the following antibodies: polyclonal rabbit-anti-rat-phospho Smad2 (Cell Signaling, Danvers, MA, # 3101, 1:1000), monoclonal rabbit-anti-rat-phospho Smad3 (Cell Signaling, Danvers, MA, # 9520, 1:1000), polyclonal rabbit-anti-rat-Smad2/3 (Cell Signaling, Danvers, MA, # 3102, 1:1000), polyclonal rabbit-anti-rat-Smad4 (Cell Signaling, Danvers, MA, # 9515), polyclonal rabbit-anti-rat-Smad7 (R&D Systems, Wiesbaden, Germany, MAB2029, 1:1000), polyclonal rabbit-anti-rat-cleaved Caspase-3 (Cell Signaling, Danvers, MA, # 9661, 1:1000), polyclonal rabbit-anti-rat-Caspase-3 (Cell Signaling, Danvers, MA, # 9662, 1:1000), polyclonal rabbit-anti-rat-poly (ADP-ribose) polymerase (PARP) (Cell Signaling, Danvers, MA, # 9542, 1:2000), monoclonal mouse-anti-rat-proliferating cell nuclear antigen (PCNA) (DAKO, Glostrup, Denmark, Clone PC10, M0879, 1:10.000). Monoclonal mouse-anti-rat- β -Actin (Cell Signaling, Danvers, MA, # 3700, 1:1000) served as a loading control. Anti-mouse IgG, HRP-linked (Cell Signaling, Danvers, MA, # 7076, 1:2000), and HRP-linked anti-rabbit IgG (Cell Signaling, Danvers, MA, # 7074, 1:2000) were used as secondary antibodies.

Table 1. Primer pairs and TaqMan probes used.

PAI-1	forward 5'-TCCGCCATCACCAACATTTT-3' reverse 5'-GTCAGTCATGCCAGCTTCTC-3' probe 5'(FAM)- CCGCCTCTCATCCTGCCT-AAGTTCTCT-(TAMRA)3'
TGFβ-1	forward 5'-CACCCGCGTGAATGGT-3' reverse 5'-GGCACTGCTTCCCGAATG-3' probe 5'(FAM)-ACCGCAACAACGCAATC-TATGACA-(TAMRA)3'
tgfbr1	forward 5'-ACCGCGTGCCAAATGAAGAGGAT-3' reverse 5'-GGTAAACCTGATCCAGACCTGAT-3'
Tgfbr2	forward 5'-GAGCAACTGCAGCGTACC-3' reverse 5'-CCAGAGTAATGTTCTGTCTC-3'
Tgfbr3	forward 5'-CTTGACAGCAGAAACAGAGG-3' reverse 5'-AAACACTTGATCTTCCAC-3'
Smad2	forward 5'-AATTACATCCAGAAACACCAC-3' reverse 5'-TGTCATACTTTGGTTCAACTG-3'
Smad3	forward 5'-CACCAGTGCTACCTCAGTGT-3' reverse 5'-TAGTGTCTCCGGGATGGAA-3'
Smad4	forward 5'-CTACTTACCACATAAC-AGCACTACCA-3' reverse 5'-GTGCTGAAGATGGCCGTTTT-3'
Smad6	forward 5'-CCCCCTATTCTCGGCTGTCT-3' reverse 5'-TGGTGGCCTCGGTTTCA-3'
Smad7	forward 5'-AGATACCCGATGGATTTTCTCAA-3' reverse 5'-TCGTTCCCGGTTTCA-3'
Smurf2	forward 5'-GGTCTCAGCAGACATAGAAATACATG-3' reverse 5'-TGTTGTGTTCTCTGTTTCAAGC-3'
SARA	forward 5'-GCCAAGTGCTATCCTAATTC-3' reverse 5'-ACTGCCCTTCTGTTGTCTGA-3'
Elastin	forward 5'-GAAAACCCCGAAGCCCT-3' reverse 5'-CCCCACTTGATATCCAGG-3'
Tenascin N	forward 5'-AGGTGGACTATTACAAGTTCGGTAT-3' reverse 5'-GCAGACCGGTGATGTCATATCTAC-3'
Collagen I α	forward 5'-AGAGCGGAGAGTACTGGATCGA-3' reverse 5'-CTGACCTGTCTCCATGTTGCA-3' probe 5'(FAM)-CAAGGCTGCAACCTGGA-TGCCATC-(TAMRA)3'
Collagen III	forward 5'-GGACCTCTGGTGCTATTG -3' reverse 5'-GAATCCAGGATACCAGTG-3'
Fibrillin	forward 5'-TGCTCTGAAAGGACCCCAATGT-3' reverse 5'-CGGACAAACAGTATGCGTTATAAC-3'
mCollagen I	forward 5'-TCACCTACAGCACCCTTGTGG -3' reverse 5'-CCCAAGTTCGGGTGTGACTC-3'
mTenascin N	forward 5'-AGAAGCTGAACCGGAAGTTGAC-3' reverse 5'-CGTCTGGAGTGGCATCTGAAA-3'
mElastin	forward 5'-GGCTTTGGACTTCTCCATT-3' reverse 5'-CCACCTTGGTATCCAGGG-3'
mMMP-2	forward 5'-ATGCGGAAGCAAGATGTG-3' reverse 5'-GTCCAGGTCAGGTGTGTAAC-3'
mβ-Actin	forward 5'-GACATCAGGAAGGATCTCTATG-3' reverse 5'-CTTCTGCATCTGTGAGCA-3'
SP-A	forward 5'-GGGATAGTAGCATGTCTGTGT-3' reverse 5'-CGTCTGCATCTGTGAGCA-3'
SP-C	forward 5'-CCTGAGTGAACACAGACACCAT-3' reverse 5'-GTCAGGAGCCGCTGGTAGTC-3'
SP-D	forward 5'-TAGAGGCTGCCTTTTCTCGTAT -3' reverse 5'-GCCGCCCTGAAGATTTTGT-3'
TIMP-2*	forward 5'-TCAAAGGACCTGACAAGGACATC-3' reverse 5'-CGCCTTCCCTGCAATTAGATAT-3' probe 5'(FAM)-TCTACACGGCCCTCTCAGCA-(TAMRA)3'

Table 1. Cont.

MMP-2*	forward 5'-CTGGAGATACAATGAAGTAAAGAAGA-AAAT-3' reverse 5'-CACGACTGCATCCAGGTTATCA-3' probe 5'(FAM)-TTTCCCAGGCTCATCGAGA-CTCC-(TAMRA)3'
GAPDH	forward 5'-ACGGGAAACCCATCACCAT-3' reverse 5'-CCAGCATACCCCATTTGA-3' probe 5'(FAM)-TTCCAGGAGCGAGATCCC-GTCAAG-(TAMRA)3'

*TIMP-1, TIMP-2 and MMP-2 were detected by TaqMan realtime-PCR analysis.

doi:10.1371/journal.pone.0026371.t001

Densitometric analysis of protein bands was performed using Advanced Image Data Analyzer-Software (Version 4.15, Fuji Photo Film Co., Omiyama, Japan) and Bio-Rad ImageLab software (Bio-Rad, Munich, Germany). Band intensities from samples were normalized for loading using the β-actin band from the same sample.

Immunostaining of lung tissue sections

Expression of Smad molecules was assessed on 1-μm tissue sections, prepared as described above for morphometric analysis. Antigen retrieval and quenching of endogenous peroxidase activity with 3% (vol/vol) H₂O for 20 min was performed. Sections were incubated with the relevant primary antibody: polyclonal rabbit-anti-rat-phospho Smad2 (Cell Signaling, Danvers, MA, # 3101, 1:1000) or monoclonal rabbit-anti-rat-phospho Smad3 (Cell Signaling, Danvers, MA, # 9520, 1:100). Immune complexes were visualized with an avidin/biotin-DAB (3,3'-diaminobenzidine) detection system (Vector Lab, Burlingame, CA, USA). Each slide was counterstained with hematoxylin.

Optimization of the multiplicity of infection (M.O.I.)

NIH/3T3, MLE-12 and mouse endothelial cells were seeded in 24-well tissue culture plates at a density of 1×10^4 /well, incubated for approximately 12 h until 50% confluent, washed with PBS and then incubated in serum-free OptiMEM medium (Invitrogen, Darmstadt, Germany; 1000 μl per well) for 30 min at 37°C before addition of the virus. To define the best suitable multiplicity of infection (M.O.I.), an adenoviral LacZ vector (AdLacZ) carrying a β-galactosidase reporter gene was used. AdLacZ was diluted in PBS to a final concentration of 1×10^6 plaque forming units (p.f.u.)/μl, applied to the cells with increasing M.O.I. (10, 50, 100, 200 and 500 μl per well), followed by incubation of the cells at 37°C for 3 h. The volume of the culture medium was then increased by addition of OptiMEM (1500 ml per well). After incubation for 6 h the medium was replaced by the appropriate culture medium containing FCS and the incubation was continued for a total of 48 h. All experiments were performed in triplicate. After 48 h of incubation cells were fixed in 2% formaldehyde/0.2% glutaraldehyde for 15 min, washed with PBS supplemented with 0.02% Nonidet P40 and analyzed for nuclear bacterial β-galactosidase activity indicated by the characteristic blue staining in a PBS solution containing K₃Fe(CN)₆ (5 mM), K₄Fe(CN)₆ (5 mM), MgCl₂ (2 mM), 0.02% Nonidet P40, 0.01% sodium deoxycholate and X-gal (5-bromo-4-chloro-3-indolyl-β-D-galactopyranoside dissolved in N,N-dimethylformamide) at a concentration of 0.8 mg/ml. The cells were stained overnight protected from light.

Infection with an adenoviral Smad7 vector

The E1A/E1B-deleted adenoviral vector AdSmad7 was diluted in PBS to a final concentration of 1×10^6 p.f.u./ μ l and applied to the cells (NIH/3T3, MLE-12, and mouse endothelial cells) at an M.O.I. of 100. The incubation was continued for a total of 48 h. All experiments were performed in triplicate.

AdSmad7-infected cells were stimulated with TGF- β 1 (2 ng/ml) for 12 and 24 h. The cells were then lysed and processed for mRNA extraction. Uninfected cells served as control.

Data analysis

The results of real-time RT-PCR were calculated based on the $\Delta\Delta C_t$ method and expressed as fold induction of mRNA expression compared to the corresponding control group (1.0-fold induction). For quantitative immunoblot analysis densitometry was performed and values were normalized to β -actin. Two-tailed Mann-Whitney test and one-way ANOVA followed by a Bonferroni post-test were used to assess the significance of differences between IUGR and control animals at given time points. A p value < 0.05 was considered as significant. All results are shown as means \pm standard error of the mean.

Results

Auxometry of neonatal and adult rats after IUGR

A marked effect of low protein diet during gestation on growth, as assessed by body length and body weight, was observed (Figure 1A). At day P1 average body weight (5.86 ± 0.092 g) of the undernourished pups (IUGR) was significantly lower than that of age-matched pups of mothers fed with normal protein (control group: 4.55 ± 0.068 g). However, by P70 the IUGR group exhibited a slightly reduced body mass (383 ± 6.32 g) in comparison with the control group (416 ± 4.61 g). This difference was not significant when tested by one-way ANOVA followed by Bonferroni post-test (Figure 1A). Thus, low protein diet during gestation led to IUGR without affecting survival or adult body weight.

Lung morphology of adult rats formerly affected by IUGR

Total lung weight at P1 and P70 did not differ between IUGR and control animals. However, alveolar development was impaired in IUGR animals, evident by fewer and larger air spaces (Figure 1B), compared to animals with appropriate birth weight. The mean linear intercept (MLI) is roughly inversely proportional to the alveolar surface (37). By P70, IUGR animals exhibited a MLI approximately 30% lower than that of the control group. To evaluate the interstitium and accumulation of ECM components we assessed septal thickness. There were no differences between IUGR and Co.

Respiratory parameters of adult rats formerly affected by IUGR

A marked effect of IUGR on dynamic respiratory compliance (C_{dyn}) was observed at P70. IUGR animals exhibited a C_{dyn} 40% lower than that of age-matched controls (Figure 1C). C_{dyn} reflects the elasticity and function of the pulmonary connective tissue. Interestingly, lung compliance was significantly lower in IUGR animals under baseline conditions.

Expression pattern of surfactant protein A (SP-A), SP-C, SP-D

To address surface tension as a regulator of lung compliance, we assessed mRNA expression of genes encoding surfactant protein A

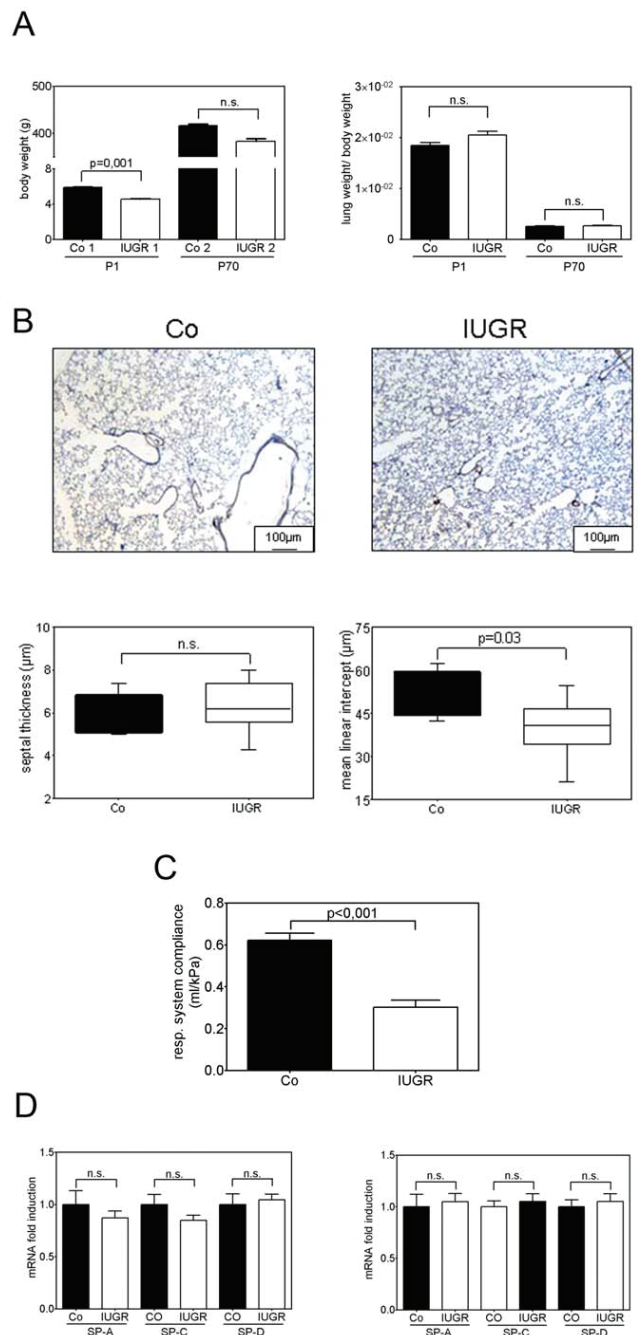


Figure 1. Body weight, respiration and physiological lung parameters of IUGR rats. A: Body weight (g) and relative lung weight (lung weight/body weight) of rats after IUGR (white bars) and control rats (black bars) at days P1 and P70; $n=8-15$ for each bar. B: Architectural changes in lung structure were evident in hematoxylin and eosin-stained lung sections from IUGR rats and control rats at day P70. Measurement of septal thickness (μ m) and mean linear intercept (MLI; μ m) in IUGR rats and control rats (CO) at day P70; $n=6-10$ for each bar. C: Assessment of respiratory system compliance by whole body plethysmography in IUGR rats (white bars) and in the control group (CO; black bars) at P70. $n=15-17$ for each bar. D: Expression pattern of genes encoding surfactant protein A (SP-A), SP-C, and SP-D. IUGR rats (white bars) and control group (black bars). $n=6-15$ for each bar. The significance for each bar is indicated by p values, IUGR vs. Co, n.s. = not significant; two-tailed Mann-Whitney test. doi:10.1371/journal.pone.0026371.g001

(SP-A), SP-C, and SP-D at P1 and P70. There was no significant difference detectable, neither at P1 nor at P70 (Figure 1D).

Effect of IUGR on TGF- β -induced ECM proteins and modulators of the ECM in neonatal and adult rat lungs

To address whether the dramatic alterations in dynamic respiratory compliance (C_{dyn}) and respiratory system resistance (Res) in IUGR animals are associated with altered expression of ECM components, we assessed the mRNA levels of genes encoding ECM molecules. Expression of collagen I, collagen III, fibrillin (Figure 2A) and the ECM regulators MMP-9 and TIMP-1 (Figure 2B) was downregulated at the critical developmental time point P1. In contrast, the expression of elastin (Eln), tenascin N (TenN) (Figure 2A), as well as that of MMP-2, a regulator of ECM remodeling enzymes, and its inhibitor TIMP-2 (Figure 2B) was

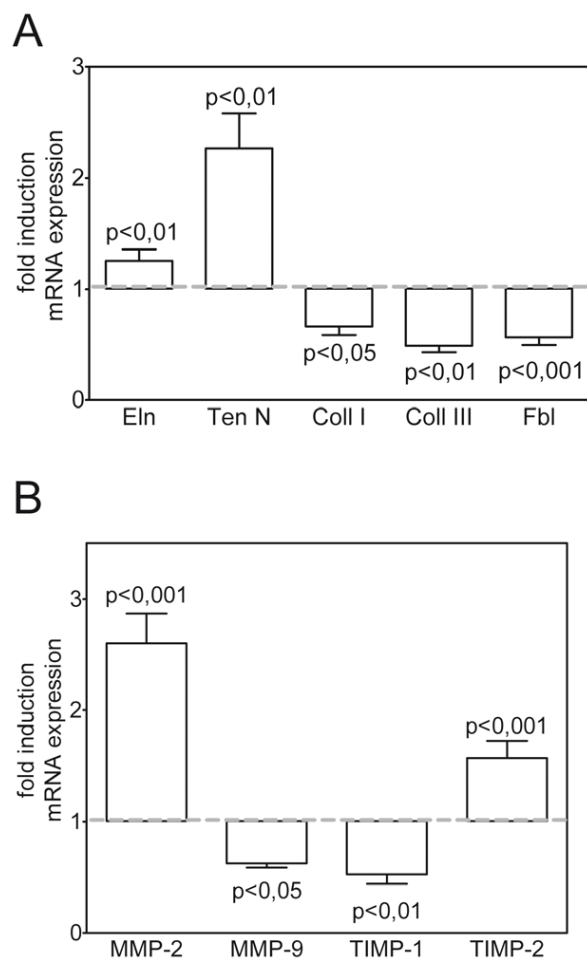


Figure 2. Effect of IUGR on the expression of extracellular matrix (ECM) proteins and modulators of the ECM in neonatal rat lungs. Expression of TGF- β -regulated genes encoding elastin (Eln), tenascin N (Ten), collagens (Coll) I, Coll III, and Fibrillin (A), and genes of ECM modulators including matrix metalloproteinase (MMP)-2, MMP-9, tissue inhibitor of metalloproteinases (TIMP)-1, and TIMP-2 (B) in lungs extracted at day P1 from neonatal rats after IUGR and control rats. The mRNA expression, illustrated as relative fold induction, was assessed by real-time PCR. The control group was normalized to 1 as indicated by a scattered line; $n = 15$ for each group. The significance for each bar is indicated by p values, IUGR vs. Co; two-tailed Mann-Whitney test. doi:10.1371/journal.pone.0026371.g002

elevated. These results indicate a dysregulated composition and remodelling of the ECM during the stage of alveolarization.

Effect of IUGR on the expression of TGF- β 1 and the methylation of CpG islands of the promoter region of TGF- β 1

To address whether the alterations in the expression of ECM components at the critical phase of lung development at P1 are associated with an altered expression of the growth factor TGF- β 1 in the neonatal lungs of IUGR rats, we measured the expression of the gene encoding TGF- β 1 and the TGF- β responsive gene PAI-1. Both TGF- β 1 mRNA and protein were decreased in IUGR pups at P1 (Figure 3A, Figure 3B), consistent with the downregulation of expression of the TGF- β -responsive gene PAI-1 at P1 (Figure 3A). TGF- β 1 protein was detected at lower amounts in lungs of IUGR animals at P70 (Figure 3B, 3C).

Next, we wanted to investigate why the expression of the ligand TGF- β 1 is changed after IUGR. Therefore we analyzed the methylation of CpG islands in the promoter region of the TGF- β 1 gene by PCR amplification of bisulfite-treated DNA, separation by agarose gel electrophoresis, and gel extraction and purification of the PCR products. Analysis of the PCR products did not reveal any significant difference of methylation in lungs of IUGR rats compared to the controls (data not shown).

Effect of IUGR on the expression of TGF- β signaling molecules in rat lungs

Next, we assessed expression of the components of TGF- β signaling by quantitative real-time PCR. The results demonstrate a significant increase of the transforming growth factor receptor type I (T β RI) and T β RIII in lungs of IUGR animals, but no changes for T β RII at P1. At P70 the expression of the receptors did not differ between the two groups (Figure 4A). The mRNA expression of the regulatory Smad2 was reduced, whereas the mRNA levels of Smad3 and Smad4 were significantly increased at P1. At P70 Smad2 expression was downregulated, while no remarkable difference for Smad3 or Smad4 was observed (Figure 4B). Expression of the inhibitory molecule of the TGF- β system, Smad7, was slightly decreased and expression of Smad-specific E3 ubiquitin protein ligase 2 (Smurf2), which inhibits Smad2 and Smad3, was significantly reduced. The expression of Smad anchor for receptor activation (Sara) as a protein presenting Smad2 and Smad3 to the TGF- β -receptors, was significantly increased (Figure 4C).

Additionally, where antibodies were available, lung homogenates at P1 and P70 were probed by immunoblotting to investigate whether IUGR due to undernourishment during gestation resulted in changes on the protein level between IUGR and control groups. Indeed, pronounced alterations were observed for some intracellular signaling components of the TGF- β system. The abundance of co-Smad4 and of inhibitory Smad7 was decreased at P1 (Figure 5A). At P70 the expression of Smad4 was unchanged, while expression of Smad7 was persistently downregulated (Figure 5A). The expression of regulatory Smad2 and Smad3, transducers of TGF- β signals, was altered neither at P1 nor at P70 (Figure 5A).

Effect of IUGR on the activity and localization of TGF- β signaling in rat lungs

The results obtained so far indicate a regulation of the expression of the TGF- β system due to IUGR. To further elucidate whether the activity of TGF- β signaling was changed in lungs of IUGR rats, we analyzed the phosphorylation of

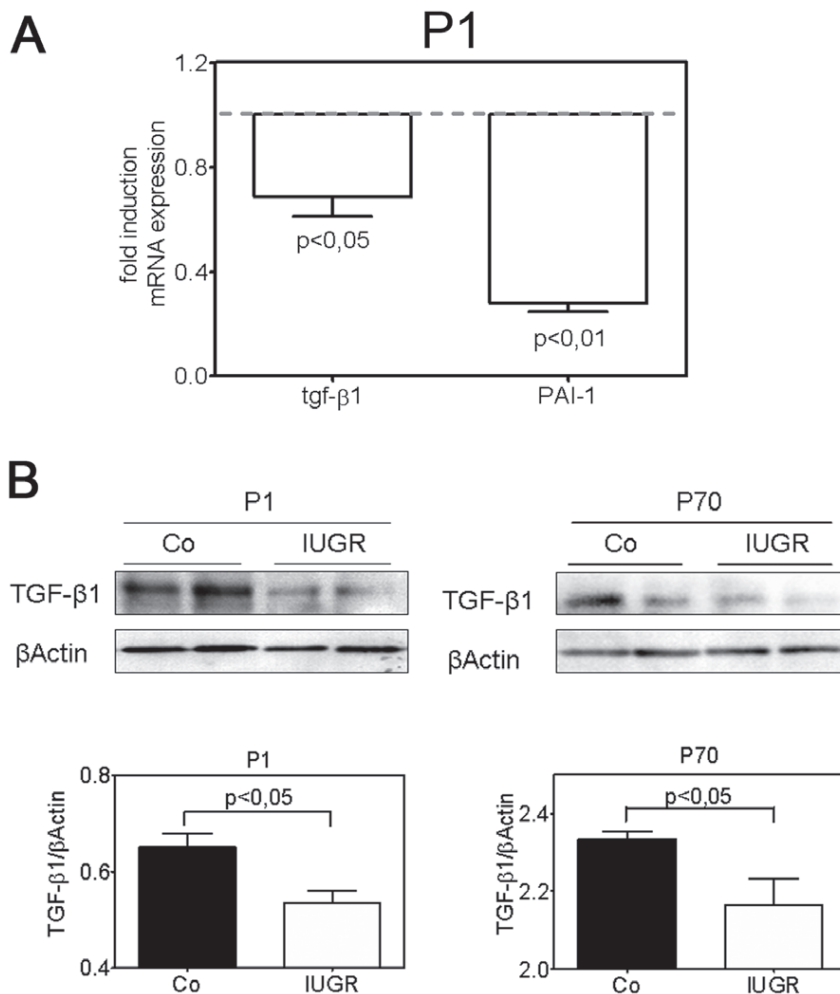


Figure 3. Effect of IUGR on the expression of TGF- β 1 in lungs of neonatal and adult rats. A: Expression of genes encoding TGF- β 1 and TGF- β -inducible plasminogen activator inhibitor-1 (PAI-1) during late lung development (day P1). The mRNA expression was assessed by quantitative real-time PCR. The control group was normalized to 1 as indicated by a scattered line; $n = 15$ for each group. The significance for each bar is indicated by p values, IUGR vs. Co; two-tailed Mann-Whitney test. B: representative immunoblots illustrating expression of TGF- β 1 in lungs extracted at day P1 and P70 from rats with and without IUGR. β -actin served as loading control. Immunoblot data were quantified for both day P1 and P70; $n = 6$ for each bar. The significance for each bar is indicated by p values, IUGR vs. Co; two-tailed Mann-Whitney test. doi:10.1371/journal.pone.0026371.g003

intracellular Smad2 and Smad3 by immunoblot. At P1 and P70 phosphorylation of Smad2 and Smad3 was significantly diminished (Figure 5B), indicating that the activity of TGF- β signaling was decreased in lungs of IUGR rats.

To localize the activity of TGF- β signaling within the different compartments of the lung we performed immunohistochemical analysis of lung tissue at P70. Consistent with the immunoblotting data, the phosphorylation of both Smad2 and Smad3 was less in the bronchi and in the alveoli of lungs after IUGR (Figure 5C).

Effect of IUGR on apoptosis in neonatal and adult rat lungs

The observed impaired pulmonary TGF- β signaling in IUGR rats is likely to influence apoptosis and proliferation during the vulnerable perinatal period and may thereby contribute to the increase in alveolar surface and lung tissue in adulthood. Therefore, we next sought to examine key markers of apoptosis and proliferation in the developing lung at P1 and in the adult lung at P70. We assessed expression of caspase-3 and polyclonal rabbit-

anti-rat-poly (ADP-ribose) polymerase (PARP) by immunoblotting. Total caspase 3 levels were reduced in lungs of IUGR rats at P1 at P70, whereas PCNA levels were not changed. Additionally, cleaved caspase-3 and the cleaved fragment of PARP were markedly diminished after IUGR at both time points, indicating decreased apoptosis in lungs after of IUGR rats (Figure 6).

Effect of the inhibition of the TGF- β signaling by adenoviral Smad7 on the expression of extracellular matrix proteins

The inhibition of TGF- β signaling by AdSmad7 was confirmed by immunoblotting of both phospho-Smad2 and phospho-Smad3. Additionally we assessed baseline transcriptional activity of the cells infected by AdSmad7. Accordingly, the induction of transcription was normalized to AdSmad7/Co (Figure 7A).

To assess the impact of TGF- β signaling on the expression of ECM components, we next performed cell culture experiments. Phosphorylation of Smad2 and Smad3 was inhibited by infecting NIH/3T3 cells (fibroblasts), MLE-12 epithelial cells and murine

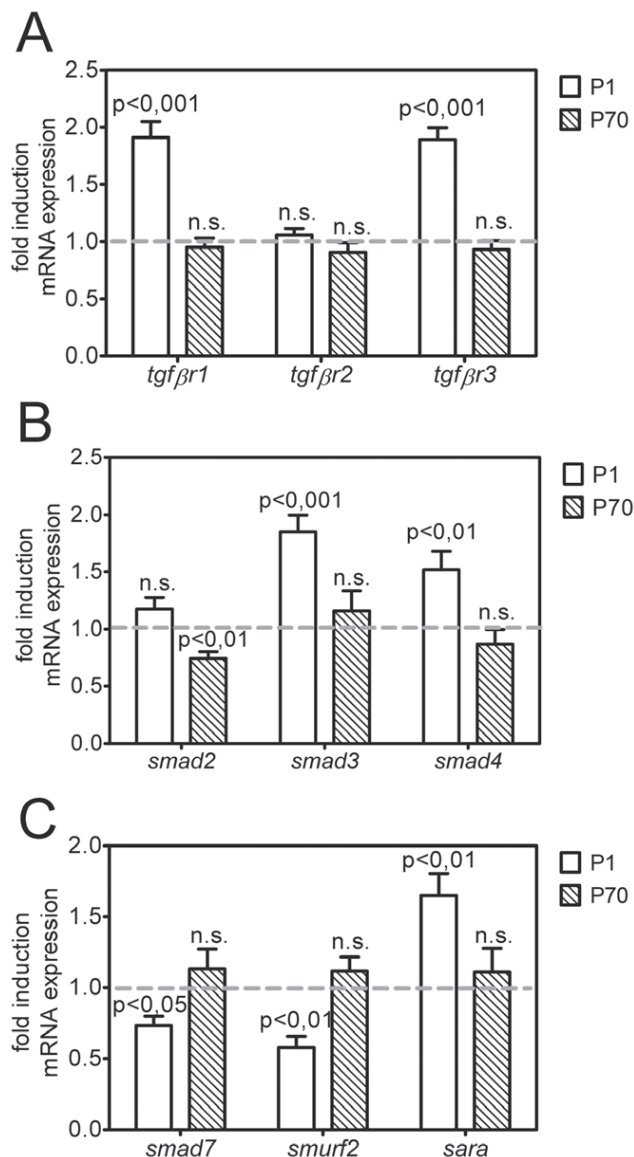


Figure 4. Expression of the TGF- β signaling machinery in lungs of neonatal and adult rats. Changes in the expression of genes encoding components of the TGF- β signaling machinery as assessed by real-time RT-PCR at days P1 and P70; $n=8-15$ for each bar. The significance for each bar is indicated by p values, IUGR vs. CO; two-tailed Mann-Whitney test. A: Expression of genes encoding the TGF- β receptors *tgfbr1*, *tgfbr2* and *tgfbr3* at P1 (white bar) and P70 (striped bar). B: Expression of genes encoding the regulatory *smad2*, *smad3* and *smad4* at days P1 (white bar) and P70 (striped bar). C: Expression of genes encoding the inhibitory *smad7*, *smurf2* and smad anchor for receptor activation (*sara*) at days P1 (white bar) and P70 (striped bar). doi:10.1371/journal.pone.0026371.g004

endothelial (mEnd) cells with a constitutively-expressing Smad7 adenoviral vector (AdSmad7). Inhibition of intracellular TGF- β signaling led to cell type-dependent expression. Collagen I was significantly downregulated in NIH/3T3 cells and slightly, but not significantly in MLE-12 and mEnd cells. Messenger RNA expression of tenascin N was slightly increased in NIH3T3 and dramatically upregulated in MLE-12, whereas no changes could be detected in mEnd. The expression of elastin increased strikingly in MLE-12 cells after inhibition of the Smad-dependent pathway.

Matrix metalloproteases-2 (MMP-2) expression was not altered in MLE-12 cells, but was down- or upregulated in NIH3T3 and mEnd cells, respectively (Figure 7B). Taken together, these data demonstrate a direct effect of the inhibition of TGF- β signaling by AdSmad7 on ECM components. The results are consistent with our *in vivo* data and underline the impact of a decreased TGF- β activity on the ECM.

Discussion

Several studies have examined ECM molecules and morphometric parameters of lungs after IUGR [38], but none so far has addressed lung function and the impact of growth factors such as TGF- β on the pulmonary system. Here, we aimed at elucidating mechanistic clues linking IUGR and subsequent changes in the pulmonary architecture.

Dynamic lung compliance is a dimension for the lung scaffold and ECM, and the pulmonary ability to distend in response to pressure. Our data demonstrate that IUGR following maternal isocaloric protein restriction during gestation leads to a reduced dynamic compliance. This is in line with studies demonstrating an airway disease in former IUGR infants [12]. Further, morphometric analysis at P70 revealed a decreased MLI after IUGR, indicating an increase of alveolar tissue, whereas there was no alteration of septal thickening. These results are in contrast to previously reported morphometric lung analyses subsequent to IUGR demonstrating an impaired alveolarization [16], [17]. However, those previous studies differ from our in various points: (1) species, (2) induction of IUGR and (3) catch up growth. Consistent with our observations, expression of both ECM components (elastin, tenascin N, collagens I and III) and ECM regulators (MMP-2 and TIMP-2) was markedly dysregulated. This is in contrast to the findings of Maritz *et al.* [38], who reported a lower number of alveoli per respiratory unit and thicker interalveolar septa in IUGR lambs. In addition, we investigated the surfactant proteins, based on the fact that lung compliance is determined by them, but did not detect any difference. The cause of IUGR is of utmost importance and determines the phenotype later in life [39]. Maritz *et al.* used a model of placental insufficiency, whereas the present study is based on a low protein diet model. That may explain, at least in part, the different observations.

How could IUGR dysregulate ECM components during lung development? The process of alveolarization is regulated by growth factor-mediated interaction of different cell types [18], [19]. The TGF- β family controls cell proliferation, transformation and apoptosis, as well as ECM deposition and remodelling [8], [18], [19]. There are studies demonstrating that several modifiers, such as RAGE-products [40] and hypoxia [41], are involved in lung disease and regulation of TGF- β signaling. Recent studies of our group did not indicate placental or fetal hypoxia subsequent to IUGR induced by low protein diet during gestation. Overexpression of TGF- β 1 during gestation leads to septal thickening and lung fibrosis [31], [42], whereas Smad3-deficient mice develop a hypoplastic lung [32], [43]. Here we show, for the first time, that IUGR in rats decreases pulmonary TGF- β signaling persistently. TGF- β 1 mRNA and protein levels were reduced immediately after birth and at P70. Such persistent changes could be the result of epigenetic modifications, for example methylation of promoter regions (CpG islands) influencing gene expression and possibly inducing gene silencing. Some studies revealed an effect of IUGR due to maternal protein restriction on DNA methylation and on the expression of essential growth or transcription factors [44], [45], [46]. We could not

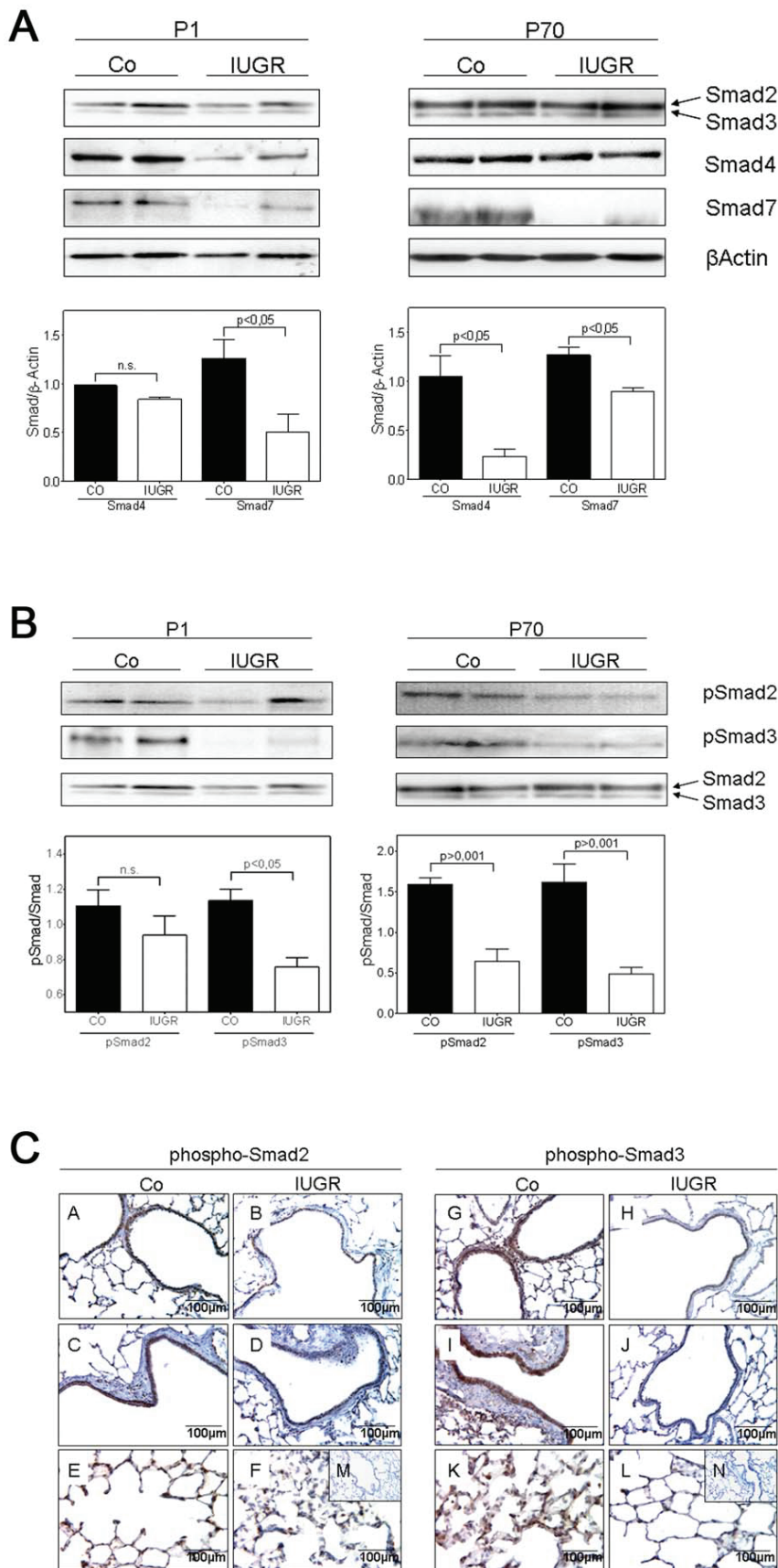


Figure 5. IUGR alters expression and phosphorylation of Smad proteins in rats. A: Representative immunoblots illustrating the expression of TGF- β -specific Smad2, Smad3, the co-Smad, Smad4, and the inhibitory Smad, Smad7, in lungs extracted at days P1 and P70 from rats with and without IUGR. β -actin served as loading control. Immunoblot data were quantified for Smad4 and Smad7 for both days P1 and P70 (Co as black bar, and IUGR as white bar); $n=4-6$ for each bar. The significance for each bar is indicated by p values, IUGR vs. CO; two-tailed Mann-Whitney test. B: The expression of active TGF- β signaling components in lung homogenates of rats with and without IUGR was analyzed by immunoblotting of phosphorylated (p) and total Smad2 and Smad3. β -actin served as loading control. Immunoblot data were quantified for pSmad2 and pSmad3 for both days P1 and P70 (Co as black bar, and IUGR as white bar); $n=4-6$ for each bar. The significance for each bar is indicated by p values, IUGR vs. CO; two-tailed Mann-Whitney test. C: Immunohistochemical localization and expression pattern of pSmad2 and pSmad3 in lungs of rats with IUGR (right column) and without IUGR (left column). A–F: representative fields illustrating the expression and localization of pSmad2 in bronchi (A–D) and in the alveoli (E–F) of lungs extracted on day P70. G–L: representative fields illustrating the expression and localization of pSmad3 in bronchi (G–J) and in the alveoli (K–L) of lungs extracted on day P70. M–N: negative control. doi:10.1371/journal.pone.0026371.g005

detect differences between IUGR and control animals. However, other epigenetic mechanisms of transcriptional regulation via transcription factors may contribute to the altered TGF- β 1 expression. In line with this, the phosphorylation of both Smad2 and Smad3 is significantly derogated at P1 and P70 in the rat lung. TGF- β regulates the expression and secretion of some ECM molecules, including collagens, fibrillin, and matrix-metabolizing enzymes [7], [8], [47]: the MMPs and their cognate inhibitors, TIMPs. During early and late lung development both ECM components and MMP-2/TIMP-1 are strongly expressed in humans [48] and mice [49], and their deposition in the ECM and its remodeling plays a pivotal role in alveolarization. In our study, we have illustrated that the levels of collagen I, collagen III, and fibrillin mRNA are consistently decreased. In animal models of arrest of alveolarization, MMP-2 is reduced and TIMP-1 is elevated [50], [51]. In contrast to these results, we demonstrate an increased alveolarization and alveolar mass after IUGR, and opposing regulation of TIMP-1 and MMP-2. Additionally, we show that inhibition of the TGF- β activity in fibroblasts by adenoviral Smad7 leads to reduced mRNA expression of TGF- β -regulated ECM molecules. However, it is essential to differentiate between the cell types of the compartments of the lung: in epithelial cells (MLE-12) inhibition of TGF- β signaling led to a tremendous upregulation of elastin and tenascin N, whereas elastin expression was unaffected in fibroblasts (NIH/3T3) and murine endothelial cells, and tenascin N expression was even decreased in murine endothelial cells. Taken together, our data *in vivo* and *in vitro* suggest that an abnormal downregulation of pulmonary TGF- β activity after IUGR has an impact on the composition and function of the ECM contributing to an impaired lung function.

What other role may the TGF- β system play during lung development in IUGR animals? Proliferation and differentiation

of type II pneumocytes are key steps in the process of alveolarization and regulated by TGF- β [52], [53]. Our study shows that IUGR may result in a decreased activation of the TGF- β system accompanied by diminished expression and cleavage of caspase-3 and reduced cleavage of PARP, indicating clearly disturbed apoptotic processes at both time points investigated. These findings are endorsed by the fact that caspase-3 is a downstream molecule of the TGF- β system [54], whereby TGF- β signaling has potent antiproliferative and pro-apoptotic effects on epithelial cells [55], [56], [57], [58]. Moreover, we demonstrate that *tgfr3* expression is significantly upregulated in IUGR lungs at P1. Consistent with these results, another group postulates that TGF- β receptor III (T β RIII) may act as a protective factor in apoptotic processes in cardiac fibroblasts by negative regulation and inhibition of TGF- β signaling [59]. Considering these data, it is conceivable that diminished TGF- β signaling in lungs after IUGR inhibits apoptosis in fibroblasts and alveolar epithelial cells, thereby contributing to an abnormal growth of pulmonary tissue (Figure 8).

Additionally, compensatory mechanisms occur in order to counter-regulate the reduced phosphorylation of Smad2/3 by downregulation of the inhibitory intracellular molecules Smad7 and Smurf2. Furthermore, phosphorylation of Smad2/3 supporting molecules, e.g. Sara, is upregulated indicating a compensation for the reduced activity of the TGF- β system.

There two major reasons for IUGR: first, placental insufficiency with a combination of hypoxemia, inflammatory reaction and nutrient restriction, second, maternal undernourishment due to low protein diet. Of the different animal models of IUGR, we chose the low protein diet model in the rat, based on the fact that it is characterized by a low birth weight, development of arterial hypertension and pronounced responsiveness to inflammatory

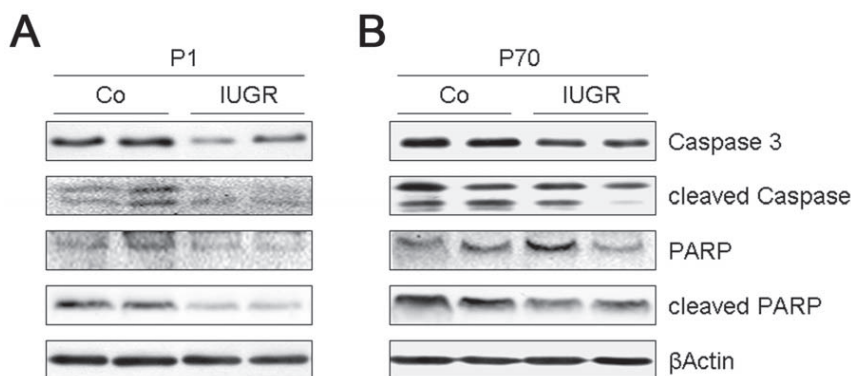
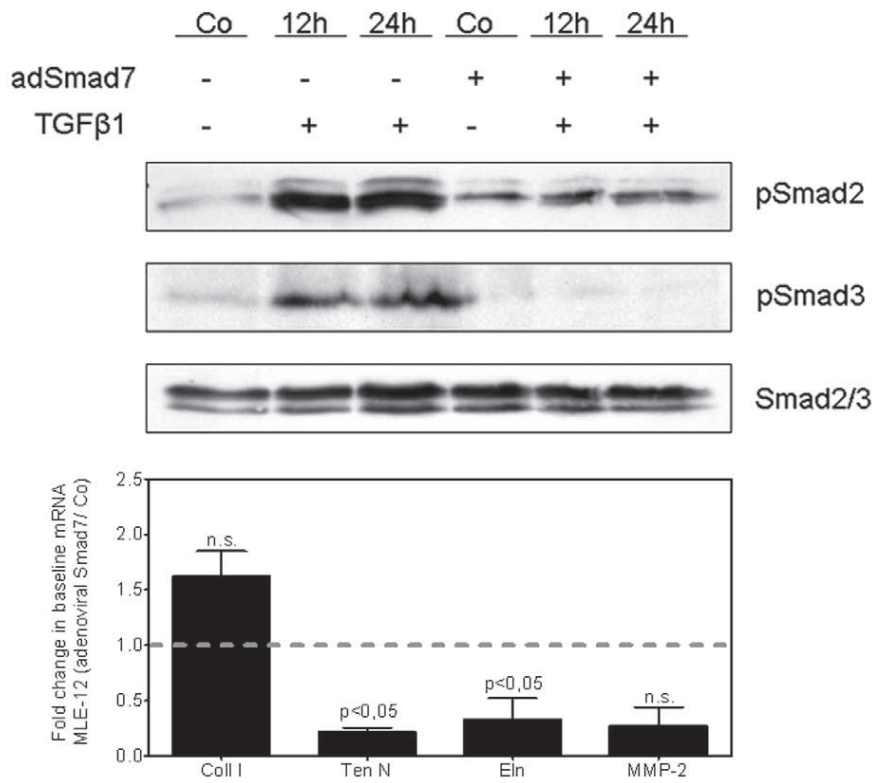


Figure 6. Effect of IUGR on apoptosis in lungs of rats at days P1 and P70. Apoptosis is assessed by cleaved caspase-3 and cleaved fragment of Poly (ADP-ribose) polymerase (PARP). A: Representative immunoblots illustrating the expression of cleaved and total caspase-3, fragments of PARP and total PARP in lung homogenates of rats with IUGR and without IUGR (Co) at day P1 (A) and P70 (B). The β -actin served as loading control; $n=4-6$ for each bar. doi:10.1371/journal.pone.0026371.g006

A



B

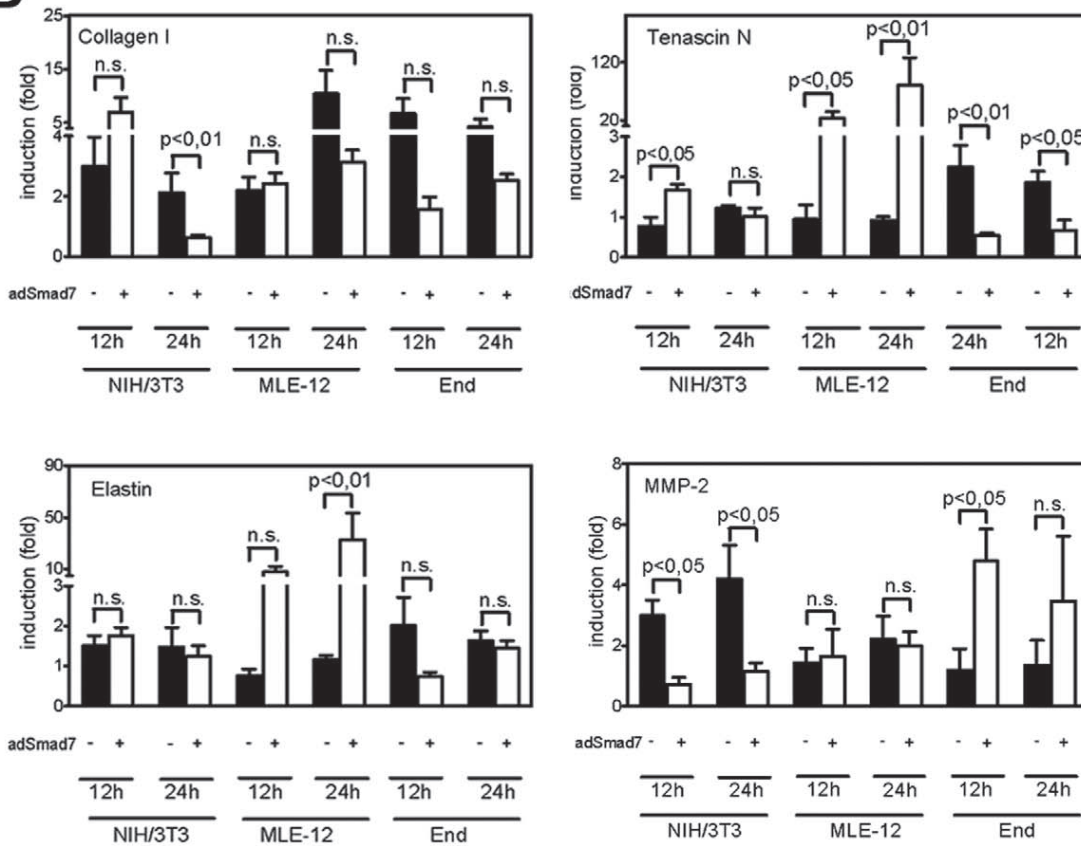


Figure 7. Effect of the inhibition of intracellular TGF-β signaling by adenoviral Smad7 overexpression on the expression of ECM components *in vitro*. A: Basal expression of components of the TGF-β signaling pathway in MLE-12 cells following infection with adenoviral Smad7 (AdSmad7) and stimulation with TGF-β1 (2 ng/ml) for either 12 h or 24 h. Representative immunoblots illustrating the expression and phosphorylation of Smad2 and Smad3 in MLE-12 cells are shown. Changes in the basal mRNA levels of genes encoding collagen I (Coll), tenascin N (TenN), elastin (Eln) and metallo-matrixproteinase-2 (MMP-2) in MLE-12 cells infected by AdSmad7. Data represent the mean relative fold change in mRNA expression assessed by real-time RT-PCR in MLE-12 cells 24 h after infection with AdSmad7. B: Induction of these four genes in native fibroblasts (NIH/3T3), alveolar cells (MLE-12) and endothelial cells (End) (black bars) and after infection with AdSmad7 (white bars) one day prior to a stimulation with TGF-β1 (2 ng/ml) for 12 h or 24 h. Fold changes were calculated by: $(\Delta\Delta C_t \text{ adSmad7, stim} / \Delta\Delta C_t \text{ adSmad7, unstim})$, and $(\Delta\Delta C_t \text{ control, stim} / \Delta\Delta C_t \text{ control, unstim})$, where adSmad7 denotes infection with AdSmad7; control, no infection with AdSmad7; stim, ligand-stimulated; unstim, unstimulated. The significance for each bar is indicated by p values, AdSmad7 vs. control. doi:10.1371/journal.pone.0026371.g007

processes. However, undernourishment is not the leading cause of IUGR in the western world, but in the developing countries. Hence, the data presented in our study may be limited to a certain group of IUGR infants and not completely alienable to IUGR induced by placental insufficiency. Furthermore, rat lungs at birth are at an earlier developmental stage than lungs of human

neonates born at term and therefore comparable to preterm infants.

Taken together, the data presented here suggest that IUGR affects lung development and lung function by at least two functional consequences: 1) IUGR attenuates TGF-β signaling after IUGR which leads to a dysregulated expression of ECM and

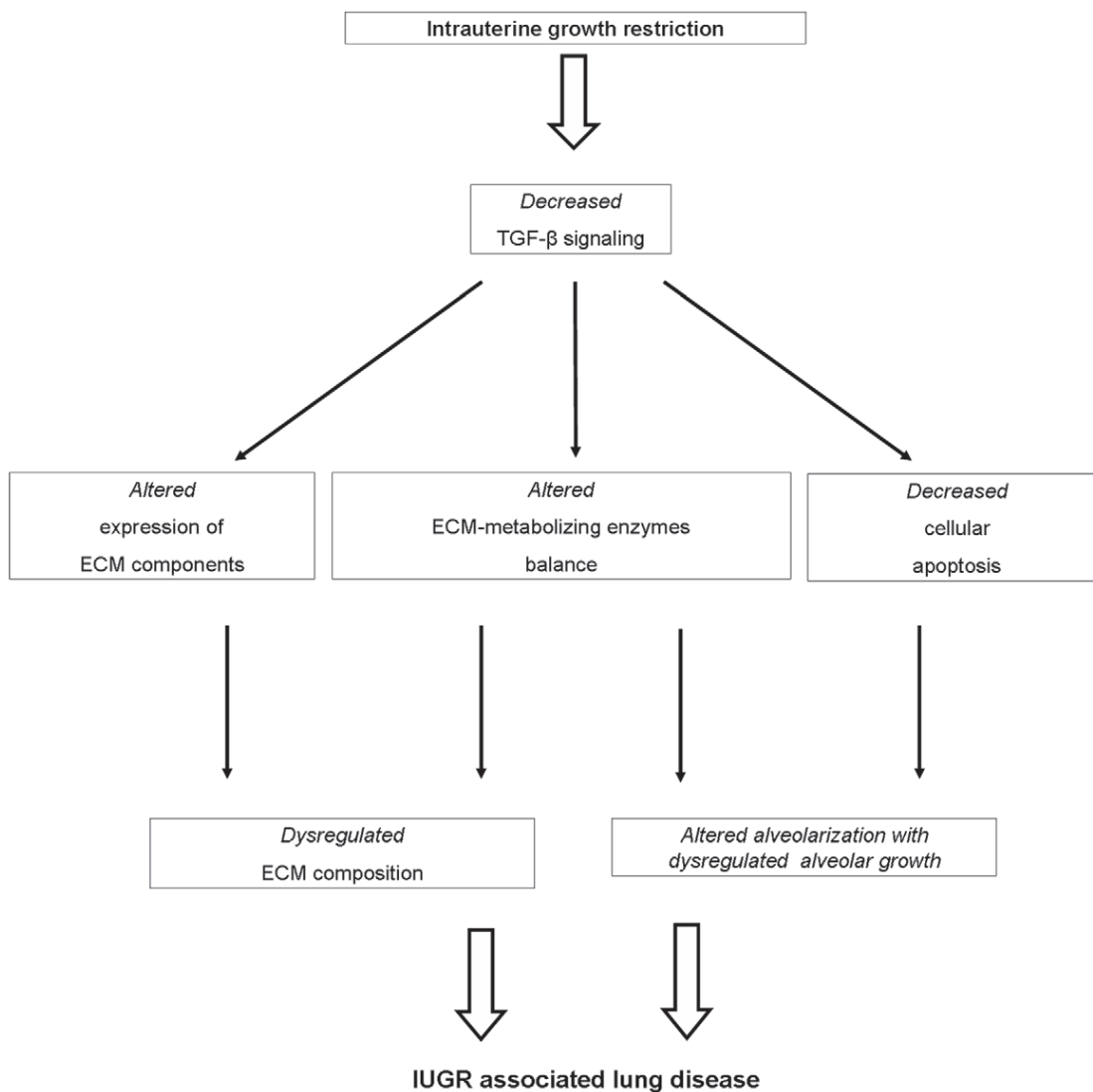


Figure 8. The role of transforming growth factor (TGF)-β signaling in lung disease subsequent to intrauterine growth restriction (IUGR). A proposed model depicting the effects of decreased TGF-β signaling during the development of IUGR-associated lung disease is shown. ECM - extracellular matrix. doi:10.1371/journal.pone.0026371.g008

ECM-remodeling components, and 2) IUGR decreases apoptosis in the lung. This significantly contributes to the altered lung development and impaired lung function seen after IUGR.

Acknowledgments

The authors gratefully acknowledge the expert technical assistance of Ida Allabauer, Julia Dobner and Yvonne Birkner.

References

- Barker DJ (1995) Intrauterine programming of adult disease. *Mol Med Today* 1: 418–423.
- Nuyt AM (2008) Mechanisms underlying developmental programming of elevated blood pressure and vascular dysfunction: evidence from human studies and experimental animal models. *Clin Sci (Lond)* 114: 1–17.
- Barker DJ (1998) In utero programming of chronic disease. *Clin Sci (Lond)* 95: 115–128.
- Torrance HL, Voorbij HA, Wijnberger LD, van Bel F, Visser GH (2008) Lung maturation in small for gestational age fetuses from pregnancies complicated by placental insufficiency or maternal hypertension. *Early Hum Dev* 84(7): 465–9.
- Anand D, Stevenson CJ, West CR, Pharoah PO (2003) Lung function and respiratory health in adolescents of very low birth weight. *Arch Dis Child* 88: 135–8.
- Chen CM, Wang LF, Su B (2004) Effects of maternal undernutrition during late gestation on the lung surfactant system and morphometry in rats. *Pediatr Res* 56: 329–335.
- Roth-Kleiner M, Post M (2003) Genetic control of lung development. *Biol Neonate* 84: 83–88.
- Roth-Kleiner M, Post M (2005) Similarities and dissimilarities of branching and septation during lung development. *Pediatr Pulmonol* 40: 113–134.
- Dezateux C, Lum S, Hoo AF, Hawdon J, Costeloe K, et al. (2004) Low birth weight for gestation and airway function in infancy: exploring the fetal origins hypothesis. *Thorax* 59: 60–66.
- Rona RJ, Gulliford MC, Chinn S (1993) Effects of prematurity and intrauterine growth on respiratory health and lung function in childhood. *Bmj* 306: 817–820.
- Boezen HM, Vonk JM, van Aalderen WM, Brand PL, Gerritsen J, et al. (2002) Perinatal predictors of respiratory symptoms and lung function at a young adult age. *Eur Respir J* 20: 383–390.
- Kotecha SJ, Watkins WJ, Heron J, Henderson J, Dunstan FD, et al. (2010) Spirometric lung function in school-age children: effect of intrauterine growth retardation and catch-up growth. *Am J Respir Crit Care Med* 181(9): 969–74.
- Langley-Evans SC, Phillips GJ, Jackson AA (1997) Fetal exposure to low protein maternal diet alters the susceptibility of young adult rats to sulfur dioxide-induced lung injury. *J Nutr* 127: 202–209.
- Plank C, Östreicher I, Hartner A, Marek I, Struwe FG, et al. (2006) Intrauterine growth retardation aggravates the course of acute mesangioproliferative glomerulonephritis in the rat. *Kidney Int* 70: 1974–1982.
- Joyce BJ, Louey S, Davey MG, Cock ML, Hooper SB, et al. (2001) Compromised respiratory function in postnatal lambs after placental insufficiency and intrauterine growth restriction. *Pediatr Res* 50: 641–649.
- Maritz GS, Cock ML, Louey S, Joyce BJ, Albuquerque CA, et al. (2001) Effects of fetal growth restriction on lung development before and after birth: a morphometric analysis. *Pediatr Pulmonol* 32: 201–210.
- Maritz GS, Cock ML, Louey S, Suzuki K, Harding R (2004) Fetal growth restriction has long-term effects on postnatal lung structure in sheep. *Pediatr Res* 55: 287–295.
- Jankov RP, Tanswell AK (2004) Growth factors, postnatal lung growth and bronchopulmonary dysplasia. *Paediatr Respir Rev* 5 Suppl A: 265–275.
- Copland I, Post M (2004) Lung development and fetal lung growth. *Paediatr Respir Rev* 5 Suppl A: 259–264.
- Warburton D, Bellusci S (2004) The molecular genetics of lung morphogenesis and injury repair. *Paediatr Respir Rev* 5, Suppl A: S283–S287.
- Joss-Moore LA, Wang Y, Yu X, Campbell MS, Callaway CW, et al. (2011) IUGR decreases elastin mRNA expression in the developing rat lung and alters elastin content and lung compliance in the mature rat lung. *Physiol Genomics*. In press.
- Joss-Moore LA, Wang Y, Ogata EM, Sainz AJ, Yu X, et al. (2011) IUGR differentially alters MeCP2 expression and H3K9Me3 of the PPAR γ gene in male and female rat lungs during alveolarization. *Birth Defects Res A Clin Mol Teratol*. In press.
- Warburton D, Bellusci S, De Langhe S, Del Moral PM, Fleury V, et al. (2005) Molecular mechanisms of early lung specification and branching morphogenesis. *Pediatr Res* 57: 26R–37R.
- Warburton D, Schwarz M, Tefft D, Flores-Delgado G, Anderson KD, et al. (2000) The molecular basis of lung morphogenesis. *Mech Dev* 92: 55–81.
- Massagué J (1998) TGF- β signal transduction. *Annu Rev Biochem* 67: 753–791.
- Morty RE, Königshoff M, Eickelberg O (2009) Transforming growth factor-beta signaling across ages: from distorted lung development to chronic obstructive pulmonary disease. *Proc Am Thorac Soc* 6(7): 607–13.
- Liu J, Tseu I, Wang J, Tanswell K, Post M (2000) Transforming growth factor b2, but not b1 and b3, is critical for early rat lung branching. *Dev Dyn* 217: 343–360.
- Zhao J, Bu D, Lee M, Slavkin HC, Hall FL, et al. (1996) Abrogation of transforming growth factor-b type II receptor stimulates embryonic mouse lung branching morphogenesis in culture. *Dev Biol* 180: 242–257.
- Zhao J, Lee M, Smith S, Warburton D (1998) Abrogation of Smad3 and Smad2 or of Smad4 gene expression positively regulates murine embryonic lung branching morphogenesis in culture. *Dev Biol* 194: 182–195.
- Zhao J, Shi W, Chen H, Warburton D (2000) Smad7 and Smad6 differentially modulate transforming growth factor β -induced inhibition of embryonic lung morphogenesis. *J Biol Chem* 275: 23992–23997.
- Vicencio AG, Lee CG, Cho SJ, Eickelberg O, Chuu Y, et al. (2004) Conditional overexpression of bioactive transforming growth factor-beta1 in neonatal mouse lung: a new model for bronchopulmonary dysplasia? *Am J Respir Cell Mol Biol* 31: 650–656.
- Chen H, Sun J, Buckley S, Chen C, Warburton D, et al. (2005) Abnormal mouse lung alveolarization caused by Smad3 deficiency is a developmental antecedent of centrilobular emphysema. *Am J Physiol Lung Cell Mol Physiol* 288: L683–L691.
- Ostlund E, Tally M, Fried G (2002) Transforming growth factor-beta1 in fetal serum correlates with insulin-like growth factor-I and fetal growth. *Obstet Gynecol* 100(3): 567–73.
- Alejandro-Alcázar MA, Michiels-Corsten M, Vicencio AG, Reiss I, Ryu J, et al. (2008) TGF-beta signaling is dynamically regulated during the alveolarization of rodent and human lungs. *Dev Dyn* 237(1): 259–69.
- Vicencio AG, Eickelberg O, Stankewich MC, Kashgarian M, Haddad GG (2002) Regulation of TGF- β ligand and receptor expression in neonatal rat lungs exposed to chronic hypoxia. *J Appl Physiol* 93: 1123–1130.
- Vicencio AG, Lee CG, Cho SJ, Eickelberg O, Chuu Y, et al. (2004) Conditional overexpression of bioactive transforming growth factor-beta1 in neonatal mouse lung: a new model for bronchopulmonary dysplasia? *Am J Respir Cell Mol Biol* 31: 650–656.
- Alejandro-Alcázar MA, Kwapiszewska G, Reiss I, Amarie OV, Marsh LM, et al. (2007) Hyperoxia modulates TGF-beta/BMP signaling in a mouse model of bronchopulmonary dysplasia. *Am J Physiol Lung Cell Mol Physiol* 292(2): L537–49.
- Maritz GS, Morley CJ, Harding R (2005) Early developmental origins of impaired lung structure and function. *Early Hum Dev* 81(9): 763–71.
- Nüsken KD, Schneider H, Plank C, Trollmann R, Nüsken E, Rascher, et al. (2011) Fetal programming of gene expression in growth-restricted rats depends on the cause of low birth weight. *Endocrinology*. In press.
- Song JS, Kang CM, Park CK, Yoon HK, Lee SY, et al. (2011) Inhibitory effect of receptor for advanced glycation end products (RAGE) on the TGF- β -induced alveolar epithelial to mesenchymal transition. *Exp Mol Med*. In press.
- Nicola T, Ambalavanan N, Zhang W, James ML, Rehan V, et al. (2011) Hypoxia-induced inhibition of lung development is attenuated by the peroxisome proliferator-activated receptor- γ agonist rosiglitazone. *Am J Physiol Lung Cell Mol Physiol* 301(1): L125–34. In press.
- Pulichino AM, Wang IM, Caron A, Mortimer J, Auger A, et al. (2008) Identification of transforming growth factor beta1-driven genetic programs of acute lung fibrosis. *Am J Respir Cell Mol Biol* 39(3): 324–36.
- Bonnaud P, Kolb M, Galt T, Robertson J, Robbins C, et al. (2004) Smad3 null mice develop airspace enlargement and are resistant to TGF-beta-mediated pulmonary fibrosis. *J Immunol* 173: 2099–2108.
- Simmons RA (2007) Developmental origins of beta-cell failure in type 2 diabetes: the role of epigenetic mechanisms. *Pediatr Res* 61: 64R–67R.
- Park JH, Stoffers DA, Nicholls RD, Simmons RA (2008) Development of type 2 diabetes following intrauterine growth retardation in rats is associated with progressive epigenetic silencing of Pdx1. *J Clin Invest* 118(6): 2316–24.
- Ke X, Schober ME, McKnight RA, O'Grady S, Caprau D, et al. (2010) Intrauterine growth retardation affects expression and epigenetic characteristics of the rat hippocampal glucocorticoid receptor gene. *Physiol Genomics* 42(2): 177–89.
- Zhao Y (1999) Transforming growth factor-beta (TGF-beta) type I and type II receptors are both required for TGF-beta-mediated extracellular matrix production in lung fibroblasts. *Mol Cell Endocrinol* 150: 91–97.
- Masumoto K, de Rooij JD, Suita S, Rottier R, Tibboel D, et al. (2005) Expression of matrix metalloproteinases and tissue inhibitors of metalloproteinases during normal human pulmonary development. *Histopathology* 47: 410–419.

Author Contributions

Conceived and designed the experiments: MAA JD HS CP. Performed the experiments: MAA LL IO CV. Analyzed the data: MAA RM HS JD. Wrote the paper: MAA.

49. Ryu J, Vicencio AG, Yeager ME, Kashgarian M, Haddad GG, et al. (2005) Differential expression of matrix metalloproteinases and their inhibitors in human and mouse lung development. *Thromb Haemost* 94: 175–183.
50. Dik WA, De Krijger RR, Bonekamp L, Naber BA, Zimmermann LJ, et al. (2001) Localization and potential role of matrix metalloproteinase-1 and tissue inhibitors of metalloproteinase-1 and -2 in different phases of bronchopulmonary dysplasia. *Pediatr Res* 50: 761–766.
51. Hosford GE, Fang X, Olson DM (2004) Hyperoxia decreases matrix metalloproteinase-9 and increases tissue inhibitor of matrix metalloproteinase-1 protein in the newborn rat lung: association with arrested alveolarization. *Pediatr Res* 56: 26–34.
52. McDevitt TM, Gonzales LW, Savani RC, Ballard PL (2007) Role of endogenous TGF-beta in glucocorticoid-induced lung type II cell differentiation. *Am J Physiol Lung Cell Mol Physiol* 292(1): L249–57.
53. Kasai H, Allen JT, Mason RM, Kamimura T, Zhang Z. (2005) TGF-beta1 induces human alveolar epithelial to mesenchymal cell transition (EMT). *Respir Res* 6: 56.
54. Freathy C, Brown DG, Roberts RA, Cain K (2000) Transforming growth factor-beta(1) induces apoptosis in rat FaO hepatoma cells via cytochrome c release and oligomerization of Apaf-1 to form a approximately 700-kd apoptosome caspase-processing complex. *Hepatology* 32: 750–760.
55. Ryan RM, Mineo-Kuhn MM, Kramer CM, Finkelstein JN (1994) Growth factors alter neonatal type II alveolar epithelial cell proliferation. *Am J Physiol Lung Cell Mol Physiol* 266: L17–L22.
56. Zhang F, Nielsen LD, Lucas JJ, Mason RJ (2004) Transforming growth factor-beta antagonizes alveolar type II cell proliferation induced by keratinocyte growth factor. *Am J Respir Cell Mol Biol* 31: 679–686.
57. Gal A, Sjöblom T, Fedorova L, Imreh S, Beug H, et al. (2008) Sustained TGF beta exposure suppresses Smad and non-Smad signalling in mammary epithelial cells, leading to EMT and inhibition of growth arrest and apoptosis. *Oncogene* 27(9): 1218–30.
58. Undevia NS, Dorscheid DR, Marroquin BA, Gugliotta WL, Tse R, et al. (2004) Smad and p38-MAPK signaling mediates apoptotic effects of transforming growth factor-beta1 in human airway epithelial cells. *Am J Physiol Lung Cell Mol Physiol* 287(3): L515–24.
59. Chu WF, Li XX, Li C, Wan L, Shi H, et al. (2010) TGFBR3, a potential negative regulator of TGF- β signaling, protects cardiac fibroblasts from hypoxia-induced apoptosis. *J Cell Physiol*. In press.

Developmental regulation of inflammatory cytokine-mediated Stat3 signaling: the missing link between intrauterine growth restriction and pulmonary dysfunction?

Miguel Angel Alejandro Alcazar · Iris Östreicher · Sarah Appel · Eva Rother · Christina Vohlen · Christian Plank · Jörg Dötsch

Received: 27 September 2011 / Revised: 5 December 2011 / Accepted: 28 December 2011
© Springer-Verlag 2012

Abstract Intrauterine growth restriction (IUGR) is a risk factor for impairment of lung function in adolescence and adulthood. Inflammatory and proliferative processes linking IUGR and perturbed extracellular matrix (ECM) as an underlying mechanism have not been addressed so far. Therefore, in this study, we aimed to investigate the developmental regulation of inflammatory and profibrotic processes in the lung subsequent to IUGR. IUGR was induced in rats by isocaloric protein restriction during gestation. Lung function was assessed with direct plethysmography at postnatal day (P) 28 and P70. Lungs were obtained at P1, P42, and P70 for assessment of mRNA, protein expression, immunohistochemistry, and gelatinolytic activity. Both respiratory system resistance and compliance were impaired subsequent to IUGR at P28 and this impairment was even more pronounced at P70. In line with these results, the expression of ECM components and metabolizing enzymes was deregulated. The deposition of collagen was increased at P70. In addition, the expression of inflammatory cytokines and both the activity and the

expression of target genes of Stat3 signaling were dynamically regulated, with unaltered or decreased expression at P1 and significantly increased expression at P70. Taken together, these data give evidence for an age-dependent impairment of lung function as a result of a developmentally regulated increase in inflammatory and profibrotic processes subsequent to IUGR.

Keywords Intrauterine growth restriction · Lung disease · Inflammation · Stat3 · Airway inflammation · Airway hyperresponsiveness

Introduction

The incidence of respiratory illness has increased during the past several decades in many parts of the world [1]. Bronchial asthma is the most common chronic childhood disease in developed countries. Its prevalence has nearly doubled over the last 2 decades, putting a serious socio-economic burden on the children and their families [2]. The pathogenesis of bronchial asthma is based on the interaction between multiple genetic and environmental factors [3]. Prenatal and postnatal influences, such as maternal smoking during gestation and recurrent respiratory tract infections during infancy can adversely affect later respiratory health [4].

Barker et al. coined the term *intrauterine programming* to reflect that a temporal change in the fetal environment such as intrauterine growth restriction (IUGR) leads to a permanent change of physiological processes later in life [5, 6]. Intrauterine growth restriction affects approximately 10% of all newborns and is a major risk factor for the development

M. A. Alejandro Alcazar (✉) · S. Appel · E. Rother · C. Vohlen · J. Dötsch
Department of Pediatrics and Adolescent Medicine,
University of Cologne,
Kerpener Strasse 62,
50937 Cologne, Germany
e-mail: miguel.alejandre-alcazar@uk-koeln.de

I. Östreicher
Department of Neonatology, Charité University Medical Center,
Berlin, Germany

C. Plank
Department of Pediatrics and Adolescent Medicine,
University of Erlangen—Nuremberg,
Nuremberg, Germany

of metabolic syndrome in adulthood [5]. Furthermore, there is an increasing body of evidence that IUGR induces changes in the developing lung with a persisting impairment of pulmonary structure and function [7–9]. In addition, recent epidemiological studies have demonstrated impaired lung function with reduced forced expiratory volume (FEV_1) in young infants following IUGR [10].

However, the molecular pathomechanisms of IUGR-associated lung disease have not been completely clarified so far. Several studies indicate that a severely perturbed extracellular matrix (ECM) metabolism contributes to the impairment of lung function and suggest a regulatory effect of IUGR on the pulmonary structure and production of ECM components [9, 11]. Both lung structure and function are already determined during early and late lung development [12, 13]. Interference with the developmental program of the lung during any of these phases may render the lung less effective in gas exchange and more susceptible to disease. Several experimental studies have demonstrated morphologic pulmonary alterations and imbalance of ECM composition in lungs of animals subsequent to IUGR [7, 8]. Additionally, analysis of lung structure in intrauterine growth restricted animals revealed an impaired development of the lung. For example, maturation of the surfactant system is controversially discussed: there are studies reporting a delayed maturation of the surfactant proteins subsequent to IUGR [14], whereas other groups either state no alterations [15, 16] or increased maturation of the surfactant proteins after IUGR [17]. In line with this developmental deregulation, Joss-Moore et al. recently suggested a pivotal role of ECM components such as elastic fibers in the pathomechanism of IUGR-associated lung disease [11]. Although several studies have investigated the synthesis of pulmonary ECM and impaired lung function associated with IUGR, the molecular mechanism linking perturbed ECM with IUGR remains largely unclear to date. Interestingly, human and animal studies demonstrate a programming of inflammatory response subsequent to IUGR [18, 19]. In line with these observations, Plank et al. highlighted a predisposition of former IUGR animals for renal fibrosis and inflammation with a strikingly upregulation of inflammatory and profibrotic marker [Interleukin-6 (IL-6), tumor necrosis factor α (TNF- α), transforming growth factor β (TGF- β)] and of ECM components (collagen I and collagen IV) [20]. It is intriguing though that pulmonary inflammatory response as a link between perturbed ECM and IUGR has not been addressed so far. However, increased expression of cytokines like Interleukin (IL)-13 [21] as well as deregulation of ECM metabolism [22] are known to be involved in the progression of respiratory diseases such as asthma. Furthermore, recent studies underline the central role of IL-6, transforming growth factor (TGF) β 1 and plasminogen activator inhibitor-1 (PAI-1) in the development and progression of dysregulated ECM and fibrosis [23, 24].

In this study, we tested the hypothesis that IUGR (1) impairs lung function in a time dependent manner, (2) deregulates both, the expression of profibrotic markers and formation and remodeling of the ECM, and (3) has an impact on pulmonary inflammatory response.

Methods

Animal procedures

All procedures performed on animals were done in accordance with the German regulations and legal requirements and were approved by the local government authorities (Regierung von Mittelfranken). Adult and neonatal Wistar rats were housed in humidity- and temperature-controlled rooms on a 12:12-h light–dark cycle. IUGR in rats was induced by isocaloric low protein diet (8% versus 17% casein) as previously described [25]. On the first postnatal day (P1) the litters were reduced to six pups per dam. During lactation and subsequent to weaning at P23 the animals were fed standard chow. We only used the male rat offspring for the experiments.

Physiological data of control animals and intrauterine growth restricted animals

Body weight was obtained at different time points: P1, P7, P14, P21, P42, P70 by weighing each animal, and weight gain as fold induction in relation birth weight was calculated. Lung weight was obtained by weighing the entire lung at P1, P21, and P70. In addition, the ratio of lung weight to body weight was obtained. Mothers were weighed during gestation at gestational day (G) 1, G7, G14, G21, and G23 as well as during lactation at postnatal day (P) 1, P7, P14, and P23 (day of weaning). Means \pm standard error of the mean were calculated.

Measurement of airway responsiveness

At the age of P28 and P70, airway responsiveness was assessed by measuring respiratory system resistance (Res) and respiratory system compliance (C_{dyn}) with direct plethysmography (FinePointe™ RC; Wellington, NC, USA). Rats were deeply anesthetized by intramuscular injection of ketamine 100 mg/kg body weight and midazolam 5 mg/kg body weight, tracheotomised and ventilated. Res and C_{dyn} were measured at baseline, and after stimulation with methacholine, a bronchoconstrictor well established for diagnosis of airway hyperresponsiveness.

Tissue preparation

Following anesthesia with ketamine (100 mg/kg body weight) and midazolam (5 mg/kg body weight), the animals were killed. Neonatal animals were euthanized by decapitation. The right lobe of the lung was removed and immediately snap-frozen in liquid nitrogen. The left lobe was inflated via tracheotomy and pressure-fixed at 20 cm H₂O with 4% (mass/vol) paraformaldehyde. Lungs were submerged in 4% (mass/vol) paraformaldehyde overnight for paraffin embedding and sectioned as described previously [26]. Paraffin sections (1 μ m) were mounted on poly-L-lysine-coated glass slides, dewaxed with xylene (3–5 min) and rehydrated in a graduated series of ethanol solutions (100%, 95%, and 70% (vol/vol), and finally PBS).

RNA extraction and real-time PCR

Total RNA was isolated from unfixed lung tissue or cultured cells as previously described [27]. Total RNA was screened for mRNA encoding genes listed in Table 1. Quantitative changes in mRNA expression were assessed by quantitative real-time PCR as described previously [25]. In all samples, the relative amount of specific mRNA was normalized to the ubiquitously expressed glyceraldehyd-3-phosphat-dehydrogenase (GAPDH), β -Actin, as well as porphobilinogen-deaminase gene. Primer pairs and TaqMan probes are listed in Table 1. Oligonucleotides were designed with Primer Express software (PerkinElmer, Foster City, CA, USA).

Western blot analysis

Protein extraction, gel electrophoresis and immunoblotting were performed as previously described [26]. Blots were probed with the following antibodies: monoclonal mouse-anti-rat-proliferating cell nuclear antigen (PCNA; DAKO, Glostrup, Denmark, Clone PC10, M0879, 1:10,000), polyclonal rabbit-anti-rat-phospho Stat3 (Cell Signaling, # 9131, 1:1,000), and monoclonal rabbit-anti-rat-Stat3 (Cell Signaling, # 9139, 1:1,000). Monoclonal mouse-anti-rat- β -Actin (Cell Signaling, MA, # 3700, 1:1,000) served as a loading control. Anti-mouse IgG, HRP-linked (Cell Signaling, # 7076, 1:2,000), and HRP-linked anti-rabbit IgG (Cell Signaling, # 7074, 1:2,000) were used as secondary antibodies.

Histology and immunostaining

Tissue preparation was performed as described previously [27]. Sections were incubated with the rabbit-anti-rat collagen I (1:100; Biogenesis, UK). Immune complexes were visualized with an avidin/biotin-DAB (3,3-diamineobenzidine) detection system (Vector Lab,

Burlingame, CA, USA). Each slide was counterstained with hematoxylin.

Gelatin zymography

Lung homogenates were incubated with non-denaturing sample buffer (62.5 mM Tris-HCl pH 6.8, 10% glycerol, 2% SDS, 0.0025% bromphenol blue) for 10 min at 37°C and then loaded onto 10% SDS-polyacrylamide gels containing 0.1% gelatin. Following gel electrophoresis, SDS was removed by washing the gel once for 30 min in renaturation buffer (2.5% Tx-100) and once more for 30 min in developing buffer (50 mM Tris-HCl pH 8, 0.2 M NaCl, 5 mM CaCl₂, 0.02% Brij 35). Developing of the gel was performed over night at 37°C in developing buffer. For staining of the gel we used 0.1% Coomassie brilliant blue in 25% isopropanol and 10% acetic acid. Imaging was performed with the Biodoc analyze system (Biometra), and densitometry of white bands was measured using the ImageJ software (NIH).

Analysis of data

The results of real-time PCR were calculated based on the $\Delta\Delta$ Ct method and expressed as fold induction of mRNA expression compared to the corresponding control group (1.0-fold induction). Densitometric measurement was performed and values were normalized to β -actin. Quantitative evaluation of the immunohistochemical results was performed with the MetaVue™ Imaging System. The Collagen I positive area in a defined area (3.2 mm²) is displayed in percent. Results are shown as means \pm standard error of the mean. Two-tailed Mann-Whitney test and two-way ANOVA followed by a Bonferroni post-test were used to assess the significance of differences between IUGR and control animals at given time points. A *p* value < 0.05 was considered as significant.

Results

Intrauterine growth retardation after low protein diet

To analyze maternal weight gain during gestation and lactation we determined maternal body weight from conception (G1) until weaning (P23; Fig. 1a, b). As expected, maternal weight gain was reduced in low protein diet (LP) dams compared to controls during gestation (Fig. 1a). In contrast, during lactation when both experimental groups of dams received standard chow, no difference in weight gain was detectable (Fig. 1b).

The number of animals per litter between control and IUGR dams was not different (15.3 \pm 0.9 pups in NP mothers

Table 1 Designed primer pairs and TaqMan probes used in this study

AP-1	Forward 5'-AAACCTTGAAAGCGCAAAACTC-3' Reverse 5'-GTGGTTCATGACTTTCTGTTAAGCT-3' Probe 5'-(FAM)-CTGGCGTCCACGGCCAACATG-(TAMRA)-3'
Collagen Ia	Forward 5'-AGAGCGGAGAGTACTGGATCGA-3' Reverse 5'-CTGACCTGTCTCCATGTTGCA-3' Probe 5'-(FAM)-CAAGGCTGCAACCTGGATGCCATC-(TAMRA)-3'
GAPDH	Forward 5'-ACGGGAAACCCATCACCAT-3' Reverse 5'-CCAGCATCACCCATTTGA-3' Probe 5'-(FAM)-TTCCAGGAGCGAGATCCCGTCAAG-TAMRA-3'
PAI-1	Forward 5'-TCCGCCATCACCAACATTTT-3' Reverse 5'-GTCAGTCATGCCAGCTTCTC-3' Probe 5'-(FAM)-CCGCTCCTCATCTGCCTAAGTTCTCT-(TAMRA)-3'
IL-6	Forward 5'-TCCAAACTGGATATAACCAGGAAAT-3' Reverse 5'-TTGTCTTCTTGTTATCTTGTAAGTTGTTCTT-3' Probe 5'-(FAM)-AATCTGCTCTGGTCTTCTGGAGTTCGGTTTCTA-(TAMRA)-3'
IL-10	Forward 5'-GAAGCTGAAGACCTCTGGATAACA-3' Reverse 5'-CCTTTGTCTGGAGCTTATATAAATCA-3' Probe 5'-(FAM)-CGCTGTCATCGATTTCTCCCCTGTGA-(TAMRA)-3'
IL-13	Forward 5'-GAGCTGAGCAACATCACACAAGA-3' Reverse 5'-TGTCAGGTCCACGCTCCAT-3' Probe 5'-(FAM)-CAGAAGACTTCCCTGTGCAACAGCAGC-(TAMRA)-3'
MCP-1	Forward 5'-CCTCCACCACTATGCAGGTCTC-3' Reverse 5'-GCACGTGGATGCTACAGGC-3' Probe 5'-(FAM)-TCACGCTTCTGGCCTGTTGTTCA-(TAMRA)-3'
OPN	Forward 5'-AAAGTGGCTGAGTTTGGCAG-3' Reverse 5'-AAGTGGCTACAGCATCTGAGTGT-3' Probe 5'-(FAM)-TCAGAGGAGAAGGCGCATTACAGCA-(TAMRA)3'
P21	Forward 5'-TGTCTTGCACCTCTGGTGTCTCA-3' Reverse 5'-CGCTTGGAGTGATAGAAATCTGTTAG-3' Probe 5'-(FAM)-CCCCTGAGAGGCCTGAAGACTCCC-(TAMRA)3'
TGFβ-1	Forward 5'-CACCCGCGTGCTAATGGT-3' Reverse 5'-GGCACTGCTTCCCGAATG-3' Probe 5'-(FAM)-ACCGCAACAACGCAATCTATGACA-(TAMRA)3'
TNF-α	Forward 5'-GACCCTCACACTCAGATCATCTTCT-3' Reverse 5'-TTGTCTTGTGAGATCCATGCCATT-3' Probe 5'-(FAM)-ACGTCGTAGCAAACCACCAAGCGGA-(TAMRA)3'
Adrenoceptor β1 ^a	Forward 5'-ATCGTAGTGGCAACGTGTTG-3' Reverse 5'-GGGACATGATGAAGAGGTTGGT-3'
Adrenoceptor β2 ^a	Forward 5'-GGATTGCCTTCCAGGAGCTT-3' Reverse 5'-TGTCTTACCGTTGCTGTTGCTA-3'
Collagen III ^a	Forward 5'-GGACCTCCTGGTGTCTATTG-3' Reverse 5'-GAATCCAGGGATAACCAGCTG-3'
Elastin ^a	Forward 5'-GAAAACCCCGAAGCCCT-3' Reverse 5'-CCCCACCTTGATATCCAGG-3'
Fibrillin I ^a	Forward 5'-TGCTCTGAAAGGACCCAATGT-3' Reverse 5'-CGGGACAACAGTATGCGTTATAAC-3'
TIMP-1 ^a	Forward 5'-GGATATGTCCACAAGTCCCAG-3' Reverse 5'-CAGGGCTCAGATTATGCCAG-3'
TIMP-2 ^a	Forward 5'-GGACCTGACAAGGACATCG-3' Reverse 5'-GATGCTAAGCGTGTTCCAG-3'

^aTIMP-1, TIMP-2, elastin, and fibrillin were detected by SYBR Green analysis

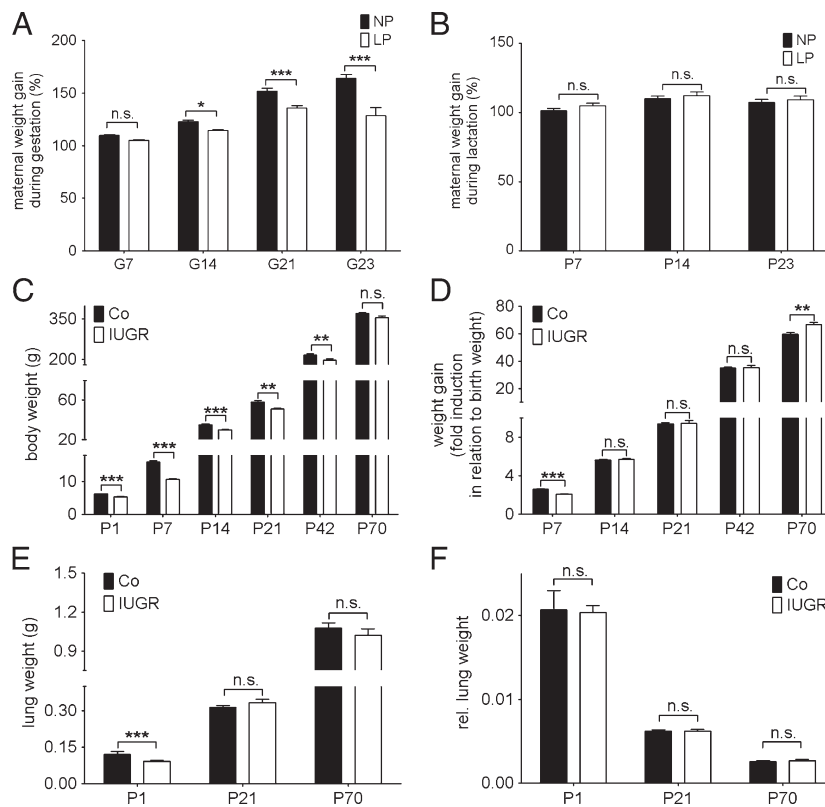


Fig. 1 Body weight, weight gain and lung weight subsequent to IUGR. **a, b** Maternal weight gain (%) during gestation (**a**) and during lactation (**b**). Body weight at gestational day (**a**) 1 is 100%, and at postnatal day (P) 1, respectively. $n=3-5$ mothers per group. Low protein diet during gestation (LP; white bars) and normal protein diet during gestation (NP; control group; black bars). **c, d** body weight (g) (**c**) and body weight gain (**d**) of rats after IUGR obtained at postnatal day (P) 1, P7, P14, P21, P42, and P70. Intrauterine growth restriction

(IUGR; white bars); control animals (Co; black bars). **e, f** lung weight (**e**) and ratios of lung weight to body weight of rats (**f**) after IUGR at P1, P21, and P70. Intrauterine growth restriction (IUGR; white bars); control animals (Co; black bars). $n=14-24$ (from three to five different litters) for each bar. The significance for each bar is indicated by p values, IUGR vs. CO and LP vs. NP. *n.s.* not significant, $**p<0.01$, $***p<0.001$; two-tailed Mann-Whitney test

versus 15.9 ± 0.8 pups in LP mothers, $p>0.05$). At day P1 the average body weight and total lung weight of the undernourished pups (IUGR) was significantly lower than those of age-matched pups of dams fed with normal protein diet (control group; Co; Fig. 1c, e). The IUGR animals remained growth restricted until P42 (Fig. 1c). However, by P70, the IUGR group demonstrated a catch-up growth with an increased weight gain over time (Fig. 1d) and nearly reached the same body mass as the control group (Fig. 1c). In line with this result, the lung also exhibited a notable catch-up growth (Fig. 1e), so that the lung weight between IUGR and control animals did not differ at P70 (Fig. 1e). In addition, we calculated the ratio of lung weight to body weight at P1, P21, and P70 to quantify relative lung weight within the two groups and did not detect any difference at either time point (Fig. 1f). Taken together, low protein diet during gestation led to IUGR and reduced lung weight at birth. Postnatal maternal alimentation with standard chow induced marked catch-up growth of lung and body weight in the offspring until P70.

Effects of IUGR and catch-up growth on the airway responsiveness

Next, we investigated the effect of IUGR on lung function over time, assessed by respiratory airway resistance (Res) and dynamic compliance (C_{dyn}). A marked, but not significant effect of IUGR on both Res and C_{dyn} was already observed at P28 (Fig. 2a, b), where IUGR animals exhibited a slightly increased Res and decreased C_{dyn} compared to the control group (Fig. 2a, b). To further examine whether this altered lung function deteriorates later in adulthood and to demonstrate that this pulmonary impairment is not just ascribable to the differences in body weight at the time of assessment but to the effects of IUGR and postnatal catch-up growth, we assessed Res and C_{dyn} at P70 as well. Strikingly, the Res was significantly increased in IUGR offspring even without methacholine challenge (Fig. 2a). In addition, the C_{dyn} was significantly decreased under baseline conditions subsequent to IUGR at P70 (Fig. 2b). However, C_{dyn} of IUGR animals was unaffected by

inhalation of methacholine, while the control group exhibited decreased C_{dyn} after inhalation of methacholine

Effect of IUGR and catch-up growth on the gene expression of adrenoceptor $\beta 1$ and $\beta 2$

To clarify whether altered expression of adrenoceptors as key molecules of the sympathetic nerve system (SNS)—known to regulate bronchoconstriction—might be responsible for the observed differences in airway responsiveness. Therefore, we measured gene expression of both adrenoceptors $\beta 1$ and $\beta 2$ by real-time RT-PCR (Fig. 3a, b). Interestingly, no difference was detectable in both genes between

IUGR and control group at P1, P42, or P70. Thus, these results give initial evidence, that there is no regulation of adrenoceptors after IUGR.

Effects of IUGR on the production of extracellular matrix components and extracellular matrix metabolizing enzymes in the lung

To address whether the dramatic impairment of lung function is associated with altered composition and production of ECM components, we assessed the expression of genes encoding pivotal ECM molecules over time. Starting at P1, the expression of ECM molecules such as coll III and fibrillin were significantly downregulated, whereas elastin and coll I α were markedly upregulated, indicating a deregulation of the ECM production (Fig. 4). At P42 and P70, we observed a striking increment of the expression of coll I α , fibrillin, and elastin (Fig. 4). These results are in line with the quantification of the expression of collagen I α as a profibrotic marker, assessed by immunostaining at P70 (Fig. 5a). We observed a considerably increased deposition of collagen I α in the different compartments of the lung (Fig. 5a, b). Next, we investigated ECM turnover assessing the expression of genes encoding the tissue inhibitors of metalloproteinases (TIMP). Interestingly, TIMP-1 and TIMP-2 were markedly upregulated on the mRNA level at P70 (Fig. 5d). Additionally, we analyzed pro-MMP-2—a target of TIMP—by gelatine zymography in total lung homogenate. In line with increased expression of TIMP-1 and TIMP-2, the abundance of pro-MMP-2 was considerably decreased at P70 (Fig. 5e).

In addition, we investigated the expression of genes encoding molecules regulating cell cycle and fibrotic process. Both, p21, a regulator of cell cycle, and AP-1, a profibrotic transcription factor and regulator of differentiation and proliferation, were significantly upregulated at P70 (Fig. 5c).

Taken together, the expression pattern and turnover of ECM components are dynamically regulated in the lung subsequent to IUGR, exhibiting an increased expression, deposition and regulation of ECM molecules at P70 over time with a concomitant increase in expression of regulators of cell cycle and senescence.

Pro-proliferative and pro-senescence state in lungs following IUGR and catch-up growth

To address proliferation and senescence as a feature of fibrotic processes, we assessed the expression of PCNA by immunoblotting. We observed an increasing expression of PCNA in the lungs subsequent to IUGR over time (Fig. 6a, b). To sum up, these results indicate an augmented proliferative state in the mature lung subsequent to IUGR.

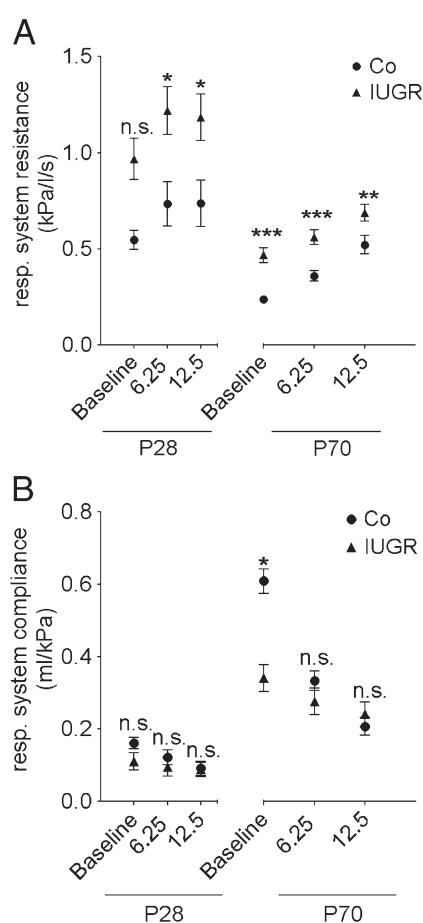


Fig. 2 Effect of IUGR and catch-up growth on respiratory function, assessment of respiratory system resistance (Res) and respiratory system compliance (C_{dyn}) by whole body plethysmography subsequent to intrauterine growth restriction (IUGR) at postnatal day 28 (P28) and P70. Res (a) and C_{dyn} (b) at P28 and P70; baseline (without nebulization), and nebulization of methacholine (two doses, 6.25 mg/ml and 12.5 mg/ml). IUGR (filled upright triangle), control (Co; filled circle). $n=4-17$ for each bar (from three to five different litters). The significance for each bar is indicated by p values, IUGR vs. CO, *n.s.* not significant; * $p<0.05$, ** $p<0.01$, *** $p<0.001$; two-way ANOVA test followed by a Bonferroni post-test (a) and two-tailed Mann–Whitney test (b)

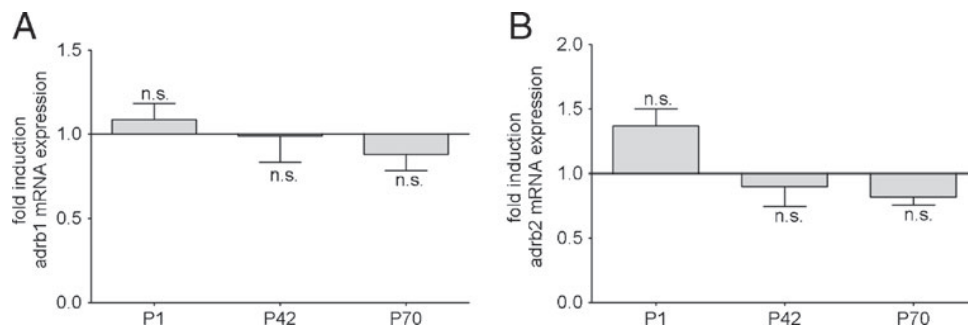


Fig. 3 Effect of IUGR and catch-up growth on the gene expression of adrenoceptor $\beta 1$ and $\beta 2$. **a** Expression of adrenoceptor $\beta 1$ (adrb1) during late lung development and adulthood (P1, P42, and P70). **b**: Expression of adrenoceptor $\beta 2$ (adrb2) at P1, P42, and P70. The mRNA expression was assessed by quantitative real-time PCR. The

control group was normalized to 1; $n=6-15$ for each group (from three to five different litters). The significance for each bar is indicated by p values, IUGR vs. Co; *n.s.* not significant; $*p<0.05$, $**p<0.01$, $***p<0.001$; two-tailed Mann-Whitney test

Developmental changes in expression of inflammatory cytokines subsequent to IUGR and catch-up growth

To further elucidate the underlying mechanism of impaired lung function, including parenchyma and airways, we assessed the expression of mRNA encoding inflammatory (Fig. 7a) and profibrotic (Fig. 7b) cytokines over time (P1, P42, and P70). We observed a dynamically regulated expression pattern for all analyzed molecules, including

Interleukin 6 (IL-6), IL-10, IL-13, tumor necrosis factor alpha (TNF- α), osteopontin (OPN), monocyte chemoattractant protein 1 (MCP-1), plasminogen activator inhibitor (PAI-1), and transforming growth factor beta 1 (TGF- $\beta 1$; Fig. 7a and b). The expression of inflammatory mediators subsequent to IUGR was decreased at P1, either non altered or considerably increased at P42, and even further increased at P70. Interestingly, the mRNA expression of proinflammatory cytokines was already upregulated at P42 and P70.

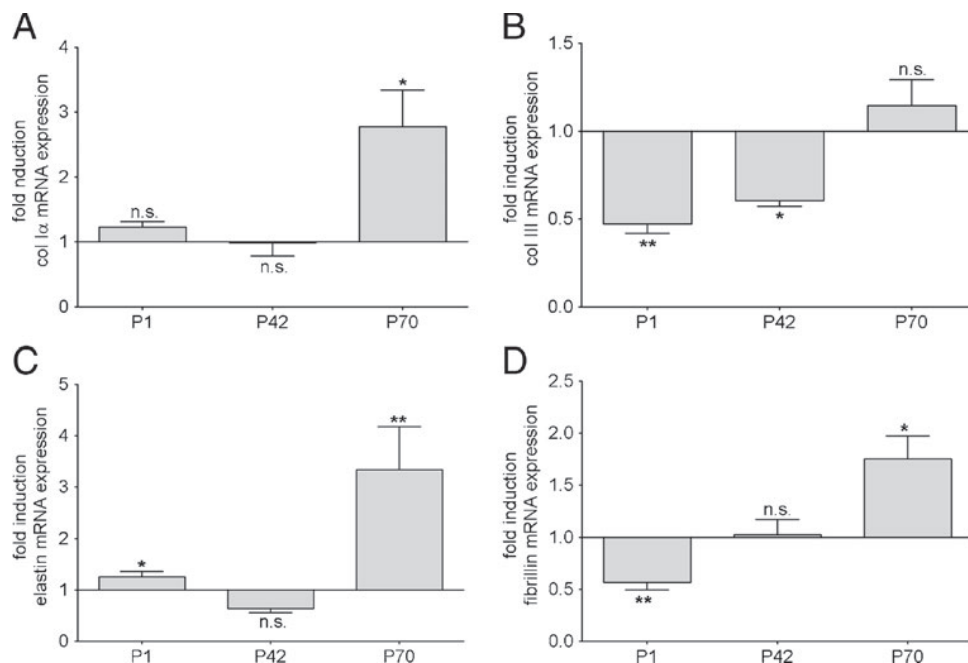


Fig. 4 Effect of IUGR on the expression of extracellular matrix (ECM) proteins and modulators of the ECM. Expression of extracellular matrix (ECM) related genes encoding collagens (Col) Ix (**a**), Col III (**b**), elastin (**c**), and fibrillin (**d**) in lungs extracted at postnatal day 1 (P1), P42, and P70 from rats after intrauterine growth restriction

(IUGR) and control rats. The mRNA expression, illustrated as relative fold induction, was assessed by real-time PCR. The control group was normalized to 1; $n=6-15$ for each group (from three to five different litters), *n.s.* not significant; $*p<0.05$, $**p<0.01$; two-tailed Mann-Whitney test

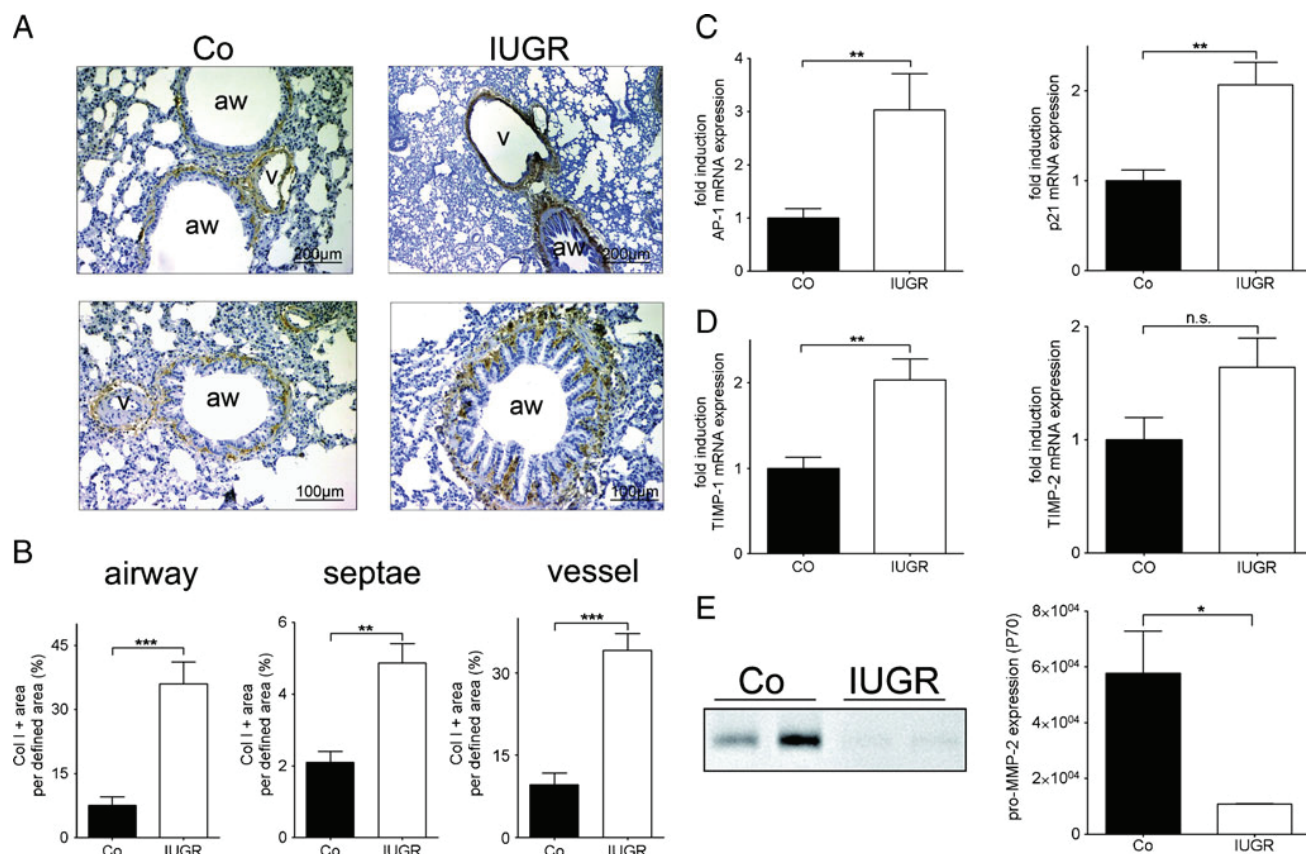


Fig. 5 Effect of IUGR and catch-up growth on ECM composition. **a, b** The expression of extracellular matrix (ECM) molecule collagen I (*col I*) in the lung was assessed by immunohistochemistry at postnatal day 70 (P70). **a** Representative pictures, illustrating positive col I staining in the alveolar septae, and in perivascular, and peribronchial tissue. **b** Quantitative evaluation of the immunohistochemical results was performed with MetaVue™ Imaging System. *V* vessel, *aw* airway. $n=4-6$ for each group (from three different litters). **c, d** The mRNA expression of genes encoding activator protein 1 (AP-1), p21, tissue inhibitor of

metalloproteinases 1 (TIMP-1), and TIMP-2 was assessed by real-time PCR at P70. $n=6-12$ for each group (from three to five different litters). **e** Analysis of MMP activity in lungs. Representative gelatin zymography of lung tissue at P70 and detection of pro-MMP2 gelatinolytic activity at ~70 kDa (**a**). Quantification pro-MMP-2 activity at P70. $n=4-6$ for each group. The significance for each bar is indicated by *p* values, IUGR (white bar) and control group (black bar), *n.s.* not significant; * $p<0.05$, ** $p<0.01$, *** $p<0.001$; two-tailed Mann-Whitney test

In contrast, the abundance of IL-10 mRNA, a mediator with anti-inflammatory effects, was decreased at P42 and unchanged at P70 (Fig. 7a). In conclusion, we observed a dynamic regulation of inflammatory mediators in animals subsequent to IUGR, starting with an attenuated inflammatory state at P1, and then an inversion over time to a markedly augmented inflammatory response.

Activation of Stat3 in the lung subsequent to IUGR and catch-up growth

To further elucidate the intracellular signaling of inflammatory cytokines and the activity of these signaling pathways, we assessed the expression and activation of Stat3 by immunoblotting (Fig. 8a and b). Consistent with the elevated expression of IL-6, we detected an increased phosphorylation of Stat3 at P70, whereas the phosphorylation was unchanged at P1 and P42. Furthermore, the target genes

of Stat3, such as TIMP-1 and AP-1 were concomitantly increased at P70 (Fig. 5c, d). In conclusion, the activation of the intracellular proinflammatory cascade as represented by Stat3 phosphorylation is markedly increased in lungs at P70 subsequent to IUGR.

Discussion

There is increasing evidence that prenatal factors, such as nutritional supply, permanently influence pivotal processes of lung development and maturation of pulmonary structures [9, 10]. The pathogenic mechanisms that results in an impairment of lung function observed in IUGR-associated lung disease are poorly understood. Although several studies have demonstrated an important role of ECM in lung disease subsequent to IUGR, the impact of pulmonary inflammation as a potential link between IUGR and

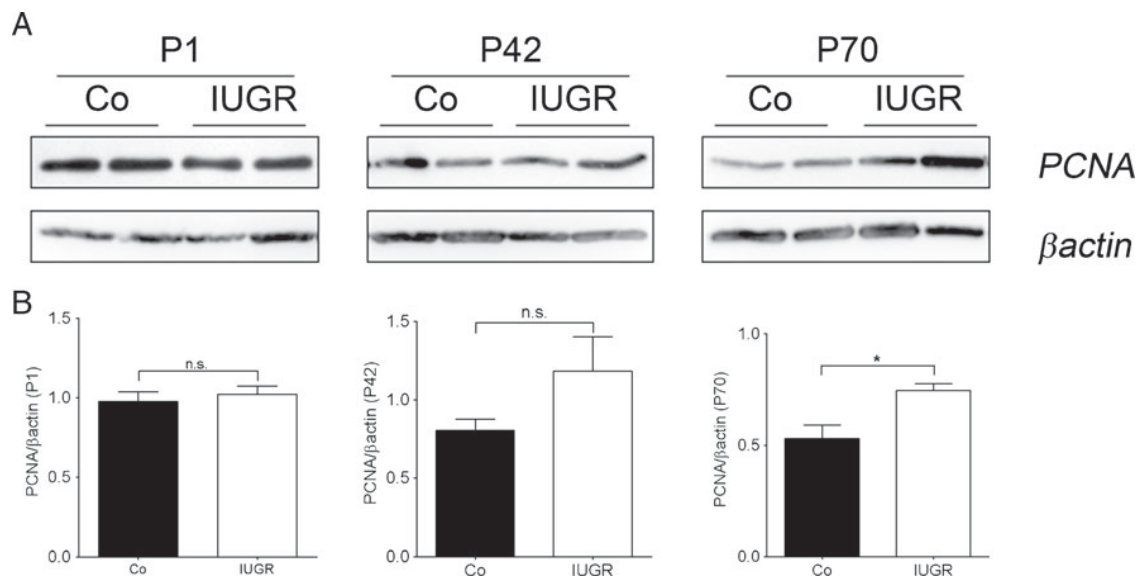
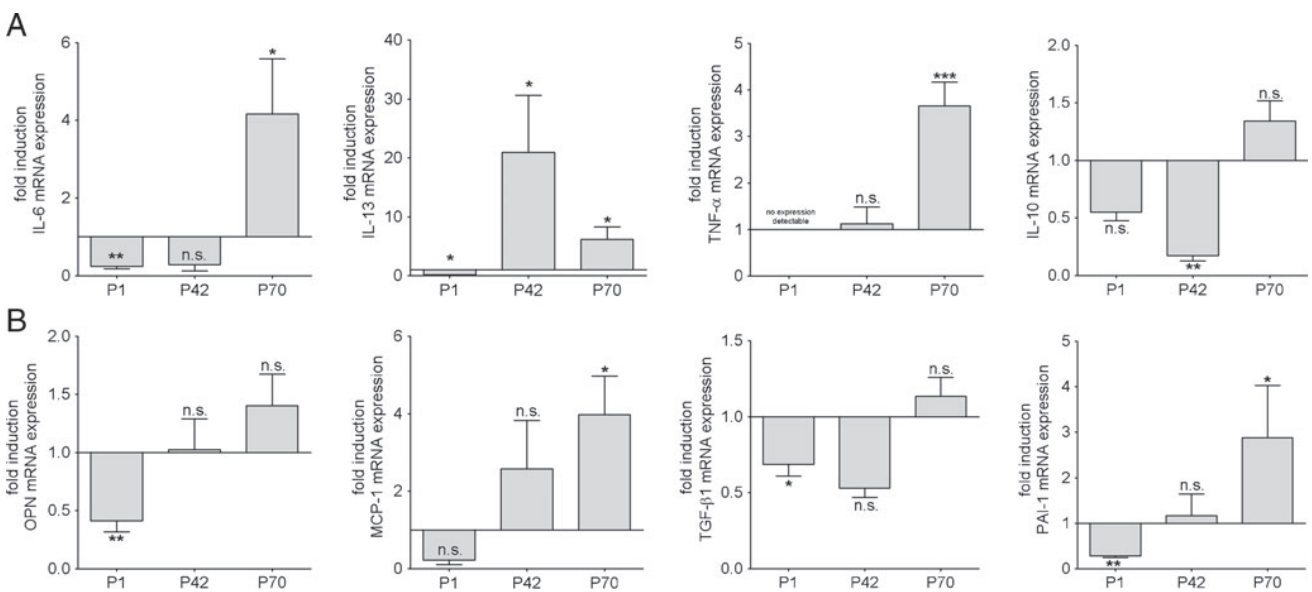


Fig. 6 Effect of IUGR and catch-up growth on proliferation. **a, b** Representative immunoblots of proliferating cell nuclear antigen (PCNA) (**a**) and the quantification of the expression by densitometric analysis (**b**) at postnatal day 1 (P1), P42, and P70, using constitutively expressed β-actin as loading control. The significance for each bar is

indicated by *p* values, intrauterine growth restriction (IUGR; white bar) and control group (black bar); *n.s.* not significant; **p*<0.05, ***p*<0.01; two-tailed Mann–Whitney test, *n*=4–6 for each group (from three to five different litters)

pulmonary disease has not been addressed to date. In this study, we aimed to examine the inflammatory processes as well as ECM over time, starting at P1 and terminating at P70.

In line with a report by Joyce et al. [28], our study shows airway hyperresponsiveness following IUGR. Obstructive lung diseases are associated with an enhanced deposition and a deregulated expression of ECM components [21].



plasminogen activator inhibitor-1 (PAI-1) at P1, P42, and P70. The mRNA expression was assessed by quantitative real-time PCR. The control group was normalized to 1; *n*=6–15 for each group (from three to five different litters). The significance for each bar is indicated by *p* values, IUGR vs. Co; *n.s.* not significant; **p*<0.05, ***p*<0.01, ****p*<0.001; two-tailed Mann–Whitney test

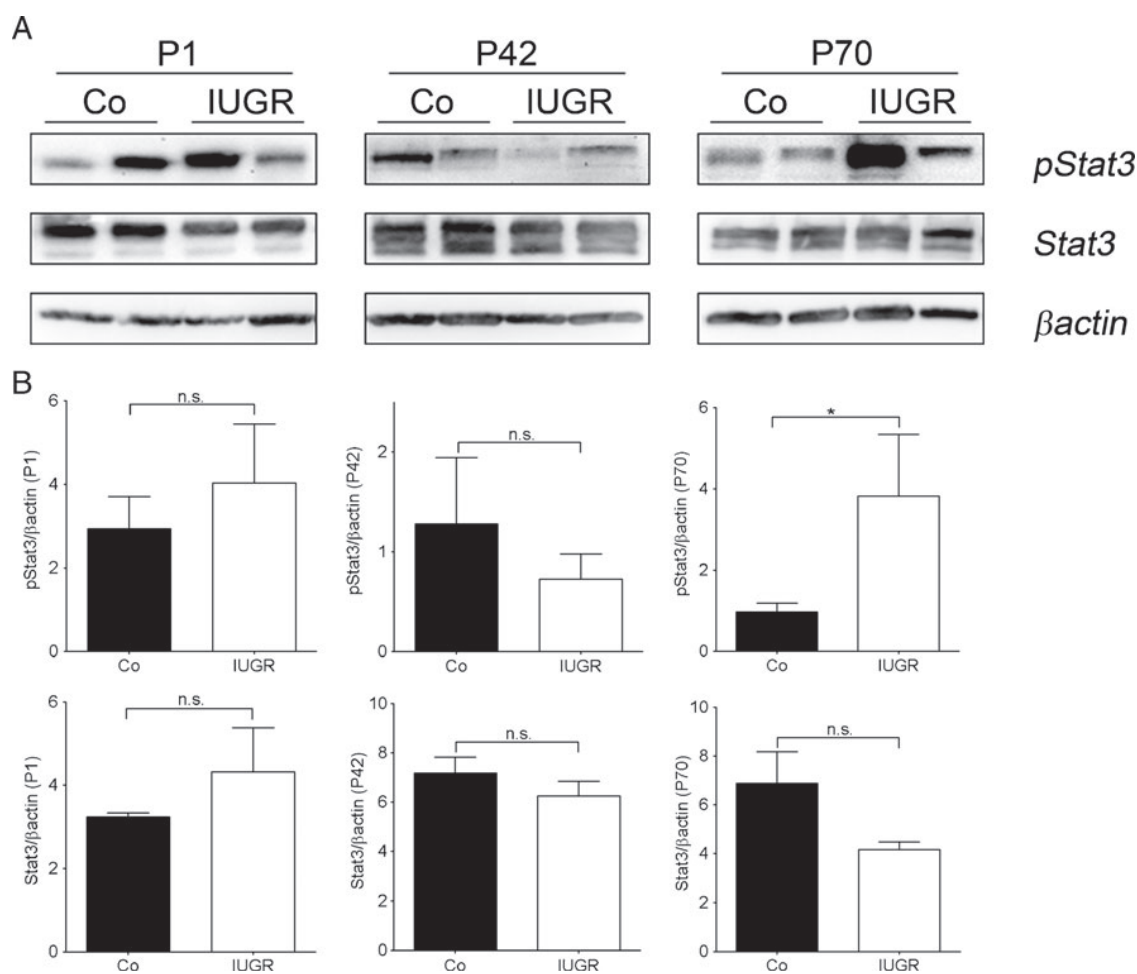


Fig. 8 Stat3 signaling in lungs subsequent to IUGR and catch-up growth. **a** Representative immunoblots, illustrating the expression and phosphorylation of Signal transducer and activator of transcription 3 (*Stat3*) in lungs subsequent to intrauterine growth restriction (*IUGR*) at postnatal day (P1), P42, and P70. Expression and phosphorylation of Stat3 was assessed by immunoblot, using constitutively expressed β -

Actin as loading control. **b** Quantification of the expression and phosphorylation of Stat3 by densitometric analysis, using β -Actin as loading control. The significance for each bar is indicated by *p* values, *IUGR* (white bars) vs. *CO* (black bars), *n.s.* not significant; **p*<0.05, ***p*<0.01; two-tailed Mann–Whitney test, *n*=4–6 for each group (from three to five different litters)

Pulmonary structure and ECM have been previously investigated and demonstrated to be affected by intrauterine growth restriction. How are the ECM components regulated over time subsequent to IUGR? Experimental studies revealed a dysregulated lung development [7] and alterations of lung structure [8] in adult animals subsequent to IUGR induced by placental insufficiency. Similarly, a very recent study of our group demonstrated that rats following IUGR exhibit an increased mean linear intercept (MLI) at P70, while septal thickness remains unaffected, indicating an elevated amount of alveolar tissue [15]. In line with these morphometric results, analysis of key enzymes regulating apoptotic processes revealed a dampened apoptosis at P1. Thus, consistent with the given dampened apoptosis during late lung development [15], and the significantly increased proliferative state shown in the present study, data we describe in both studies give a strong body of evidence that the

balance between apoptosis and proliferation is perturbed and proliferation is favored the more development and age proceed. Furthermore, the results in the present study demonstrate a decreased production of ECM at P1 (collagen III and fibrillin) and an increasing deposition of ECM molecules, such as collagen I α and fibrillin at P70. Even more interesting than the dynamic regulation of the gene expression of ECM components is the evidence of an augmented deposition of collagen I α in the different compartments of the lung at P70, indicating profibrotic processes. Experimental studies of Maritz et al. [8, 29] support these profibrotic processes shown in this study giving evidence of a persistently thicker blood–air barrier and thicker septa. In accordance with dysregulated lung morphology, we demonstrated the reduced MLI in a previous study. Here, we show a deregulation of ECM deposition, finally leading to loss of function and thereby to impaired lung function. However, possibly, the profibrotic

processes in our animal model with catch-up growth are in an initial state and therefore P70 is too early for the animals to exhibit a thickening of the septal wall. Later time points will be essential to get a broader understanding of the dynamics and the consequences of the deregulated ECM.

The ECM is deposited by fibroblasts and is continuously remodeled by matrix remodeling proteases. MMP-2 and TIMP-2 are strongly expressed in rodents during lung development [30] and in fibrotic processes [31], indicating a pivotal role and finely tuned regulation of matrix remodeling in the lung. In our study, we have illustrated that IUGR markedly decreased the protein expression of pro-MMP-2 at P70. Interestingly, this deregulation was accompanied by a significantly increased expression of the inhibitors of metalloproteinases, TIMP-1 and TIMP-2, and an augmented deposition of collagen I α in the lung. In conclusion, our data collectively suggest that IUGR would swing the balance in favor of interstitial ECM deposition and would prevent turnover of ECM components in the lung. In addition, we demonstrate an elevation of p21 at P70. Several studies report the impact of p21 on the regulation of cell cycle and cell aging/senescence, by inhibiting the activity of cyclin-dependent kinases [32]. Regulation of p21 expression is mediated by various pathways, such as Stat-signaling [33], activated by inflammatory cytokines.

It is intriguing that inflammatory response over time and pulmonary inflammation as a potential pathomechanism for impaired regulation of tissue remodeling and subsequent fibrosis in IUGR animals has not been addressed to date. First, we chose to quantify mRNA expression of several genes encoding cytokines known to have an important impact on inflammatory processes. Strikingly, this study clearly reveals a continuously increasing expression of inflammatory cytokines, such as IL-6, IL-13 and PAI-1, starting being markedly decreased at P1 and significantly upregulated at later time points (P42 and P70). These findings are in line with studies demonstrating a predisposition for fibrosis and inflammation in other organs subsequent to IUGR [20] and the notable role of IL-6 in the pathomechanism of fibrosis [34]. For example, Plank et al. illustrated the devastating course of thy1-glomerulonephritis in IUGR-rats with clear features of renal inflammation and fibrosis [25]. Consistent with these results, the renal expression of IL-6, PAI-1, and MCP-1 was dramatically upregulated and the kidneys displayed an increased deposition of ECM in a rat model of glomerulonephritis following IUGR [25]. However, inflammatory cytokines, such as IL-6, are not just crucial for inflammatory processes but also for normal lung development. Interestingly, we demonstrated a significant downregulation of IL-6 at the transition from saccular to alveolar phase at P1. The diminished abundance of IL-6 at this crucial stage of late lung development may contribute to the deregulation of lung morphogenesis. The evidence that

IL-6 mediates the catch-up growth of hypoplastic lungs [35] demonstrates its impact on lung development and underlines our idea. At P42 and P70, however, the picture is reversed: the expression of IL-6, IL-13, PAI-1, and TNF- α is significantly increased. Airway overexpression of IL-6 contributes to subepithelial fibrosis with collagen deposition [36]. The elevated expression of IL-6 could be a link to the observed catch-up growth in animals subsequent to IUGR in our model. Zhu and colleagues [37] showed in mice that an overexpression of IL-13 in the lungs causes an asthmatic phenotype with mononuclear inflammation, subepithelial fibrosis, and airway obstruction. Furthermore, Hattori and colleagues [38] demonstrated that PAI-1-deficient mice are protected from bleomycin-induced pulmonary fibrosis. PAI-1 and the plasminogen system play an important role in airway remodeling by inhibiting MMP and therefore preventing degradation of ECM as it is seen in asthmatic lung diseases [39]. To highlight the incremental inflammatory response induced by IUGR, we analyzed the intracellular signaling of several cytokines, focusing on the Stat3 pathway and its target genes, such as TIMP-1 and AP-1. The decision to focus on Stat3 signaling was based two crucial findings in our group: first, previous studies of Plank et al. demonstrated in an experimental model of glomerulonephritis that IUGR aggravates the course of the disease and led to fibroproliferative processes, impairment of renal function and increased inflammatory response. Interleukin-6 (IL-6) was the cytokine with the most striking increment in gene expression [25]. Interestingly, this cytokine is also elevated in the present study. Furthermore, the downstream pathway of IL-6 is Stat3-mediated. Second, very recent experiments from our group focusing on renal endocrine function subsequent to catch-up growth show also a strong increment in IL-6 gene expression. In accordance with these findings investigation of Stat3 signaling in the present study demonstrates a significant deregulation. Strikingly, we detected an augmentation in phosphorylation over time, starting with no changes at P1 and terminating with a significant increment on phosphorylation compared to the control group at P70. The fact that the increment of inflammatory response is paralleled by elevated expression and deposition of ECM components is especially interesting and leads to the assumption that inflammation may be a potential underlying mechanism of the profibrotic pulmonary processes. Furthermore, this study demonstrates that pulmonary impairment subsequent to IUGR is accompanied by postnatal catch-up growth. This may represent an additional pathogenetic factor for the impairment of the lung seen in our animals. However, that cannot be completely clarified in our study and require further experiments.

The impact and the underlying mechanisms of increased inflammatory response in IUGR-associated lung disease remains poorly understood. Epigenetics is one of the key

mechanisms widely discussed and increasingly recognized in the broad field of developmental programming. Several studies demonstrated persistent changes in methylation of promoter regions of crucial developmental genes following fetal and postnatal programming, ultimately leading to physiological dysfunction [40–43]. In the present study, expression of numerous cytokines is increased in lungs after IUGR. Before addressing epigenetics, it will thus be crucial to identify the key player in mediating the observed inflammatory response. Intensive research is encouraged to delineate the underlying mechanism and to find treatment strategies to improve or even prevent lung diseases caused by IUGR. It will be promising to determine the effect of an anti-inflammatory therapy on the development of IUGR-associated lung diseases in further studies in order to address the question whether such treatment strategies may help to prevent the onset of pulmonary damage and improve long term lung function following IUGR.

Taken together, the present results demonstrate that IUGR impairs lung function, leads to a dynamic upregulation of inflammatory signaling and subsequently to a profibrotic remodeling of ECM over time. Thus, this study does not only contribute to a better general understanding of pathological consequences in the increasingly important clinical group of IUGR infants, but also elucidates the pathomechanistic aspects of IUGR-associated lung disease. This will ultimately allow defining more effective preventive and therapeutic strategies of pulmonary disease.

Acknowledgments The authors thank Ida Allabauer and Julia Dobner for expert technical assistance and Andrea Hartner (Department of Pediatric and Adolescent Medicine, University Hospital Erlangen, Germany) for access to microscopy facilities. The animal experiments were in part supported by a grant to Jörg Dötsch, Christian Plank, and Wolfgang Rascher by the Deutsche Forschungsgemeinschaft, Bonn, Germany; SFB 423, Collaborative Research Centre of the German Research Foundation: Kidney Injury: Pathogenesis and Regenerative Mechanisms, Project B13 and by a grant to Christian Plank and Miguel Angel Alejandro Alcázar by the Erlanger Leistungsbezogene Anschubfinanzierung und Nachwuchsförderung (ELAN) Erlangen, Köln Fortune, University of Cologne.

Disclosure The authors declare no conflict of interest.

References

- Meetoo D (2008) Chronic diseases: the silent global epidemic. *Br J Nurs* 17:1320–1325
- Ljustina-Pribic R, Petrovic S, Tomic J (2010) Childhood asthma and risk factors. *Med Pregl* 63:516–521
- Bloomberg GR (2011) The influence of environment, as represented by diet and air pollution, upon incidence and prevalence of wheezing illnesses in young children. *Curr Opin Allergy Clin Immunol* 11:144–149. doi:10.1097/ACI.0b013e3283445950
- Gilliland FD, Li YF, Peters JM (2001) Effects of maternal smoking during pregnancy and environmental tobacco smoke on asthma and wheezing in children. *Am J Respir Crit Care Med* 163:429–436
- Barker DJ (1995) Intrauterine programming of adult disease. *Mol Med Today* 1:418–423
- Nuyt AM (2008) Mechanisms underlying developmental programming of elevated blood pressure and vascular dysfunction: evidence from human studies and experimental animal models. *Clin Sci (Lond)* 114:1–17. doi:10.1042/CS20070113
- Lipsett J, Tamblyn M, Madigan K, Roberts P, Cool JC, Runciman SI, McMillen IC, Robinson J, Owens JA (2006) Restricted fetal growth and lung development: a morphometric analysis of pulmonary structure. *Pediatr Pulmonol* 41:1138–1145
- Maritz GS, Cock ML, Louey S, Suzuki K, Harding R (2004) Fetal growth restriction has long-term effects on postnatal lung structure in sheep. *Pediatr Res* 55:287–295. doi:10.1203/01.PDR.0000106314.99930.65
- Maritz GS, Morley CJ, Harding R (2005) Early developmental origins of impaired lung structure and function. *Early Hum Dev* 81:763–771. doi:10.1016/j.earlhumdev.2005.07.002
- Kotecha SJ, Watkins WJ, Heron J, Henderson J, Dunstan FD, Kotecha S (2010) Spirometric lung function in school-age children: effect of intrauterine growth retardation and catch-up growth. *Am J Respir Crit Care Med* 181:969–974. doi:10.1164/rccm.200906-0897OC
- Joss-Moore LA, Wang Y, Yu X, Campbell MS, Callaway CW, McKnight RA, Wint A, Dahl MJ, Dull RO, Albertine KH et al (2011) IUGR decreases elastin mRNA expression in the developing rat lung and alters elastin content and lung compliance in the mature rat lung. *Physiol Genomics* 43:499–505. doi:10.1152/physiolgenomics.00183.2010
- Warburton D, Bellusci S (2004) The molecular genetics of lung morphogenesis and injury repair. *Paediatr Respir Rev* 5:S283–287
- Copland I, Post M (2004) Lung development and fetal lung growth. *Paediatr Respir Rev* 5:S259–264
- Orgeig S, Crittenden TA, Marchant C, McMillen IC, Morrison JL (2010) Intrauterine growth restriction delays surfactant protein maturation in the sheep fetus. *Am J Physiol Lung Cell Mol Physiol* 298:L575–583. doi:10.1152/ajplung.00226.2009
- Alejandre Alcazar MA, Morty RE, Lenzian L, Vöhlen C, Oestreicher I, Plank C, Schneider H, Dotsch J (2011) Inhibition of TGF-beta signaling and decreased apoptosis in IUGR-associated lung disease in rats. *PLoS One* 6:e26371. doi:10.1371/journal.pone.0026371
- Cock ML, Albuquerque CA, Joyce BJ, Hooper SB, Harding R (2001) Effects of intrauterine growth restriction on lung liquid dynamics and lung development in fetal sheep. *Am J Obstet Gynecol* 184:209–216. doi:10.1067/mob.2001.108858
- Gagnon R, Langridge J, Inchley K, Murotsuki J, Possmayer F (1999) Changes in surfactant-associated protein mRNA profile in growth-restricted fetal sheep. *Am J Physiol* 276:L459–465
- Amarilyo G, Oren A, Mimouni FB, Ochshorn Y, Deutsch V, Mandel D (2011) Increased cord serum inflammatory markers in small-for-gestational-age neonates. *J Perinatol* 31:30–32. doi:10.1038/jp.2010.53
- Desai M, Gayle DA, Casillas E, Boles J, Ross MG (2009) Early undernutrition attenuates the inflammatory response in adult rat offspring. *J Matern Fetal Neonatal Med* 22:571–575. doi:10.1080/14767050902874105
- Plank C, Nusken KD, Menendez-Castro C, Hartner A, Oestreicher I, Amann K, Baumann P, Peters H, Rascher W, Dotsch J (2010) Intrauterine growth restriction following ligation of the uterine arteries leads to more severe glomerulosclerosis after mesangio-proliferative glomerulonephritis in the offspring. *Am J Nephrol* 32:287–295. doi:10.1159/000319045
- Wynn TA (2003) IL-13 effector functions. *Annu Rev Immunol* 21:425–456. doi:10.1146/annurev.immunol.21.120601.141142

22. Gueders MM, Foidart JM, Noel A, Cataldo DD (2006) Matrix metalloproteinases (MMPs) and tissue inhibitors of MMPs in the respiratory tract: potential implications in asthma and other lung diseases. *Eur J Pharmacol* 533:133–144. doi:10.1016/j.ejphar.2005.12.082
23. Pedroza M, Schneider DJ, Karmouty-Quintana H, Coote J, Shaw S, Corrigan R, Molina JG, Alcorn JL, Galas D, Gelinas R et al (2011) Interleukin-6 contributes to inflammation and remodeling in a model of adenosine mediated lung injury. *PLoS One* 6:e22667. doi:10.1371/journal.pone.0022667
24. Wygrecka M, Jablonska E, Guenther A, Preissner KT, Markart P (2008) Current view on alveolar coagulation and fibrinolysis in acute inflammatory and chronic interstitial lung diseases. *Thromb Haemost* 99:494–501. doi:10.1160/TH07-11-0666
25. Plank C, Ostreicher I, Hartner A, Marek I, Struwe FG, Amann K, Hilgers KF, Rascher W, Dotsch J (2006) Intrauterine growth retardation aggravates the course of acute mesangioproliferative glomerulonephritis in the rat. *Kidney Int* 70:1974–1982. doi:10.1038/sj.ki.5001966
26. Alejandro-Alcazar MA, Kwapiszewska G, Reiss I, Amarie OV, Marsh LM, Sevilla-Perez J, Wygrecka M, Eul B, Kobrich S, Hesse M et al (2007) Hyperoxia modulates TGF-beta/BMP signaling in a mouse model of bronchopulmonary dysplasia. *Am J Physiol Lung Cell Mol Physiol* 292:L537–549. doi:10.1152/ajplung.00050.2006
27. Alejandro Alcazar MA, Boehler E, Amann K, Klaffenbach D, Hartner A, Allabauer I, Wagner L, von Horsten S, Plank C, Dotsch J (2011) Persistent changes within the intrinsic kidney-associated NPY system and tubular function by litter size reduction. *Nephrol Dial Transplant* 26:2453–2465. doi:10.1093/ndt/gfq825
28. Joyce BJ, Louey S, Davey MG, Cock ML, Hooper SB, Harding R (2001) Compromised respiratory function in postnatal lambs after placental insufficiency and intrauterine growth restriction. *Pediatr Res* 50:641–649
29. Maritz GS, Cock ML, Louey S, Joyce BJ, Albuquerque CA, Harding R (2001) Effects of fetal growth restriction on lung development before and after birth: a morphometric analysis. *Pediatr Pulmonol* 32:201–210. doi:10.1002/ppul.1109
30. Ryu J, Vicencio AG, Yeager ME, Kashgarian M, Haddad GG, Eickelberg O (2005) Differential expression of matrix metalloproteinases and their inhibitors in human and mouse lung development. *Thromb Haemost* 94:175–183. doi:10.1267/THRO05010175
31. Oggionni T, Morbini P, Inghilleri S, Palladini G, Tozzi R, Vitulo P, Fenoglio C, Perlini S, Pozzi E (2006) Time course of matrix metalloproteases and tissue inhibitors in bleomycin-induced pulmonary fibrosis. *Eur J Histochem* 50:317–325
32. Sherr CJ, Roberts JM (1995) Inhibitors of mammalian G1 cyclin-dependent kinases. *Genes Dev* 9:1149–1163
33. Chin YE, Kitagawa M, Su WC, You ZH, Iwamoto Y, Fu XY (1996) Cell growth arrest and induction of cyclin-dependent kinase inhibitor p21 WAF1/CIP1 mediated by STAT1. *Science* 272:719–722
34. Saito-Fujita T, Iwakawa M, Nakamura E, Nakawatari M, Fujita H, Moritake T, Imai T (2011) Attenuated lung fibrosis in interleukin 6 knock-out mice after C-ion irradiation to lung. *J Radiat Res (Tokyo)* 52:270–277
35. Nogueira-Silva C, Moura RS, Esteves N, Gonzaga S, Correia-Pinto J (2008) Intrinsic catch-up growth of hypoplastic fetal lungs is mediated by interleukin-6. *Pediatr Pulmonol* 43:680–689. doi:10.1002/ppul.20840
36. Gharaee-Kermani M, Phan SH (2005) Molecular mechanisms of and possible treatment strategies for idiopathic pulmonary fibrosis. *Curr Pharm Des* 11:3943–3971
37. Zhu Z, Homer RJ, Wang Z, Chen Q, Geba GP, Wang J, Zhang Y, Elias JA (1999) Pulmonary expression of interleukin-13 causes inflammation, mucus hypersecretion, subepithelial fibrosis, physiologic abnormalities, and eotaxin production. *J Clin Invest* 103:779–788. doi:10.1172/JCI5909
38. Hattori N, Mizuno S, Yoshida Y, Chin K, Mishima M, Sisson TH, Simon RH, Nakamura T, Miyake M (2004) The plasminogen activation system reduces fibrosis in the lung by a hepatocyte growth factor-dependent mechanism. *Am J Pathol* 164:1091–1098. doi:10.1016/S0002-9440(10)63196-3
39. Kucharewicz I, Kowal K, Buczek W, Bodzenta-Lukaszyk A (2003) The plasmin system in airway remodeling. *Thromb Res* 112:1–7. doi:10.1016/j.thromres.2003.10.011
40. Simmons RA (2007) Role of metabolic programming in the pathogenesis of beta-cell failure in postnatal life. *Rev Endocr Metab Disord* 8:95–104. doi:10.1007/s11154-007-9045-1
41. Pinney SE, Simmons RA (2010) Epigenetic mechanisms in the development of type 2 diabetes. *Trends Endocrinol Metab* 21:223–229. doi:10.1016/j.tem.2009.10.002
42. Plagemann A, Harder T, Brunn M, Harder A, Roepke K, Wittrock-Staar M, Ziska T, Schellong K, Rodekamp E, Melchior K et al (2009) Hypothalamic proopiomelanocortin promoter methylation becomes altered by early overfeeding: an epigenetic model of obesity and the metabolic syndrome. *J Physiol* 587:4963–4976. doi:10.1113/jphysiol.2009.176156
43. Plagemann A, Roepke K, Harder T, Brunn M, Harder A, Wittrock-Staar M, Ziska T, Schellong K, Rodekamp E, Melchior K et al (2010) Epigenetic malprogramming of the insulin receptor promoter due to developmental overfeeding. *J Perinat Med* 38:393–400. doi:10.1515/JPM.2010.051

Nephrol Dial Transplant (2011) 26: 2453–2465

doi: 10.1093/ndt/gfq825

Advance Access publication 2 March 2011

Persistent changes within the intrinsic kidney-associated NPY system and tubular function by litter size reduction

Miguel Angel Alejandro Alcázar^{1,2}, Eva Boehler², Kerstin Amann³, Daniela Klaffenbach², Andrea Hartner², Ida Allabauer², Leona Wagner⁴, Stephan von Hörsten⁵, Christian Plank² and Jörg Dötsch¹

¹Department of Pediatric and Adolescent Medicine, University of Cologne, Cologne, Germany, ²Department of Pediatric and Adolescent Medicine, University of Erlangen-Nuremberg, Erlangen, Germany, ³Department of Pathology, University of Erlangen-Nuremberg, Erlangen, Germany, ⁴Department of Molecular Biology, University of Halle/Saale, Halle, Germany and ⁵Experimental Therapy, Franz-Penzoldt Center, University of Erlangen-Nuremberg, Erlangen, Germany

Correspondence and offprint requests to: Miguel Angel Alejandro Alcázar; E-mail: miguel.alejandre-alcazar@uk-koeln.de

Abstract

Background. Intrauterine growth restriction (IUGR) is associated with an increased risk of renal diseases in adulthood. However, while low-birth-weight-infants often undergo accelerated postnatal growth, the impact of postnatal environmental factors such as nutrition and early postnatal stressors on renal development and function remains unclear. In this context, Neuropeptide Y (NPY) may act as a critical factor. NPY is a sympathetic coneurotransmitter involved in blood pressure regulation

and tubular function. Yet, little is known about the expression and function of endogenous NPY in the kidney and the functional relevance for the transmission of persistent postnatal-induced effects.

Methods. (1) IUGR was induced in Wistar rats by isocaloric protein restriction in pregnant dams. (2) Litter size was reduced to 6 (LSR6) or 10 (LSR10) male neonates. To differentiate the effect of postnatal nutrition and stressors, we additionally included home-cage-control animals without any postnatal manipulation. Animals were sacrificed at Day 70.

Results. Litter size reduction (LSR) to 6 but not IUGR increased messenger RNA expression of endogenous NPY and down-regulated the NPY-receptors Y1 and Y2. Furthermore, dipeptidylpeptidase IV (DPPIV)—an enzyme that cleaves NPY—was decreased after LSR. Expression and the phosphorylation of mitogen-activated protein kinase 42/44 (intracellular signalling pathway of the receptor Y1) were altered. An impaired renal function with pronounced kaliuresis and natriuresis was observed at Day 70 after LSR.

Conclusions. Postnatal nutrition and stressors such as LSR lead to dysregulated signalling of NPY. These data demonstrate that factors in the early postnatal environment exert important changes in the tubular function, which may predispose to corresponding pathology.

Keywords: NPY, NPY receptor Y1; Kaliuresis; Natriuresis; postnatal environment; IUGR

Introduction

Epidemiological studies have shown an association between low-birth-weight (LBW) and an increased risk of cardiovascular and renal diseases [1–6]. Several animal models have replicated the consequences of intrauterine growth restriction (IUGR). IUGR was induced either by protein restriction during gestation [7] or by uterine artery ligation [8]. Barker *et al.* [9, 10] coined the concept of ‘perinatal programming’ postulating that early perinatal events predispose for diseases in later life. However, epidemiological data have revealed that LBW itself is not the only factor that predisposes for diseases in later life. The mechanisms by which the pre- and postnatal environment programmes renal function are still unclear [11–14].

Newborns with LBW undergo early postnatal over-nutrition. Enhanced early nutrition of LBW infants may be adverse for the postnatal development of the kidney and hypertension [15]. The sympathetic nerve system (SNS) among other systems plays a pivotal role in the development of renal hypertension and tubular function [16, 17]. Data from Vásárhelyi [18] show an association between LBW and natriuresis in later life. Lenaerts *et al.* and McDonough [16, 19, 20] indicate a role of the SNS in the aetiology of increased renal sodium excretion. The role of the early postnatal stressors, such as litter size reduction (LSR), in the development of hypertension and imbalance of renal homeostasis has not been addressed so far. Neuropeptide Y (NPY) is a 36 aminoacid coneurotransmitter, which affects renal function in several direct and indirect ways. It is released from renal sympathetic nerves [21–23] and acts directly via NPY-receptors, especially Y1 and Y2 on renal tubules leading to alterations of intrarenal tubular transport processes and renin release [24]. It has been shown that NPY regulates natriuresis, diuresis [25–27] and kaliuresis via the NPY-receptor Y1 [26, 28, 29]. NPY-receptor Y1 is a G-Protein-coupled receptor, transducing extracellular stimuli into intracellular signals. One

intracellular signalling pathway which plays a pivotal role is the mitogen-activated protein kinase (MAPK) 42/44 [30] and an activation of Na⁺-K⁺-ATPase [28, 31, 32]. G-protein receptors activate the phosphorylation of MAPK 42/44. Activated MAPK 42/44 pathway has been reported to regulate Na⁺/Pi cotransporter in the renal tubuli and to control the activity of the Na⁺-K⁺-ATPase. Initial evidence for a role of endogenous NPY in the regulation of renovascular function has come from studies on reserpinized pigs [32]. In addition, several studies demonstrate that NPY inhibits renin release and lowers plasma renin activity [26, 33–35] via Y1-receptor [26, 35, 36]. Renin, as part of the Renin-Angiotensin-Aldosterone-System (RAAS) plays a pivotal role in the regulation of natriuresis and kaliuresis.

Studies in rats show that neonatal perturbations can exert a significant behavioural and biological effect, which translates into various adaptational changes within the adult animal [37–39]. Most studies have focused on early stressors such as maternal deprivation, neonatal handling and infection [40–42]. They agree that such early life events alter among others, NPY release and signal transduction [43–46]. Therefore, the aim of this study was to investigate the effects of altered prenatal and early postnatal management on renal function in later life and to elucidate the possible associated alterations of endogenous NPY-system.

Materials and methods

Animal procedures

All procedures performed on animals were done in accordance with guidelines of the American Physiological Society and were approved by the local government authorities (AZ # 621-2531.31-11/02 and AZ # 621-2531.31-14/05; Regierung von Mittelfranken). Virgin female Wistar rats were obtained from our own colony and were housed in a room maintained at 22 ± 2°C, exposed to a 12-h dark/light cycle. The animals were allowed unlimited access to standard chow (#1320; Altromin, Lage, Germany) and tap water. Two simultaneous sets of experiments, completely independent from each other were performed. The first included pre- and postnatal nutritional interventions, the second was restricted to postnatal interventions only.

- (1) Intrauterine growth restriction (IUGR) was induced in Wistar rats by isocaloric protein restriction in pregnant dams as previously described [7]. They were fed either a normal protein (Co) diet containing 17.0% protein (casein) or a low-protein (IUGR) isocaloric diet containing 8.0% protein (casein) throughout pregnancy. Rats delivered spontaneously at Day 23 of pregnancy. On the first day of life, the litters were reduced to six male pups per dam. During lactation, dams were fed standard chow. The offspring were nursed by their own mothers until weaned at Day 23 to standard chow. Male animals were sacrificed at Day 70 defining four groups: IUGR 6 (six animals, three dams), Non IUGR 6 (six animals, three dams), IUGR 10 (six animals, three dams) and non-IUGR 10 (six animals, three dams).
- (2) In the model of postnatal LSR, the litters were either reduced to 10 (LSR10) or 6 (LSR6) pups on the first day of life. Each group (LSR6 and LSR10) was formed of males from three to five different litters. During lactation, rat mothers were fed standard chow. The weaning was at Day 23 after birth. We included home-cage-control (HCC, mean litter size of 16) animals without any postnatal manipulation during lactation, rat mothers were fed standard chow. After weaning, animals were equally fed ad libitum with standard chow. HCC, LSR10 and LSR6 animals were sacrificed at Day 70 of life defining three groups: HCC (five animals, three dams), LSR10 (ten animals, four dams), LSR6 (eight animals, three dams).

Table 1. Designed primer pairs and TaqMan probes used in this study

NPY	Forward 5'-AGCAGAGGACATGGCCAGATAC-3' Reverse 5'-TGAAATCAGTGTCTCAGGGCTG-3' Probe 5'-(FAM)-CAATCTCATCACCAGACAGAGATATGGCAAGA-(TAMRA)-3'
Y1	Forward 5'-CCACCTCACGGCCATGAT-3' Reverse 5'-TGGAAATTTTTGTTTCAGGAATCC-3' Probe 5'-(FAM)-TCCACCTGCGTCAACCCCATCTTTA-(TAMRA)-3'
Y2	Forward 5'-GGTGAGTTGCCCCCTGATC-3' Reverse 5'-ACCACCTGCACCTCAACCA-3'; Probe 5'-(FAM)-AGCCGGAGCTCATAGACAGCACCAA-(TAMRA)-3'
Renin	Forward 5'-ACCAGGGCACTTTCCTACTACGT-3' Reverse 5'-GAGACCCCTTCATGGTGATC-3' Probe 5'-(FAM)-AGCATCAGCAAGGCCGGCTCC-(TAMRA)-3'
MCR	Forward 5'-CCAAGTACTTCCAGGATTTAAAAAC-3' Reverse 5'-AACGATGATAGACACATCCAAGAATACT-3' Probe 5'-(FAM)-TGCCTCTCGAGGACCAAATCACCT-(TAMRA)-3'
ATR1a	Forward 5'-TCACAGTGTGCGCGTTTCAT-3' Reverse 5'-TGGTAAGGCCAGCCCTAT-3' Probe 5'-(FAM)-TGAGTCTCGGAATTCGACGCTCCC-(TAMRA)-3'
ATR1b	Forward 5'-TTCTGCTCACGTGTCTCAG-3' Reverse 5'-GATGATGCAGGTGACTTTGG-3' Probe 5'-(FAM)-TGAAGTCTCGCCTCCGCCGC-(TAMRA)-3'
GAPDH	Forward 5'-ACGGGAAACCCATCACCAT-3' Reverse 5'-CCAGCATCACCCATTGA-3' Probe 5'-(FAM)-TTCCAGGAGCGAGATCCCGTCAAG-TAMRA-3'
β -Actin	Forward 5'-TGAGTGCCTGACGGTCAAG-3' Reverse 5'-TGCCACAGGATTCCATACCC-3' Probe 5'-(FAM)-CACTATCGGCAATGAGCGTTCCG-(TAMRA)-3'

Physiological data of animals after IUGR and/or LSR

Body weight (gram) and body length (centimeter) was obtained at different time points: birth, Day 23 and Day 70 by weighing each animal. Body length was obtained by measuring from nose to anus and tail length beginning at tail insertion at birth.

Metabolic studies

Metabolic studies including standardized analyses of renal function were performed at the age of 70 days. The following protocol was carried out at each time point: 24 h before sacrifice, the animals were housed individually in a metabolic cage for 24 h allowing exact quantification of food and water intake as well as urine excretion. Next, a retro-orbital blood sample of 2 mL was collected at the end of the 24-h period. Haemoglobin, potassium and sodium concentration in plasma were analysed. Fractional ex-

cretion of sodium (FeNa) and fractional excretion of potassium (FeK) was calculated:

$$\text{FeNa (\%)} : \frac{(\text{urine-sodium} \times \text{plasma creatinine})}{(\text{plasma-sodium} \times \text{urine creatinine})}$$

$$\text{FeK (\%)} : \frac{(\text{urine-potassium} \times \text{plasma creatinine})}{(\text{plasma-potassium} \times \text{urine creatinine})}$$

Tissue preparation

At Day 70, the experiment was terminated as previously described [7]. Then, the kidneys were excised and a portion was immediately placed frozen in liquid nitrogen. For histology, another portion of renal tissue was fixed in 4% paraformaldehyde in phosphate-buffered saline (PBS; 20

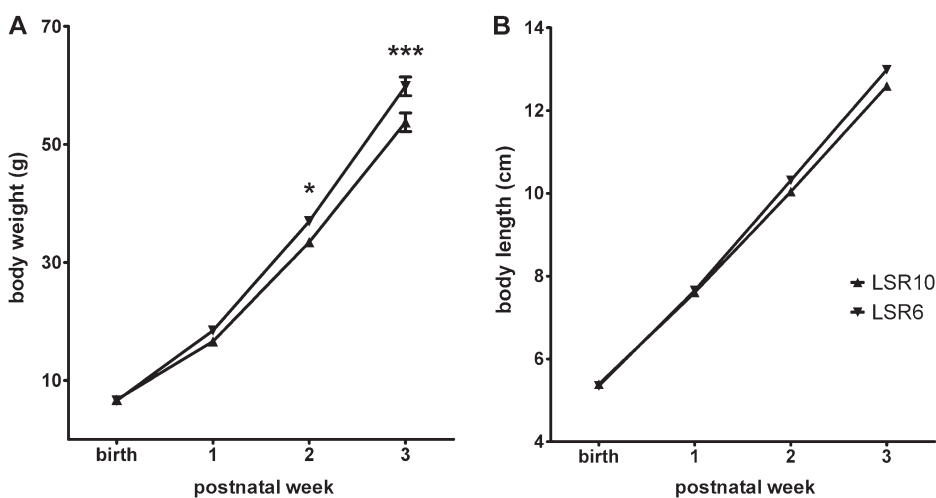
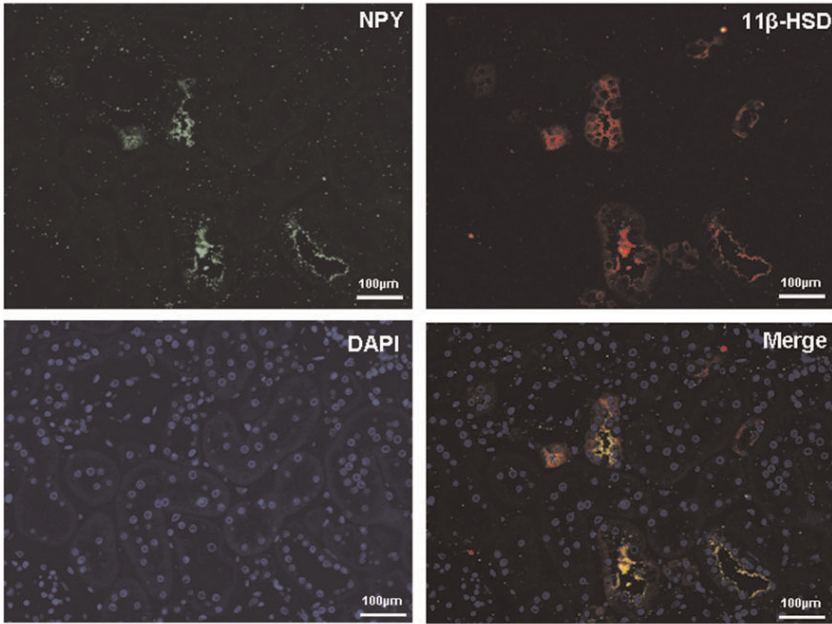


Fig. 1. Physiological data of animals with LSR to either 10 or 6. (A) Body weight (g) and (B) body length (cm) per week from birth until Week 3. Animals after LSR to 6 (LSR6, inverted triangles) have in the first 3 weeks after birth an increased body weight gain compared to animals with LSR to 10 (LSR10, triangles). At Weeks 2 and 3, the group with LSR6 has a significant increased body weight per week compared to the control group with LSR10 (* $P < 0.05$, *** $P < 0.001$; two-way ANOVA test and Bonferroni correction).

A Co-localization of NPY and 11 β -HSD in the distal tubuli



B Co-localization of NPY and 11 β -HSD in the collecting tubuli

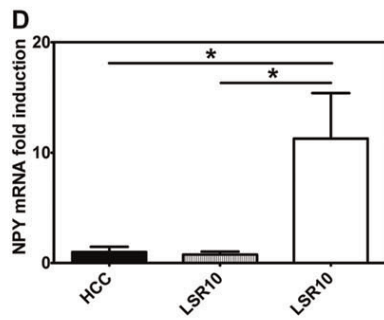
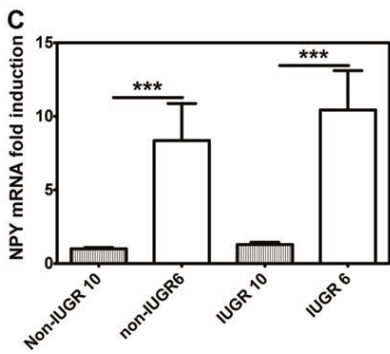
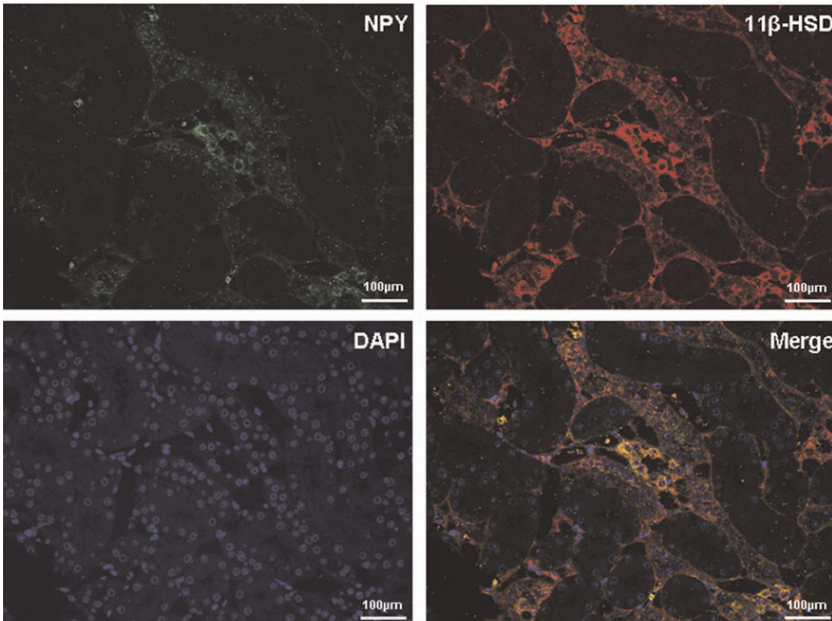


Fig. 2. Continues

mM Tris-Cl, 137 mM NaCl; pH7.6). Electrolytes in serum and urine samples were analysed with the automatic analyser Integra 800 (Roche Diagnostics, Mannheim, Germany).

RNA extraction and real-time polymerase chain reaction

RNA extraction and quantitative real-time reverse transcription-polymerase chain reaction (RT-PCR) analysis was performed as described previously [7] for NPY, NPY-receptor Y1 (Y1), Y2, mineral corticoid receptor (MCR), renin, angiotensin receptor (ATR) 1a and ATR1b. The results were confirmed by normalization to 'housekeeping genes' β -actin and glyceraldehyde-3-phosphate dehydrogenase (GAPDH). Primer pairs and TaqMan probes used are listed in Table 1. Unless otherwise indicated, the oligonucleotides for each gene investigated were designed as previously described [7].

Protein isolation and immunoblotting

Protein extraction from rat kidneys, gel electrophoresis and immunoblotting were performed as described previously [47]. Blots were probed with: rabbit anti-phospho-p42/44 MAPK (Thr202/Tyr204) (catalogue number 4370, 1:1000; Cell Signalling Technology, New England Biolabs, Frankfurt, Germany), p42/44 MAPK (catalogue number 9102, 1:1000; Cell Signalling, New England Biolabs), mouse anti-5E8 (DPPIV) (catalogue number HM3021, 1:625; Cell Sciences, Canton, MA), while goat anti- β -actin (designated I-19, catalogue number SC-1616, 1:1000; Santa Cruz Biotechnology, San Francisco, CA) served as loading control. Horseradish peroxidase-conjugated anti-rabbit (catalogue number 7074, 1:1500; Cell Signalling Technology, Minneapolis, MA) and anti-goat (catalogue number 305-035-045, 1:1500; Jackson ImmunoResearch Laboratories, Suffolk, UK) was used with a dilution 1:1500. Densitometric analysis of the bands was performed using Advanced Image Data Analyzer-Software (Version 4.15; Fuji Photo Film Co., Omiyama, Japan) and normalized to total amount of β -actin per lane. Pixel densities were corrected for background staining in the same film.

Immunohistochemistry

Immunohistochemistry was performed as previously described [7, 47]. The expression was assessed with rabbit anti-NPY (catalogue number NA1233, 1:100; Biotrend, Cologne, Germany), goat anti-NPY-receptor 1 (catalogue number Cs21990, 1:400; Santa Cruz Biotechnology, San Francisco), sheep anti-11 β -hydroxysteroid dehydrogenase Type 2 (11 β -HSD2) (catalogue number AB1296, 1:200; Chemicon) and mouse anti-smooth muscle actin (catalogue number M0851, 1:200; Dako). Immune complexes were visualized with fluorescent secondary antibodies: Cy3 goat anti-rabbit (catalogue number 111-166-003, 1:400; Jackson ImmunoResearch Laboratories), Alexa 488 donkey anti-goat (catalogue number A11055, 1:400; Invitrogen, Karlsruhe, Germany) and Cy2 donkey anti-mouse (catalogue number 715-226-150, 1:400; Jackson ImmunoResearch Laboratories). Cell nuclei were labelled with 4',6-diamidino-2-phenylindole (DAPI) (catalogue number D1306, 1:1000; Invitrogen).

For the immunohistochemical analysis of DPPIV, the sections were treated as previously explained. After quenching of endogenous peroxidase activity with 1.5% (vol/vol) H₂O₂ (35%), 20% methanol and 0.1 M PBS for 20 min at room temperature, sections were incubated with blocking buffer (catalogue number AL120R500; DCS, Hamburg, Germany) for 45 min at room temperature. The expression was assessed with mouse anti-5E8 (DPPIV) (catalogue number HM3021, 1:100; Cell Sciences, Canton, MA). Immune complexes were visualized with an avidin/biotin-DAB (3,3'-diaminobenzidine) detection system (Vector Lab, Burlingame, CA, USA).

Tissue-specific DPPIV-like enzymatic activity

Synthesis of the histochemical substrate H-Gly-L-Pro-1-hydroxy-4-naphthylamide hydrochloride as well as histochemistry were conducted

as previously described [48]. As a further control for specificity and in addition to the use of DPPIV-deficient animals, this histochemical activity assay was also performed using a DPPIV-specific inhibitor, which was added to the incubation solution in a final concentration of 2 μ M. Light microscopy investigations were carried out on a Nikon Eclipse 80i microscope (Nikon GmbH, Duesseldorf, Germany) and representative pictures were taken with a MicroFire digital microscope camera (Optronics, Goleta, CA).

Analysis of data

The results of RT-PCR were calculated based on the $\Delta\Delta$ Ct method as described in detail previously [7] and expressed as fold induction of mRNA expression compared to the corresponding control animal groups. Mean mRNA expression in control animals was defined as 1.0-fold induction. For quantitative immunoblot analysis, a densitometry was performed normalized to β -actin of the same animal probe.

Two tailed Mann-Whitney test, one-way analysis of variance (ANOVA) test, two-way ANOVA test, Bonferroni correction test and Dunnett's test were used to test significance at the given time points. A P-value <0.05 was considered significant. The procedures were carried out using the GraphPad Prism software (Version 4.0; GraphPad Software, San Diego, CA). Values are displayed as means \pm standard deviations of the mean.

Results

Localization of NPY, NPY-receptor Y1 and DPPIV in the kidney

NPY and Y1-receptor localization in the kidney. NPY and Y1-receptor were detected in both the renal cortex and renal medulla. NPY is localized perinuclear and in the cytoplasm (Figure 2A and B). Both NPY (Figure 2A and B) and Y1-receptor (Figure 3A) were colocalized with 11 β -HSD, a marker of distal tubuli and collecting ducts of the renal cortex and renal medulla. Y1-receptor was observed in the cytoplasm and in the membrane of the cells of the distal and collecting renal duct (Figure 3A).

NPY and Y1-receptor are colocalized in the kidney. NPY and Y1-receptor were detectable in both the cells of the distal and the collecting ducts of the kidney. A coimmunostaining demonstrated a colocalization of NPY and Y1 in the tubuli of the renal cortex (Figure 4A) and in the renal medulla (Figure 4B).

NPY and Y1-receptor are colocalized in the macula densa. NPY was determined in the tubuli of the renal cortex and medulla by immunofluorescence. Furthermore, it was demonstrated that NPY is localized adjacent to the macula densa, characterized by a positive staining for actin and loco tipico in the renal morphology (Figure 5A). NPY and Y1-receptor are colocalized adjacent to the glomeruli in loco tipico of the macula densa (Figure 5B).

Fig. 2. Continued

Fig. 2. Localization of NPY in the kidney and the expression pattern after LSR and IUGR. (A and B) NPY expression is assessed with immunofluorescence (green), nuclear staining with DAPI (blue). The localization of NPY in the kidney was shown with colocalization with 11 β -HSD (red) as a marker for the distal (A) and the collecting tubuli (B) of the kidney. Colocalization of NPY and 11 β -HSD in the distal and collecting tubuli is yellow (merge). (C and D) Two independent animal models: one model of IUGR combined with LSR (C) and the other, postnatal LSR only (D). The mRNA expression of NPY is not altered after IUGR (IUGR6 versus non-IUGR6, IUGR10 versus non-IUGR10) but significantly increased after LSR to 6 (non-IUGR-6 versus non-IUGR10, IUGR6 versus IUGR10; LSR6 versus LSR10 and HCC) (C and D). (*P < 0.05, ***P < 0.001; one-way ANOVA test and Bonferroni correction).

A Co-localization of Y1-receptor and 11 β -HSD in the distal and collecting tubuli

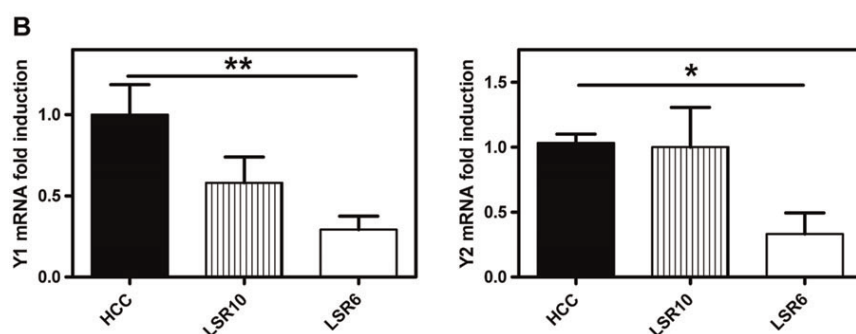
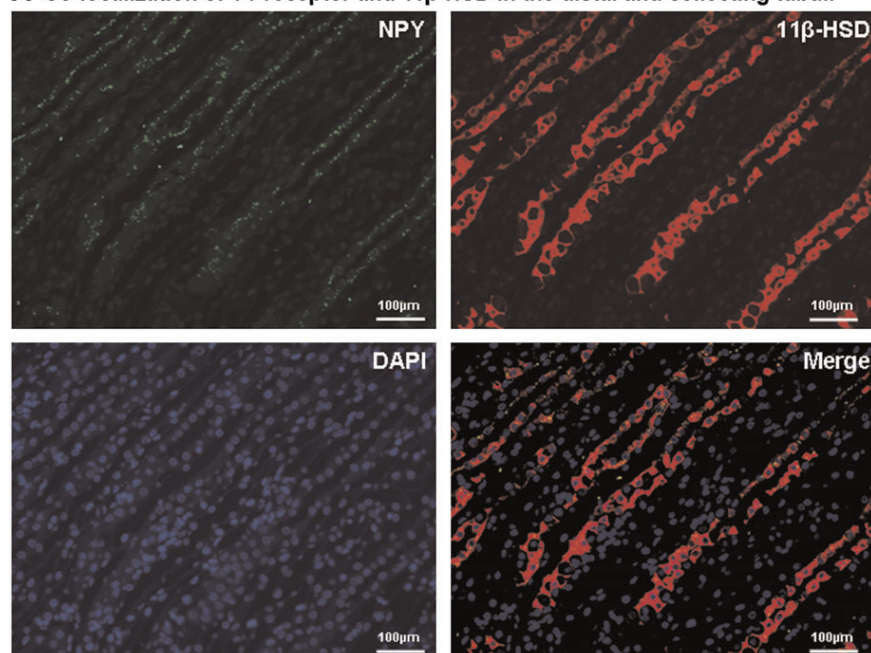


Fig. 3. Localization of Y1-receptor in the kidney and the expression pattern of Y1- and Y2-receptor after LSR. (A) Y1-receptor expression is assessed with immunofluorescence (green), nuclear staining with DAPI (blue). The renal localization of Y1-receptor is shown by colocalization with 11 β -HSD (red) as a marker for the distal and collecting tubuli of the kidney. Colocalization of Y1-receptor and 11 β -HSD in the distal and collecting is yellow (merge). (B) The mRNA expression of Y1- and Y2-receptor is significantly decreased after LSR to 6. (* $P < 0.05$, ** $P < 0.01$; one-way ANOVA test and Bonferroni correction).

Localization and activity of DPPIV in the kidney. DPPIV was detectable in the cortex (Figure 6A), in renal ducts (Figure 6A) and in glomeruli (Figure 6A). However, there was almost no staining for DPPIV in the medulla (Figure 6A). The activity of DPPIV was detected in the cortex and proximal and distal tubuli (Figure 6B).

IUGR and the NPY-system

IUGR after low protein diet. Low protein (LP) diet of the pregnant dams (IUGR) led to a reduction of birth weight, body length and tail length at birth in their offspring in comparison to litters of normal protein-fed dams (non-IUGR). The offspring of the IUGR mothers reached body weight of the offspring of non-IUGR mothers until Day 42. At Day 70, body weight was comparable in both groups (Table 2). In respect to LSR, we demonstrated a significant increased weight gain in the group with a litter size of 6 (IUGR 6, non-IUGR 6) compared to the group with a litter size of 10 (IUGR 10, non-IUGR 10) at Day 23. At Day 70,

body weight was comparable in all groups (non-IUGR10, non-IUGR6, IUGR10 and IUGR6) (Table 2).

mRNA expression of endogenous NPY in the kidney after IUGR. No alteration of the mRNA expression of NPY was detected after IUGR without LSR (IUGR10) at Day 70 (Figure 2C). Whereas both the group after IUGR with LSR to 6 (IUGR6) and the group without IUGR but with LSR to 6 (non-IUGR6) showed an up to 10-fold induction of the mRNA expression of NPY compared with the analogical groups with LSR to 10 (IUGR10; non-IUGR10) at Day 70 after birth (Figure 2C).

The impact of postnatal LSR on the NPY-system and tubular function

Physiological data after LSR: diuresis, haemoglobin, plasma sodium and plasma sodium. Diuresis was not altered after LSR. It was comparable in LSR6, LSR10 and HCC. Neither alterations in the haemoglobin

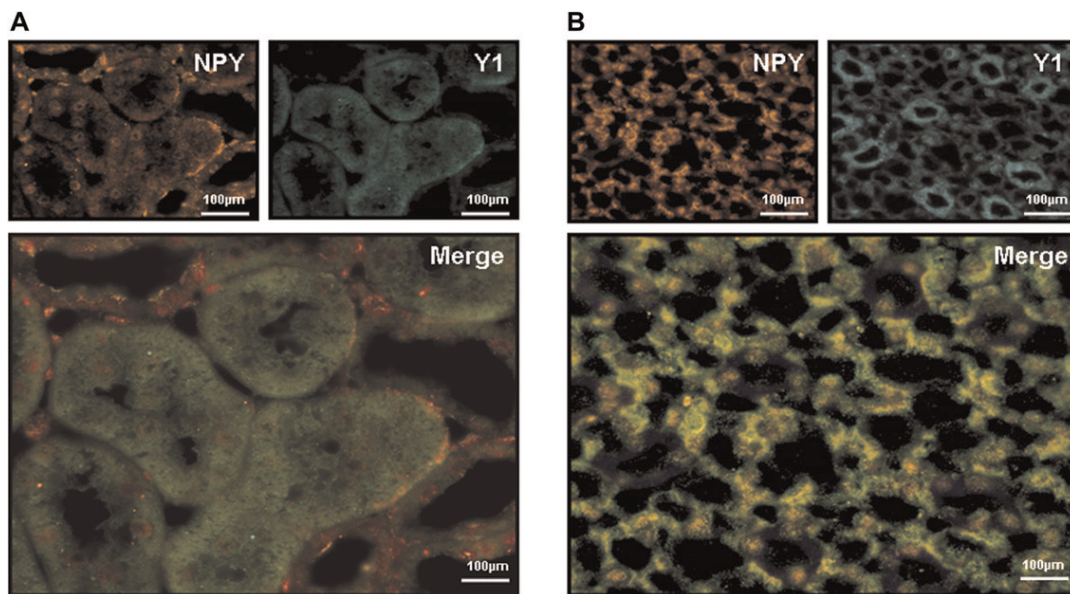


Fig. 4. Colocalization of NPY and Y1-receptor in the kidney. The expression of NPY and Y1 in the kidney is demonstrated by immunofluorescence. Both Y1-receptor (green) and NPY (red) are detectable in the tubuli of both the renal cortex (A) and in the renal medulla (B). Colocalization (yellow) of NPY and Y1-receptor is observed in the membrane of the tubuli of the renal cortex (A) and in the collecting ducts of the renal medulla (B).

concentration nor hyponatraemia or hypokalaemia were detectable after LSR (Table 3).

Excreted fraction of the filtered sodium (FeNa) and potassium (FeK) after LSR. Metabolic studies at Day 70 demonstrated that both FeNa and FeK (Figure 8C and D) are significantly increased after LSR6 (postnatal LSR, no IUGR). Additionally, absolute excretion of potassium (Figure 8B) but not absolute excretion of sodium (Figure 8A) was increased after LSR, while diuresis was only slightly affected (Table 3). Natriuresis and kaliuresis was linked to postnatal LSR only.

Postnatal growth after LSR. No differences in body weight or body length were observed at Day 1 after birth. Reduction of the litter size to 6 (LSR6) led to a significant increased weight in weeks 2 and 3 after birth (Figure 1A), whereas body length was not different from the control group (LSR10) (Figure 1B).

mRNA expression of NPY and NPY-receptor 1 and 2 (Y1, Y2) after LSR. A LSR to 6 after birth led to an up to 10-fold induction of the mRNA expression of NPY (Figure 2D) and a decrease of the Y1- and Y2-mRNA at Day 70 of life (Figure 3B) compared to the control group (HCC) and, respectively, LSR10.

mRNA expression of renin, MCR, ATR1a, ATR1b after LSR. Renin expression is significantly up-regulated (Figure 5C), whereas MCR and ATR1a expression (Figure 5C) did not change after LSR (LSR6, LSR10) compared to the control group (HCC). ATR1b expression was decreased after LSR to 6 compared to LSR10 and HCC (Figure 5C).

Localization and activity of DPPIV in the kidney and expression after LSR. Localization and activity of DPPIV was predominantly detectable in the renal cortex and almost not in the medulla. Protein analysis in our study demonstrated a decrease of DPPIV expression after LSR to 6 (LSR6) compared to the control group with LSR to 10 (LSR10) or without LSR (HCC) (Figure 6C).

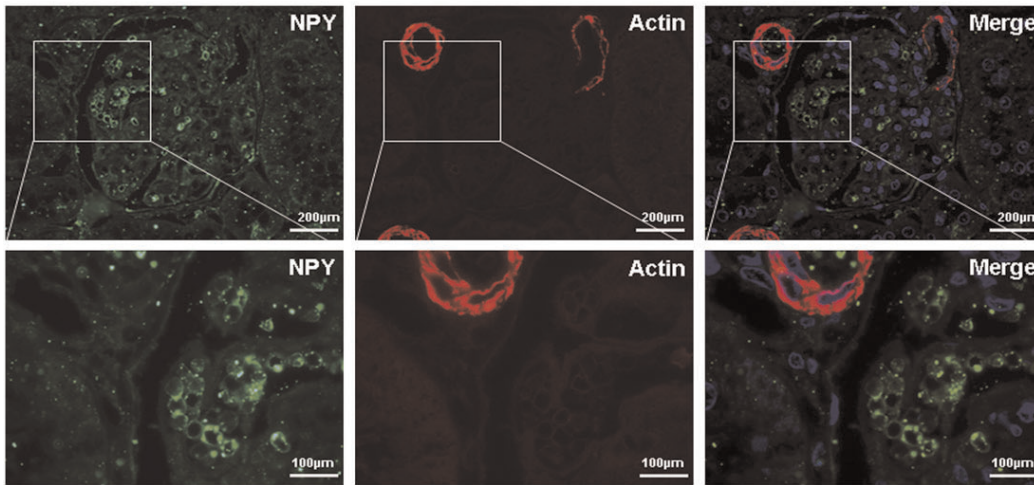
MAPK 42/44 and its phosphorylation are dysregulated after LSR. LSR6 led to decrease of phosphorylation of MAPK 42/44 compared to the control group (LSR10, HCC). Furthermore, an increase of total MAPK 42/44 was detected after LSR to 6 (LSR6) (Figure 7).

Discussion

This is the first study demonstrating early postnatally acquired alterations of the kidney physiology. LSR immediately after birth leads to an altered expression pattern of endogenous NPY and NPY-receptor 1 (Y1), which is associated with an impaired tubular function resulting in increased natriuresis and kaliuresis at Day 70 after birth. In contrast, IUGR itself does not alter the mRNA expression of NPY.

IUGR is associated with an increased sodium excretion in the renal ducts after IUGR in piglets [49]. Furthermore, LBW leads to increased sympathetic nerve traffic [50]. That may be the link between low birth weight and altered tubular function. It is well known that the postnatal environment influences kidney development and nephron number. Bearing in mind the differences in the animal models, Wlodek *et al.* [51, 52] showed that both IUGR and LSR impair renal function in later life. Consistently, Boubred *et al.* [53] showed that early postnatal overfeeding induced

A Localization of NPY and Actin as a marker of the macula densa



B Co-localization of NPY and Y1-receptor adjacent to the glomerulus

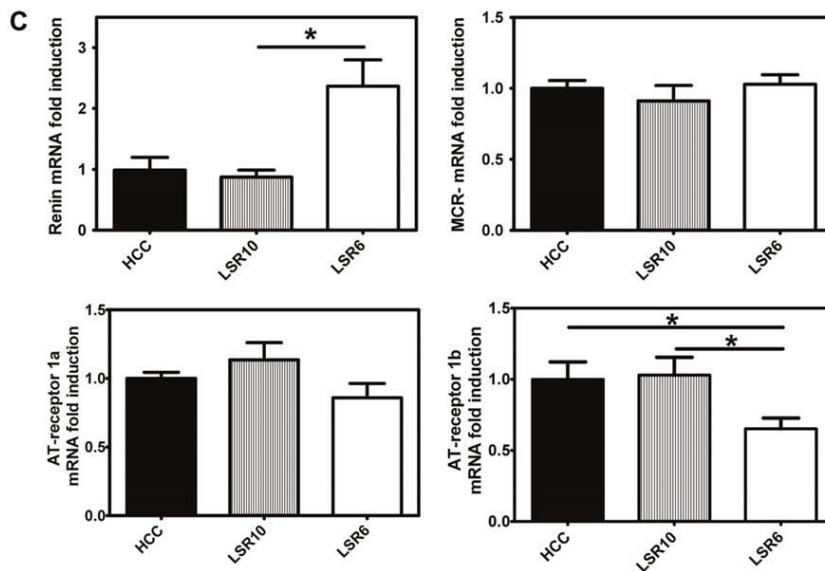
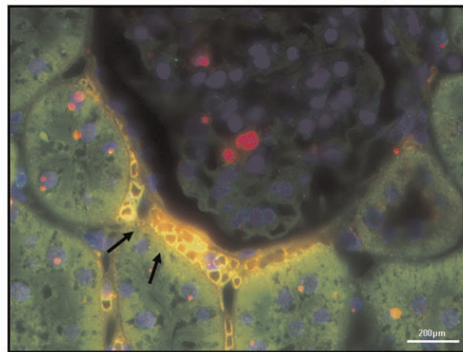


Fig. 5. Colocalization of NPY and Y1-receptor in the macula densa and dysregulation of renin after LSR. **(A)** Localization of NPY is assessed with immunofluorescence. NPY (green) is localized adjacent to the macula densa (red; actin-positive staining and loco tipico). Merge shows the adjacent localization of NPY to the macula densa. Where high-magnification images (lower row) are derived from the low magnification image (upper row), the magnified area is demarcated with a solid-lined box. **(B)** NPY (red) and Y1-receptor (green) localization is assessed with immunofluorescence. There is co-staining adjacent to the glomerulus in loco tipico of the macula densa (yellow, arrow). **(C)** The mRNA expression of renin but not of MCR and ATR1a is increased after LSR to 6 (LSR6) compared to control group without LSR (HCC). Additionally the expression of ATR1b is decreased after LSR6 compared to the control. (* $P < 0.05$; one-way ANOVA test and Bonferroni correction).

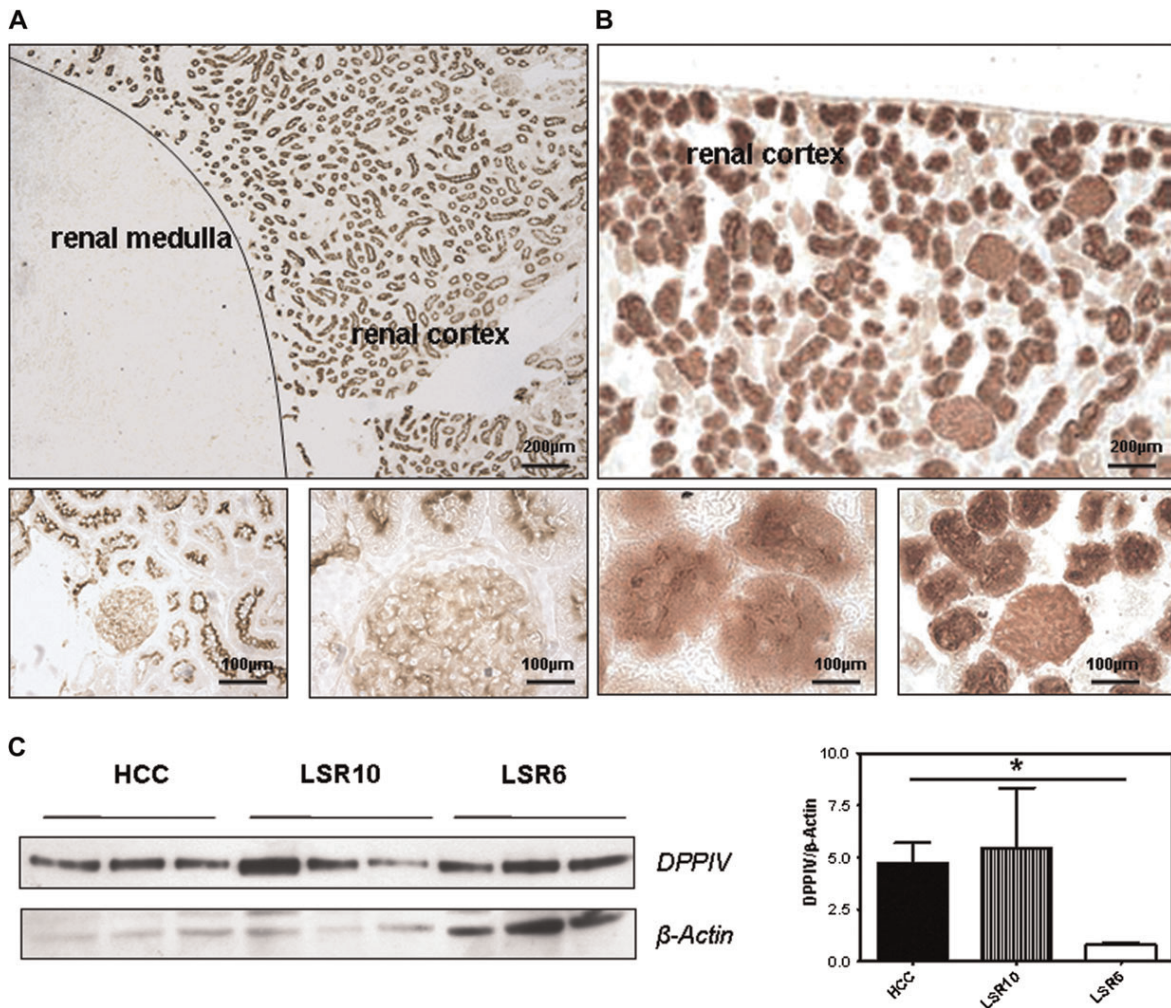


Fig. 6. Protein expression of DPPiV after LSR and its activity and the localization in the kidney. DPPiV is a peptidase known to cleave peptide hormones such as NPY. Therefore, we assessed immunohistochemistry to characterize the localization (A) and the activity (B) within the kidney. It is expressed and active ubiquitously in the renal cortex (A,B), in the tubuli (A,B) and in the glomeruli (A,B). Almost no staining was detectable in the renal medulla (A,B). Analysis of the protein expression was assessed with western blotting. Densitometric analysis showed a significant down-regulation of DPPiV in the animals with LSR to 6 (LSR6) compared with the control group without LSR (HCC) (D). (*P < 0.05; one-way ANOVA test and Bonferroni correction).

Table 2. Physiological data of IUGR animals and controls with and without LSR^a

	Non-IUGR 10	Non-IUGR 6	IUGR 10	IUGR 6
Birth weight (g)		6.2 ± 0.43 (n = 39)		5.405 ± 0.403 (n = 22)
Body length at birth (cm)		5.0 ± 0.17 (n = 39)		4.88 ± 0.1 (n = 39)
Tail length at birth (cm)		1.63 ± 0.95 (n = 39)		1.46 ± 0.1 (n = 39)
Body weight at weaning Day 23 (g)	51.8 ± 5.8 (n = 9)	69.00 ± 6.1 (n = 24)***	50.95 ± 6.7 (n = 6)	60.97 ± 3.15 (n = 12)*
Body weight at Day 70 (g)	351.9 ± 21.28 (n = 9)	373.6 ± 18.07 (n = 12)	379.9 ± 16.52 (n = 6)	354.7 ± 24.41 (n = 11)

^aValues are given as means ± standard deviations. ***P < 0.001, respectively, *P < 0.05 versus non-IUGR. ***P < 0.001: non-IUGR10 versus non-IUGR6, *P < 0.05: non-IUGR6 versus IUGR6.

by LSR in rat enhances postnatal nephrogenesis but the blood pressure, and the glomerulosclerosis score are still elevated. Additionally, Boubred *et al.* [54] demonstrated that reduced nephron number alone due to IUGR may not be sufficient to induce physiological alterations, and early postnatal overfeeding acts as a ‘second hit’. Our data shows that LSR and not IUGR itself leads to increased postnatal weight gain. Furthermore, we could demonstrate that LSR but not IUGR is associated with an up-regulation

of the mRNA expression of NPY. Hence, there seems to be an association between increased postnatal weight gain due to LSR and the dysregulation of the NPY-system. Therefore, we focused this study on the effect of LSR on the NPY-system and renal function.

Our data demonstrate a significant up-regulation of the mRNA expression of NPY and a down-regulation of the Y1- and Y2-receptor after LSR to 6. Already a litter size of 10 slightly downregulates the Y1-receptor, whereas the

NPY-expression is not altered yet. Maybe the up-regulation of NPY after LSR to 6 is a compensatory mechanism to the decreased expression of the Y1-receptor.

The results demonstrated in this study show that post-natal LSR to 6 alters tubular function. A significant increase of both natriuresis and kaliuresis was observed at Day 70 after birth. Additionally, a slight increment of diuresis was measured. One underlying mechanism of renal tubular function is the RAAS. Therefore, we analysed renin, the mineralcorticoid receptor, and the angiotensin (AT) receptors. No changes in the group with LSR compared to the control group without LSR were detectable with regard to mRNA expression of the mineralcorticoid receptor and AT-receptor 1a in the kidney, whereas renin mRNA expression is increased and AT-receptor 1b is decreased at Day 70 after birth. Renin release is regulated by multiple mechanisms. Several studies describe a direct effect of NPY on the renin release [33, 35, 36]. Consistent with the localization of NPY next to the macula densa—shown in our study—it can directly act through a paracrine effect on the macula densa and influence the

expression of renin. According to Aubert *et al.* [34] NPY inhibits renin release in the kidney. Hence, the RAAS activation would be suppressed and less aldosterone is secreted. Consequently, that leads to increased natriuresis and decreased kaliuresis. The expression of one of the corresponding receptors of RAAS (AT-receptor 1b) is decreased in the LSR6-group. That can be reactive to the increased expression of renin. These findings may have an influence on renal blood flow and blood pressure. Further studies will have to address blood pressure after LSR. In our study, the expression of endogenous NPY is increased and the Y1-receptor is decreased. Consistent with the decreased expression of the Y1-receptor, we observe less phosphorylation of MAPK42/44 due to a reduced activation through G-protein coupled receptors. The activity of the NPY-system through Y1-receptors seems to be decreased. That leads to a diminished activity of Na⁺-K⁺-ATPase and of Na⁺/Pi cotransporter in the renal tubuli. In addition, these results may explain why renin expression is not suppressed but increased. Activation of the RAAS is the consequence. That may contribute to the increase of kaliuresis.

To demonstrate that NPY is expressed endogenously in the renal tubular cells and not just as previously described in the end of the sympathetic nerves, we analysed the localization of NPY and Y1-receptor with a renal tubular marker. Both NPY and Y1-receptor are localized in the distal tubuli and collecting ducts of the renal system. We conclude that endogenous renal NPY is expressed not just in the end of sympathetic nerves but also and predominantly in the renal tubular cells itself and may have paracrine effects in the kidney.

Table 3. Physiological data of animals with and without LSR

	HCC	LSR10	LSR6
Diuresis (mL/24 h)	0.504 ± 0.116	0.562 ± 0.136	0.595 ± 0.193
Haemoglobin (g/dL)	14.9 ± 0.725	14.62 ± 0.691	15.21 ± 1.208
Na ⁺ -concentration plasma (mmol/L)	144.0 ± 4.355	138.6 ± 2.970	136.4 ± 1.734
K ⁺ -concentration plasma (mmol/L)	2.602 ± 0.112	2.583 ± 0.366	2.807 ± 0.396

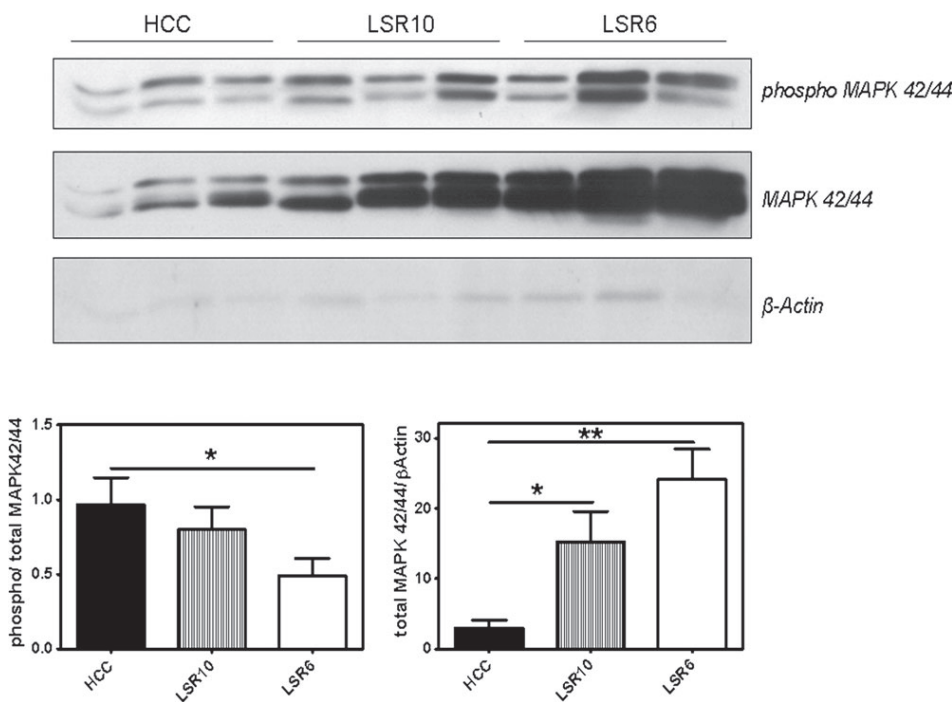


Fig. 7. MAPK 42/44 and its phosphorylation after LSR. Analysis of the phosphorylation of MAPK 42/44 and total MAPK 42/44 after LSR to 6 (LSR6) was assessed by western blotting. Densitometric analysis demonstrated a decreased phosphorylation of MAPK 42/44, whereas the expression of total MAPK 42/44 after LSR to 6 (LSR6) was increased. (* $P < 0.05$, ** $P < 0.01$; one-way ANOVA test and Bonferroni correction).

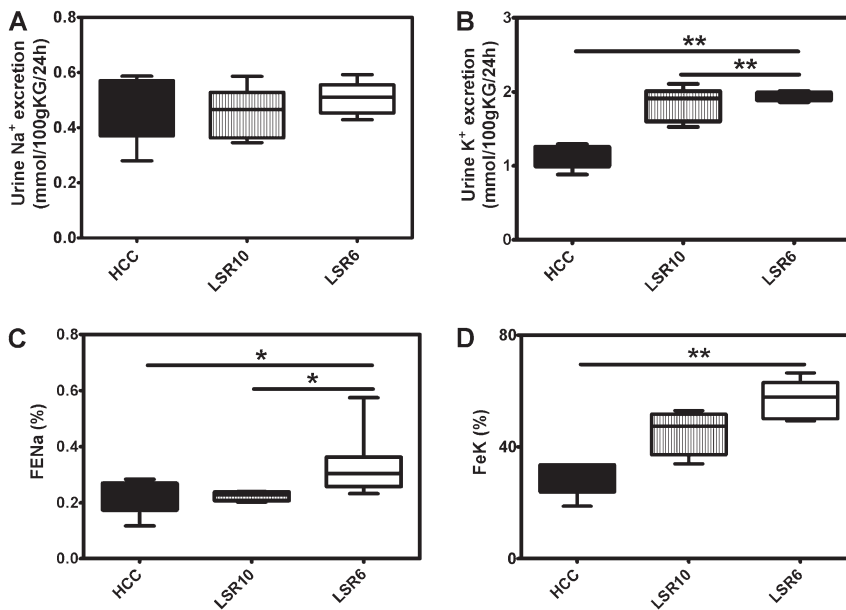


Fig. 8. Natriuresis and kaliuresis after LSR. Analysis of sodium and potassium excretion in the urine for 24 h revealed an alteration of the renal homeostasis after LSR. An increase is shown in absolute kaliuresis (**B**) but no alteration of absolute excretion of sodium (**A**) after LSR to 6 (LSR6) compared to the control group without any LSR (HCC). Both excreted fraction of the filtered sodium (FeNa) (**C**) and excreted fraction of the filtered potassium (FeK) (**D**) were increased significantly after LSR6 compared to the control group. (* $P < 0.05$, ** $P < 0.01$; one-way ANOVA test and Bonferroni correction).

NPY is inactivated by several peptidases, one key regulator is DPPIV. It is a peptidase with the capability of hydrolyzing postproline bonds and it cleaves NPY. Some previous studies have described an expression of DPPIV in the kidney, but none have addressed the expression pattern within the kidney. This study demonstrates that it is predominantly localized and active immunohistochemically in the renal cortex, especially in renal ducts and in the glomeruli, and also slightly in the renal medulla. Furthermore, DPPIV is significantly decreased after LSR6 on protein level. Consequently, we assume that NPY is less cleaved in the kidney of LSR6 animals due to the insufficient level of its regulating peptidase. Hence, the NPY levels are increased.

Additional extrarenal factors may influence renal function and body weight, i.e. SNS or metabolic syndrome. That may have an impact on the expression of the NPY-system and its signalling. Further investigations are necessary to elucidate these issues.

To sum up, LSR and increased postnatal weight gain lead to increased natriuresis and kaliuresis in this animal model. A potential underlying mechanism may be seen in the intrinsic kidney-associated NPY-system. On the one hand, NPY influences kaliuresis indirectly through renin via the Y1-receptor. In addition, NPY also has a direct RAAS-independent effect on kaliuresis and natriuresis via Y1-/Y2-receptor. Both receptors are G-Protein-coupled receptors acting via MAPK42/44. Due to reduced expression of Y1-receptor, its intracellular signalling through MAPK 42/44 is significantly decreased. The NPY-system regulates both kaliuresis and natriuresis and may be a potential mechanism in the tubular dysfunction after LSR.

In conclusion, we provide direct experimental evidence in rats illustrating that tubular function is influenced by the

postnatal environment. Furthermore, this study also shows a potential role of the endogenous NPY-system in the regulation of tubular function as well as a mediating system transmitting early in life acquired physiological changes. Given that the NPY-system is also amenable to pharmacological and genetic manipulation in the kidney, it provides a potential target in this context.

Acknowledgements. The authors gratefully acknowledge the expert technical assistance of Ida Allabauer, Jenny Stiller and Miriam Reutelschöfer.

The animal experiments were supported by a grant to J.D., C.P. and K.A. by the Deutsche Forschungsgemeinschaft, Bonn, Germany; SFB 423, Collaborative Research Centre of the German Research Foundation: Kidney Injury: Pathogenesis and Regenerative Mechanisms, projects B13 and Z2.

Conflict of interest statement. all authors declare that there is no conflict of interest concerning this study.

References

- Painter RC, Roseboom TJ, Bleker OP. Prenatal exposure to the Dutch famine and disease in later life: an overview. *Reprod Toxicol* 2005; 20: 345–352
- Roseboom TJ, van der Meulen JH, Ravelli AC *et al.* Blood pressure in adults after prenatal exposure to famine. *J Hypertens* 1999; 17: 325–330
- Ravelli AC, van Der Meulen JH, Osmond C *et al.* Obesity at the age of 50 y in men and women exposed to famine prenatally. *Am J Clin Nutr* 1999; 70: 811–816
- de Rooij SR, Painter RC, Holleman F *et al.* The metabolic syndrome in adults prenatally exposed to the Dutch famine. *Am J Clin Nutr* 2007; 86: 1219–1224
- Lackland DT, Bendall HE, Osmond C *et al.* Low birth weights contribute to high rates of early-onset chronic renal failure in the southeastern United States. *Arch Intern Med* 2000; 160: 1472–1476
- Lackland DT, Egan BM, Fan ZJ *et al.* Low birth weight contributes to the excess prevalence of end-stage renal disease in African Americans. *J Clin Hypertens (Greenwich)* 2001; 3: 29–31

7. Plank C, Ostreicher I, Hartner A *et al.* Intrauterine growth retardation aggravates the course of acute mesangioproliferative glomerulonephritis in the rat. *Kidney Int* 2006; 70: 1974–1982
8. Schreuder MF, Van Wijk JA, Fodor M *et al.* Influence of intrauterine growth restriction on renal function in the adult rat. *J Physiol Biochem* 2007; 63: 213–219
9. Barker DJ. Intrauterine programming of adult disease. *Mol Med Today* 1995; 1: 418–423
10. Barker DJ. *In utero* programming of chronic disease. *Clin Sci (London)* 1998; 95: 115–128
11. Adair LS, Cole TJ. Rapid child growth raises blood pressure in adolescent boys who were thin at birth. *Hypertension* 2003; 41: 451–456
12. Barker DJ, Osmond C, Forsén TJ *et al.* Trajectories of growth among children who have coronary events as adults. *N Engl J Med* 2005; 353: 1802–9
13. Huxley RR, Shiell AW, Law CM. The role of size at birth and postnatal catch-up growth in determining systolic blood pressure: a systematic review of the literature. *J Hypertens* 2000; 18: 815–831
14. Symonds ME, Stephenson T, Budge H. Early determinants of cardiovascular disease: the role of early diet in later blood pressure control. *Am J Clin Nutr* 2009; 89: 1523–1529
15. Singhal A, Cole TJ, Fewtrell M *et al.* Promotion of faster weight gain in infants born small for gestational age: is there an adverse effect on later blood pressure? *Circulation* 2007; 115: 213–220
16. Ojeda NB, Johnson WR, Dwyer TM *et al.* Early renal denervation prevents development of hypertension in growth-restricted offspring. *Clin Exp Pharmacol Physiol* 2007; 34: 1212–1216
17. Jansson T, Lambert GW. Effect of intrauterine growth restriction on blood pressure, glucose tolerance and sympathetic nervous system activity in the rat at 3–4 months of age. *J Hypertens* 1999; 17: 1239–1248
18. Vászrhelyi B, Dobos M, Reusz GS *et al.* Normal kidney function and elevated natriuresis in young men born with low birth weight. *Pediatr Nephrol* 2000; 15: 96–100
19. Lenaerts A, Codden T, Meunier JC *et al.* Effects of clonidine on diuretic response in ascitic patients with cirrhosis and activation of sympathetic nervous system. *Hepatology* 2006; 44: 844–9
20. McDonough AA. Mechanisms of proximal tubule sodium transport regulation that link extracellular fluid volume and blood pressure. *Am J Physiol Regul Integr Comp Physiol* 2010; 298: 851–861
21. Chevendra V, Weaver LC. Distribution of splenic, mesenteric and renal neurons in sympathetic ganglia in rats. *J Auton Nerv Syst* 1991; 33: 47–53
22. Grouzmann E, Alvarez-Bolado G, Meyer C *et al.* Localization of neuropeptide Y and its C-terminal flanking peptide in human renal tissue. *Peptides* 1994; 15: 1377–1382
23. Knight DS, Fabre RD, Beal JA. Identification of noradrenergic nerve terminals immunoreactive for neuropeptide Y and vasoactive intestinal peptide in the rat kidney. *Am J Anat* 1989; 184: 190–204
24. Bischoff A, Michel MC. Renal effects of neuropeptide Y. *Pflugers Arch* 1998; 435: 443–453
25. Bischoff A, Erdbrügger W, Smits J *et al.* Neuropeptide Y-enhanced diuresis and natriuresis in anaesthetized rats is independent of renal blood flow reduction. *J Physiol* 1996; 495: 525–534
26. Bischoff A, Avramidis P, Erdbrügger W *et al.* Receptor subtypes Y1 and Y5 are involved in the renal effects of neuropeptide Y. *Br J Pharmacol* 1997; 120: 1335–1343
27. Bischoff A, Stickan-Verfürth M, Michel MC. Renovascular and tubular effects of neuropeptide Y are discriminated by PP56 (D-myo-inositol 1,2,6-triphosphate) in anaesthetized rats. *Pflugers Arch* 1997; 434: 57–62
28. Bischoff A, Michel MC. Neuropeptide Y enhances potassium excretion by mechanisms distinct from those controlling sodium excretion. *Can J Physiol Pharmacol* 2000; 78: 93–99
29. Callanan EY, Lee EW, Tilan JU *et al.* Renal and cardiac neuropeptide Y and NPY receptors in a rat model of congestive heart failure. *Am J Physiol Renal Physiol* 2007; 293: 1811–1817
30. Lei J, Mariash CN, Bhargava M *et al.* T3 increases Na-K-ATPase activity via a MAPK/ERK1/2-dependent pathway in rat adult alveolar epithelial cells. *Am J Physiol Lung Cell Mol Physiol* 2008; 294: 749–754
31. Hansel DE, Eipper BA, Ronnett GV. Neuropeptide Y functions as a neuroproliferative factor. *Nature* 2001; 410: 940–4
32. Modin A, Pernow J, Lundberg JM. Repeated renal and splenic sympathetic nerve stimulation in anaesthetized pigs: maintained overflow of neuropeptide Y in controls but not after reserpine. *J Auton Nerv Syst* 1994; 49: 123–134
33. Hackenthal E, Aktories K, Jakobs KH *et al.* Neuropeptide Y inhibits renin release by a pertussis toxin-sensitive mechanism. *Am J Physiol* 1987; 252: 543–550
34. Aubert JF, Walker P, Grouzmann E *et al.* Inhibitory effect of neuropeptide Y on stimulated renin secretion of awake rats. *Clin Exp Pharmacol Physiol* 1992; 19: 223–228
35. Ahlborg G, Lundberg JM. Inhibitory effects of neuropeptide Y on splanchnic glycogenolysis and renin release in humans. *Clin Physiol* 1994; 14: 187–196
36. Evéquo D, Aubert JF, Nussberger J *et al.* Effects of neuropeptide Y on intrarenal hemodynamics, plasma renin activity and urinary sodium excretion in rats. *Nephron* 1996; 73: 467–472
37. von Horsten S, Dimitrijevic M, Markovic BM *et al.* Effect of early experience on behavior and immune response in the rat. *Physiol Behav* 1993; 54: 931–940
38. Blom JM, Benatti C, Alboni S *et al.* Early postnatal chronic inflammation produces long-term changes in pain behavior and N-methyl-D-aspartate receptor subtype gene expression in the central nervous system of adult mice. *J Neurosci Res* 2006; 84: 1789–1798
39. Kwak HR, Lee JW, Kwon KJ *et al.* Maternal social separation of adolescent rats induces hyperactivity and anxiolytic behavior. *Korean J Physiol Pharmacol* 2009; 13: 79–83
40. O'Mahony SM, Marchesi JR, Scully P *et al.* Early life stress alters behavior, immunity, and microbiota in rats: implications for irritable bowel syndrome and psychiatric illnesses. *Biol Psychiatry* 2009; 65: 263–267
41. Avitsur R, Hunziker J, Sheridan JF. Role of early stress in the individual differences in host response to viral infection. *Brain Behav Immun* 2006; 20: 339–348
42. Shanks N, Lightman SL. The maternal-neonatal neuro-immune interface: are there long-term implications for inflammatory or stress-related disease? *J Clin Invest* 2001; 108: 1567–1573
43. Kruschinski C, Skripuletz T, Bedoui S *et al.* Postnatal life events affect the severity of asthmatic airway inflammation in the adult rat. *J Immunol* 2008; 180: 3919–3925
44. Shanks N, Windle RJ, Perks PA *et al.* Early-life exposure to endotoxin alters hypothalamic-pituitary-adrenal function and predisposition to inflammation. *Proc Natl Acad Sci U S A* 2000; 97: 5645–5650
45. Liu D, Diorio J, Tannenbaum B, Caldji C *et al.* Maternal care, hippocampal glucocorticoid receptors, and hypothalamic-pituitary-adrenal responses to stress. *Science* 1997; 277: 1659–1662
46. Stephan M, Straub RH, Breivik T *et al.* Postnatal maternal deprivation aggravates experimental autoimmune encephalomyelitis in adult Lewis rats: reversal by chronic imipramine treatment. *Int J Dev Neurosci* 2002; 20: 125–132
47. Alejandre-Alcázar MA, Kwapiszewska G, Reiss I *et al.* Hyperoxia modulates TGF-beta/BMP signaling in a mouse model of bronchopulmonary dysplasia. *Am J Physiol Lung Cell Mol Physiol* 2007; 292: 537–549
48. Schade J, Stephan M, Schmiedl A *et al.* Regulation of Expression and Function of Dipeptidyl Peptidase 4 (DP4), DP8/9, and DP10 in Allergic Responses of the Lung in Rats. *J Histochem Cytochem* 2008; 56: 147–155
49. Bauer R, Walter B, Ihring W *et al.* Altered renal function in growth-restricted newborn piglets. *Pediatr Nephrol* 2000; 14: 735–739
50. Giapros V, Papadimitriou P, Challa A *et al.* The effect of intrauterine growth retardation on renal function in the first two months of life. *Nephrol Dial Transplant* 2007; 22: 96–103
51. Wlodek ME, Westcott K, Siebel AL *et al.* Growth restriction before or after birth reduces nephron number and increases blood pressure in male rats. *Kidney Int* 2008; 74: 187–195
52. Moritz KM, Mazzuca MQ *et al.* Uteroplacental insufficiency causes a nephron deficit, modest renal insufficiency but no hypertension with ageing in female rats. *J Physiol* 2009; 11: 2635–2646

53. Boubred F, Buffat C, Feruerstein JM *et al.* Effects of early postnatal hypernutrition on nephron number and long-term renal function and structure in rats. *Am J Physiol Renal Physiol* 2007; 293: 1944–1949
54. Boubred F, Daniel L, Buffat C *et al.* Early postnatal overfeeding induces early chronic renal dysfunction in adult male rats. *Am J Physiol Renal Physiol* 2009; 297: 943–951

Received for publication: 13.7.10; Accepted in revised form: 20.12.10

Early Postnatal Hyperalimentation Impairs Renal Function via SOCS-3 Mediated Renal Postreceptor Leptin Resistance

Miguel Angel Alejandre Alcazar, Eva Boehler, Eva Rother, Kerstin Amann, Christina Vohlen, Stephan von Hörsten, Christian Plank, and Jörg Dötsch

Department of Pediatric and Adolescent Medicine (M.A.A.A., E.R., C.V., J.D.), University of Cologne, D-50937 Cologne, Germany; and Departments of Pediatric and Adolescent Medicine (E.B., C.P.), Pathology (K.A.), and Experimental Therapy (S.v.H.), Franz-Penzoldt Center, University Hospital Erlangen, D-91054 Erlangen, Germany

Early postnatal hyperalimentation has long-term implications for obesity and developing renal disease. Suppressor of cytokine signaling (SOCS) 3 inhibits phosphorylation of signal transducer and activator of transcription (STAT) 3 and ERK1/2 and thereby plays a pivotal role in mediating leptin resistance. In addition, SOCS-3 is induced by both leptin and inflammatory cytokines. However, little is known about the intrinsic-renal leptin synthesis and function. Therefore, this study aimed to elucidate the implications of early postnatal hyperalimentation on renal function and on the intrinsic-renal leptin signaling. Early postnatal hyperalimentation in Wistar rats during lactation was induced by litter size reduction at birth (LSR) either to LSR10 or LSR6, compared with home cage control male rats. Assessment of renal function at postnatal day 70 revealed decreased glomerular filtration rate and proteinuria after LSR6. In line with this impairment of renal function, renal inflammation and expression as well as deposition of extracellular matrix molecules, such as collagen I, were increased. Furthermore, renal expression of leptin and IL-6 was up-regulated subsequent to LSR6. Interestingly, the phosphorylation of Stat3 and ERK1/2 in the kidney, however, was decreased after LSR6, indicating postreceptor leptin resistance. In accordance, neuropeptide Y (NPY) gene expression was down-regulated; moreover, SOCS-3 protein expression, a mediator of postreceptor leptin resistance, was strongly elevated and colocalized with NPY. Thus, our findings not only demonstrate impaired renal function and profibrotic processes but also provide compelling evidence of a SOCS-3-mediated intrinsic renal leptin resistance and concomitant up-regulated NPY expression as an underlying mechanism. (*Endocrinology* 153: 1397–1410, 2012)

Childhood obesity is becoming a worldwide epidemic, with a continuous increase in prevalence that has tripled in the last 3 decades (1). Projections of the International Obesity Task Force indicate that by 2020 the prevalence of childhood overweight and obesity will be more than 35% in Europe and more than 45% in the United States (2). Obesity entails a risk for chronic kidney disease (CKD) (3, 4), independent of diabetes and hypertension (5). In accordance with these studies, the incidence of CKD and end-stage renal disease is increasing in our society. Moreover, there are further sequelae of obesity, such as

cardiovascular disease (6) and inflammation. However, these data are alarming and underline obesity being a threat not only to adults but also to children and adolescents (7, 8).

The term of fetal programming of diseases in adulthood was coined by Barker (9). Specifically, they postulate that an insult, acting during a phase of sensitivity in prenatal

Abbreviations: CKD, Chronic kidney disease; DAPI, 4',6-diamidino-2-phenylindole; ECM, extracellular matrix; GSI, glomerulosclerosis index; HCC, home-cage control; HKC8, human kidney cells; 11 β HSD, 11 β -hydroxysteroid dehydrogenase; LSR, litter size reduction at birth; M1, murine renal cortical collecting duct cells; MAP, mean arterial pressure; MC, mesangium cell; mEnd, murine endothelial cell; NPY, neuropeptide Y; P, postnatal day; PAI, plasminogen activator inhibitor; PC-12, pheochromocytoma cell line; PCNA, proliferating cell nuclear antigen; pH_A, postnatal hyperalimentation; RAAS, renin-angiotensin-aldosterone system; RR_{diast}, diastolic pressure; RR_{syst}, systolic pressure; SNS, sympathetic nervous system; SOCS-3, suppressor of cytokine signaling 3; Stat3, signal transducer and activator of transcription 3; THP, Tamm-horsefall protein; TIMP, tissue inhibitor of metalloproteinases.

ISSN Print 0013-7227 ISSN Online 1945-7170
Printed in U.S.A.

Copyright © 2012 by The Endocrine Society
doi: 10.1210/en.2011-1670 Received August 24, 2011. Accepted December 14, 2011.
First Published Online January 17, 2012

period, induces physiological alterations predisposing for disease later in life. Plagemann (10) extended the concept of fetal programming on postnatal events, such as nutritional factors. This association was named metabolic programming and defines a basic biological phenomena that putatively underlie relationships between nutritional experiences of early life and organogenesis as well as future disease in adolescence and adulthood (10, 11). Regarding renal development, nephrogenesis is predominantly completed prenatally in the human. However, renal maturation proceeds postnatally and consists of increment of glomerular size together with tubular length. In accordance, a few studies demonstrated that postnatal nutrition influences nephrogenesis and renal maturation in human and rodents (12–14). Moreover, early postnatal hyperalimentation (pHA) (15) induced by increased food intake during lactation period leads to metabolic programming and is therefore known to be a risk factor for development of obesity and obesity-related diseases (10, 11, 16).

Leptin is a 16-kDa protein, encoded by the *ob* gene and mainly produced in adipocytes. In accordance, hyperleptinemia is closely linked to obesity and further partially contributes to renal damage not only due to its profibrotic effects but also as a stimulator of the sympathetic nervous system (SNS). Leptin-mediated sympathetic stimulation is thought to play a pivotal role in obesity-related nephropathy (1). Interestingly, recent studies have demonstrated that placenta, skeletal muscle, and kidney are additional sites of leptin synthesis (17, 18). Leptin exerts diverse actions (19), extending beyond those involved in regulation of appetite and body weight. Some of these include proliferation, sympathetic nervous activation, fibrosis, and inflammation (20–22). In addition, leptin induces the synthesis of TGF- β 1 in glomerular endothelial cells and sensitizes mesangial cells to the effects of physiological levels of TGF- β 1 (20, 23). In line with this, glomerular expression of type IV collagen is significantly enhanced in leptin treated animals (24).

Leptin exerts its function via ObRb initiating tyrosine phosphorylation by Janus tyrosine kinase 2. Phosphorylated Janus tyrosine kinase 2 recruits signal transducer and activator of transcription 3 (Stat3). Next, phosphorylated Stat3 dimerizes and translocates to the nucleus regulating gene expression (25), such as suppressor of cytokine signaling 3 (SOCS-3), which acts as a leptin and IL-6 inducible inhibitor of leptin signaling and thereby presents one postreceptor cause of leptin resistance (26, 27). Furthermore, leptin regulates the expression of neuropeptide Y (NPY) via Stat3 signaling (28, 29); NPY is a coneurotransmitter of the SNS and among other functions a regulator of inflammatory response and renal function (30) (31). Moreover, recent studies demonstrated that early pHA

results in early onset of leptin resistance in the arcuate nucleus (32).

However, to date, the role of intrinsic renal leptin signaling and its impact on renal function subsequent to early pHA remains to be elucidated. Therefore, here we tested the hypothesis that early pHA contributes to impaired renal function via altered intrinsic renal leptin signaling in a rat model.

Materials and Methods

Animal procedures

All procedures performed on animals were approved by the local government authorities (Regierung von Mittelfranken, AZ no. 621-2531.31-11/02 and AZ no. 621-2531.31-14/05). Virgin female Wistar rats were obtained from our own colony and were housed in a room maintained at 22 ± 2 C, exposed to a 12-h dark, 12-h light cycle. The animals were allowed unlimited access to standard chow (no. 1320; Altromin, Lage, Germany) and tap water. The litter size reduction at birth (LSR) occurred at either LSR10 or LSR6 pups on the first day of life as previously described (30). During lactation rat mothers were fed standard chow. The weaning was at postnatal day (P) 23. We included home-cage control (HCC; mean litter size of 16) animals without any postnatal manipulation during lactation.

HCC, LSR10, and LSR6 animals were killed at P70 defining three groups: HCC (five animals), LSR10 (10 animals), and LSR6 (eight animals).

Cell culture

Five different cell lines were used: 1) murine endothelial cells (mEnd), 2) rat mesangium cells (MC), 3) human kidney cells (HKC8), 4) murine renal cortical collecting duct cells (M1), and 5) rat pheochromocytoma cell line (PC-12). All cell lines were maintained and passaged according to the recommendations of the American Type Culture Collection (<http://www.atcc.org>). The mEnd were kindly provided by Professor Dr. H. Schneider (University Hospital of Erlangen).

Physiological data of animals after litter size reduction

Body weight (grams) and body length (centimeters) were obtained at five time points: birth, postnatal wk 1, wk 2, wk 3, and wk 10 by weighing each animal. Body length was obtained by measuring from nose to tail insertion.

Metabolic studies and physiological parameters

Metabolic studies including standardized analyses of renal function and blood pressure were performed at the age of P70. The following protocol was carried out at each time point: 24 h before the animals were killed, the animals were housed individually in a metabolic cage for 24 h, allowing exact quantification of food and water intake as well as urine excretion. On the day the animals were killed, all animals were instrumented with femoral catheters under 5 mg/kg midazolam and 100 mg/kg ketamine anesthesia ip for intraarterial blood pressure measurements. At the end of the operation, animals were antagonized

with 0.2 ml atipamezole (5 mg/ml; Antisedan; Pfizer GmbH, Karlsruhe, Germany). Two hours after anesthesia, mean arterial blood pressure was recorded on a polygraph (Hellige, Freiburg, Germany) in conscious rats for 30 min in the animals' home cages as described previously (33). Retroorbital blood samples of 2 ml were obtained at the time the animals were killed. Creatinine in serum and urine samples was analyzed with the automatic analyzer Integra 800 (Roche Diagnostics, Mannheim, Germany).

Leptin ELISA

Measurement of leptin levels was performed using commercial available ELISA systems (Leptin DuoSet; R&D Systems, Minneapolis, MN) according to the manufacturer's instruction and as described previously (34).

Tissue preparation

The kidneys were excised and a portion was immediately frozen in liquid nitrogen at P70. For histology, another portion of renal tissue was fixed in 4% paraformaldehyde in PBS (20 mM Tris-Cl; 137 mM NaCl, pH7.6).

RNA extraction and semiquantitative and real time PCR

Total RNA was isolated from unfixed renal tissue or cultured cells and semiquantitative PCR was performed as previously described (33), using the 7500 real-time PCR system (Applied Biosystems, Foster City, CA). In all probes the relative amount of the specific mRNA was normalized to the ubiquitously expressed β -actin and glyceraldehyde-3-phosphate dehydrogenase gene. The primers and Taq-Man probes are listed in Table 1.

Protein isolation and immunoblotting

Protein isolation and immunoblotting were performed as described elsewhere (30). In brief, blots were probed with the following antibodies: monoclonal rabbit-antirat-phospho-p42/44 MAPK (ERK1/2) (Cell Signaling, Danvers, MA; no. 4370, 1:1000), polyclonal rabbit-antirat-p42/44 MAPK (ERK1/2) (Cell Signaling; no. 9102, 1:1000), polyclonal rabbit-antirat-phospho-Stat3 (Cell Signaling; no. 9131, 1:1000), monoclonal rabbit-antirat-Stat3 (Cell Signaling; no. 9139, 1:1000), poly-

TABLE 1. Designed primer pairs and TaqMan probes used in this study

Primers	(5'–3')
NPY	Forward, AGCAGAGGACATGGCCAGATAC Reverse, TGAAATCAGTGTCTCAGGGCTG Probe (FAM), CAATCTCATCACCAGACAGAGATATGGCAAGA (TAMRA)
Y1	Forward, CCACCTCACGGCCATGAT Reverse, TGGAAATTTTTGTTTCAGGAATCC Probe (FAM), TCCACCTGCGTCAACCCCATCTTTA (TAMRA)
Leptin	Forward, ATGACACCAAACCCCTCATCAAG Reverse, TGAAGTCCAAACCGGTGACC Probe (FAM), TCAATGACATTTACACACGCAGTCGG (TAMRA)
ObRa	Forward, TCAGAGCACCCAGGGAACC Reverse, ATAGCCCCTTGCTCTTCATCAG Probe (FAM), TCAGAGTCAACCCCTCAGTTAAATATGCAACGCT (TAMRA)
ObRb	Forward, CAGGTGCTATCTCTGAAGTAAG Reverse, GATAGGCCAGGTTAAGTGACG Probe (FAM), TCACATACAGAAATCCCAGTGTAAACAAAACC (TAMRA)
IL-6	Forward, TCCAAACTGGATATAACCAGGAAAT Reverse, TTGTCTTCTTGTTATCTTGTAAGTTGTTCTT Probe (FAM), AATCTGCTCTGGTCTTCTGGAGTTCCGTTTCTA (TAMRA)
IL-10	Forward, GAAGCTGAAGACCCTCTGGATACA Reverse, CCTTTGCTTGGAGCTTATTAATAATCA Probe (FAM), CGTGTTCATCGATTTCTCCCCTGTGA (TAMRA)
PAI-1	Forward, TCCGCCATCACCACATTTT Reverse, GTCAGTCATGCCAGCTTCTC Probe (FAM), CCGCTCCTCATCCTGCCTAAGTTCTCT (TAMRA)
β -Actin	Forward, TGAGCTGCCTGACGGTCAG Reverse, TGCCACAGGATTCCATACCC Probe (FAM), CACTATCGGCAATGAGCGGTTCCG (TAMRA)
GAPDH	Forward, TGTGAAGCTCATTTCTGGTATGA Reverse, CTCTCTTGTCTCAGTATCCTTGCT Probe (FAM), CCAAGGAGTAAGAAACCCTGGACCACCC (TAMRA)
Adrenoceptor 1a	Forward, GCTGCTCAAGTTTTCTCGAGAGA Reverse, AAGACCCAATGGGCATCACTAG
Adrenoceptor 1d	Forward, GTCCTGCCCTGGGCTCTCT Reverse, GGGTAGATGAGCGGGTTTAC
Adrenoceptor β 1	Forward, ATCGTAGTGGCAACGTGTTG Reverse, GGGACATGATGAAGAGTTGGT
Adrenoceptor β 2	Forward, GGATTGCCCTCCAGGAGCTT Reverse, TGTCCTACCGTTGCTGTTGCTA

GAPDH, Glyceraldehyde-3-phosphate dehydrogenase.

clonal rabbit-antirat-IL-6 (Abcam, Cambridge, UK; 6672, 1:400), and monoclonal mouse-antirat-proliferating cell nuclear antigen (PCNA) (Dako, Glostrup, Denmark; clone PC10, M0879, 1:1000), and polyclonal rabbit-antirat-Socs3 (Cell Signaling; no. 2923, 1:1000), whereas monoclonal mouse-antirat- β -actin (Cell Signaling; no. 3700, 1:1000) served as a loading control. Antimouse IgG, horseradish peroxidase-linked (Cell Signaling; no. 7076, 1:2000), and antirabbit IgG, horseradish peroxidase-linked (Cell Signaling; no. 7074, 1:2000) were used as secondary antibody.

Renal histology

The degree of mesangial matrix expansion and sclerosis within the glomerulus as an index of progression was determined on periodic acid-Schiff-stained paraffin sections using a scoring system [glomerulosclerosis index (GSI)] as described before (35). Using light microscopy at a magnification of $\times 400$, the glomerular score (0–4) of each animal was derived as the mean of 100 randomly sampled glomeruli, and the resulting index in each

animal was expressed as a mean of all scores obtained. For evaluation of vascular damage, 20 vessels per kidney were randomly sampled using hematoxylin-eosin stained sections at a magnification of $\times 200$ and graded using a semiquantitative scoring system with a score from 0 to 4: score 0, no vascular damage; score 4, vascular fibrinoid necrosis.

Tubulointerstitial damage was assessed on periodic acid-Schiff-stained paraffin sections at a magnification of $\times 200$ using a semiquantitative scoring system (tubulointerstitial lesion score) (35). Here interstitial fibrosis, inflammation, tubular dilatation, and tubular atrophy were graded (0–3) in 20 randomly selected fields per kidney.

All histological studies were carried out by an investigator unaware of the experimental group to which each kidney belonged.

Immunofluorescence

Immunostaining was assessed as previously described (30, 35). Sections were incubated with the relevant primary antibody: rabbit-

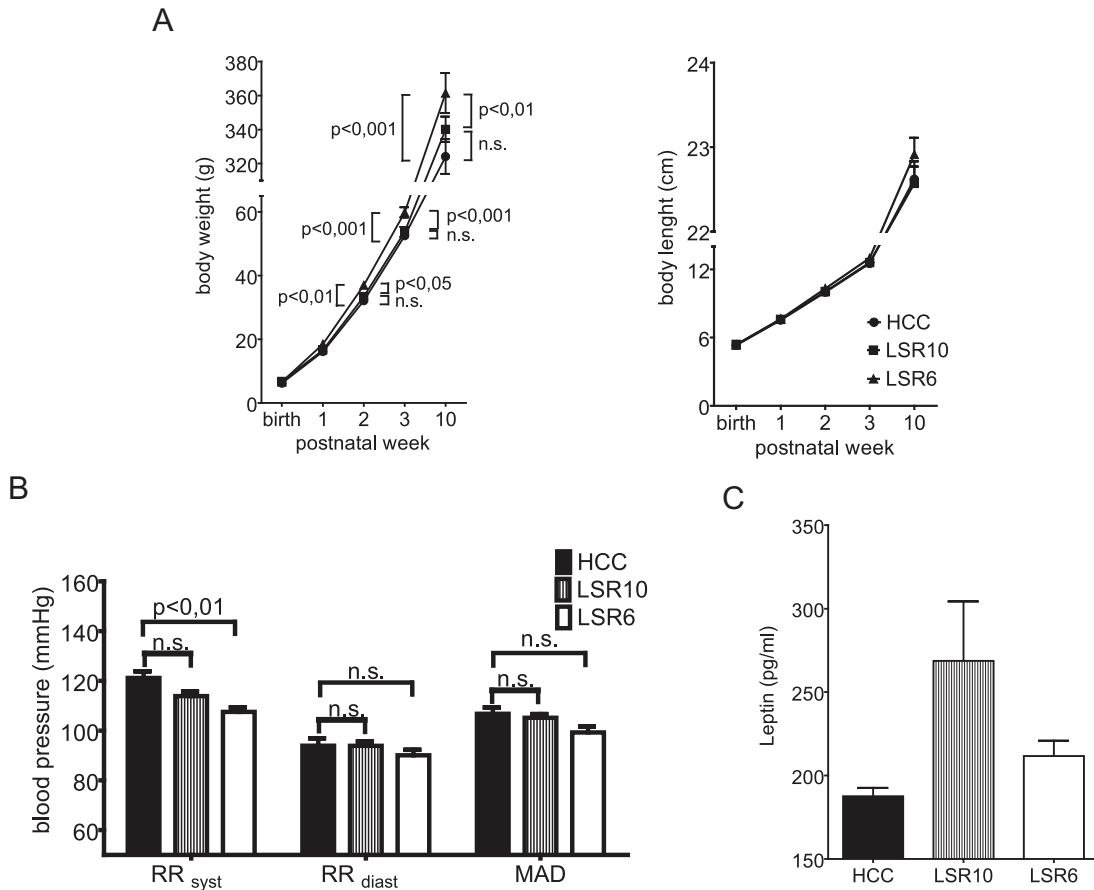


FIG. 1. Physiological parameters after litter size reduction. A, Body weight (grams) and body length (centimeters) at postnatal wk 1, postnatal wk 2, postnatal wk 3, and postnatal wk 10. Animals after litter size reduction to 6 (LSR6, \blacktriangle) exhibit from the postnatal wk 2 forward an increased body weight compared with either animals with litter size reduction to 10 (LSR10, \blacksquare) or the HCC group (\bullet). At postnatal wk 3 (time of weaning), LSR6 has a significant increased weight compared with LSR6 and HCC, whereas there is no difference between LSR10 and HCC. Interestingly, at postnatal wk 10, the difference in weight persists to be significant between both LSR6 and LSR10, and in accordance, the group LSR10 was significantly heavier than the HCC group. With regard to body length, there was no difference between the groups detected. B, Systolic and diastolic blood pressure (RR_{sys} and RR_{diast}) and MAP (millimeters of mercury) at P70: rats after LSR6 (white bar) exhibit a significantly decreased RR_{sys} compared with LSR10 (striped bar) and HCC (black bar). Regarding RR_{diast} and MAP, no significance difference was measured. C, Plasma leptin levels in the blood at P70: leptin concentrations in plasma (picograms per milliliter) were slightly elevated after LSR6 and LSR10. Significance for each bar is indicated by P values (two way ANOVA test and Bonferroni posttest). n.s., Not significant.

anti-NPY (Biotrend; Cologne, Germany; NA1233, 1:1000), goat anti-NPY receptor 1 (catalog no. Cs21990; Santa Cruz Biotechnologies, San Francisco, CA; 1:400), rabbit-anti-leptin (Acris, Herford, Germany; SP5130P, 1:50), rabbit-anti-Socs3 (Abcam, Cambridge UK; ab16030, 1:100), goat-anti-Tamm-horsefall protein (THP) (ICN Biomedical, Eschwege, Germany; 55140, 1:500), sheep anti-11 β -hydroxysteroid dehydrogenase (11 β HSD) type 2 (Chemicon, Billerica, MA; AB1296, 1:200), mouse-anticalbindin (Swant, Bellinzona, Switzerland; 300, 1:200). Immune complexes were visualized with fluorescent secondary antibodies: Cy3 goat antirabbit (catalog no. 111-166-003; Jackson ImmunoResearch, Suffolk, UK; 1:400), Alexa 488 donkey antigoat (catalog no. A11055; Invitrogen, Karlsruhe, Germany; 1:400), and Cy2 donkey antimouse (catalog no. 715-226-150; Jackson ImmunoResearch; 1:400). Cell nuclei were labeled with 4',6-diamidino-2-phenylindole (DAPI; catalog no. D1306; Invitrogen; 1:1000).

Quantitative immunostaining

Tissue preparation was performed as described elsewhere (30). Sections were incubated with the relevant primary antibody: rabbit-antirat-collagen I (Biogenesis; 1:100) and goat-antirat-collagen IV (Southern Biotech, BIOZOL Diagnostica Vertrieb GmbH, Eching, Germany, AL; 1:500). Immune complexes were visualized with an avidin/biotin-3,3'-diaminobenzidine detection system (Vector Laboratories, BIOZOL Diagnostica Vertrieb GmbH, Eching, Germany). Each slide was counterstained with hematoxylin.

Quantitative evaluation of the immunohistochemical results was performed with a MetaVue imaging system (Molecular De-

vices, Sunnyvale, CA). Collagen positive area in a defined area (3.2 mm²) is displayed in percentage.

Analysis of data

The results of real-time RT-PCR were calculated based on the change in delta delta cycle threshold value method and expressed as fold induction of mRNA expression compared with the HCC (1.0-fold induction). Values are shown as means \pm SEM. A two-tailed Mann-Whitney *U* test, one-way ANOVA followed by a Dunn's test and a two-way ANOVA followed by a Bonferroni posttest were used to test significance at the given time points. A *P* < 0.05 was considered as significant.

Densitometric analysis of protein bands was performed using Advanced Image Data Analyzer software (version 4.15; Fuji Photo Film Co., Omiyama, Japan) and Bio-Rad ImageLab software (Bio-Rad, Munich, Germany). Band intensities from samples were normalized for loading using the β -actin band from the same sample.

Results

Increased weight gain during lactation without hyperleptinemia or hypertension subsequent to litter size reduction

We characterized initially the phenotype of the animals after early pHA at P70. To assess renal function and leptin

signaling subsequent to early pHA and before the onset of metabolic syndrome, we chose P70. That age enables to differentiate between the effects early postnatal nutrition and metabolic syndrome induced diseases. Body weight during lactation period (postnatal wk 2 and 3) and at postnatal wk 10 was significantly increased after litter size reduction to 10 (LSR10) and LSR6 compared with the HCC (Fig. 1A). Body length did not differ between the groups (Fig. 1A). To rule out a pronounced metabolic syndrome at P70, we assessed leptin levels in plasma (picograms per milliliter) and blood pressure [systolic (RR_{sys}; millimeters of mercury), diastolic (RR_{diast}; millimeters of mercury), and mean arterial pressure (MAP)]. We found no evidence that MAP was altered. In contrast, we measured a significantly lowered RR_{sys} after LSR6, whereas RR_{diast} was unchanged (Fig. 1B). Leptin levels in plasma were slightly but not significantly increased in LSR10 and LSR6 compared with HCC (Fig. 1C). Glucose levels did not differ in the three groups (data not

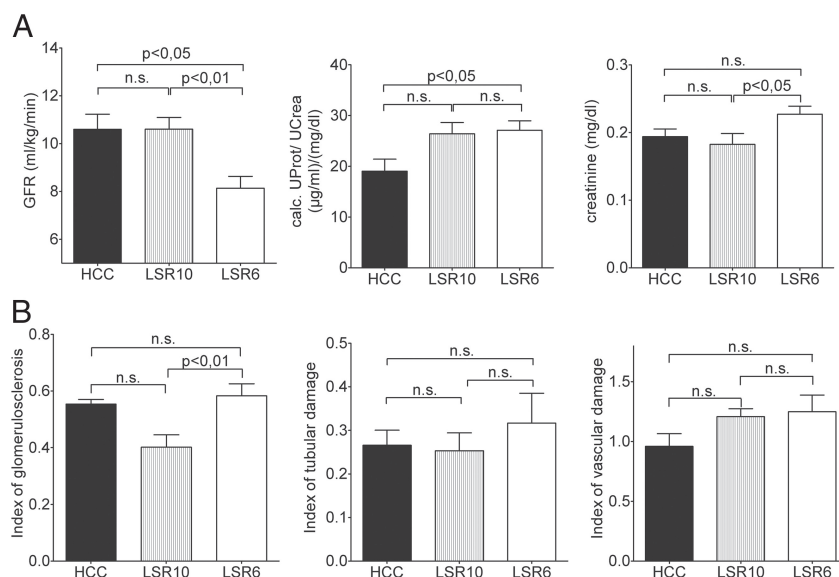


FIG. 2. Renal physiological parameters and indices of renal damage after litter size reduction at P70. A, Analysis of glomerular filtration rate (GFR) and protein excretion in the urine for 24 h and creatinine level in the serum revealed an impaired renal function after litter size reduction to 6 (LSR6) at P70: rats after litter size reduction to 6 (LSR6; white bar) exhibit reduced GFR (milliliters per kilogram per minute) compared with LSR10 (striped bar) and HCC (black bar). The protein excretion [calc. UProt/Ucrea (micrograms per milliliter)/(milligrams per deciliter)] was significantly increased in LSR6 compared with HCC. In addition, creatinine (milligrams per deciliter) in the serum was markedly elevated in the LSR6. B, Indices of glomerulosclerosis (GSI), tubulointerstitial damage (TSI), and vascular damage (VI) after litter size reduction. Significance for each bar is indicated by *P* values (one way ANOVA test and Dunn's posttest). n.s., Not significant.

shown). Taken together, LSR6 leads to a persistent increased weight gain. Furthermore, the rats display no significant hyperleptinemia, normal glucose plasma levels (data not

shown), no glycosuria, and rather a hypotensive than a hypertensive state at P70.

Impaired glomerular and tubular function after early pHA

To assess renal function the animals then underwent metabolic analysis in metabolic cages for 24 h at P70. The glomerular filtration rate (GFR) was significantly decreased and protein excretion elevated. In addition, we recently demonstrated that early pHA leads to an increase of both excreted fraction of the filtered sodium and excreted fraction of the filtered potassium (30). Furthermore, measurement of creatinine in the serum clearly showed an increased creatinine level subsequent to LSR6. To further histologically evaluate renal damage, we assessed immunohistochemistry and applied indices for glomerular, tubulointerstitial, and vascular damage. They were slightly increased after LSR6 but did not reach significance at such an early time P70 (Fig. 2B). Thus, early pHA impairs renal function, in particular leading to decreased GFR and proteinuria.

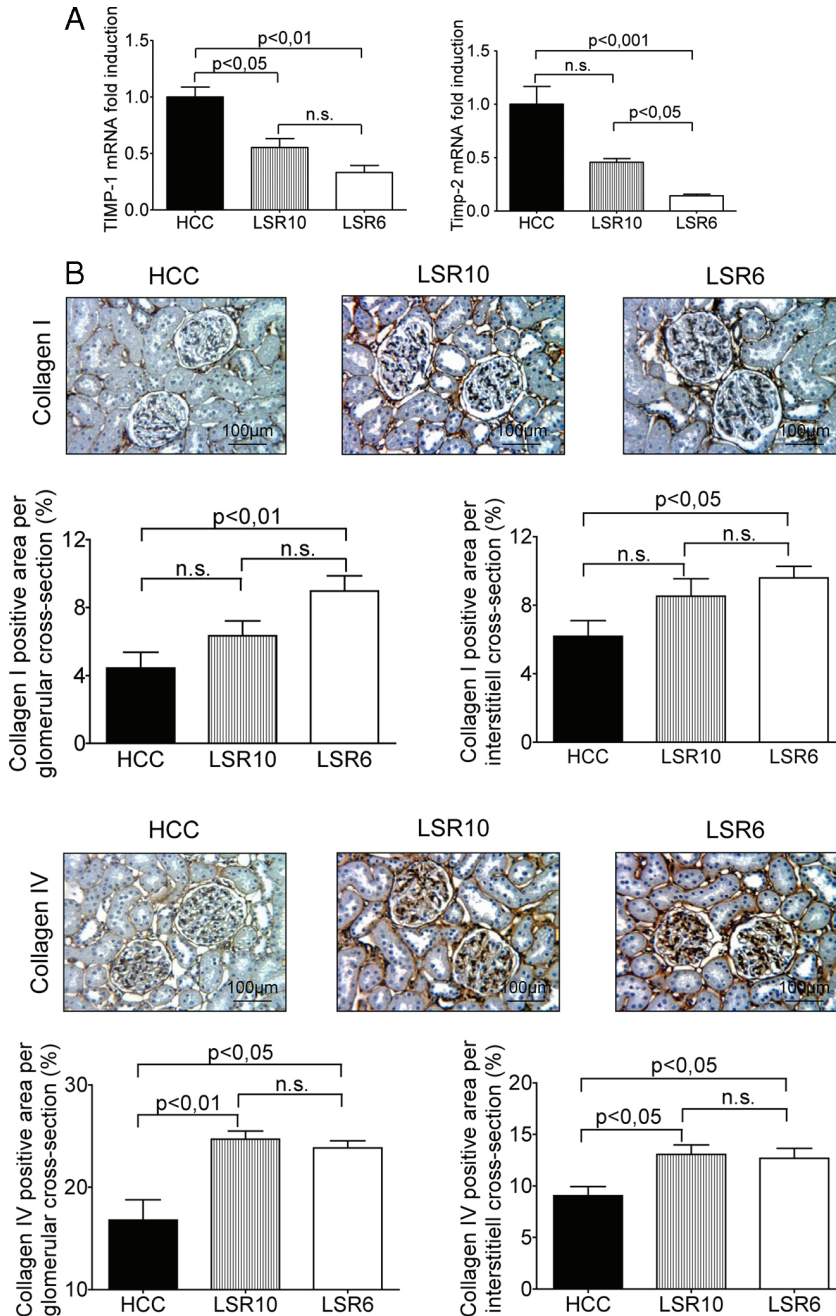


FIG. 3. Decreased expression of ECM-metabolizing enzymes and increased renal deposition of collagen I and collagen IV after early pHA at P70. A, Expression of leptin signaling target genes encoding ECM-metabolizing enzymes TIMP-1 and TIMP-2 was assessed by quantitative RT-PCR. B, The deposition of the ECM components collagen I and collagen IV in the glomerulus and in the interstitium was detected by immunohistochemistry. The areas illustrated were representative for the staining pattern observed in five to 10 different kidneys. Semiquantitative analysis of the expression of collagen I and collagen IV in the glomerulus and interstitium was assessed by the MetaVue imaging system (Molecular Devices). Litter size reduction to 6 (LSR6; white bar), LSR10 (striped bar), and HCC (black bar) are shown. Significance for each bar is indicated by P values (one way ANOVA test and Dunn’s posttest). n.s., Not significant.

Dysregulated proliferation and extracellular matrix composition after early pHA

To elucidate whether early pHA has long-term effect on proliferation and extracellular matrix (ECM), we assessed immunostaining for collagen I and collagen IV. Semiquantitative evaluation demonstrates an increased positive staining for both collagen I and collagen IV in glomeruli and tubulointerstitium (Fig. 3B). In addition, the gene expression of ECM-metabolizing enzymes, such as tissue inhibitor of metalloproteinases (*TIMP*)-1 and *TIMP*-2 were considerably down-regulated (Fig. 3A). Finally, we assessed immunoblotting for PCNA and detected a significant up-regulation at P70 after LSR6 (Fig. 4A). Additionally, we examined PCNA by immunostaining for differentiation of glomerular and tubulointerstitial compartment. Both glomeruli and tubulointerstitium showed in-

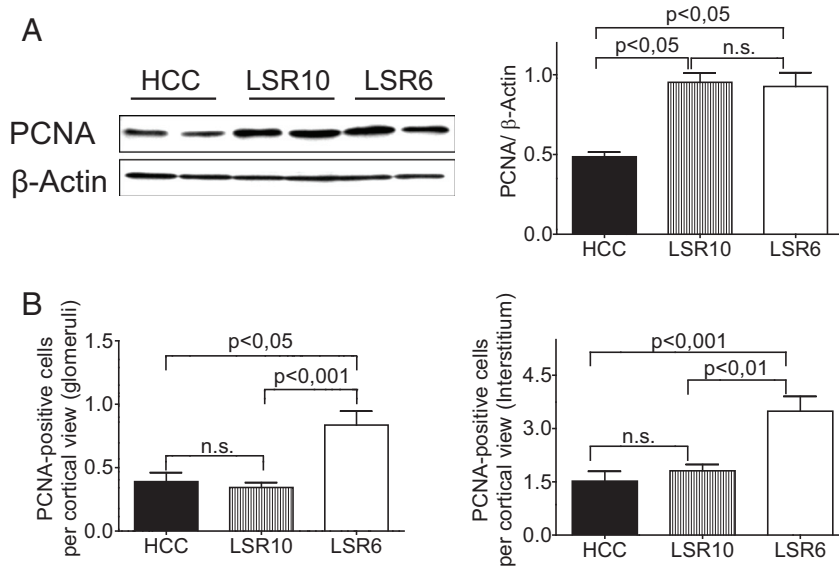


FIG. 4. Increased renal intrinsic proliferative processes after early pHA at P70. **A**, Expression of PCNA as a marker for proliferation was assessed by immunoblotting, using constitutively expressed β -actin as loading control. These data were quantified by densitometric analysis. **B**, Proliferative effect after postnatal hyperalimentation was assessed by quantification of PCNA-positive cell in glomeruli and interstitium. Litter size reduction to 6 (LSR6; white bar), LSR10 (striped bar), and HCC (black bar) are shown. Significance for each bar is indicated by *P* values (one way ANOVA test and Dunn's posttest). n.s., Not significant.

creased positive staining for PCNA in the animals after LSR6 (Fig. 4B). Taken together, these results give strong evidence of dysregulated proliferation and profibrotic processes subsequent to early pHA.

Increased expression of renal-specific leptin expression after early pHA

The results obtained so far indicate a vital role of early pHA in renal physiology and an impact on regulation of profibrotic processes before histological changes are seen. To gain a mechanistic view, we analyzed the expression pattern of the obesity-related peptide hormone leptin and leptin receptors (*ObRb*, *ObRa*) by quantitative RT-PCR. The mRNA expression of genes encoding *leptin* and *ObRb* was significantly increased in the LSR6 (Fig. 5A). To further differentiate the localization of leptin within the kidney, we assessed immunocytochemistry. Leptin was colocalized with THP, a marker of the thick ascending limb of the Henle's loop (Fig. 5B). To determine a regulation of ObR subsequent to an increment of leptin expression, we assessed the expression of ObR by immunoblotting. We did not detect any notable alterations after early pHA (Fig. 5C). We next assessed mRNA expression of leptin in the retroperineal and epigonadal tissue and compared the expression of leptin in adipose tissue to kidney subsequent to early pHA (LSR6). There was no difference in leptin expression in the adipose tissue within the

groups (Fig. 5D). On the contrary, as expected, the expression of leptin was clearly higher in the adipose tissue than in the kidney in the LSR6 (Fig. 5E). In summary, our findings show a striking increase of renal-specific expression and a distinct renal localization of leptin subsequent to early pHA, whereas the expression of leptin is not altered in white adipose tissue.

Inhibition of intrinsic renal STAT3 and ERK1/2 signaling after early pHA

To analyze the activation of the Stat3 and Erk1/2 pathway, we performed immunoblotting (Fig. 6, A and B). Phosphorylation of both Stat3 and Erk1/2 was already decreased after LSR10 and even more predominantly after LSR6 compared with the control group (HCC), demonstrating an additional litter size-dependent effect on phosphorylation. Unphosphorylated Stat3 was significantly increased (Fig. 6A), whereas total, unphosphorylated Erk1/2 was unchanged (Fig. 6B). Thus, the activation of Stat3 and Erk1/2 signaling is strongly attenuated after early pHA.

Functional impact of inhibition of intrinsic renal STAT3 and ERK1/2 signaling on leptin target genes after early pHA

To further delineate functional impact of inhibition of leptin signaling pathway, we analyzed mRNA expression of corresponding target genes, such as *IL-10* (Fig. 7A), *TIMP-1*, and *TIMP-2* (Fig. 3A). Phosphorylated Stat3 and Erk1/2 induce *IL-10*, *TIMP-1*, and *TIMP-2* expression. Consistently, the mRNA expression of *IL-10*, *TIMP-1*, and *TIMP-2* is decreased in the group of LSR10 and LSR6 due to the reduced degree of phosphorylation of Stat33 and Erk1/2.

Next, we continued our study with the expression pattern of another pivotal target gene of leptin signaling: NPY, a conerurotransmitter of the sympathetic system, and its receptor NPY receptor 1 (Y1). Strikingly, the mRNA expression of NPY was significantly increased in LSR6, whereas Y1 was significantly decreased (Fig. 6C). To further differentiate the expression of *NPY* and *NPY receptor Y1* within renal compartments, we analyzed endothelial cells (mouse), MC (rat), HKC8 (human), and the M1 cell line (derived from the mouse cortical collecting duct) with PCR and immunocytochemistry. Consistent with

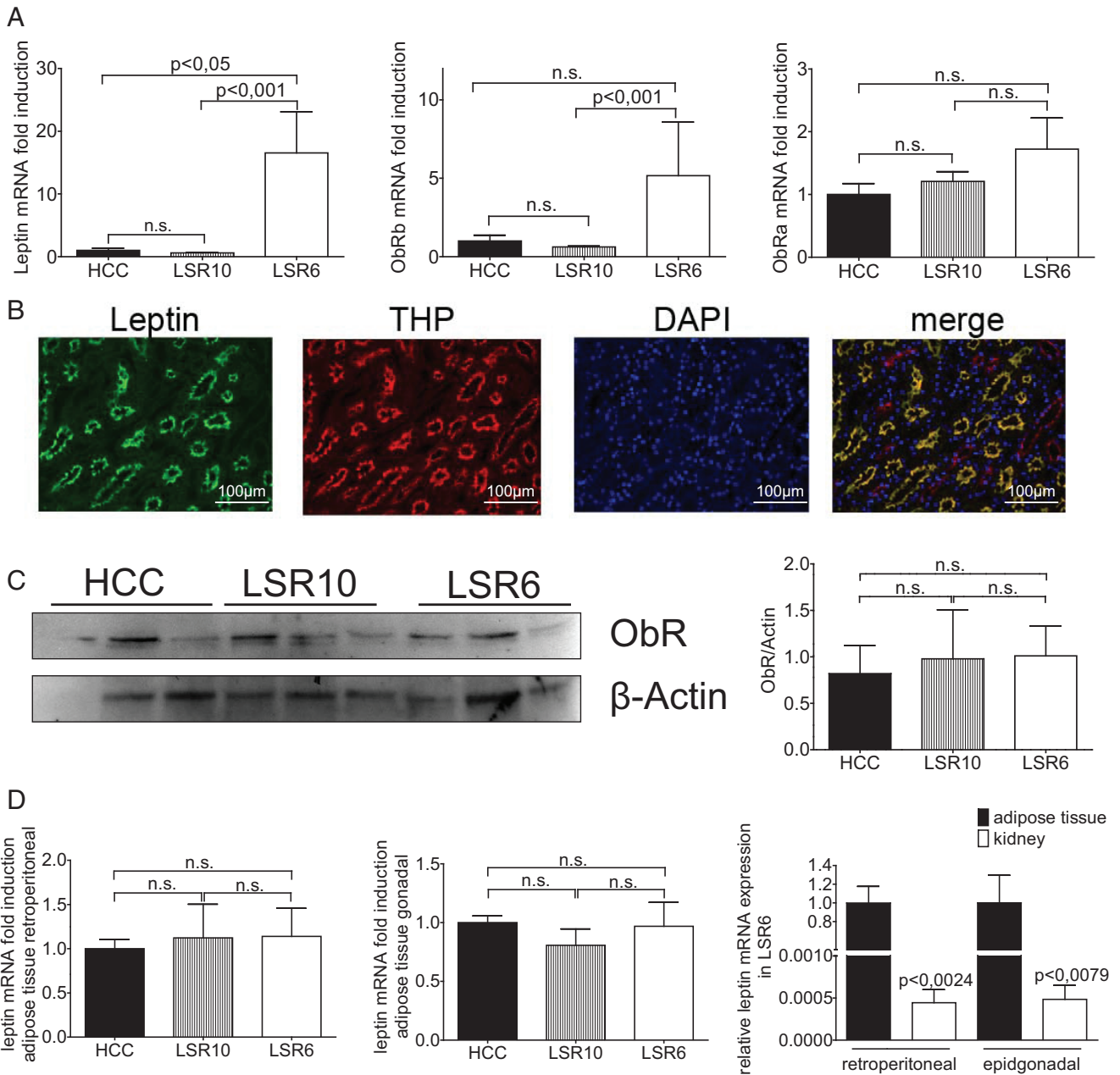


FIG. 5. Intrinsic renal and adipose tissue expression of leptin, obese receptor b (*ObRb*), and *ObRa* after early pHA at P70. **A**, Renal leptin and leptin receptor expression at P70 and renal localization of leptin: mRNA expression of the genes encoding leptin, obese receptor b (*ObRb*), and *ObRa* (alternative splice form of *ObRb*) was assessed by quantitative real-time PCR. The mRNA expression of leptin and *ObRb* was significantly and of *ObRa* slightly increased in the group of litter size reduction to 6 (LSR6, white bar) compared with LSR10 (striped bar) and HCC (black bar). **B**, The localization of leptin in the renal distal tubuli and collecting ducts was examined by coimmunostaining with THP. **C**, Expression of leptin receptor (*ObR*) was assessed by immunoblot in LSR6 (white bar), LSR10 (striped bar), and HCC (black bar); β -actin was used as loading control. The results were analyzed and quantified by densitometry. **D**, The mRNA expression of leptin in retroperitoneal and epididymal adipose tissue was assessed by quantitative real-time-PCR. LSR6 (white bar), LSR10 (striped bar), and HCC (black bar). **E**, Comparison of the mRNA expression of leptin in adipose tissue (retroperitoneal and epididymal, black bar) and kidney (white bar) in LSR6. Significance for each bar is indicated by *P* values (one way ANOVA test and Dunn's posttest). n.s., Not significant.

the mRNA results, *NPY* was expressed in endothelial, MC, and M1 cells but not in HKC8 cells. The *Y1* receptor was detectable in all four cell lines. PC-12 (rat) served as a positive control (Fig. 6C). Taken together, these results demonstrate a functional impact of the renal specific reduced leptin signaling on its specific target genes.

Renal-specific proinflammatory state and altered expression of renal adrenoceptors after early pHA

The results obtained so far demonstrate an impaired leptin signaling with subsequent regulation of target genes encoding inflammatory cytokines (*IL-10*), and neurotransmitter (*NPY*). To elucidate whether this intrinsic

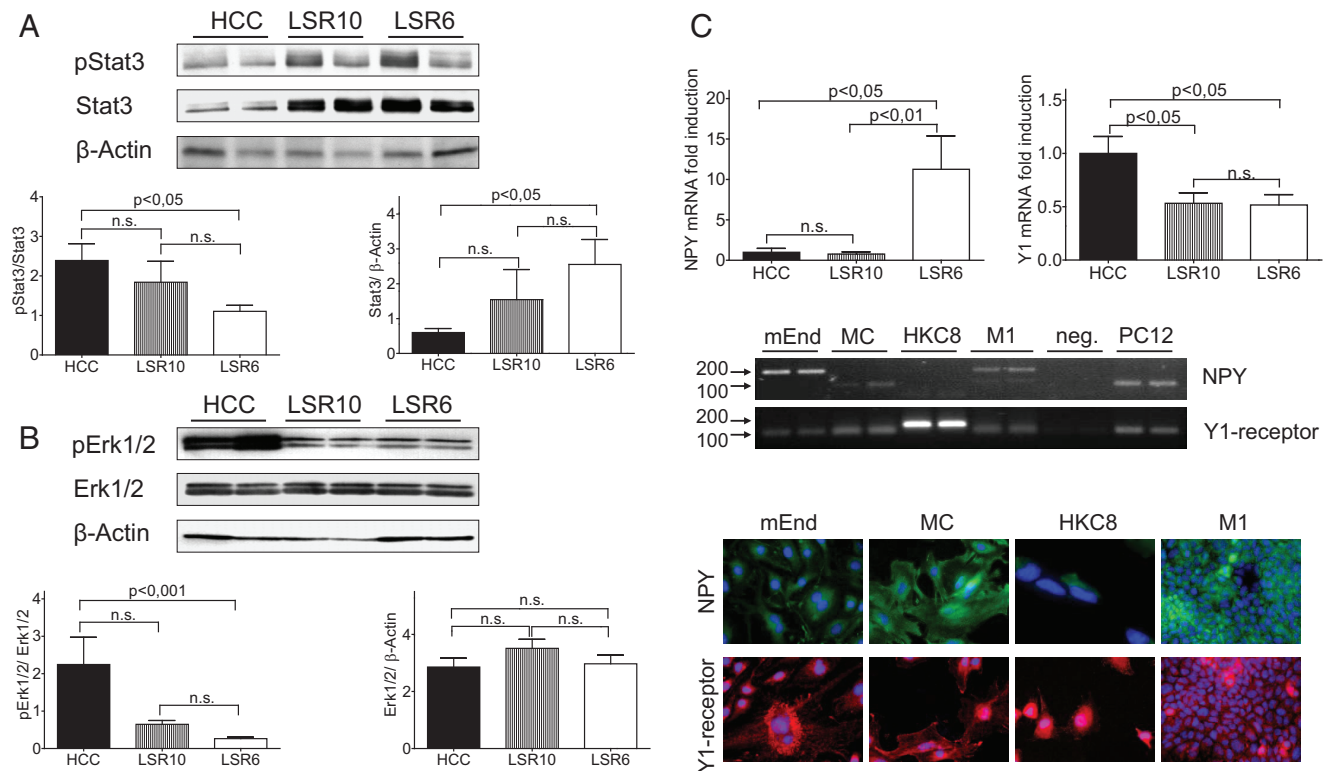


FIG. 6. Early postnatal hyperalimantation inhibits the phosphorylation of both Stat3 and Erk1/2 after early pHA at P70. **A**, Expression and phosphorylation of Stat3 was assessed by immunoblot, using constitutively expressed β -actin as loading control. These data were quantified by densitometric analysis. **B**, Protein expression and phosphorylation of Erk1/2 was monitored by immunoblot; β -actin was used as loading control. The results were analyzed and quantified by densitometry. **C**, Expression of *NPY* and the *NPY*-receptor 1 (*Y1*) *in vitro* and *in vivo* after litter size reduction: a significant increase of mRNA expression of *NPY* and reduced of *Y1* after litter size reduction to 6 (LSR6) compared with LSR10 and HCC is seen. Additionally, *in vitro* analysis by RT-PCR revealed the mRNA expression pattern of *NPY* and *Y1* in different compartments of the kidney [mEnd, MC, HKC8, and cortical collecting duct cells (M1)]. PC-12 served as positive control for *NPY* and *Y1*. *NPY* mRNA was detected in the mEnd, MC, and M1 cells but not in HKC8 cells, whereas mRNA expression of *Y1* was detectable in all cell lines. Immunocytochemistry for expression of *NPY* and *Y1* in these cell lines demonstrates a positive staining for *NPY* in mEnd, MC, and M1 cells but not in HKC8-cells and for *Y1* in all cell lines. Litter size reduction to 6 (LSR6; white bar), LSR10 (striped bar), and HCC (black bar) is shown. The significance for each bar is indicated by *P* values (one way ANOVA test and Dunn's posttest). n.s., Not significant.

renal leptin resistance goes along with a dysregulated inflammatory and sympathetic response after pHA, we analyzed renal cytokine expression and expression of adrenoceptors in the animals. We demonstrated that early pHA increases markedly the expression of *IL-6* and plasminogen activator inhibitor (PAI)-1 after LSR10 and even more pronounced after LSR6 (Fig. 7A). Additionally, we confirmed the mRNA expression data for *IL-6* with immunoblotting (Fig. 7A). Interestingly, we detected a significant up-regulation of mRNA expression of adrenoceptors- $\alpha 1a$ and - $\alpha 1d$ compared with the HCC, whereas adrenoceptors- $\beta 1$ and - $\beta 2$ were significantly down-regulated (Fig. 7B). Taken together, these data underline the clear effect of pHA on the regulation of the inflammatory response and the sympathetic nerve system.

Up-regulation of STAT3 and ERK1/2 inhibitor SOCS-3 after early pHA

It remains unclear what specifically leads to an intrinsic renal postreceptor leptin resistance subsequent to early

pHA. To further identify the underlying mechanism of the inhibition of the Stat3 and Erk1/2 signaling pathway, we analyzed SOCS-3, an inhibitor of phosphorylation of Stat3 and Erk1/2. Strikingly, immunoblotting of SOCS-3 demonstrates an up-regulation of SOCS-3 after pHA (Fig. 8A). To further delineate the renal compartment of localization of SOCS-3, we assessed immunohistochemical analysis: first, we could demonstrate a colocalization of SOCS-3 with 11 β HSD (a marker for the distal tubules in the cortex and outer medulla), calbindin (calbindin is found in distal convoluted tubule with the signal extending into the connecting ducts), and THP (a marker of the proximal tubules) (Fig. 8B), but no staining was detectable in the glomeruli (Fig. 8C).

To show next that SOCS-3 is colocalized with *NPY* in the kidney, *NPY* was detectable in the glomeruli, the distal (costaining with 11 β HSD), and the proximal (costaining with THP) tubulus system (Fig. 8C). Additionally, we could demonstrate a colocalization of SOCS-3 and *NPY*.

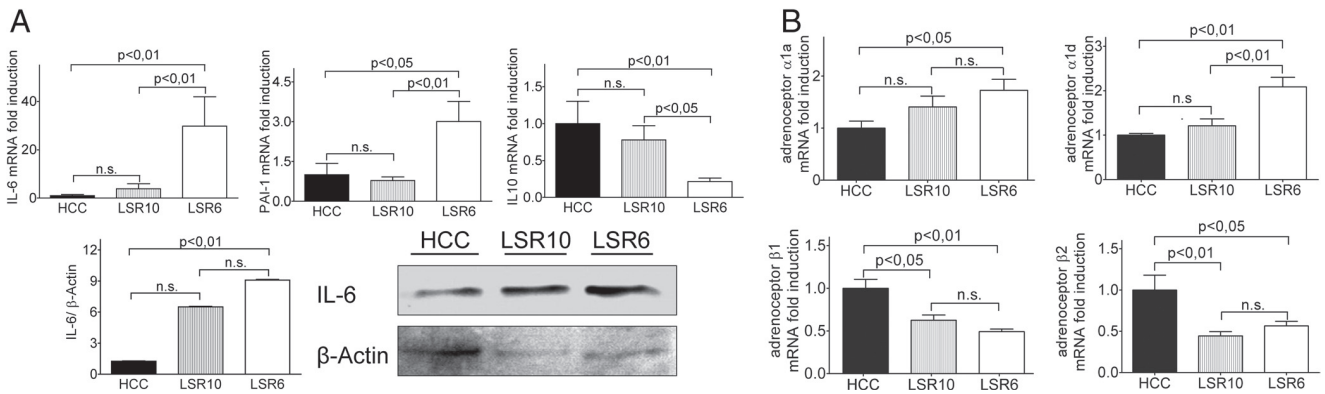


FIG. 7. Intrinsic renal inflammatory state and expression of genes encoding adrenoceptors- $\alpha 1a$, - $\alpha 1d$, - $\beta 1$, and - $\beta 2$ after early pHA at P70. **A**, Intrinsic renal inflammatory state after early pHA at P70: mRNA expression of genes encoding *IL-6*, *IL-10*, and *PAI-1* was assessed by quantitative real-time-PCR. Litter size reduction to 6 (LSR6; white bar) showed a dramatic increased mRNA expression of inflammatory cytokines *IL-6* and *PAI-1* and decreased mRNA expression of antiinflammatory and leptin-inducible gene *IL-10* compared with LSR10 (striped bar) and HCC (black bar). Quantification of immunoblotting of *IL-6* showed an increased renal protein expression of *IL-6* after LSR6 compared with LSR10 and HCC. **B**, Intrinsic renal expression of genes encoding adrenoceptor- $\alpha 1a$, adrenoceptor- $\alpha 1d$, adrenoceptor- $\beta 1$, and adrenoceptor- $\beta 2$ was assessed by quantitative real-time-PCR. Litter size reduction to 6 (LSR6; white bar) exhibited a significant increased expression of adrenoceptor- $\alpha 1a$ compared with HCC (black bar) and an increased expression of adrenoceptor- $\alpha 1d$ compared with LSR10 (striped bar) and HCC. The expression of adrenoceptor- $\beta 1$ and adrenoceptor- $\beta 2$ was significantly down-regulated in the LSR6 and LSR10 group compared with HCC. Significance for each bar is indicated by *P* values (one way ANOVA test and Dunn's posttest). n.s., Not significant.

To sum up, SOCS-3, a crucial mediator of postreceptor leptin resistance is significantly up-regulated in the kidneys subsequent to pHA and specifically localized with leptin's target gene *NPY*.

Discussion

This study demonstrates for the first time a renal postreceptor leptin resistance with impaired glomerular and tubular function in rats after early pHA (15). Moreover, our findings give strong evidence that early pHA leads not only to an increased renal expression of proinflammatory (such as *IL-6*) but also to a dramatic up-regulation of renal-specific leptin resistance. Clinical studies support these results demonstrating elevated serum inflammatory markers in overweight children and adolescents (36) as well as in patients with CKD (37). Arising evidence for obesity-related nephropathy in infant, adolescent, and adult humans (8, 9, 38, 39) endorses these results.

Note that in the presented study, the impaired glomerular and tubular function was not (or not yet) accompanied by a metabolic syndrome. We could detect neither increased glucose levels nor hypertension or hyperleptinemia subsequent to early pHA. This is consistent with several studies giving evidence that obese individuals often develop progressive renal dysfunction before the occurrence of diabetes and severe hypertension (40, 41).

Obesity is a self-perpetuating and devastating process: adipose tissue-secreted adipocytokines, such as *IL-6* and *PAI-1*, exert inflammatory and atherosclerotic effects, increase sympathetic activity, contribute to insulin resis-

tance and hypertension, and impair renal function. In addition to cytokines, there are also peptide hormones (such as leptin) linked to pHA obesity-related diseases (42). Leptin exerts both systemic and organ specific function. Accordingly, there are several studies demonstrating an intrinsic renal synthesis (18) and function of leptin (17, 20, 21). Notable among these are profibrotic, proliferative effects (17, 23), and stimulation of SNS (22). Leptin affects blood pressure through stimulation of the central and peripheral sympathetic nervous systems. In the present study, leptin plasma levels were not significantly elevated in the group after early pHA, and accordingly, blood pressure was not increased. However, the intrinsic renal expression of leptin and its receptor (*obRb*) is strikingly up-regulated after early pHA. Thus, intrinsic renal leptin may exhibit an auto- and paracrine effect, independent of circulating leptin secreted by adipose tissue.

Both *IL-6* and leptin have direct impact on the regulation of renal cell proliferation (20, 24), differentiation, and production of components and metabolizing enzymes of the ECM (17, 43–45) via Stat3 and Erk1/2. This is in line with data presented in our study giving strong evidence that an elevated expression of leptin goes along with dysregulated ECM turnover: decreased expression of ECM metabolizing enzymes (*TIMP-1* and *TIMP-2*) and increased deposition of collagen I and collagen IV in the renal interstitium and glomeruli. In this context, intrinsic renal leptin could play a vital role mediating proliferative and profibrotic effect.

The intracellular pathway of leptin occurs predominantly via phosphorylation of Stat3 and Erk1/2. Target

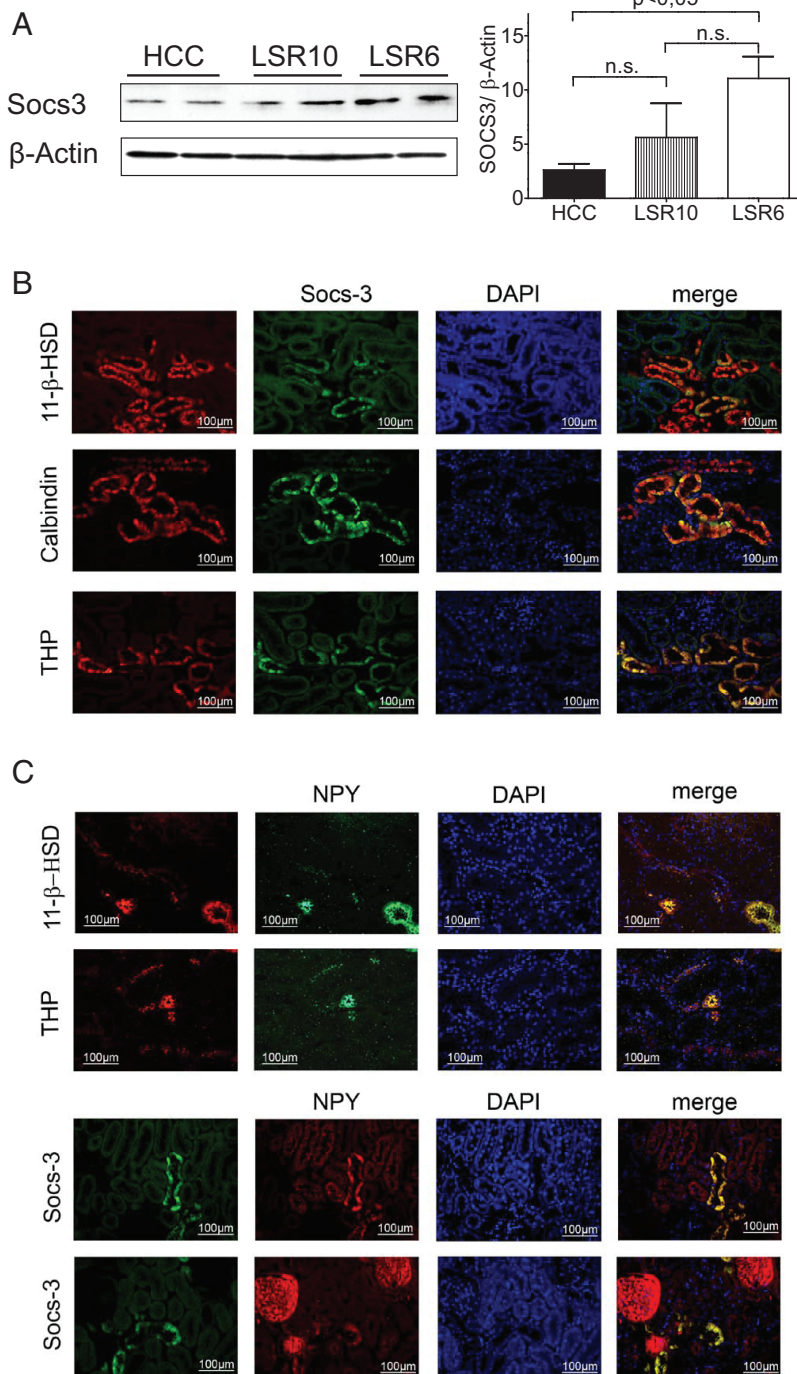


FIG. 8. Renal localization and expression of SOCS-3 after early pHA at P70. **A**, Expression of SOCS-3 was assessed by immunoblot, using constitutively expressed β -actin as loading control. These data were quantified by densitometric analysis. Litter size reduction to 6 (LSR6; white bar), LSR10 (striped bar), and HCC (black bar) are shown. Significance for each bar is indicated by *P* values (one way ANOVA test and Dunn's posttest). n.s., Not significant. **B**, Localization of SOCS-3 was detected by immunofluorescence staining. Representative sections are illustrated, using SOCS-3 (green) and 11 β HSD (red) as a marker for the distal tubules in the cortex and outer medulla, calbindin as a marker of the distal convoluted tubule and the connecting ducts, THP (red) as a marker of the proximal tubules, and DAPI (blue) as a nuclear marker. **C**, The renal localization of NPY (red) and the colocalization of NPY with SOCS-3 (green) was assessed by immunofluorescence. Colocalization of NPY (green) with 11 β HSD (red) and THP (red) and DAPI (blue) as a nuclear marker are illustrated. SOCS-3 (green) and NPY (red) colocalization is illustrated below.

genes, such as *TIMP-1* and *TIMP-2* (46, 47), and antiinflammatory cytokines such as *IL-10* (48) are up-regulated through leptin signaling, whereas the sympathetic neurotransmitter *NPY* is inhibited (28, 29). We report in our study a decreased expression of genes encoding *IL-10*, *TIMP-1*, and *TIMP-2* and an increased expression of *NPY* after pHA. These findings are consistent with reduced phosphorylation of Stat3 and Erk1/2 observed subsequent to pHA. Thus, increased *NPY* expression and the impaired Stat3 and Erk1/2 signaling display a peripheral leptin resistance subsequent to pHA. In addition to regulatory function regarding energy homeostasis, *NPY* has direct proinflammatory and renal tubular function affecting natriuresis and kaliuresis via *NPY* receptors Y1 and Y2 (30, 31). Thus, *NPY* and the neuroimmune interaction might enhance the inflammatory response after early pHA and contribute to the obesity-related nephropathy. The question arose as to how an increased renal *NPY* expression exerts greater inflammatory effect via a decreased expression Y1 receptor. Sympathetic nerve system activation results in the release of *NPY* concomitantly with catecholamines. *NPY* as a sympathetic neurotransmitter exerts its inflammatory effects mainly via Y1 receptor, which is present on the surface of inflammatory cells, particularly macrophages and granulocytes (31, 49, 50). Therefore, the inflammatory action of *NPY* may not be mediated by renal Y1 receptors but by granulocytes and/or macrophages and thereby secondary exert inflammatory response on renal tissue. Furthermore, *NPY* has inhibitory effect on renin release (51) and also secondary on the renin-angiotensin-aldosterone system (RAAS). We already demonstrated dysregulation of the RAAS and especially a down-regulation of angiotensin receptor II in kidney subsequent to early pHA (30). In line with this, the regulatory effect of *NPY* on RAAS and SNS may be a potential cause of the slight hypotensive phenotype sub-

sequent to pHA at P70. Further studies are necessary to elucidate in detail the short- and long-term effect of early pHA on blood pressure.

Hyperalimentation is known to induce leptin resistance subsequent to hyperleptinemia. But how could intrinsic renal leptin resistance be mediated without systemic hyperleptinemia and an underlying metabolic syndrome? There is also controversially discussed obesity-induced leptin-independent leptin resistance (52): 1) endoplasmic reticulum stress-associated leptin resistance (53) and 2) inflammation (IL-6) and therefore postreceptor-mediated leptin resistance (27, 45). SOCS-3 is an inhibitor of Stat3 and Erk1/2 phosphorylation and is thought to be causal for postreceptor leptin resistance (27). This is the first study to our knowledge so far addressing the renal expression of SOCS-3. SOCS-3 is strikingly up-regulated subsequent to pHA. Interestingly, we did not detect SOCS-3 in the glomeruli. Hence, in the glomeruli, leptin can exert its glomerular proliferative effect. Rodrigues *et al.* (28) support our findings demonstrating that pHA leads to a higher SOCS-3 expression in the hypothalamus. Regarding its functional role, however, Gomez-Guerrero and colleagues (54) gave evidence that SOCS-3 improves renal function in diabetic rodents and reduces renal lesions in an animal model of diabetic nephropathy. In contrast to our study, interestingly, SOCS-3 was localized not only in the interstitial compartment of diabetic kidneys but also in the glomeruli. These facts indicate that the underlying pathomechanism of hyperglycemia induced renal damage is different from the mechanism investigated in our study subsequent to pHA.

Injury to the developing and maturing kidney, like obesity and early pHA, may disrupt critical signaling pathways that regulate cell proliferation, ECM composition, and renal function. There are numerous underlying mechanisms discussed: 1) cytokines (IL-6, PAI-1) secreted by adipose tissue or other organs directly induce renal cell proliferation and fibrotic processes; 2) hyperleptinemia due to obesity and pHA stimulate sympathetic activity and thereby contributes to renal damage; and 3) hyperleptinemia-independent intrinsic renal leptin resistance leads to increased expression of NPY and altered expression of ECM-metabolizing enzyme and ECM components, and enhances proinflammatory processes. In the context of increased sympathetic activity subsequent to pHA, it is noteworthy that pHA increases the expression of renin (30). In line with this, we observed in our study a down-regulation of adrenoceptors- α 1a and - α 1d after early pHA, whereas adrenoceptor- β 1 and - β 2 were significantly up-regulated, indicating a regulation of the sympathetic system after pHA. However, because we have not

focused on the regulation of the sympathetic nerve system in this study, this idea requires further investigation.

In conclusion, early pHA contributes to impaired renal function in later life. This study presents evidence for a role of SOCS-3 in mediating postreceptor leptin resistance and subsequent regulation of sympathetic activity (NPY) and inflammatory response in the underlying pathomechanism of pHA-induced nephropathy. A more profound understanding of the underlying mechanistic aspects of early postnatal hyperalimentation will ultimately allow defining more effective preventional and therapeutic strategies of nephropathy in childhood and beyond.

Acknowledgments

The authors gratefully acknowledge the expert technical assistance of Ida Allabauer, Miriam Reutelshöfer, and Julia Dobner.

Address all correspondence and requests for reprints to: Miguel Angel Alejandro Alcázar, Department of Pediatrics, University of Cologne, Kerpener Strasse 62, D-50937 Cologne, Germany. E-mail: miguel.alejandre-alcazar@uk-koeln.de.

The animal experiments were supported by a grant from the Deutsche Forschungsgemeinschaft, Bonn, Germany (to J.D., C.P., and K.A.); Grant SFB 423, Collaborative Research Centre of the German Research Foundation: Kidney Injury: Pathogenesis and Regenerative Mechanisms, Project B13 and Z2.

Disclosure Summary: All authors declare that there is no conflict of interest concerning this study.

References

1. Zoccali C, Mallamaci F 2011 Adiponectin and leptin in chronic kidney disease: causal factors or mere risk markers? *J Ren Nutr* 21:87–91
2. Wang Y, Chen X, Klag MJ, Caballero B 2006 Epidemic of childhood obesity: implications for kidney disease. *Adv Chronic Kidney Dis* 13:336–351
3. Adelman RD 2002 Obesity and renal disease. *Curr Opin Nephrol Hypertens* 11:331–335
4. Cleal JK, Poore KR, Boullin JP, Khan O, Chau R, Hambidge O, Torrens C, Newman JP, Poston L, Noakes DE, Hanson MA, Green LR 2007 Mismatched pre- and postnatal nutrition leads to cardiovascular dysfunction and altered renal function in adulthood. *Proc Natl Acad Sci USA* 104:9529–9533
5. Coresh J, Selvin E, Stevens LA, Manzi J, Kusek JW, Eggers P, Van Lente F, Levey AS 2007 Prevalence of chronic kidney disease in the United States. *JAMA* 298:2038–2047
6. Hall JE, Crook ED, Jones DW, Wofford MR, Dubbert PM 2002 Mechanisms of obesity-associated cardiovascular and renal disease. *Am J Med Sci* 324:127–137
7. Savino A, Pelliccia P, Chiarelli F, Mohn A 2010 Obesity-related renal injury in childhood. *Horm Res Paediatr* 73:303–311
8. Zoccali C, Mallamaci F 2011 Does adipose tissue have a key role in inflammation in CKD? *J Intern Med* 269:407–409
9. Barker DJ 1995 Intrauterine programming of adult disease. *Mol Med Today* 1:418–423

10. Plagemann A 2005 Perinatal programming and functional teratogenesis: impact on body weight regulation and obesity. *Physiol Behav* 86:661–668
11. Simmons RA 2007 Role of metabolic programming in the pathogenesis of β -cell failure in postnatal life. *Rev Endocr Metab Disord* 8:95–104
12. Boubred F, Buffat C, Feuerstein JM, Daniel L, Tsimaratos M, Oliver C, Lelièvre-Pégorier M, Simeoni U 2007 Effects of early postnatal hypernutrition on nephron number and long-term renal function and structure in rats. *Am J Physiol Renal Physiol* 293:F1944–F1949
13. Boubred F, Daniel L, Buffat C, Feuerstein JM, Tsimaratos M, Oliver C, Dignat-George F, Lelièvre-Pégorier M, Simeoni U 2009 Early postnatal overfeeding induces early chronic renal dysfunction in adult male rats. *Am J Physiol Renal Physiol* 297:F943–F951
14. Gubhaju L, Sutherland MR, Black MJ 2011 Preterm birth and the kidney: implications for long-term renal health. *Reprod Sci* 18:322–333
15. Gharraee-Kermani M, Phan SH 2005 Molecular mechanisms of and possible treatment strategies for idiopathic pulmonary fibrosis. *Curr Pharm Des* 11:3943–3971
16. Plagemann A, Heidrich I, Götz F, Rohde W, Dörner G 1992 Obesity and enhanced diabetes and cardiovascular risk in adult rats due to early postnatal overfeeding. *Exp Clin Endocrinol* 99:154–158
17. Wolf G, Chen S, Han DC, Ziyadeh FN 2002 Leptin and renal disease. *Am J Kidney Dis* 39:1–11
18. Meissner U, Hänisch C, Ostreicher I, Knerr I, Hofbauer KH, Blum WF, Allabauer I, Rascher W, Dötsch J 2005 Differential regulation of leptin synthesis in rats during short-term hypoxia and short-term carbon monoxide inhalation. *Endocrinology* 146:215–220
19. Alejandro-Alcázar MA, Kwapiszewska G, Reiss I, Amarie OV, Marsh LM, Sevilla-Pérez J, Wygrecka M, Eul B, Köbrich S, Hesse M, Schermuly RT, Seeger W, Eickelberg O, Morty RE 2007 Hyperoxia modulates TGF- β /BMP signaling in a mouse model of bronchopulmonary dysplasia. *Am J Physiol Lung Cell Mol Physiol* 292:L537–L549
20. Wolf G, Hamann A, Han DC, Helmchen U, Thaïss F, Ziyadeh FN, Stahl RA 1999 Leptin stimulates proliferation and TGF- β expression in renal glomerular endothelial cells: potential role in glomerulosclerosis. *Kidney Int* 56:860–872
21. Aizawa-Abe M, Ogawa Y, Masuzaki H, Ebihara K, Satoh N, Iwai H, Matsuoka N, Hayashi T, Hosoda K, Inoue G, Yoshimasa Y, Nakao K 2000 Pathophysiological role of leptin in obesity-related hypertension. *J Clin Invest* 105:1243–1252
22. Haynes WG, Sivitz WI, Morgan DA, Walsh SA, Mark AL 1997 Sympathetic and cardiorenal actions of leptin. *Hypertension* 30:619–623
23. Han DC, Isono M, Chen S, Casaretto A, Hong SW, Wolf G, Ziyadeh FN 2001 Leptin stimulates type I collagen production in db/db mesangial cells: glucose uptake and TGF- β type II receptor expression. *Kidney Int* 59:1315–1323
24. Wolf G, Ziyadeh FN 2006 Leptin and renal fibrosis. *Contrib Nephrol* 151:175–183
25. Auwerx J, Staels B 1998 Leptin. *Lancet* 351:737–742
26. Myers MG, Cowley MA, Münzberg H 2008 Mechanisms of leptin action and leptin resistance. *Annu Rev Physiol* 70:537–556
27. Lubis AR, Widia F, Soegondo S, Setiawati A 2008 The role of SOCS-3 protein in leptin resistance and obesity. *Acta Med Indones* 40:89–95
28. Rodrigues AL, de Moura EG, Passos MC, Trevenzoli IH, da Conceição EP, Bonono IT, Neto JF, Lisboa PC 2011 Postnatal early overfeeding induces hypothalamic higher SOCS3 expression and lower STAT3 activity in adult rats. *J Nutr Biochem* 22:109–117
29. Bates SH, Stearns WH, Dundon TA, Schubert M, Tso AW, Wang Y, Banks AS, Lavery HJ, Haq AK, Maratos-Flier E, Neel BG, Schwartz MW, Myers Jr MG 2003 STAT3 signalling is required for leptin regulation of energy balance but not reproduction. *Nature* 421:856–859
30. Alejandro Alcázar MA, Boehler E, Amann K, Klaffenbach D, Hartner A, Allabauer I, Wagner L, von Hörsten S, Plank C, Dötsch J 2011 Persistent changes within the intrinsic kidney-associated NPY system and tubular function by litter size reduction. *Nephrol Dial Transplant* 26:2453–2465
31. Straub RH, Schaller T, Müller LE, von Hörsten S, Jessop DS, Falk W, Schölmerich J 2000 Neuropeptide Y cotransmission with norepinephrine in the sympathetic nerve-macrophage interplay. *J Neurochem* 75:2464–2471
32. Glavas MM, Kirigiti MA, Xiao XQ, Enriori PJ, Fisher SK, Evans AE, Grayson BE, Cowley MA, Smith MS, Grove KL 2010 Early overnutrition results in early-onset arcuate leptin resistance and increased sensitivity to high-fat diet. *Endocrinology* 151:1598–1610
33. Plank C, Nüsken KD, Menendez-Castro C, Hartner A, Ostreicher I, Amann K, Baumann P, Peters H, Rascher W, Dötsch J 2010 Intrauterine growth restriction following ligation of the uterine arteries leads to more severe glomerulosclerosis after mesangioproliferative glomerulonephritis in the offspring. *Am J Nephrol* 32:287–295
34. Ostreicher I, Meissner U, Plank C, Allabauer I, Castrop H, Rascher W, Dötsch J 2009 Altered leptin secretion in hyperinsulinemic mice under hypoxic conditions. *Regul Pept* 153:25–29
35. Amann K, Rump LC, Simonaviciene A, Oberhauser V, Wessels S, Orth SR, Gross ML, Koch A, Bielenberg GW, Van Kats JP, Ehmke H, Mall G, Ritz E 2000 Effects of low dose sympathetic inhibition on glomerulosclerosis and albuminuria in subtotal nephrectomized rats. *J Am Soc Nephrol* 11:1469–1478
36. Neuman G, Sagi R, Shalitin S, Reif S 2010 Serum inflammatory markers in overweight children and adolescents with non-alcoholic fatty liver disease. *Isr Med Assoc J* 12:410–415
37. Teplan Jr V, Vyhnanek F, Gürllich R, Haluzik M, Racek J, Vyhnankova I, Stollóv á M, Teplan V 2010 Increased proinflammatory cytokine production in adipose tissue of obese patients with chronic kidney disease. *Wien Klin Wochenschr* 122:466–473
38. Kasiske BL, Crosson JT 1986 Renal disease in patients with massive obesity. *Arch Intern Med* 146:1105–1109
39. Adelman RD, Restaino IG, Alon US, Blowey DL 2001 Proteinuria and focal segmental glomerulosclerosis in severely obese adolescents. *J Pediatr* 138:481–485
40. Henegar JR, Bigler SA, Henegar LK, Tyagi SC, Hall JE 2001 Functional and structural changes in the kidney in the early stages of obesity. *J Am Soc Nephrol* 12:1211–1217
41. Morales E, Valero MA, León M, Hernández E, Praga M 2003 Beneficial effects of weight loss in overweight patients with chronic proteinuric nephropathies. *Am J Kidney Dis* 41:319–327
42. Velkoska E, Cole TJ, Morris MJ 2005 Early dietary intervention: long-term effects on blood pressure, brain neuropeptide Y, and adiposity markers. *Am J Physiol Endocrinol Metab* 288:E1236–E1243
43. Fernández-Riejos P, Najib S, Santos-Alvarez J, Martín-Romero C, Pérez-Pérez A, González-Yanes C, Sánchez-Margalet V 2010 Role of leptin in the activation of immune cells. *Mediators Inflamm* 2010:568343
44. Eder K, Baffy N, Falus A, Fulop AK 2009 The major inflammatory mediator interleukin-6 and obesity. *Inflamm Res* 58:727–736
45. Galic S, Oakhill JS, Steinberg GR 2010 Adipose tissue as an endocrine organ. *Mol Cell Endocrinol* 316:129–139
46. Lin S, Saxena NK, Ding X, Stein LL, Anania FA 2006 Leptin increases tissue inhibitor of metalloproteinase I (TIMP-1) gene expression by a specificity protein 1/signal transducer and activator of transcription 3 mechanism. *Mol Endocrinol* 20:3376–3388
47. Nakamura K, Nonaka H, Saito H, Tanaka M, Miyajima A 2004 Hepatocyte proliferation and tissue remodeling is impaired after liver injury in oncostatin M receptor knockout mice. *Hepatology* 39:635–644
48. Braunschweig A, Poehlmann TG, Busch S, Schleussner E, Markert UR 2011 Signal transducer and activator of transcription 3 (STAT3) and suppressor of cytokine signaling (SOCS3) balance controls cy-

- toxicity and IL-10 expression in decidual-like natural killer cell line NK-92. *Am J Reprod Immunol* 66:329–335
49. Dimitrijević M, Stanojević S, Mičić S, Vujić V, Kovacević-Jovanović V, Mitić K, von Hörsten S, Kosec D 2006 Neuropeptide Y (NPY) modulates oxidative burst and nitric oxide production in carrageenan-elicited granulocytes from rat air pouch. *Peptides* 27:3208–3215
50. Bedoui S, Lechner S, Gebhardt T, Nave H, Beck-Sickingler AG, Straub RH, Pabst R, von Hörsten S 2002 NPY modulates epinephrine-induced leukocytosis via Y-1 and Y-5 receptor activation *in vivo*: sympathetic co-transmission during leukocyte mobilization. *J Neuroimmunol* 132:25–33
51. Aubert JF, Walker P, Grouzmann E, Nussberger J, Brunner HR, Waeber B 1992 Inhibitory effect of neuropeptide Y on stimulated renin secretion of awake rats. *Clin Exp Pharmacol Physiol* 19:223–228
52. White CL, Whittington A, Barnes MJ, Wang Z, Bray GA, Morrison CD 2009 HF diets increase hypothalamic PTP1B and induce leptin resistance through both leptin-dependent and -independent mechanisms. *Am J Physiol Endocrinol Metab* 296:E291–E299
53. Ozcan L, Ergin AS, Lu A, Chung J, Sarkar S, Nie D, Myers Jr MG, Ozcan U 2009 Endoplasmic reticulum stress plays a central role in development of leptin resistance. *Cell Metab* 9:35–51
54. Ortiz-Muñoz G, Lopez-Parra V, Lopez-Franco O, Fernandez-Vizcarra P, Mallavia B, Flores C, Sanz A, Blanco J, Mezzano S, Ortiz A, Egidio J, Gomez-Guerrero C 2010 Suppressors of cytokine signaling abrogate diabetic nephropathy. *J Am Soc Nephrol* 21:763–772



Join The Endocrine Society and network with
endocrine thought leaders from around the world.

www.endo-society.org/join

Hypothalamic JNK1 and IKK β Activation and Impaired Early Postnatal Glucose Metabolism after Maternal Perinatal High-Fat Feeding

Eva Rother, Ruth Kuschewski, Miguel Angel Alejandro Alcazar, André Oberthuer, Inga Bae-Gartz, Christina Vohlen, Bernhard Roth, and Jörg Dötsch

Department of Pediatrics, University Hospital of Cologne, 50924 Cologne, Germany

Hypothalamic inflammation has been demonstrated to be an important mechanism in the pathogenesis of obesity-induced type 2 diabetes mellitus. Feeding pregnant and lactating rodents a diet rich in saturated fatty acids has consistently been shown to predispose the offspring for the development of obesity and impaired glucose metabolism. However, hypothalamic inflammation in the offspring has not been addressed as a potential underlying mechanism. In this study, virgin female C57BL/6 mice received high-fat feeding starting at conception until weaning of the offspring at postnatal d 21. The offspring developed increased body weight, body fat content, and serum leptin concentrations during the nursing period. Analysis of hypothalamic tissue of the offspring at postnatal d 21 showed up-regulation of several members of the toll-like receptor 4 signaling cascade and subsequent activation of c-Jun N-terminal kinase 1 and I κ B kinase- β inflammatory pathways. Interestingly, glucose tolerance testing in the offspring revealed signs of impaired glucose tolerance along with increased hepatic expression of the key gluconeogenic enzyme phosphoenolpyruvate carboxykinase. In addition, significantly increased hepatic and pancreatic *PGC1 α* expression suggests a role for sympathetic innervation in mediating the effects of hypothalamic inflammation to the periphery. Taken together, our data indicate an important role for hypothalamic inflammation in the early pathogenesis of glucose intolerance after maternal perinatal high-fat feeding. (*Endocrinology* 153: 770–781, 2012)

In diet-induced obesity, the hypothalamus has been shown to become dysfunctional due to the development of inflammation. Important mediators of this inflammatory response include saturated fatty acids (stearic acid) and several cytokines, including TNF α and IL-6 (1–4). Hypothalamic inflammation subsequently leads to central resistance to fuel-sensing hormones (*i.e.* leptin and insulin) and loss of the homeostatic control of food intake and energy expenditure (5–8). In detail, hypothalamic inflammation mediated by TNF α directly attenuates the anorexigenic effect of leptin with a notable reduction in local leptin signaling and an increase in *SOCS3* expression (3). Additionally, hypothalamic TNF α action has been shown to have functional impact on several peripheral organs: centrally applied TNF α reduces the expression of thermo-

genic proteins in brown adipose tissue and skeletal muscle and impairs insulin secretion in isolated pancreatic islets (3, 9). Consistently, these effects are blunted in TNF α receptor knockout mice (3, 10). In addition, Calegari *et al.* (4) could demonstrate that intracerebroventricular injection of either saturated fatty acids or low doses of TNF α leads to dysfunctional insulin secretion and activates the expression of a number of markers of apoptosis in pancreatic islets via activation of the toll-like receptor 4 (TLR4) signaling cascade. Thus, fatty acid-induced hypothalamic inflammation and the resulting central and peripheral consequences represent a crucial pathomechanism for the development of obesity and type 2 diabetes.

Increasing evidence from human and animal studies supports the idea that maternal consumption of a high-fat

ISSN Print 0013-7227 ISSN Online 1945-7170
Printed in U.S.A.

Copyright © 2012 by The Endocrine Society
doi: 10.1210/en.2011-1589 Received August 5, 2011. Accepted November 11, 2011.
First Published Online December 6, 2011

For editorial see page 543

Abbreviations: FOXO1, Forkhead box protein 1; G6, gestational d 6; HFD, high-fat diet; IKK α/β , I κ B kinase- α/β ; ipGTT, ip glucose tolerance test; pSAPK/JNK, stress-activated protein kinase/c-Jun N-terminal kinase; P21, postnatal d 21; PEPCCK, phosphoenolpyruvate carboxykinase; PGC1 α , peroxisome proliferator-activated receptor γ coactivator 1- α ; qPCR, quantitative PCR; TLR4, toll-like receptor 4.

diet (HFD) during early fetal life puts the offspring at a lifelong risk for obesity and related negative metabolic outcomes (*i.e.* type 2 diabetes mellitus) (11–15). It is conceivable that the fetal and neonatal hypothalamus acts as an important target for maternal nutritional and hormonal cues during gestation and lactation. However, the underlying molecular mechanisms remain unclear to date. Several reports document deregulated expression of hypothalamic neuropeptides and hormone receptors involved in homeostatic control in newborn and adult rats after maternal perinatal HFD feeding (16, 17). In addition, chronic maternal high-fat feeding has been shown to induce changes in hypothalamic melanocortin expression and IL-1 β signaling in the offspring of nonhuman primates (18). This is further supported by observations in other brain regions that document increased IL-1 β , IL-6, and TLR4 expression in the offspring of obese rat dams, which is associated with changes in anxiety and spatial learning in adulthood (15, 19). Thus, it is clear that maternal constitution and dietary choice has profound influence on innate immune response within the brain of the offspring with subsequent lifelong functional consequences. Data on hypothalamic inflammation in the offspring after maternal HFD feeding are sparse. Therefore, this study aimed to 1) determine the potential hypothalamic inflammatory response in the offspring at postnatal d 21 (P21) as a consequence of increased maternal dietary fat intake throughout gestation and lactation, 2) elucidate which intracellular signaling pathways are involved, and 3) investigate the timely order of onset of central and peripheral inflammation in relation to the metabolic phenotype.

Materials and Methods

Animals

All animal procedures were conducted in compliance with protocols approved by local government authorities (Bezirksregierung Köln) and were in accordance with National Institutes of Health guidelines. Mice (C57BL/6) were bred locally at a designated animal unit of the University Hospital of Cologne (Cologne, Germany). Virgin female mice were housed individually and were maintained at 22 C on a 12-h light, 12-h dark cycle. They were mated at 10 wk of age (~22 g in body weight) and assumed to be pregnant when a vaginal plug was expelled. Immediately after detection of vaginal plugging, dams were fed *ad libitum* either a standard laboratory chow (no. 1310; Altromin, Lage, Germany) containing 40% carbohydrates, 22.5% protein, and 5.0% fat (13% of calories from fat) or a high-fat-containing diet (HFD) (no. C1057) containing 26.9% carbohydrates, 21% protein, and 35.1% fat (55.2% of calories from fat). Water was available *ad libitum*, and food was withdrawn only if required for an experiment. Body weight of the pups was monitored daily starting immediately after birth (P1). On P3, litter size was adjusted to six for each litter. Smaller litters were ex-

cluded from the experiment. On P21, the dams underwent an ip glucose tolerance test (ipGTT) and were subsequently killed. In a subset of male pups ($n = 6$ –12 per group, five to 10 distinct litters), ipGTT was performed at P21. These animals were excluded from further organ analysis. The remaining male pups were killed on P21. The hypothalamus was dissected as previously described (20), and samples of liver and pancreatic tissue were taken out and immediately frozen at -80 C for further analysis. Both epigonadal fat pads were dissected, and their weight was determined.

Body weight measurement

Body weight in dams was monitored on gestational d 6 (G6), G12, and G18 and P1 and P21. Male pups were weighed daily between P1 and P21.

Analytical procedures

Blood glucose values were determined from whole venous blood using an automatic glucose monitor (GlucoMen; A. Menarini Diagnostics, Berlin, Germany). Random fed blood glucose levels were measured 2–3 h after beginning of the light phase with free access to food/lactating dam. Serum leptin and insulin were measured by ELISA using mouse standards according to the manufacturer's guidelines [mouse leptin ELISA (EZML-82K) with a sensitivity of 0.05 ng/ml and intraassay variation of 8.35% and mouse insulin ELISA (EZRMI-13K) with a sensitivity of 0.01 ng/ml and intraassay variation of 1.06%; Millipore Corp., Billerica, MA].

Intraperitoneal glucose tolerance test

Glucose tolerance tests were performed as previously described (21). Briefly, animals were fasted overnight (16–17 h). After determination of fasted blood glucose levels, each animal received an ip injection of 20% glucose (10 ml/kg body weight = 2 g glucose/kg body weight). Blood glucose levels were measured after 15, 30, 60, and 120 min.

Insulin signaling

Mice were anesthetized by ip injection of a mixture of midazolam (5 mg/kg) and ketamine (100 mg/kg), and adequacy of the anesthesia was ensured by loss of pedal reflexes. The abdominal cavity of the mice was opened, and 125- μ l samples containing 5 U regular human insulin (Actrapid; Novo Nordisk Pharma GmbH, Mainz, Germany) diluted in 0.9% saline were injected into the inferior vena cava. Sham injections were performed with 125 μ l of 0.9% saline. Livers and hypothalami were harvested 5 min after injection, and proteins were extracted from tissues for Western blot analysis.

RNA isolation and microarray analyses

Total RNA was isolated from dissected hypothalamic, pancreatic, and liver tissue as previously described (22), followed by deoxyribonuclease treatment to remove any contaminating genomic DNA. Microarray experiments of mice hypothalamic RNA were performed as single-color experiments using 4 \times 44K Mouse (v2) Whole Genome Arrays from Agilent Technologies (Santa Clara, CA). For each sample, 1 μ g total RNA was linearly amplified and transcribed to Cy3-labeled cRNA using the Low Input Quick Amp Labeling Kit and hybridized to the array using the Gene Expression Hybridization Kit (both from Agilent Tech-

nologies) according to the manufacturer's protocol. After washing and scanning, microarray raw data were extracted using Agilent's Feature Extraction Software (version 10.8). Principal component analysis and hierarchical cluster analysis were performed using the Rosetta Resolver software version 7.2 (Rosetta Inpharmatics LCC, Seattle, WA). For hierarchical cluster analysis, gene expression values were transformed to Z-scores, and cosine correlation and average linkage were used as metric and heuristic criteria, respectively.

mRNA quantification by quantitative PCR (qPCR)

Total RNA was screened for mRNA encoding TLR4, myeloid differentiation primary response gene 88 (*MyD88*), IL-1 receptor-associated kinase 1 (*IRAK1*), TNF receptor-associated factor 6 (*Traf6*), TNF α , IL-6, proopiomelanocortin (*POMC*), cocaine and amphetamine regulated transcript (*CART*), agouti-related peptide (*AgRP*), neuropeptide Y (*NPY*), orexin, TRH, phosphoenolpyruvate carboxykinase (*PEPCK*), forkhead box protein 1 (*FOXO1*), peroxisome proliferator-activated receptor γ coactivator 1- α (*PGC1 α*). Quantitative changes in mRNA expression were assessed by quantitative real-time PCR as described previously using the IQ TM SYBR-Green Supermix and a Bio-Rad iQ5-Cycler (Bio-Rad Laboratories, Hercules, CA) or the 7500 real-time PCR system (Applied Biosystems, Foster City, CA) (22). In all samples, the relative amount of specific mRNA was normalized to the ubiquitously expressed β -actin gene. Oligonucleotides were designed with Primer Express software (PerkinElmer, Foster City, CA). Primer pairs and TaqMan probes are listed in Table 1.

Western blotting

Frozen dissected hypothalamic, pancreatic, and liver tissue was homogenized in lysis buffer as previously described (24). Protein concentration was determined with a Bio-Rad DC protein assay (Bio-Rad). Lysates resolved on a 10% reducing SDS-PAGE gel were transferred to a nitrocellulose membrane. Blots were probed with the following antibodies: monoclonal rabbit antimouse phospho-I κ B kinase- α/β (IKK α/β) (Cell Signaling, Danvers, MA; no. 3101, 1:1000), monoclonal rabbit antimouse phospho-Akt (Cell Signaling; no. 4058, 1:1000), polyclonal rabbit antimouse phospho-stress-activated protein kinase/c-Jun N-terminal kinase (pSAPK/JNK) (Thr183/Tyr185) (Cell Signaling; no. 9251), monoclonal rabbit antimouse IKK β (Cell Signaling; no. 2370, 1:1000), polyclonal rabbit antimouse Akt (Cell Signaling; no. 9272, 1:1000), polyclonal rabbit antimouse SAPK/JNK (Cell Signaling; no. 9252, 1:2000). Monoclonal mouse antimouse β -actin (Cell Signaling; no. 3700, 1:1000) served as a loading control. Antimouse IgG, horseradish peroxidase-linked (Cell Signaling; no. 7076, 1:2000), and horseradish peroxidase-linked antirabbit IgG (Cell Signaling; no. 7074, 1:2000) were used as secondary antibodies.

Analysis of data

The results of real-time RT-PCR were calculated based on the delta-deltaCt method and expressed as fold induction of mRNA expression compared with the corresponding control group (1.0-fold induction). Densitometric analysis of protein bands was performed using Bio-Rad ImageLab software (Bio-Rad, Munich, Germany). Band intensities were normalized to the β -actin band. Values are shown as means \pm SEM. Two tailed Mann-Whitney U

test and one-way ANOVA followed by a Dunn's *post hoc* test was used to test significance of differences between HFD and control animals at given time points. Over time, ANOVA was used to test significance of body weight changes and blood glucose levels during glucose tolerance testing. A *P* value <0.05 was considered significant.

Results

To investigate the effects of increased maternal dietary fat intake on the offspring, we characterized the experimental (HFD) and control dams throughout pregnancy and lactation. Litter size and pregnancy length did not differ between both groups (data not shown). Maternal body weight gain was monitored throughout the experiment and revealed no significant difference between control and HFD dams at either time point (Fig. 1A). Moreover, random fed blood glucose levels were measured on G6 and G12. There was no difference in random fed blood glucose levels between normal chow- and HFD-fed dams at either time point (Fig. 1B). To evaluate whether HFD dams developed impaired glucose tolerance over the 6-wk period of HFD feeding (conception until weaning), we performed ipGTT in the dams at the end of lactation (P21). However, there was no detectable difference in plasma glucose clearance between HFD and control dams (Fig. 1C). Taken together, HFD dams presented no alterations in the assessed parameters of energy and glucose homeostasis throughout pregnancy and lactation.

Next, offspring of both HFD and control dams were metabolically characterized. Interestingly, offspring of HFD dams was significantly lighter than control offspring at the day of birth but gained weight more rapidly throughout the first 2 wk of lactation resulting in a significantly increased body weight from P16 onward (*P* < 0.01 on P16, *P* < 0.001 on P17, and *P* = 0.0001 from P18–P21) (Fig. 2A). The increased body weight in HFD offspring was accompanied by significantly increased white adipose tissue mass at P21 represented by a 2-fold increase in weight of epigonadal fat pad (*P* = 0.009) (Fig. 2B). Along with increased fat mass, serum leptin levels at P21 were significantly elevated in HFD offspring compared with controls (*P* = 0.004) (Fig. 2C).

To assess the effects of maternal high-fat feeding during pregnancy and lactation on parameters of glucose homeostasis, we first determined random fed and fasting blood glucose levels. Random fed blood glucose levels were slightly increased in HFD offspring at P15 (*P* = 0.036) (Fig. 2D). However, fasting blood glucose levels as well as serum insulin levels at P21 were comparable between both groups (data not shown). Strikingly, glucose tolerance testing at P21 revealed significantly increased plasma glu-

TABLE 1. Primer pairs and TaqMan probes

Gene	Sequence (5'–3')
<i>β</i> -Actin	
Forward	TGACAGGATGCAGAAGGAGATTACT
Reverse	GCCACCGATCCACACAGAGT
Probe	(FAM)–ATCAAGATCATTGCTCCTCCTGAGCGC– (TAMRA)
<i>TNFα</i>	
Forward	GGCTGCCCGACTACGT
Reverse	GACTTTCCTGGTATGAGATAGCAA
Probe	(FAM)–CCTCACCCACACCGTCAGCCG– (TAMRA)
<i>IL-6^a</i>	
Forward	ACAAAGCCAGAGTCCTTCAGAGA
Reverse	CCTTCTGTGACTCCAGCTTATCTGT
<i>TLR4</i>	
Forward	GGTGAGAAATGAGCTGGTAAAGAATT
Reverse	GCAATGGCTACACCAGGAATAAA
Probe	(FAM)–TGCCCCGCTTTCACCTCTGCC– (TAMRA)
<i>MyD88</i>	
Forward	TGGCCATCTGCCTAGTAAAGCT
Reverse	CAGTAGCAGATAAAGGCATCGAAAA
Probe	(FAM)–TTGATGACCCCTTAGGACAAAACGCC– (TAMRA)
<i>IRAK1</i>	
Forward	TAGCTTGCTGCTGCATGCA
Reverse	CCTGCCTGAAGCCCTTCTAGT
Probe	(FAM)–AGAGGCCCCCATGACCCAGGTATAC– (TAMRA)
<i>TRAF6</i>	
Forward	ATCTCGAGGATCATCAAGTACATTGT
Reverse	TGTGTGTATTAACCTGGCACTTCTG
Probe	(FAM)–TTGTCCCCAGTGCCAACGTCCTTT– (TAMRA)
<i>AgRP</i>	
Forward	GAAGAAGCTCAAGAGTAAACGCATT
Reverse	GGAGCCACGCCCATCTG
Probe	(FAM)–TTGGCACTGCCTCCCACACTGG– (TAMRA)
<i>NPY</i>	
Forward	AGCAGAGGACATGGCCAGATAC
Reverse	TGAAATCAGTGTCACAGGGCTG
Probe	(FAM)–GTAAACCTTCGATTCCGACCTC– (TAMRA)
Orexin	
Forward	GCGCAGAGCTAGAGCCACAT
Reverse	TGCTAAAGCGGTGGTAGTTACG
Probe	(FAM)–CTGCTCTGGTCGCGGCTGTCC– (TAMRA)
<i>POMC</i>	
Forward	GACACGTGGAAGATGCCGAG
Reverse	CAGCGAGAGGTCGAGTTTGC
Probe	(FAM)–CAACCTGCTGGCTTGCATCCGG– (TAMRA)
<i>CART</i>	
Forward	GAAGAAGCTCAAGAGTAAACGCATT
Reverse	CCGATCCTGGCCCCTTT
Probe	(FAM)–CTACGAGAAGAAGTACGGCCAAGTCCCC– (TAMRA)
<i>TRH</i>	
Forward	GGATGGAGTCTGATGTCACCAA
Reverse	TCTGTTTCTTCCCAGCTTCTTTG
Probe	(FAM)–ATGGAAGTCAGAGGATGC– (TAMRA)
<i>PGC1α</i>	
Forward	TGAAAAAAGAAGTCCCATAACACAA
Reverse	TTCCACACTTAAGGTTTCGCTCAATA
Probe	(FAM)–CACCAATGACCCCAAGGGTTCCC– (TAMRA)
<i>FOXO1^a</i>	
Forward	CAATGGCTATGGTAGGATGG
Reverse	TTTAAATGTAGCCTGCTCAC
<i>PEPCK</i>	
Forward	CCACAGCTGCTGCAGAACAC
Reverse	GAAGGTCGCATGGCAAA
Probe	(FAM)–AGGGCAAGATCATCATGCACGACCC– (TAMRA)

^a *IL-6* and *FOXO1* were measured by the SYBR-Green method. No probe was needed.

cose levels 15 and 30 min after ip glucose administration in HFD offspring when compared with controls ($P < 0.001$ and $P < 0.0001$) (Fig. 2E).

To investigate central processes that might possibly contribute to the metabolic phenotype at P21, we next performed genome-wide gene expression arrays with hy-

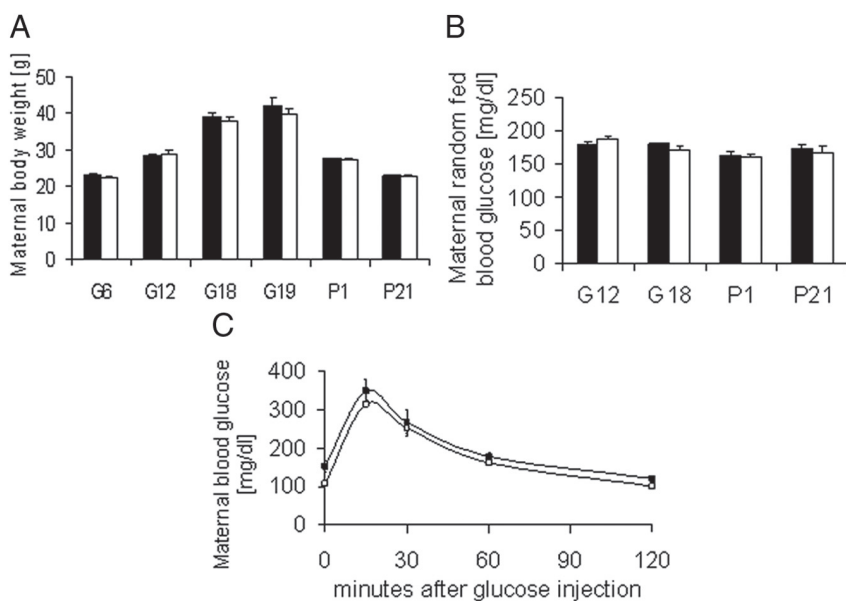


FIG. 1. A, Maternal mean body weight (\pm SEM) in control (black bars) and HFD (white bars) dams during pregnancy (G6, G12, G18, and G19) and lactation (P1 and P21). B, Random fed blood glucose levels in control (black bars) and HFD (white bars) on G12 and G18 and on P1 and P21. C, ipGTT in control (■) and HFD (□) dams at P21. Per group, $n = 8$; G, gestational day.

pothalamic tissue of HFD and control offspring at P21. Intriguingly, unsupervised principal component analysis revealed that global gene expression information differed markedly between the two cohorts, suggesting profound maternal diet-induced changes in the gene expression pattern in the hypothalami of HFD offspring (Fig. 3A). For analysis of selected candidate genes associated with inflammation, expression information of a panel of 41 genes was extracted from whole-genome microarray expression profiles. Expression information of these inflammation-associated candidates allowed a clear separation of both groups (HFD *vs.* control) in a supervised hierarchical cluster analysis (Fig. 3B). For validation of the microarray data and to further evaluate changes in expression of the most prominent candidate genes in fatty acid-induced inflammation, quantitative PCR was performed in hypothalami of control and HFD offspring at P21. Hypothalamic expression of *TNF α* was slightly reduced after maternal HFD feeding, but expression of *IL-6* was significantly increased in the hypothalamus of HFD offspring compared with controls at P21 ($P = 0.018$) (Fig. 4A). Interestingly, in both microarray and qPCR experiments, hypothalamic expression of *TLR4* was markedly increased in offspring of HFD-fed dams ($P = 0.018$) (Figs. 3B and 4B). Moreover, expression of downstream members of the TLR4 inflammatory response machinery (*MyD88*, *IRAK1*, and *TRAF6*) were also significantly increased in both microarray and qPCR analyses of hypothalami after maternal

HFD feeding at P21 ($P = 0.005$; $P = 0.017$; $P = 0.014$) (Fig. 4B).

To evaluate the functional consequence of the observed increase in expression levels of proinflammatory genes in the hypothalamus of HFD offspring at P21, we next determined the protein amounts and phosphorylation of inflammation mediating kinases JNK1 and IKK β in hypothalamic tissue of HFD and control offspring at P21. Total amounts of both JNK1 and IKK β were significantly increased in the hypothalamus of HFD offspring compared with controls at P21 ($P = 0.024$ and $P = 0.036$) (Fig. 4, C and D). Moreover, HFD offspring showed a robust increase in phosphorylated protein amount of both JNK1 and IKK β compared with controls ($P = 0.024$ and $P = 0.024$) (Fig. 4, C and D), indicating increased intracellular inflammatory signaling within the hypothalamus.

Taken together, maternal HFD feeding-induced up-regulation of *IL-6* and genes involved in the TLR4 signaling cascade with subsequently increased inflammatory signaling on the level of JNK1 and IKK β in the hypothalamus of the offspring at P21.

To next assess whether increased hypothalamic inflammation is associated with functional changes in the neuronal networks known to be involved in the regulation of energy and glucose homeostasis, we determined expression levels of orexigenic (*AgRP* and *NPY*) and anorexigenic (*orexin*, *POMC*, *CART*, and *TRH*) neuropeptides in the hypothalamus of HFD and control offspring at P21. Interestingly, expression levels of both orexigenic and anorexigenic neuropeptides tended to be increased in HFD offspring compared with controls, indicating a generally disturbed regulatory environment after maternal HFD feeding ($P = 0.027$ for *AgRP*, $P = 0.053$ for *orexin*, $P = 0.051$ for *POMC*, and $P = 0.054$ for *TRH*) (Fig. 4E).

Furthermore, we tested whether the observed hypothalamic inflammation might be part of a multi-organ inflammatory response resulting from maternal HFD feeding. Focusing on liver and pancreas as two major regulators of glucose balance, we next determined local mRNA levels of *TNF α* , *IL-6*, and members of the TLR4 signaling cascade at P21. Interestingly, we did not detect an increase in hepatic or pancreatic expression levels in HFD offspring compared with controls at P21 (Fig. 5, A–D). Additionally, we quantified protein amounts of JNK1 in liver of HFD and control offspring at P21. Again,

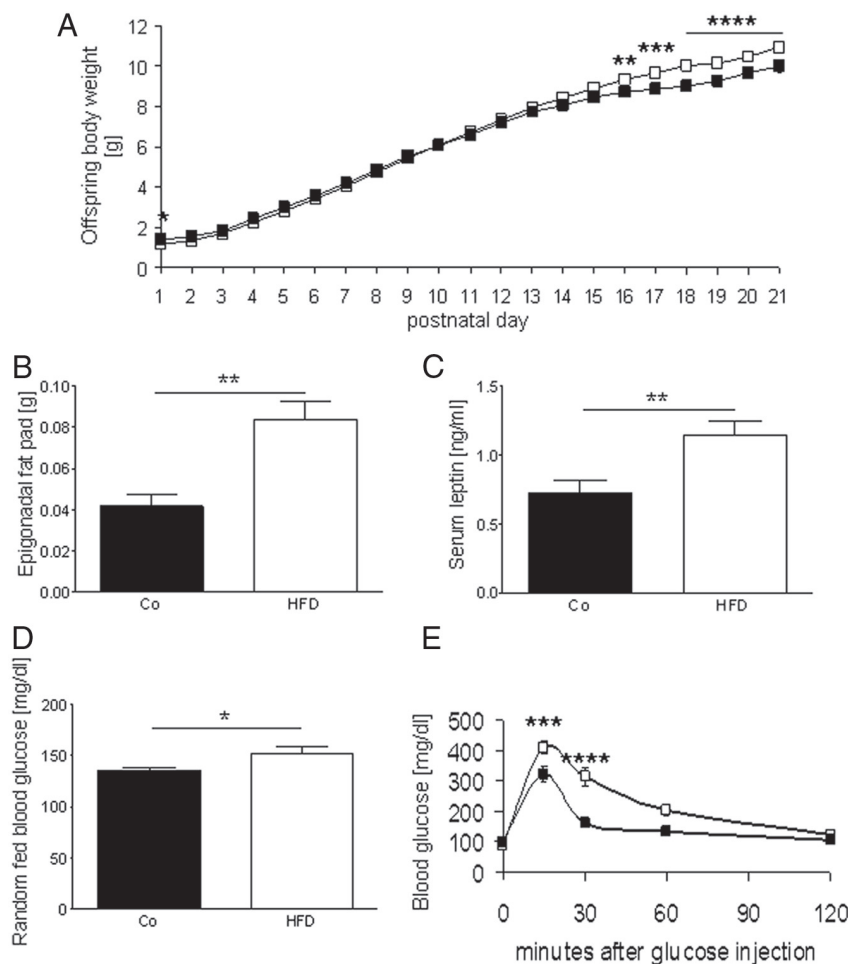


FIG. 2. A, Mean body weight (\pm SEM) of control (■) and HFD (□) male offspring between P1 and P21. B, Epigonadal fat pad weight in control (black bars) and HFD (white bars) male offspring at P21. C, Serum leptin levels in control (black bars) and HFD (white bars) male offspring at P21. D, Random fed blood glucose levels in control (black bars) and HFD (white bars) male offspring at P15. E, ipGTT in control (■) and HFD (□) male offspring at P21. Per group, $n = 6$ –18 (five to 12 different litters). *, $P < 0.05$; **, $P < 0.01$; ***, $P < 0.001$; ****, $P < 0.0001$. Co, Control.

we did not observe a difference in either total or phosphorylated protein amounts of hepatic JNK1 (Fig. 5E). Based on these findings, it can be hypothesized that HFD induces a local IL-6 and TLR4-mediated hypothalamic inflammation as an early event in the pathogenesis of glucose intolerance after maternal perinatal HFD feeding.

Fatty acid-induced hypothalamic inflammation has been shown to alter β -cell function via sympathetic innervation of the pancreas (4). Moreover, pancreatic expression levels of *PGC1 α* have been demonstrated to rise upon sympathetic nerve input and therefore serve as a measure of sympathetic innervation (4). Thus, we next determined expression levels of *PGC1 α* in liver and pancreatic tissue of HFD and control offspring at P21. In liver, *PGC1 α* expression showed a significant 2-fold increase ($P = 0.016$) (Fig. 6A). In pancreatic tissue, *PGC1 α* expression

even underwent an almost 30-fold induction after maternal HFD feeding ($P = 0.036$) (Fig. 6B).

To investigate whether hepatic insulin resistance might be responsible for the observed increase in *PGC1 α* expression, we quantified insulin-stimulated AKT phosphorylation in the liver of HFD and control offspring at P21. Phosphorylation of AKT was slightly increased after insulin stimulation in HFD offspring compared with controls at P21, arguing against hepatic insulin resistance at that stage (Fig. 6C).

Finally, we also assessed expression of the key gluconeogenic enzyme *PEPCK* in the liver of HFD and control offspring. *PEPCK* expression is known to be directly regulated by *PGC1 α* via the forkhead transcription factor *FOXO1* (25–27). Interestingly, hepatic mRNA levels of *PEPCK* showed a significant 4-fold induction in HFD offspring at P21 ($P = 0.012$) (Fig. 6D). Hepatic *FOXO1* expression was also significantly increased ($P = 0.009$) (Fig. 6D).

Discussion

This study aimed to determine the effects of maternal perinatal HFD feeding on the metabolic phenotype and parameters of inflammation in the hypothalamus of the offspring at P21. Metabolic characterization of the offspring revealed an expected, yet compared with other studies early onset of increased body weight, increased white adipose tissue mass, and hyperleptinemia within the first 3 wk of life (11, 28). Interestingly, HFD offspring also presented early signs of impaired glucose metabolism at P21. In detail, fasting blood glucose levels were unaltered, but random fed blood glucose levels were significantly increased and plasma glucose clearance in an ipGTT was delayed. This impairment in glucose tolerance is of special interest, because neonatal rat pups (P1) have already been shown to display elevated blood glucose levels immediately after birth with simultaneous up-regulation of hepatic gluconeogenic genes after maternal HFD feeding (29). Moreover, up-regulation of gluconeogenic enzymes has also been demonstrated in adult (P70) offspring after maternal

metabolic characterization of the offspring revealed an expected, yet compared with other studies early onset of increased body weight, increased white adipose tissue mass, and hyperleptinemia within the first 3 wk of life (11, 28). Interestingly, HFD offspring also presented early signs of impaired glucose metabolism at P21. In detail, fasting blood glucose levels were unaltered, but random fed blood glucose levels were significantly increased and plasma glucose clearance in an ipGTT was delayed. This impairment in glucose tolerance is of special interest, because neonatal rat pups (P1) have already been shown to display elevated blood glucose levels immediately after birth with simultaneous up-regulation of hepatic gluconeogenic genes after maternal HFD feeding (29). Moreover, up-regulation of gluconeogenic enzymes has also been demonstrated in adult (P70) offspring after maternal

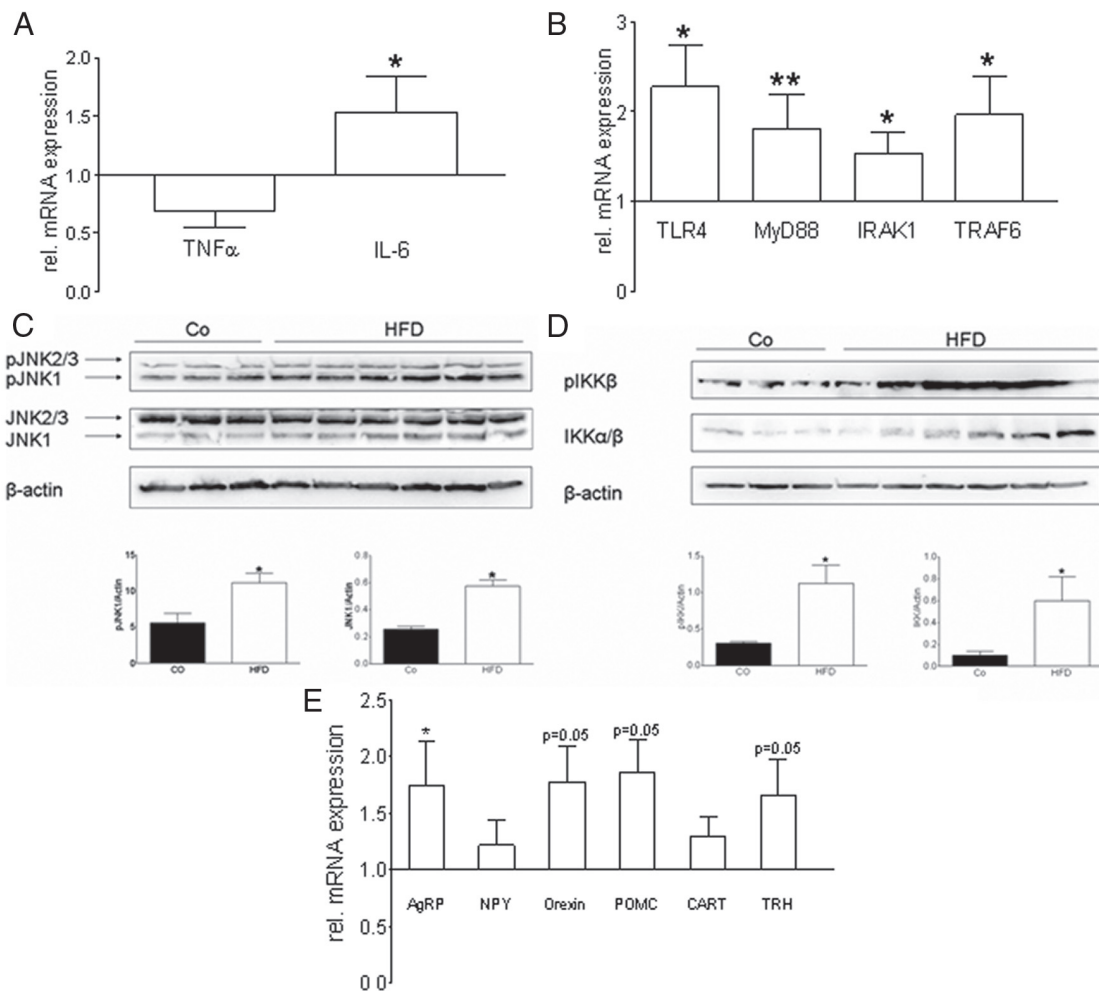


FIG. 4. A, Relative hypothalamic mRNA expression of TNF α and IL-6 in HFD offspring at P21 determined by qPCR. Average expression level in control offspring was set to 1. B, Relative hypothalamic mRNA expression of TLR4, MyD88, IRAK1, and TRAF6 in HFD offspring at P21 determined by qPCR. Average expression level in control offspring was set to 1. C, Western blot analysis of protein extracted from hypothalamic tissue of control and HFD male offspring at P21. Quantification of JNK1 and pJNK1 relative to loading control (β -actin) in control (*black bars*) and HFD (*white bars*) offspring. D, Western blot analysis of protein extracted from hypothalamic tissue of control and HFD male offspring at P21. Quantification of IKK β and pIKK β relative to loading control (β -actin) in control (*black bars*) and HFD (*white bars*) offspring. E, Relative hypothalamic mRNA expression of hypothalamic neuropeptides (AgRP, NPY, orexin, POMC, CART, and TRH) in HFD offspring at P21 determined by qPCR. Average expression level in control offspring was set to 1. Per group, $n = 6-10$ (five to eight different litters) for qPCR; $n = 3-6$ per group (three to six different litters) for Western blots. *, $P < 0.05$; **, $P < 0.01$. Co, Control.

induces inflammatory response in rodents (6, 31). We detected marked up-regulation of TLR4 and several members of its downstream signaling cascade in the hypothalamus of HFD offspring, which can be seen independently of local TNF α activity because hypothalamic TNF α expression is even reduced at the same time. Subsequently, phosphorylation of JNK1 and IKK β was significantly increased at P21. The association between increased expression of key molecules of the TLR4 signaling cascade and simultaneous activation of JNK1 and IKK β is a novel finding and suggests a role of TLR4-mediated hypothalamic inflammation in the pathogenesis of obesity and type 2 diabetes. Furthermore, it provides a potential link between HFD-induced hypothalamic inflammation and perinatal programming of metabolic disease. The fact

that among the studied organs the hypothalamus is the first tissue to show signs of inflammation is especially intriguing. First, this demonstrates once more an evident vulnerability of the fetal and neonatal hypothalamus to maternal nutritional and hormonal cues. Second, it supports the hypothesis that the observed metabolic phenotype might indeed result from changes in central regulatory systems rather than being caused by peripheral effects of nutritional or hormonal factors. One recent rodent study described hypothalamic TLR4/nuclear factor- κ B activation as a consequence of maternal perinatal consumption of a diet rich in *trans* fatty acids (32). Interestingly, the offspring presented with accelerated postweaning body weight gain and impaired satiety sensing as adults despite the fact that the general amount of maternal fatty acid

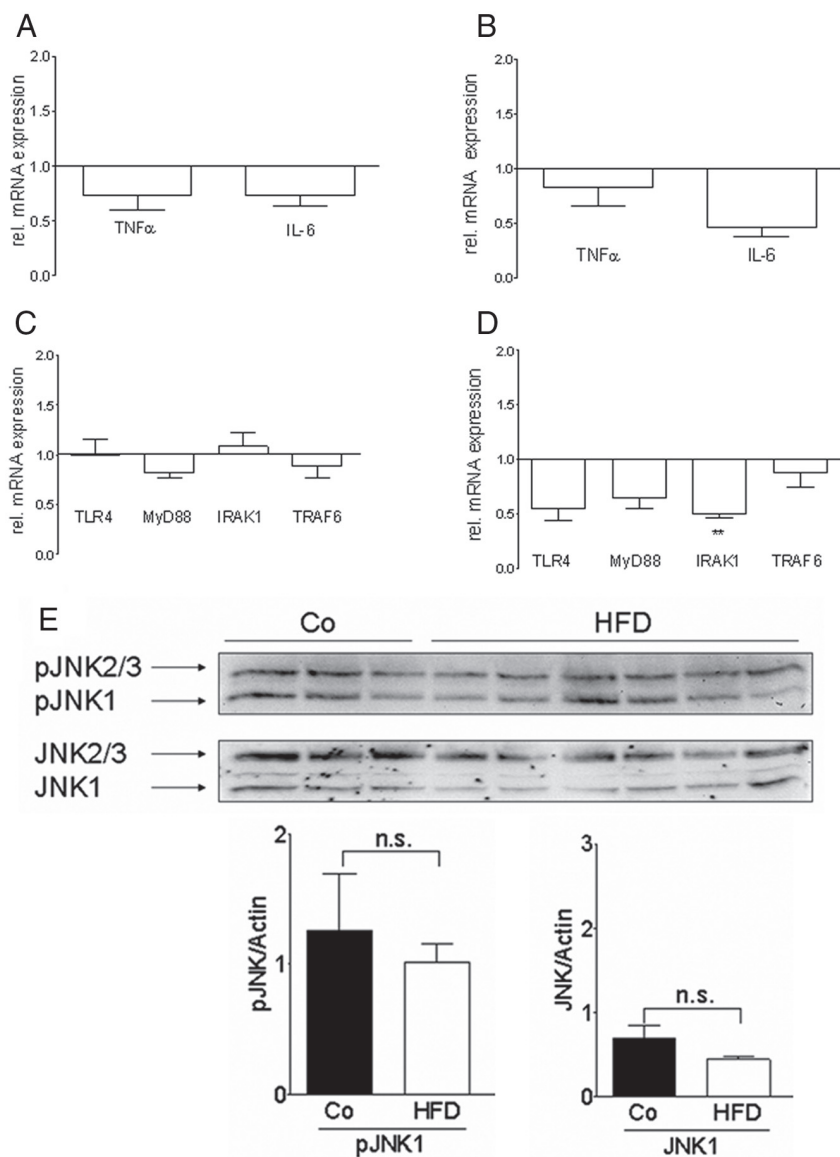


FIG. 5. A, Relative hepatic mRNA expression of TNF α and IL-6 in HFD offspring at P21 determined by qPCR. Average expression level in control offspring was set to 1. B, Relative pancreatic mRNA expression of TNF α and IL-6 in HFD offspring at P21 determined by qPCR. Average expression level in control offspring was set to 1. C, Relative hepatic mRNA expression of TLR4, MyD88, IRAK1, and TRAF6 in HFD offspring at P21 determined by qPCR. Average expression level in control offspring was set to 1. D, Relative pancreatic mRNA expression of TLR4, MyD88, IRAK1, and TRAF6 in HFD offspring at P21 determined by qPCR. Average expression level in control offspring was set to 1. E, Western blot analysis of protein extracted from liver of control and HFD male offspring at P21. Quantification of JNK1 and pJNK1 is relative to loading control (β -actin) in control (black bars) and HFD (white bars) offspring. Per group, $n = 6-10$ (five to eight different litters) for qPCR; $n = 3-6$ per group (three to six different litters) for Western blots. **, $P < 0.01$. Co, Control.

intake did not differ between experimental and control groups. Thus, the inflammatory response within the hypothalamus must be crucial for the resulting metabolic predisposition, independent of an inflammation-causing factor.

It is conceivable that in our experimental setting direct action of altered levels of circulating adipokines or cytokines may act in concert with nutritional factors to mod-

ulate hypothalamic inflammation. In light of elevated serum leptin levels in HFD offspring at P21, it is important to appreciate that leptin itself is able to modulate the inflammatory response in mouse glial cells (33). In addition, leptin can potentiate microglial activation in response to lipopolysaccharides, indicating that leptin has an important role in microglial function and inflammation (34). Furthermore, changes in circulating as well as locally released cytokines might contribute to the observed hypothalamic inflammatory response. Therefore, determining serum cytokine levels as well as assessing from which cell type or nuclear region the observed increase in hypothalamic cytokine expression in HFD offspring at P21 arises will help to better understand the underlying inflammatory processes.

With regard to the regulatory impact of the observed increase in inflammatory response in our experimental group, the interpretation of the observed trend toward an increased hypothalamic expression of both orexigenic and anorexigenic neuropeptides at P21 is demanding. Previous studies have shown that postnatal overnutrition results in hyperleptinemia and increased hypothalamic *NPY* and *POMC* mRNA levels in adult rats (35). Furthermore, hypothalamic TNF α action has been shown to influence hypothalamic *NPY*, *AgRP*, and *POMC* mRNA levels (9). Moreover, exposure of adult mice to HFD was recently associated with reactive gliosis within the hypothalamus, thereby affecting the structure of the blood-brain barrier such that the *POMC* and *NPY* cell bodies and their dendrites may become less accessible to blood vessels (36). Thus, changes in neuropeptide expression in

our experimental setting might also be a result of reactive gliosis and subsequently disturbed hypothalamic cytoarchitecture. Histological studies will help to clarify whether and to what extent gliosis or proliferative neuronal processes within the hypothalamus might play a role in the context of altered neuropeptide expression in the offspring of HFD-fed dams.

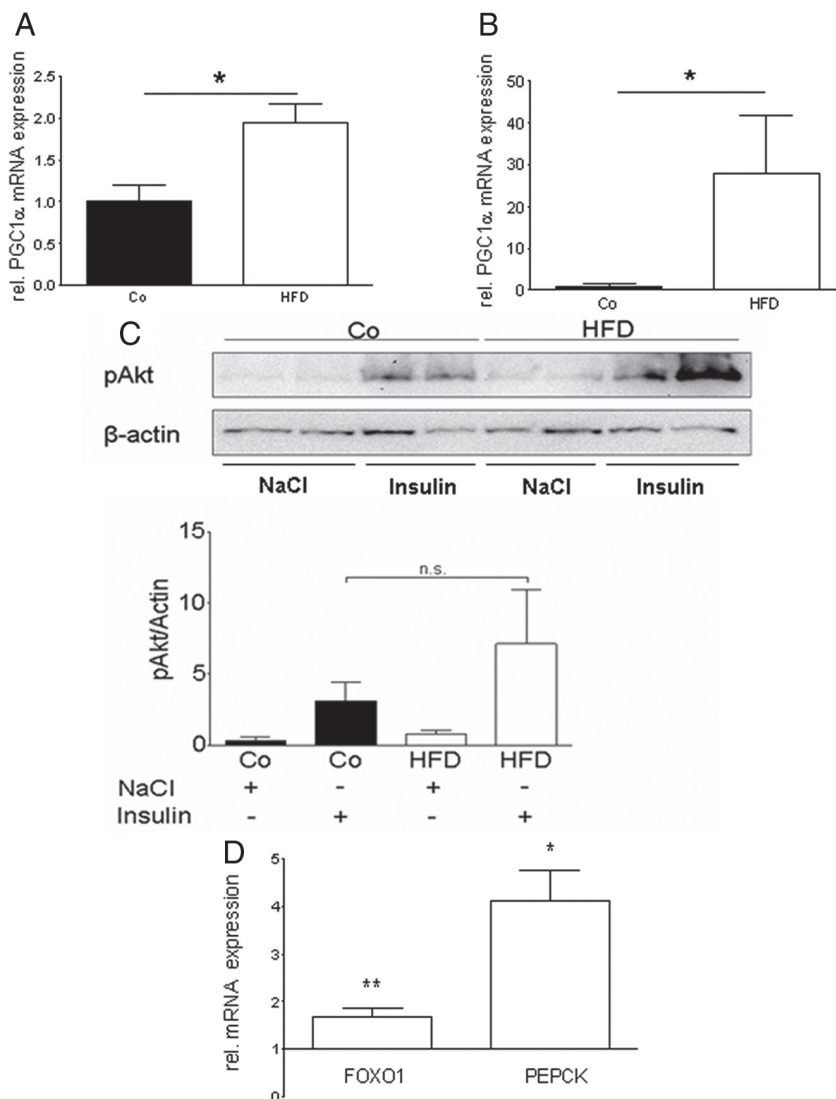


FIG. 6. A, Relative hepatic mRNA expression of PGC1 α in control (black bar) and HFD (white bar) offspring at P21 determined by qPCR. Average expression level in control offspring was set to 1. B, Relative pancreatic mRNA expression of PGC1 α in control (black bar) and HFD (white bar) offspring at P21 determined by qPCR. Average expression level in control offspring was set to 1. C, Insulin-stimulated AKT phosphorylation in liver of control (black bars) and HFD (white bars) male offspring at P21. D, Relative hepatic mRNA expression of FOXO1 and PEPCK in HFD offspring at P21 determined by qPCR. Average expression level in control offspring was set to 1. Per group, $n = 6$ – 10 per group (five to eight different litters) for qPCR; $n = 3$ – 6 per group (three to six different litters) for Western blots. *, $P < 0.05$; **, $P < 0.01$. Co, Control.

Several groups have very recently demonstrated that hypothalamic inflammation results in altered sympathetic innervation and subsequent dysfunction in peripheral organs (4, 37). In detail, obesity-associated activation of IKK β and NF κ B in the mediobasal hypothalamus in adult mice has been shown to induce hypertension via sympathetic up-regulation (37). Furthermore, fatty acid-induced hypothalamic inflammation has been shown to cause pancreatic islet dysfunction via modulation of the sympathetic innervation (4). Taking this into account, it is

conceivable that early hypothalamic inflammation after maternal HFD feeding in our animal model may also result in altered sympathetic innervation of peripheral organs. Peripheral expression of the transcriptional coactivator PGC1 α has previously been shown to increase upon fatty acid-induced hypothalamic inflammation and lead to a loss of first-phase insulin secretion (4). This up-regulation is dependent on sympathetic innervation of the organ, because sympathectomy in the animals returns peripheral PGC1 α levels and insulin secretion capacity back to normal (4). Moreover, PGC1 α has been shown to directly increase gluconeogenic gene expression via the forkhead transcription factor FOXO1 in the liver and to suppress membrane depolarization in pancreatic β -cells with subsequent impairment of insulin secretion (25, 26, 38). Thus, PGC1 α is an important modulator of several key mechanisms in the control of glucose homeostasis. Interestingly, PGC1 α expression was markedly increased in liver as well as pancreatic tissue of HFD offspring at P21. This supports the hypothesis of an elevated sympathetic tone after hypothalamic inflammation, which results in disturbed regulation of glucose homeostasis. Independent of sympathetic innervation, insulin can directly suppress PGC1 α expression in the liver via phosphorylation of AKT (39). Thus, hepatic insulin resistance with subsequently reduced AKT phosphorylation could provide an explanation for elevated hepatic PGC1 α mRNA levels. Interestingly, we did not detect signs of hepatic insulin resistance as assessed

by quantification of insulin-stimulated AKT phosphorylation in HFD offspring at P21. Thus, hepatic insulin action is unlikely to contribute to the disturbance in glucose homeostasis in our animal model at this stage during development. However, we cannot rule out that the observed hyperleptinemia and subsequently increased central leptin action might further contribute to enhanced sympathetic outflow to the periphery (40, 23). Functional analysis of leptin's action on hypothalamic neurons in HFD offspring will be necessary to

properly evaluate leptin's contribution to sympathoactivation at P21.

Taken together, maternal HFD consumption during gestation and lactation leads to accelerated body weight and body fat gain, impaired glucose tolerance, and most importantly, hypothalamic inflammation at P21 in the offspring. Expression analysis of hepatic and pancreatic tissue suggests increased sympathetic innervation of both organs. This in turn contributes to the development of impaired glucose tolerance by up-regulation of gluconeogenesis and presumably disturbance of insulin secretion. A fuller understanding of the molecular mechanisms leading to this predisposition will ultimately allow the development of effective preventive strategies against perinatal programming of obesity and type 2 diabetes.

Acknowledgments

We thank the Department of Pediatric Oncology and Hematology at the University of Cologne for kindly providing access to their microarray scanning facility and Leona Plum for critical reading of the manuscript.

Address all correspondence and requests for reprints to: Eva Rother, M.D., Department of Pediatrics, University Hospital of Cologne, Kerpener Strasse 62, 50924 Cologne, Germany. E-mail: eva.rother@uni-koeln.de.

This work was supported by Köln Fortune (25/2009 and 69/2010) to E.R. and the Deutsche Forschungsgemeinschaft (DO 682/8-1) to J.D.

Disclosure Summary: The authors have nothing to disclose.

References

- Choi SJ, Kim F, Schwartz MW, Wisse BE 2010 Cultured hypothalamic neurons are resistant to inflammation and insulin resistance induced by saturated fatty acids. *Am J Physiol Endocrinol Metab* 298:E1122–E1130
- Arruda AP, Milanski M, Romanatto T, Solon C, Coope A, Alberici LC, Festuccia WT, Hirabara SM, Ropelle E, Curi R, Carvalheira JB, Vercesi AE, Velloso LA 2010 Hypothalamic actions of tumor necrosis factor α provide the thermogenic core for the wastage syndrome in cachexia. *Endocrinology* 151:683–694
- Arruda AP, Milanski M, Coope A, Torsoni AS, Ropelle E, Carvalho DP, Carvalheira JB, Velloso LA 2011 Low-grade hypothalamic inflammation leads to defective thermogenesis, insulin resistance, and impaired insulin secretion. *Endocrinology* 152:1314–1326
- Calegari VC, Torsoni AS, Vanzela EC, Araújo EP, Morari J, Zoppi CC, Sbragia L, Boschero AC, Velloso LA 2011 Inflammation of the hypothalamus leads to defective pancreatic islet function. *J Biol Chem* 286:12870–12880
- De Souza CT, Araujo EP, Bordin S, Ashimine R, Zollner RL, Boschero AC, Saad MJ, Velloso LA 2005 Consumption of a fat-rich diet activates a proinflammatory response and induces insulin resistance in the hypothalamus. *Endocrinology* 146:4192–4199
- Milanski M, Degasperis G, Coope A, Morari J, Denis R, Cintra DE, Tsukumo DM, Anhe G, Amaral ME, Takahashi HK, Curi R, Oliveira HC, Carvalheira JB, Bordin S, Saad MJ, Velloso LA 2009 Saturated fatty acids produce an inflammatory response predominantly through the activation of TLR4 signaling in hypothalamus: implications for the pathogenesis of obesity. *J Neurosci* 29:359–370
- Thaler JP, Choi SJ, Schwartz MW, Wisse BE 2010 Hypothalamic inflammation and energy homeostasis: resolving the paradox. *Front Neuroendocrinol* 31:79–84
- Posey KA, Clegg DJ, Printz RL, Byun J, Morton GJ, Vivekanandan-Giri A, Pennathur S, Baskin DG, Heinecke JW, Woods SC, Schwartz MW, Niswender KD 2009 Hypothalamic proinflammatory lipid accumulation, inflammation, and insulin resistance in rats fed a high-fat diet. *Am J Physiol Endocrinol Metab* 296:E1003–E1012
- Arruda AP, Milanski M, Velloso LA 2011 Hypothalamic inflammation and thermogenesis: the brown adipose tissue connection. *J Bioenerg Biomembr* 43:53–58
- Romanatto T, Roman EA, Arruda AP, Denis RG, Solon C, Milanski M, Moraes JC, Bonfleur ML, Degasperis GR, Picardi PK, Hirabara S, Boschero AC, Curi R, Velloso LA 2009 Deletion of tumor necrosis factor- α receptor 1 (TNFR1) protects against diet-induced obesity by means of increased thermogenesis. *J Biol Chem* 284:36213–36222
- Howe GJ, Sloboda DM, Kamal T, Vickers MH 2009 Maternal nutritional history predicts obesity in adult offspring independent of postnatal diet. *J Physiol* 587:905–915
- Zhang X, Strakovsky R, Zhou D, Zhang Y, Pan YX 2011 A maternal high-fat diet represses the expression of antioxidant defense genes and induces the cellular senescence pathway in the liver of male offspring rats. *J Nutr* 141:1254–1259
- Catalano PM, Hauguel-De Mouzon S 2011 Is it time to revisit the Pedersen hypothesis in the face of the obesity epidemic? *Am J Obstet Gynecol* 204:479–487
- Boney CM, Verma A, Tucker R, Vohr BR 2005 Metabolic syndrome in childhood: association with birth weight, maternal obesity, and gestational diabetes mellitus. *Pediatrics* 115:e290–296
- Bilbo SD, Tsang V 2010 Enduring consequences of maternal obesity for brain inflammation and behavior of offspring. *FASEB J* 24:2104–2115
- Gupta A, Srinivasan M, Thamadolok S, Patel MS 2009 Hypothalamic alterations in fetuses of high fat diet-fed obese female rats. *J Endocrinol* 200:293–300
- Page KC, Malik RE, Ripple JA, Anday EK 2009 Maternal and postweaning diet interaction alters hypothalamic gene expression and modulates response to a high-fat diet in male offspring. *Am J Physiol Regul Integr Comp Physiol* 297:R1049–R1057
- Grayson BE, Levasseur PR, Williams SM, Smith MS, Marks DL, Grove KL 2010 Changes in melanocortin expression and inflammatory pathways in fetal offspring of nonhuman primates fed a high-fat diet. *Endocrinology* 151:1622–1632
- White CL, Pistell PJ, Purpera MN, Gupta S, Fernandez-Kim SO, Hise TL, Keller JN, Ingram DK, Morrison CD, Bruce-Keller AJ 2009 Effects of high fat diet on Morris maze performance, oxidative stress, and inflammation in rats: contributions of maternal diet. *Neurobiol Dis* 35:3–13
- Gropp E, Shanabrough M, Borok E, Xu AW, Janoschek R, Buch T, Plum L, Balthasar N, Hampel B, Waisman A, Barsh GS, Horvath TL, Brüning JC 2005 Agouti-related peptide-expressing neurons are mandatory for feeding. *Nat Neurosci* 8:1289–1291
- Könner AC, Janoschek R, Plum L, Jordan SD, Rother E, Ma X, Xu C, Enriori P, Hampel B, Barsh GS, Kahn CR, Cowley MA, Ashcroft FM, Brüning JC 2007 Insulin action in AgRP-expressing neurons is required for suppression of hepatic glucose production. *Cell Metab* 5:438–449
- Plank C, Ostreicher I, Hartner A, Marek I, Struwe FG, Amann K, Hilgers KF, Rascher W, Dötsch J 2006 Intrauterine growth retardation aggravates the course of acute mesangioproliferative glomerulonephritis in the rat. *Kidney Int* 70:1974–1982

23. Harlan SM, Morgan DA, Agassandian K, Guo DF, Cassell MD, Sigmund CD, Mark AL, Rahmouni K 2011 Ablation of the leptin receptor in the hypothalamic arcuate nucleus abrogates leptin-induced sympathetic activation. *Circ Res* 108:808–812
24. Alejandro-Alcázar MA, Kwapiszewska G, Reiss I, Amarie OV, Marsh LM, Sevilla-Pérez J, Wygrecka M, Eul B, Köbrich S, Hesse M, Schermuly RT, Seeger W, Eickelberg O, Morty RE 2007 Hyperoxia modulates TGF- β /BMP signaling in a mouse model of bronchopulmonary dysplasia. *Am J Physiol Lung Cell Mol Physiol* 292:L537–L549
25. Matsumoto M, Pocai A, Rossetti L, Depinho RA, Accili D 2007 Impaired regulation of hepatic glucose production in mice lacking the forkhead transcription factor Foxo1 in liver. *Cell Metab* 6:208–216
26. Rodgers JT, Lerin C, Haas W, Gygi SP, Spiegelman BM, Puigserver P 2005 Nutrient control of glucose homeostasis through a complex of PGC-1 α and SIRT1. *Nature* 434:113–118
27. Cheng Z, Guo S, Copps K, Dong X, Kollipara R, Rodgers JT, Depinho RA, Puigserver P, White MF 2009 Foxo1 integrates insulin signaling with mitochondrial function in the liver. *Nat Med* 15:1307–1311
28. Ashino NG, Saito KN, Souza FD, Nakutz FS, Roman EA, Velloso LA, Torsoni AS, Torsoni MA 2 May 2011 Maternal high-fat feeding through pregnancy and lactation predisposes mouse offspring to molecular insulin resistance and fatty liver. *J Nutr Biochem* 10.1016/j.jnutbio.2010.12.011
29. Strakovsky RS, Zhang X, Zhou D, Pan YX 2011 Gestational high fat diet programs hepatic phosphoenolpyruvate carboxykinase gene expression and histone modification in neonatal offspring rats. *J Physiol* 589:2707–2717
30. Ainge H, Thompson C, Ozanne SE, Rooney KB 2011 A systematic review on animal models of maternal high fat feeding and offspring glycaemic control. *Int J Obes (Lond)* 35:325–335
31. Moraes JC, Coope A, Morari J, Cintra DE, Roman EA, Pauli JR, Romanatto T, Carnevali JB, Oliveira AL, Saad MJ, Velloso LA 2009 High-fat diet induces apoptosis of hypothalamic neurons. *PLoS One* 4:e5045
32. Pimentel GD, Lira FS, Rosa JC, Oliveira JL, Losinskas-Hachul AC, Souza GI, das Gracas T do Carmo M, Santos RV, de Mello MT, Tufik S, Seelaender M, Oyama LM, Oller do Nascimento CM, Watanabe RH, Ribeiro EB, Pisani LP 2 May 2011 Intake of *trans* fatty acids during gestation and lactation leads to hypothalamic inflammation via TLR4/NF κ Bp65 signaling in adult offspring. *J Nutr Biochem* 10.1016/j.jnutbio.2010.12.003
33. Hosoi T, Okuma Y, Nomura Y 2000 Expression of leptin receptors and induction of IL-1 β transcript in glial cells. *Biochem Biophys Res Commun* 273:312–315
34. Lafrance V, Inoue W, Kan B, Luheshi GN 2010 Leptin modulates cell morphology and cytokine release in microglia. *Brain Behav Immun* 24:358–365
35. Ikenasio-Thorpe BA, Breier BH, Vickers MH, Fraser M 2007 Prenatal influences on susceptibility to diet-induced obesity are mediated by altered neuroendocrine gene expression. *J Endocrinol* 193:31–37
36. Horvath TL, Sarman B, García-Cáceres C, Enriori PJ, Sotonyi P, Shanabrough M, Borok E, Argente J, Chowen JA, Perez-Tilve D, Pfluger PT, Brönneke HS, Levin BE, Diano S, Cowley MA, Tschöp MH 2010 Synaptic input organization of the melanocortin system predicts diet-induced hypothalamic reactive gliosis and obesity. *Proc Natl Acad Sci USA* 107:14875–14880
37. Purkayastha S, Zhang G, Cai D 2011 Uncoupling the mechanisms of obesity and hypertension by targeting hypothalamic IKK- β and NF- κ B. *Nat Med* 17:883–887
38. Yoon JC, Xu G, Deeney JT, Yang SN, Rhee J, Puigserver P, Levens AR, Yang R, Zhang CY, Lowell BB, Berggren PO, Newgard CB, Bonner-Weir S, Weir G, Spiegelman BM 2003 Suppression of β -cell energy metabolism and insulin release by PGC-1 α . *Dev Cell* 5:73–83
39. Southgate RJ, Bruce CR, Carey AL, Steinberg GR, Walder K, Monks R, Watt MJ, Hawley JA, Birnbaum MJ, Febbraio MA 2005 PGC-1 α gene expression is down-regulated by Akt-mediated phosphorylation and nuclear exclusion of FoxO1 in insulin-stimulated skeletal muscle. *FASEB J* 19:2072–2074
40. Rahmouni K 2010 Leptin-induced sympathetic nerve activation: signaling mechanisms and cardiovascular consequences in obesity. *Curr Hypertens Rev* 6:104–209